NTNU
Norwegian University of
Science and Technology

Impacts of climate change on the floods in Lake Victoria

Henry Jacob Okany

Hydropower Development
Submission date: July 2017
Supervisor: Knut Alfredsen, IBM

Norwegian University of Science and Technology
Department of Civil and Environmental Engineering

NTNU – Trondheim
Norwegian University of
Science and Technology

Faculty of Engineering
Science and Technology
Department of Hydraulic and
Environmental Engineering

Impacts of climate change on floods in Lake Victoria.

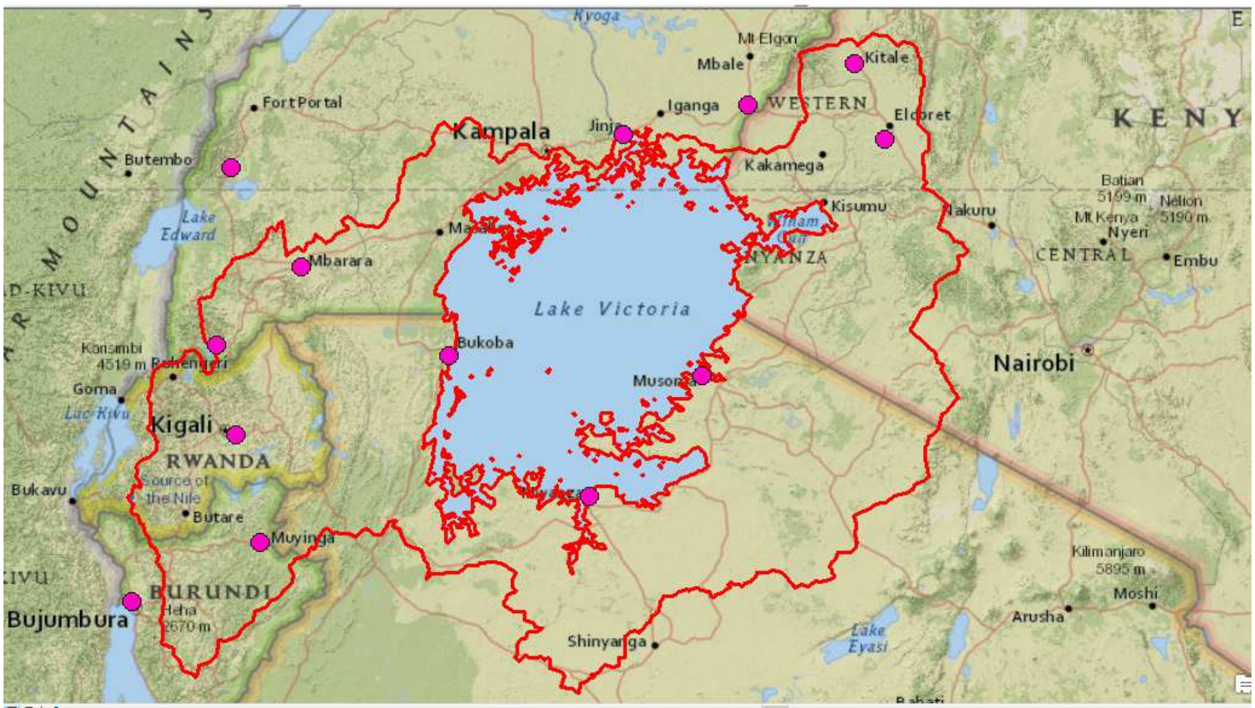

Okany Henry Jacob

Hydropower Development

Submission Date: July 2017

Supervisor: Professor Knut Alfredsen IVM

Co-supervisor: Emmanuel Jjunju, SWECO

Master's Thesis

Impacts of Climate Change on the Floods in Lake Victoria

A thesis submitted in fulfilment of the requirements for the M.Sc. degree in Hydropower Development

Under

Faculty of Engineering Science and Technology

Department of Hydraulics and Environmental Engineering

Trondheim, July 2017

Author:

Okany Henry Jacob

Supervisor:

Professor Knut Alfredsen

Declaration of Authorship

I, Okany Henry Jacob, hereby declare that this master's thesis titled "**Impacts of climate change on Flood in Lake Victoria**" and the work presented in it are my own and has been generated by me as the result of my own original research.

I confirm that:

1. This work was done wholly or mainly while in candidature for a research degree at the Norwegian University of Science and Technology.
2. Where any part of this thesis has previously been submitted for a degree or any other qualification at this University or any other institution, this has been clearly stated.
3. Where I have consulted the published work of others, this is always clearly attributed.
4. Where I have quoted from the work of others, the source is always given. With the exception, of such quotations, this thesis is entirely my own work.
5. I have acknowledged all main sources of help.
6. This thesis is based on work done by myself with the guidance of my supervisor Professor Knut Alfredsen and Co-supervisor Emmanuel Jjunju

Signature: Okany Henry Jacob

Date and Place: July 2017, Trondheim, Norway

ABSTRACT

The effect of climate change not only touches every corner of our planet's ecosystem, however, the water cycle is no exception due to the processes involved which are highly dependent on temperature changes. Therefore, impacts of climate change on flood levels is one issue of important issues to be addressed now due to the lifetime of new infrastructure and the need to determine design floods that are relevant for the future climatic conditions.

Lake Victoria being at one of the centres of diverse attractions draws a lot of studies on climate change. This study therefore was undertaken to investigate the of changes in future floods from the basin inflows to the lake on current infrastructure and the need to adapt to changes in the future. Projecting the future inflows from the catchment was assessed using tow model runs obtained from two Global Circulation Models (GCMs). Two scenarios defined by Representative Concentration Pathways (RCP), RCP45 and RCP85 were used for the climate change studies. Daily precipitation, temperature and aggregated inflows from the catchment over the period of 1980-2005 was used for to compare with future projections for 2041-2065 and 2073-2097. Projections by the GCMs was used on the Delta Change approach.

A gridded resolution of 0.25^{o} x 0.25^{o} (50x50km) was used by ENKI framework an HBV distributed model to simulate the inflows and estimate the evaporation both from the land and from the lake. and estimated the evaporation from and precipitation on Lake Victoria. The total annual precipitation is expected to increase by 3% and 6% for the period 2041-2065 and 2073-2097 scenarios respectively.

The future design flood from the future GCM simulations is not expected to exceed the historical design flood.

1 Introduction

1.1 Background

Impacts on flood levels is one issue of climate change that is important to address already now due to the lifetime of new infrastructure and the need to determine design floods that are relevant for the future climatic conditions. At the same time, we also need to investigate the effect of changes in future floods on current infrastructure and the need to adapt to changes in the future. In this study the flood generation for Lake Victoria in Uganda should be investigated under future climate scenarios, and changes evaluated against the current design criteria for the hydropower installations. A hydrological model was setup which simulated the inflow (from the land- runoff) and estimated the evaporation from and precipitation on Lake Victoria.

Motivation

Uganda has greater focus on development of hydropower plants to sustain her growing economy. However, a lot of planning for the major hydropower plants have been concentrated on the Nile River whose source of water is from Lake Victoria, which derives its waters from the tributaries and precipitation on the lake. Moreover, some of the plants were constructed at the source of the river as early as 1950s and more are being planned along the same river at various sites.

Climate change brings along changes in the hydrological patterns in the catchment and as a result will affect the infrastructure built on the water course. It was therefore under this idea that an investigation into the changes of flood generations for Lake Victoria were conceived and a study of how they would impact these infrastructures done.

1.2 Objective of the Project

The main objective of this study is to investigate the effect of climate change in future floods generated from the catchment on current infrastructure built on the Victoria Nile stretch and the need to adapt to changes in the future. Reference will be on the design floods inflow into the Lake Victoria and how they will impact on the safety of the dams in this area in relation to previous design floods.

2. **Main Questions for the Thesis**

The main objective of this study is to investigate the effect of climate change in future floods on current infrastructure built on the Victoria Nile stretch and the need to adapt to changes in the future. Reference will be on the design floods inflow from Lake Victoria catchment and how they will impact on the safety of the dams in this area in relation to earlier design floods.

The main questions for the thesis can be stated as follows:

1. Prepare data for the setup and calibration of the hydrological model. This involves the preparation of the outflow series from the lake and the input climatic data for the model. It will be of interest to look at alternatives to gauged precipitation and/or temperature, e.g. reanalysis datasets or satellite data.
2. Prepare and set up the model for Lake Victoria. It should be paid special attention to how the lake is handled in the model, including evaluation of necessary routing. Attention will also be paid on the individual contributions from the lake and the run off from the land using the distributed model set up in determining the inflows.
3. Downscale regional data from CORDEX Africa for several GCMs. Perform necessary bias correction and evaluate if historical RCM data can be used to drive the hydrological simulation by comparing it with the historical data. Use the hydrological model from 2) and simulate the flow for the control period. Compute the design flood and evaluate this against data from the observed flow series and from design floods for the infrastructure.
4. Simulate the lake for the future downscaled data. Perform a flood frequency analysis on the future runoff data.
5. Evaluate the results from 4) both with regards to changes in design flood for the hydropower infrastructure and with regards to the uncertainty in the downscaling.
6. Discussions of the results and suggest recommendations where necessary.

3 Supervision, data information input

Professor Knut Alfredsen will be the formal supervisor for the thesis work and assisted by Dr. Emmanuel Jjunju as co-supervisor.

Discussion with and input from colleagues and other research or engineering staff at NTNU, SINTEF, power companies or consultants are recommended. Significant inputs from others shall, however, be referenced in a convenient manner.

The research and engineering work carried out by the candidate in connection with this thesis shall remain within an educational context. The candidate and the supervisors are therefore free to introduce assumptions and limitations, which may be considered unrealistic or inappropriate in a contract research or a professional engineering context.

4 Report format and reference statement

The thesis report shall be in the format A4. It shall be typed by a word processor and figures, tables, photos etc. shall be of good report quality. The report shall include a summary, a table of content, a list of literature formatted according to a common standard and other relevant references. A signed statement where the candidate states that the presented work is his own and that significant outside input is identified should be included.

The report shall have a professional structure, assuming professional senior engineers (not in teaching or research) and decision makers as the main target group.

The thesis shall be submitted no later than 15th of July 2017.

Trondheim 13th of January 2017

____

Knut Alfredsen

Professor

Acknowledgement

First and foremost, I want to thank the Almighty God for the health, the knowledge acquired and for the journey through the completion of the course.

I must say I am very blessed to be part of the researchers on the Lake Victoria Basin and I believe the knowledge gained from it will be transformed to the best of my ability.

Special thanks goes to my Supervisor, Prof Knut Alfredsen for the immense guidance and support during the project time and amazing experiences not in class but outside the class times too.

My sincere gratitude to Dr. Emmanuel Jjunju for his precious expertise and time invested in helping me out on this journey. I also want to take this chance to thank Dr. Teklu T. Hailegeorgis for the ENKI model setup and his extra input in this study based on his expertise.

I would also like to thank the non-teaching stuff; Abebe Girmay for the great help at all stages of the research and to my fellow course mates for the support and the togetherness.

To my parents and my siblings, I will say thank you for moral, mental and emotional support. And to my lovely wife and my sweet daughters, I owe you the greatest patience while I was away from you and I thank God for keeping you all safe and healthy.

List of Acronyms and Abbreviations

CORDEX- Coordinated Regional Climate Downscaling Experiment

DWD- Directorate of Water Development

DWRM- Department of Water Resource Management

ECMWF: European Center for Medium-Range Weather Forecasts

ENSEMBLES- Ensemble Based Predictions of climate change and their impacts

GCM-General Circulation Model

GHCN-D-Global Historical Climatology Network- Daily

IPCC- Intergovernmental panel on climate change

LVEMP: Lake Victoria Environment Project

MOCH- Met Office Hadley center

NASA- National Aeronautics and Space Administration

NOAA: National Oceanic and Atmospheric Administration

PEST -Parameter Estimator

RCM- Regional Climate Model

RCP- Representative Concentration Pathways

UNMA: Uganda National Meteorological Authority

List of Figures

Table of Contents

2 Literature Review and Previous studies on Lake Victoria Catchment

2.1 Background and previous studies

Water extraction for hydropower on River Nile is permitted in line with an agreed water release curve for Lake Victoria which discharges directly into the upstream Nalubaale and Kiira power facilities. This curve was established in the 1950's with Egypt and other countries influenced by the Nile River. Discharge is dependent on lake levels and Uganda's Water Resources Management Department (WRMD) is the responsible agency for monitoring the agreement. Within the WRMD, the Ugandan Directorate of Water Development is responsible for permitting the use of the water for power generation purposes. The 100+ year average discharge from the lake is 870 cubic meters per second (m^3/s.) During the day, flows may vary between 400 m^3/s and 1300 m^3/s but rarely are the extremes reached and more typically the flows vary between 575 m^3/s to 1150 m^3/s.

To make necessary hydrological analysis, data such as the runoff series, precipitation, temperature, wind speed, humidity, radiation, lake levels and lake outflows were obtained from reanalysis and observed gauges. Runoff data for the sub-catchments was obtained from a previous study done by the Lake Victoria Environment Project (LVEMP-2005). ENKI tool was used for the calibration and simulation of the inflows from the catchment.

The ENKI hydrological modelling framework, developed by SINTEF was employed for the calibrations and simulations of the inflows to the lake. The ENKI model employed the use of Priestley Taylor for estimating the precipitation on and evaporation from the lake. The temperature used for the study was from the reanalysis data (which is comparable with the observed.

At the inception of the study, the reference for the design floods was on the outflow from the lake. However, since the outflow is regulated, focus was put into the inflow for investigation. The main objective of this study is to investigate the effect of climate change in future floods on current infrastructure built on the Victoria Nile stretch and the need to adapt to changes in the future. If time allows, an impact of these floods in relation to the dam safety in relation to the earlier design floods will be studied.

The East African lakes have exhibited and left traces of dramatic climatic fluctuations over both historical and recent geologic time (Nicholson & Flohn, 1980, Nicholson, 1997). The river Nile is one of the longest rivers in the world with 6,700km from Lake Victoria to the Mediterranean Sea.

Lake Victoria has been of interest in the context of water balance because it is the source of the Nile and because of its abrupt fluctuations and anomalous hydrological behaviour. Its variability plays a regulatory role for the annual Nile flow, hence any changes in the lake's water balance have significant consequences for riparian countries dependent on Nile water. It has been the subject of several major hydrological investigations, commencing in the early 1930s (e.g. Hurst & Phillips; 1933; de Baulny & Baker, 1970; WMO, 1974, 1981). The later studies, including those of Flohn & Burkhardt (1985) and Kite (1981), have universally underscored the apparent discrepancies between water balance estimates and lake level fluctuations. In particular, it has been difficult to reproduce the dramatic two-metre rise of Victoria between 1961 and 1964. The problem appears to be in the estimation of rainfall over the lake surface (Kite, 1981; Piper et al., 1986). This is not only the largest term in the water balance, but it is also very difficult to assess. However, it is impossible to completely rule out the inaccuracy in evaporation estimates as the root of the "imbalance". One source of error appears to be associated with the rainfall enhancement over the lake that is produced by the nocturnal lake induced circulation system (Flohn & Fraedrich, 1966; Fraedrich, 1968). In this article, we re-examine Lake Victoria's water balance, making two modifications compared to past studies. Most importantly, lake rainfall is estimated from catchment rainfall using a relationship between the two that was derived using satellite data (Ba & Nicholson, in press). Secondly, evaporation is estimated using both the Penman formula and the energy balance approach, and sensitivity studies are performed to determine the influence of input data on the estimates. Our results are compared with past studies and used to reproduce lake-level fluctuations during the period 1956-4978. In a subsequent paper, the model will be utilized to interpret the lake's earlier history in terms of regionally-averaged rainfall.

2.2 Geography and hydrology of Lake Victoria catchment

Victoria is the largest in Africa, with a surface area of 68 800 km2 . Its mean depth is only 40 m; its maximum depth is about 92 m (Spigel & Coulter, 1996). Lake Victoria receives inflow from 17 tributaries, the largest of which is the Kagera (Howell et al, 1988). However, these contribute less than 20% of the water entering the lake, the rest being provided by rainfall. Most of the region would be characterized as arid or semiarid; however, around Lake Victoria mean annual rainfall is 1200-1600 mm in most areas (Fig. 3).

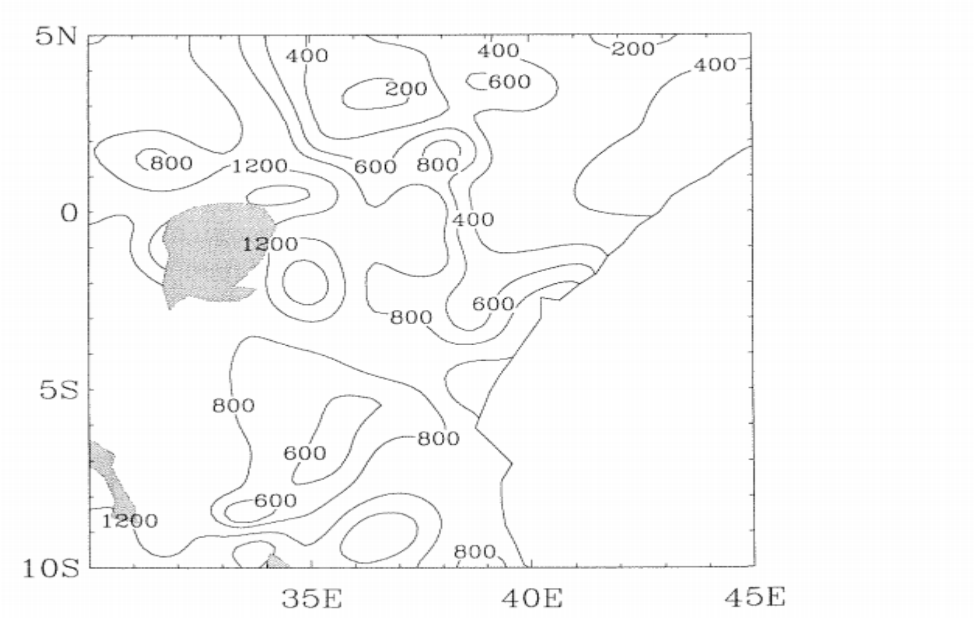

Figure 2-1: Mean annual rainfall mm over East Africa (1930-1994)

The most recent water balance estimate, was that of Piper et al. (1986) which gives mean annual rainfall over the lake as 1850 mm and mean annual evaporation over the lake as 1595 mm. Rainfall over the lake is not only the biggest term in its water balance; it is also the most variable The only outflow is via the White Nile, which exits the lake near Jinja, Uganda. It flows through lakes Kyoga then Albert (now Mobutu Sese Seko) before crossing into the Sudan. Near Khartoum it links with the Blue Nile, which drains the Ethiopian highlands, to form the main Nile flow through Egypt. Thus, Lake Victoria is the source of the White Nile and it also provides 14% of the total Nile flow. The importance of this contribution lies in its relative constancy, a result of the regulating influence of Victoria and the upstream lakes. The rise and fall of these lakes, particularly Victoria, therefore regulates Nile flow. The Lakr Victoria Catchment totals some 197, 000 km2 , and is, hence, nearly three times as large as the lake itself. The catchment includes areas in Rwanda, Burundi, Uganda, Kenya and Tanzania. The northeastern sector (50 000 km2) is relatively steep and forested, a similarly sized southeastern sector drains somewhat drier and flatter land. In the southwest, the Kagera drains some 60 000 km2 in the mountains of Rwanda and Burundi, although some of the runoff is lost as it passes through a system of lakes and swamps. The remaining 30 000 km2 area of the catchment in the northwest contributes little inflow to the lake (Howell et al., 1988).

Previous Studies of Lake Victoria Catchment

Daily rainfall data show a nocturnal peak in rainfall over the lake's centre and along its western shore, as well as an afternoon peak along the eastern shore (Fig. 5). The 25-30% enhancement is also supported by a satellite analysis of rainfall over Lake Victoria (Ba & Nicholson, in press). Table 1 presents a summary of the water balance calculations by various studies. The range in values of mean annual rainfall, 1145-1850 mm, partially reflects different periods of calculation, but the estimates are nevertheless widely divergent. Similarly, inflow and outflow vary by a factor of nearly two. The various estimates of evaporation range from 1130 to 1595 mm/ year . The differences largely reflect methods of calculation and assumptions concerning meteorological variables and lake temperature. In general, it appears that the calculations based on energy balance are lower than those produced using the Penman formula.

Table of previous mean annual water balance components (mm) for Lake Victoria studies by Yin et al (1998)

Ref Source	P (mm)	E (mm)	I (mm)	O (mm)	D[P+I-E-O] (mm)	Period	Rmks
Hurst (1952)	1420	1350	230	305	-5		
Merelieu (1961)	1145	1130	238	305	-52		
De Baulny et al (1970)	1630	1523	260	306	61	1925-59	
Krishnamurty (1973)	1471	1471	265	344	-79		
WMO (1974, 1981)	1636	1458	238	426	-10		
Kite (1982)	1660	1590	420	570	-80	1970-74	
Flohn (1983)	1690	1470	280	450	0	1945-84	
Hasterrath et al (1983)	1650	1500	250	400	0		
Flohn et al (1985)	1630	1470		500		1650-79	
Piper et al (1986)	1558	1595	256	343	-124	1956-78	
Howell (1988)	1810	1593	343	524	36	1956-78	

Sene et al(1994)	1850	1595	343	500	98	1925-90	
Spigel et al (1996)	1450	1370	260	340	0		
Balek (1997)	1476	1401	241	316	0		
Yin et al (1998)	1791	1551	338	524	54	1956-78	
Ba and Nicholson(1998)							P=1.3533Pc-87
Sutcliffe and Parks (1999)		1595					
Yin and Nicholson (2001)	1500-1600						Centre of lake

Table 2-1Previous Studies on Lake Victoria Basin

3 Theory Review

3.1 Introduction

Predicting of water processes behavior is the main aim of hydrological modeling. Many methods and researches have been made to solve that problem. Some of the methods become very popular and broadly used such as:

- Scaling from neighboring catchment;
- Using hydrological modeling for predicting runoff.

A great challenge in hydrological predictions for ungauged basins comes from insufficient understanding of important physical hydrological processes. The concept of hydrological modeling is that physical properties of the catchment converted to numerical value which calls parameters. In this study the aim was focused on application of regional modeling for estimating runoff from Lake Victoria Catchment. The concept of regional modeling is to use the parameters calculated from the catchments with available data series and to apply the same set of average best calibrated parameters to the sub-catchments within the same region.

3.2 Hydrological Modelling and its components

The quantitative description of the characteristics of water is the subject of hydrological modeling. The environment in which hydrological cycle takes place is treated as system and the mechanisms that underlie the processes embedded in models of these systems. The models can then be manipulated and used to simulate system responses. By simulating various alternatives, the consequences of the utilization can be assessed. Using different sets of meteorological input data allows the consequences to be estimated under different climatic conditions (Singh, 1995)

Modeling requires a system view of the hydrological cycle (Figure 3-1 and figure 3-2 describe two approaches to view hydrological cycle). The physical hydrological cycle should be divided in three parts in order to be described as various systems which represent whole complexity of natural water movement processes. Such subsystems are:

- The atmospheric water system containing the processes of precipitation, evaporation and transpiration;
- The surface water system, responsible for the processes of snow accumulation and melt, overland flow, surface runoff, subsurface and groundwater outflow and runoff to streams and the ocean;

- The subsurface water system containing the processes of infiltration, ground water recharge, subsurface flow and groundwater flow.

The objective of hydrological system analysis is to study the system operation and predict its internal states and output. The inputs and outputs are measurable hydrological variables and the model's structure is a set of equations linking input to output. (Killingtveit and Sælthun, 1995)

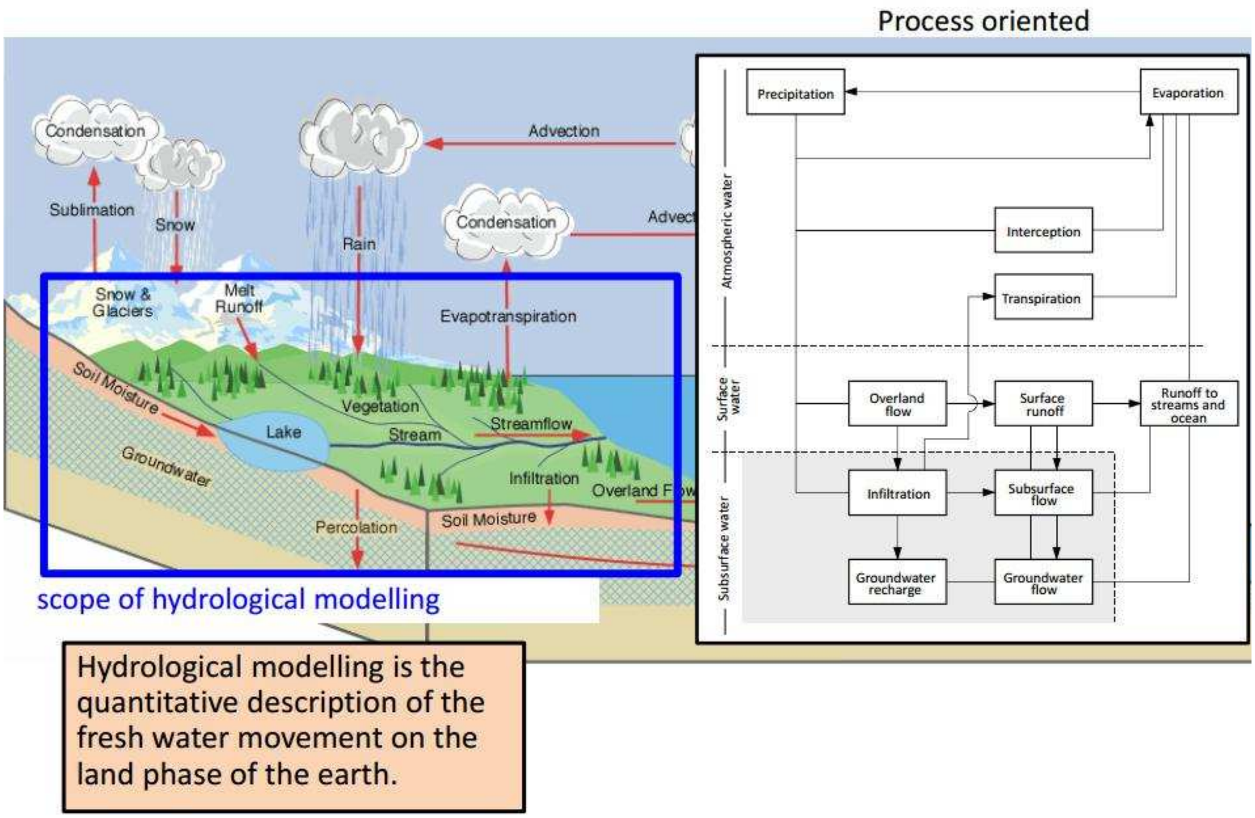

Figure 3-1: Hydrological Cycle for physical hydrological modelling (Rinde, 2016)

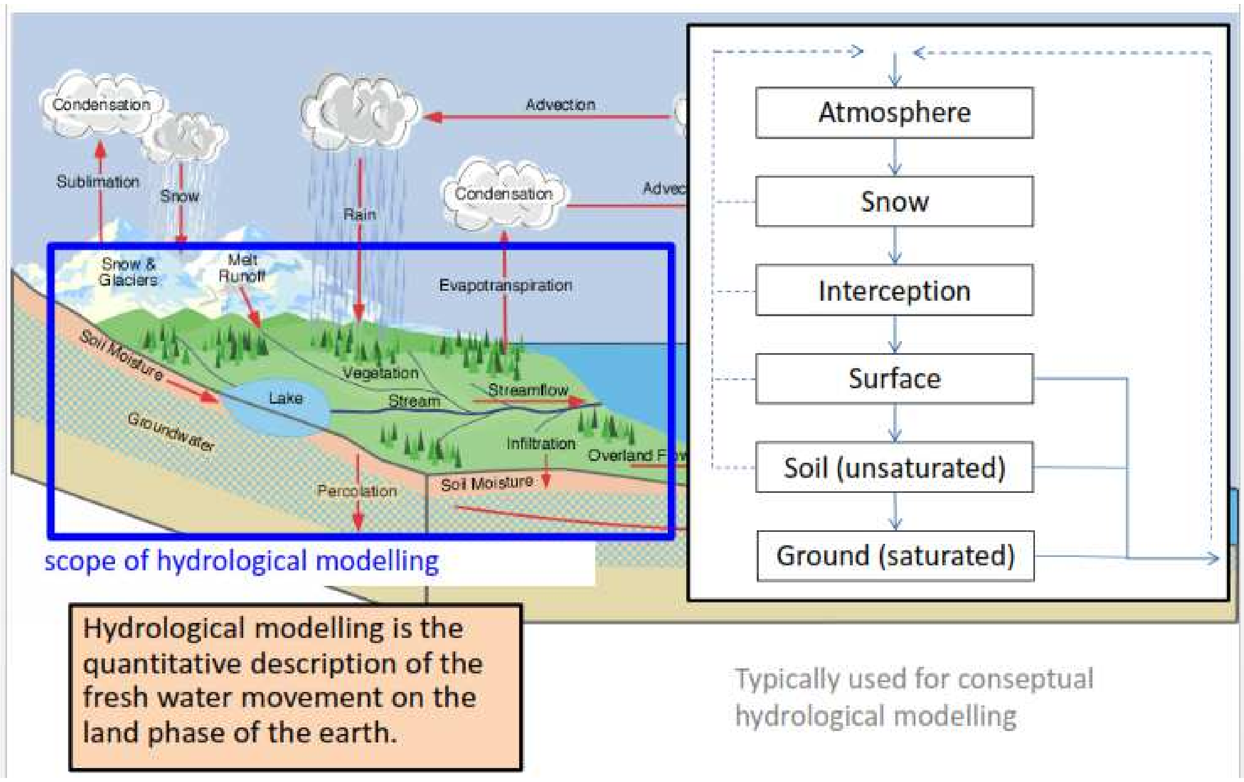

Figure 3-2 Hydrological cycle for conceptual modeling

Figure 3-2 Hydrological cycle typically used for conceptual hydrological modelling

The input and the output of the model can be described as a function of time *I(t)* input and *O(t)* output. The system performs a transformation of the input into output by a transformation operator or equation. Due to great complications of natural processes it is not possible to describe all the physical phenomena within the watershed with exact physical laws.

Knowing the concept of natural water movement, it is possible to construct the model representing the most important processes, and their interaction within the total system. A conceptual knowledge of the physical system will still be valuable to determine the main processes, and to develop a simplified but useful model. (Killingtveit and Sælthun, 1995)

The catchment represents the elementary unit for most hydrological models. The runoff from a catchment is a function of a complex series of processes. Water from precipitation is moving through a series of storages in for example snow (in cold regions), soil and groundwater, through the influence of gravity. Finally, after a short or long delay, the water flows out as river runoff, but some also as evaporation back to the atmosphere and groundwater flow below the soil surface is closely linked to precipitation falling on the contributing catchment.

The catchment represents the elementary unit for most hydrological models. (Rinde, 2016)

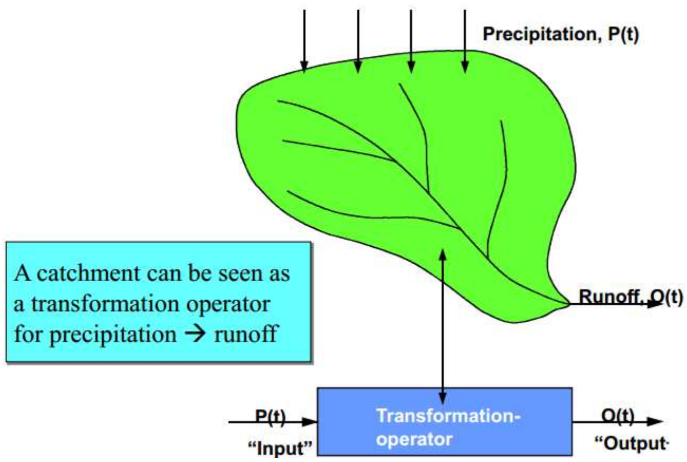

Figure 3-4 Catchment hydrological transformation operator (Rinde, 2016)

Within each catchment there are three main steps that should be identified and included in any rainfall-runoff model (Rinde, 2016):

- The first one is to understand how much areal precipitation is within the catchment. It is important to determine the average value for the rainfall, hence it is not always easy to obtain the average precipitation, based on several available point measurements

- The second important issue is to determine the amount of water which generates the stream from catchment

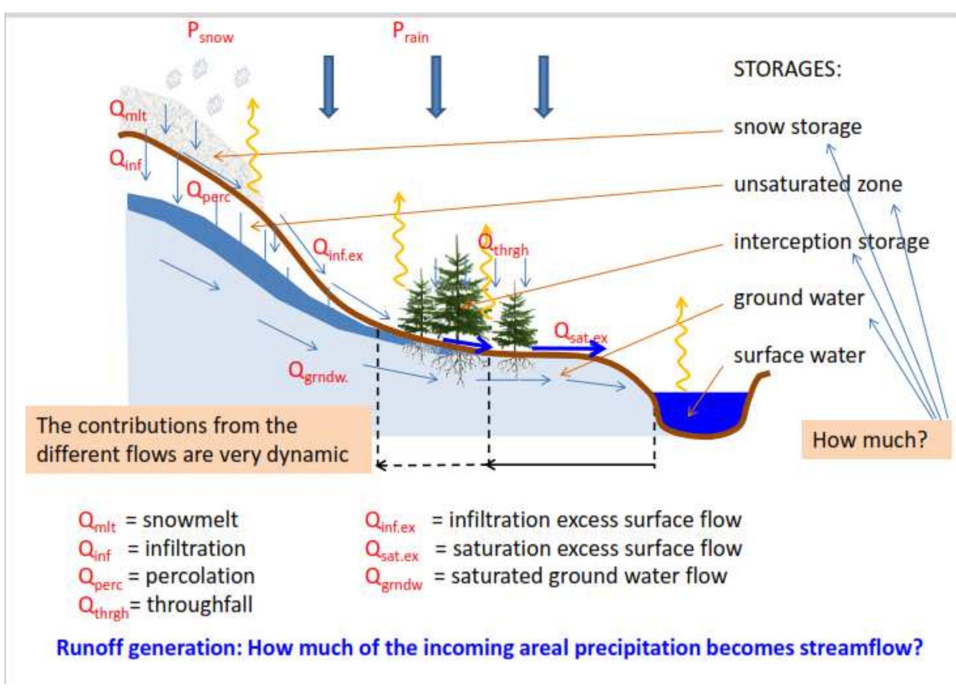

Figure 3-3

- Movement of water from the source to the outlet point is the next issue which should be considered. In the countries with cold climate the storage of snow and snow melt process should be included as part of the model.

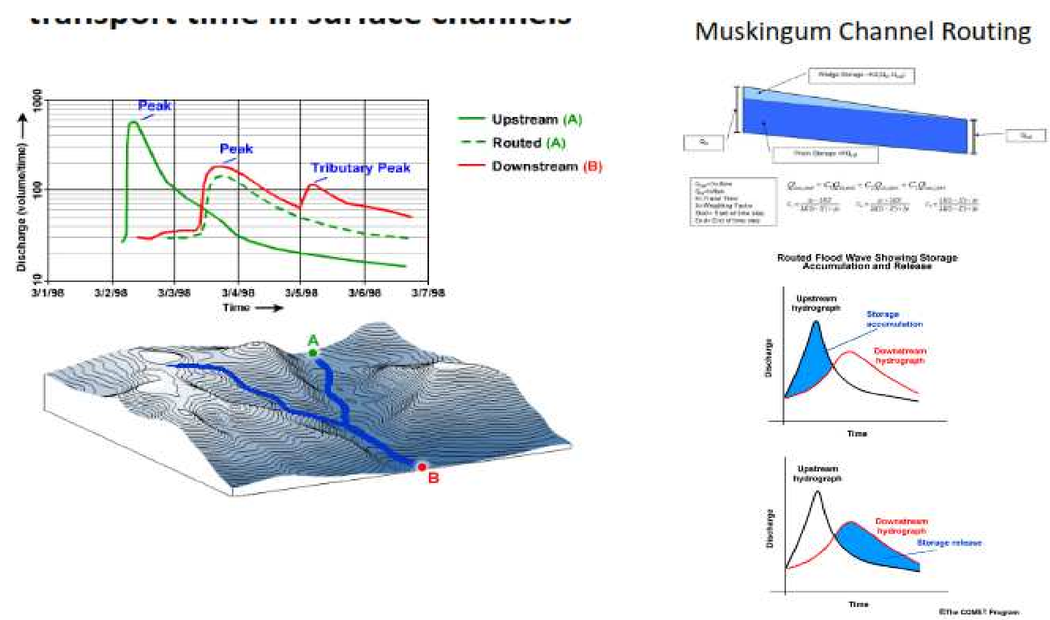

Figure :3-5 Water movement from source to outlet

In all the above three steps of rainfall-runoff modelling, (Beven, 2000) derived a model process link generation, shown in the figure 3-6

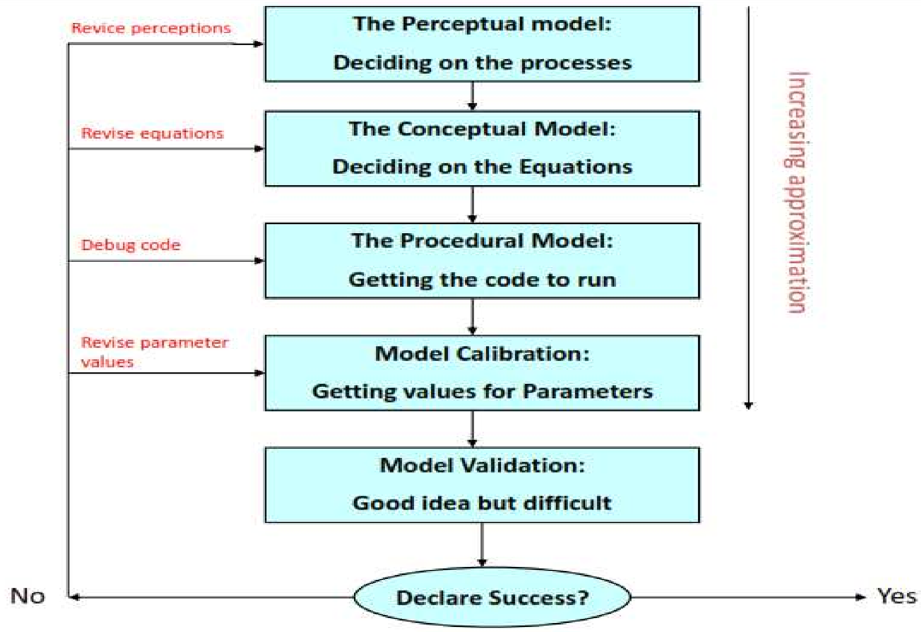

Figure 3-6: Steps in the modelling process (Beven, 2000)

3.3 Hydrological Model Classification

There are two main classes of hydrological models:

1) Physical model which is the real scaled down and minimized copy of the object or
2) Abstract models. In this model, mathematical equations describe the processes. The equations can be set as description of the system and represent the algorithm, which in turn can be coded to the computer program.

The hydrological model classification are further divided into three :

- Randomness (deterministic or stochastic)
- Spatial variation (lumped or distributed)
- Time variability (time-depended, time -independent)

In terms of complexity, the simplest type of model is a deterministic lumped time-independent model. The most complex type is the stochastic model with space variation in three dimensions and with time variation. (Killingtveit and Sælthun, 1995)

In this study, focus was put into the distributed hydrological model which utilizes spatial distributions of input variables and spatial distributions of physical properties in a catchment in combination with algorithms that calculate spatially distributed hydrologic behaviour. This type of model attempts to increase the simulation accuracy by accounting explicitly for the areal distribution of the spatially non-uniform quantities and processes.

Figure 3-6 details the structural classification of the hydrological models.

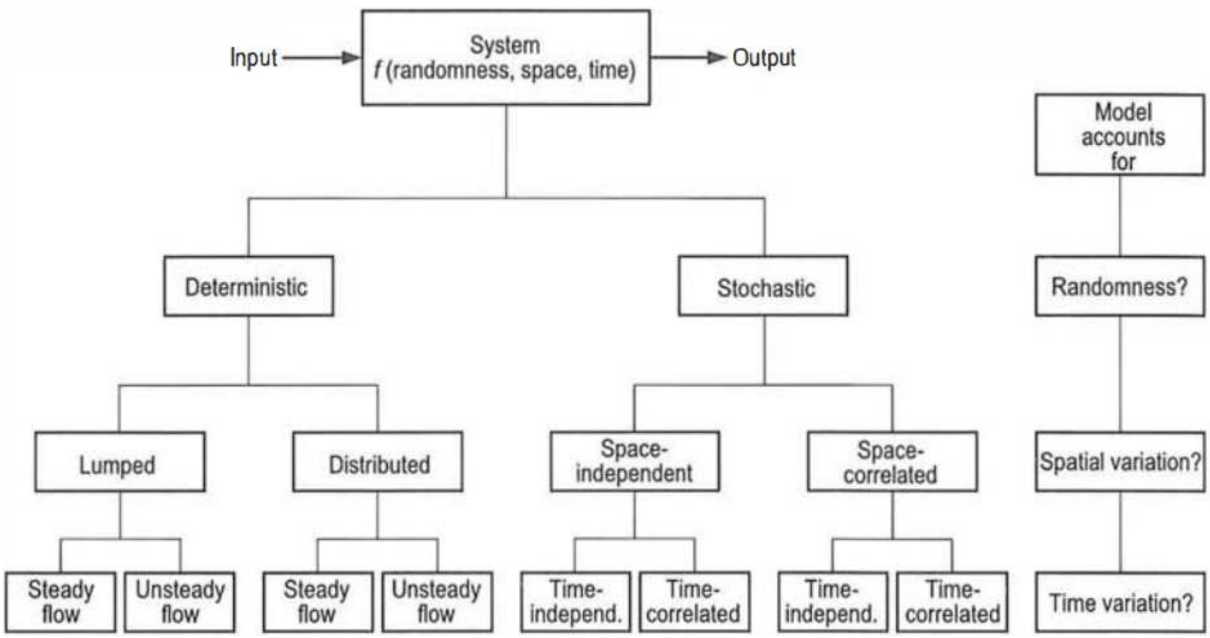

Figure 3-7: Classification of hydrological models adapted from (Chow et al., 1988)

However, a lumped model is the model in which a catchment is handled as one homogeneous unit and the model parameters applied to the whole catchment area.

Within distributed model the input parameters should be determined for each grid, e.g. soil type, land use and elevation are different within each sell of the catchment. Schematic representations of the lumped and distributed hydrological models are shown on Figure 3-4.

The distributed rainfall-runoff models are: The System Hydrologique Europeen (SHE) model, IHDM, LANDPINE-NTNU, ENKI-SINTEF. (Rinde, 2013c)

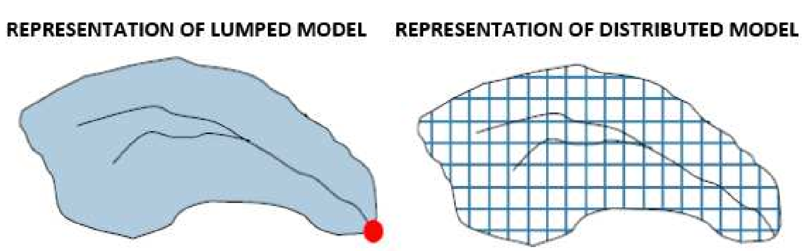

Figure 3-8: Representation of a Lumped and Distributed Model

3.4 Regional Modelling

Regional hydrological modelling or hydrological macro modelling implies a repeated use of a model everywhere within a region using a global set of parameters. Spatial variability is the major source of uncertainties in parameter calibration on rainfall-runoff relationships for runoff simulations (Milly and Dunne 2002).

For sites without observations or with limited observations, the model application needs to be based on the global parameters. In a distributed hydrological model, the parameters are determined for each fundamental unit (grid cell) of the model based on physiographic factors, e.g. topography, soil type and vegetation class of the units. The same global parameter values are used everywhere where the physiographic factors for a fundamental unit falls into the same classes. Parameters of lumped conceptual models can be regionalised by using multiple regression to relate them to catchment characteristics. In the split sample and proxy basin tests (Klemes, 1986), the model is calibrated on some of the data and then validated on data from time periods and catchments not used in the calibration.

Regional parameters ought to be robust, physical based, and have a low dependence on the catchment and time period used for calibration. The calibration and validation results are only utilized within the region.

3.5 Regional Modelling with ENKI

The ENKI framework for hydrological modeling was invented by SINTEF Energy Research and Statkraft Companies. The ENKI modeling system contains tools for regional model setting and calibration. The objective of ENKI regional modeling is to calibrate the set of parameters in different catchments within selected region and to validate the obtained results.

The best set of parameters should be used for extracting discharge in ungauged sites.

ENKI utilizes a multi objective method for the various catchments and iterates the many ranges of parameters to produce best fit by temporal performance, R^2, which named as Nash efficiency. (Shrestha, 2012)

The other method employed on the regional modeling is the Bayesian method which is based on the estimation of probability distribution of the parameters. Parameter sets are given probability based on a quality measure describing the goodness of fit between observed and simulated values. Both the multi-objective method and the Bayesian methods consider the uncertainty in the choice of parameter sets values.

The ENKI framework has prebuilt subroutines of which the HBV-model is within the framework. Enki therefore was configured for the regional model calibration in the LVB i.e. the aggregated HBV-model output for a set of gauged sub-catchments is calibrated at the same time and evaluated based on the average response. The best parameter sets of the region, obtained by the regional model calibration, were deemed fit for all the sub-catchments of the region enabling an estimation of the uncertainty also for ungauged catchments. This, in contrast to the traditional one catchment approach, where the calibrated parameters could be used only for the basin they were derived for. The regional model allows for various responses from various parts of the catchments, and emphasizes interpolation and downscaling of input data.

3.6 Enki Modelling System

3.6.1 Introduction

The ENKI framework operates on the principle of gridded data input from the catchment. Based on the geographical region and process data, a library of subroutines are built for the functionality of ENKI. A subroutine is an instance of a method, which implements the simulation equations, which for each time step are organised by user-specified order. All process data are GIS data; in raster form, as point-vector data, or as discrete variables. For each time step (each day), the framework reads a new time slice from the input database into the region, and writes a time slice from the region to the output database.

New routines were coded and compiled as dynamic-link libraries (dlls) using the Microsoft Visual Studio and dynamically added to the ENKI framework. The required input static maps such as elevation and land use were prepared in ArcGIS (http://www.esri.com) and converted to Idrisi raster files using Geospatial Data Abstraction Library (GDAL) for use as input in ENKI. The input and output databases in ENKI are based on the NetCDF. ENKI allows import of TAB-delimited text file input time series and export of output time series for instance to MS-excel for further processing of the results. The input climate forcing from gauging stations on a 1x1 km2 grids were imported using the Inverse Distance Weighted (IDW) interpolation routine in ENKI.

3.6.2 The Enki Model Structure

The input data for ENKI model are observations of precipitation, air temperature, radiation, wind speed, relative humidity and runoff. Similar to the HBV model, a distributed version of the Swedish Meteorological and Hydrological Institute (SMHI)-HBV model (Bergström, 1976) was used in the ENKI framework. The model contains two conceptual reservoirs. The upper reservoir contains two outlets while the lower reservoir has only one outlet. The response routine has five free parameters namely very quick and quick upper reservoir recession coefficients (respectively k_2 and k_1), slow base flow recession coefficient (k_0), percolation rate (*Perc*) and upper reservoir storage threshold (UZ_t). The runoff from the upper reservoir conceptually represents flow from overland and shallow depths while the runoff from lower zone represents a base flow from ground water:

$$Rf_l = Q_{UZ} + Q_{LZ} = \Big(max\big(0, k_2(UZ - UZ_t)\big) + (k_1\, min(UZ, UZ_t))\Big) + k_0 LZ,$$

where the Rf_l is the total runoff from the land grid cell, and the Q_{UZ} and Q_{LZ} respectively are outflows from the upper and lower zones in mm. The soil moisture accounting is based on a non-linear function that partitions the infiltration from rainfall and snowmelt (*I*) into recharge (*R*) to upper reservoir and change in soil moisture storage (Δ_{SM}):

$$R = I\left(\frac{\text{SM}}{\text{FC}}\right)^{\beta},$$

where β is the 'non-linearity parameter' controlling the shape of the partitioning curve, *SM* is the actual soil moisture and *FC* is the field capacity or the maximum soil moisture holding capacity of the soil. If *SM/FC* exceeds *LP*, actual evapotranspiration (*AET*) is assumed equal to the potential (*PET*) otherwise the actual evapotranspiration decreases linearly with the decrease in soil moisture storage (i.e. *AET/PET = SM/LP*). The soil moisture accounting involves three free parameters *FC*, β and *LP*.

The ENKI framework divided into two parts: the model and the region. The model part contains the equations and it navigates which one should be used. The equations or subroutines, operates in particular order. The region links the model (set of subroutine) to the region which contains all properties of the region such as catchment size, elevation, all maps, raster and all parameters which are used within equations in model

The ENKI hydrological model framework considered as flexible, due to availability of different subroutines. By changing combinations of subroutine, user is able to create a unique model. The HBV model is organised in different way with standard set of equations. The model structure for ENKI is shown in Figure 3-6.

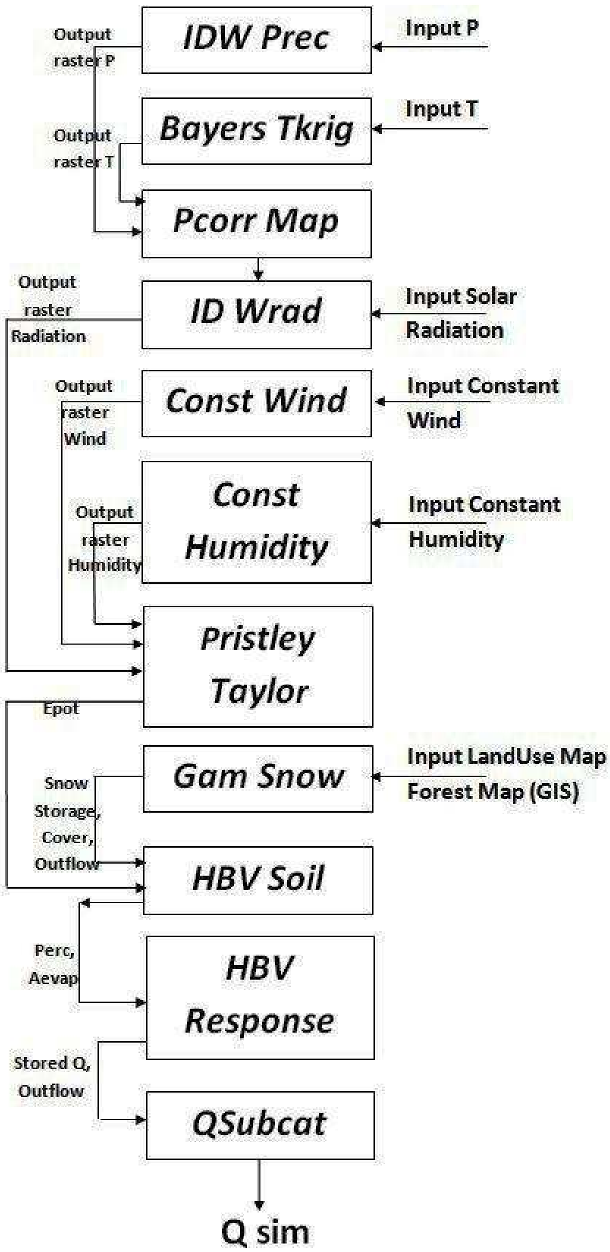

Figure 3-9: Structure of ENKI Model

3.6.3 The Precipitation and the other climate data interpolation

The subroutines named IDWPrec and Bayes Tkrig were used in calculating the precipitation and air temperature in each cell for each day. It uses Inverse – Distance Weighted method to interpolate the precipitation and Bayes kriging air temperature along the region on 1x1 km^2 grids.

Spatial variability of rainfall is a major source of uncertainties in parameter calibration based on rainfall-runoff relationships for runoff simulation (see Milly and Dunne 2002a, 2002b; Syed et al., 2003). Haile et al. (2009) based on their study on the space-time variability of rainfall in the vicinity of the Lake Tana (over mountainous and Lake adjacent areas) using hourly observations from gauges and satellite sensor reported that the variation of rainfall in the Lake Tana basin is affected by terrain elevation and distance from the center of the Lake, where heavy rainfall events are frequent at stations relatively close to the Lake. Measurement of rainfall from radar and satellite would allow spatial distributed observations to understand the spatial variability of rainfall fields. However, several studies demonstrated the limitations of such remotely sensed measurements especially for calibration of rainfall-runoff parameters and continuous runoff simulation. Tetzlaff and Uhlenbrook (2005) investigated the use of radar observations for a distributed event-based runoff simulation but noted that in most cases model efficiencies were poorer and percentage deviations of simulated runoff from the observed were higher for radar data than ground station data, and extensive radar data adjustment using ground station data is required. Also noted was a general rainfall underestimation by data from radar or satellites (Zhu et a., (2014), this could underestimate peak floods, and overestimate low–middle rainfall rate. Harris et al. (2007) noted that correction for satellite derived rainfall need to consider season and flow regime beyond a simple bias adjustment to minimize false peak flows and missing true peak flows. Satellite rainfall products may improve runoff simulation when only integrated with ground (point) rainfall measurements and there is a need for recalibration of parameters of rainfall-runoff models (e.g. Ciabatta et al., 2016).

3.6.4 Gam Snow Routine

This routine deals with the snow. In the catchment under study, there was no snow and hence was not considered in the model. However, the required input parameters for this routine are temperature, radiation, precipitation, wind speed and humidity.

3.6.5 Priestley-Taylor Evapotranspiration

The Priestley-Taylor method for calculating evapotranspiration is utilized within ENKI framework for entire model. (Priestley & Taylor 1972)

$PET = \alpha \frac{\Delta}{(\Delta+\gamma)}(Rn - G)$….Eqn (1)

Where α is the Priestley-Taylor constant (and mostly assumed mean value as 1.26), Δ is the slope of saturation vapour pressure curve at air temperature at 2m, γ is the psychometric constant (0.67 $hPaK^{-1}$), Rn is the net radiation = net shortwave radiation (SRn) + the net longwave radiation (LRn). G is the soil/ground heat flux = 0.12*Rn

The Priestley-Taylor equation, a simplification of the Penman equation, which was used to allow calculations of evapotranspiration under conditions where soil water supply limits evapotranspiration. The Priestley-Taylor method is appropriate for use when detailed meteorological measurements are not available.

3.6.6 The Soil Moisture Routine

In the soil moisture routine, precipitation here would be received as an output from the snow or the direct precipitation. As earlier stated in the Snow routine, in the study area, the snow was not taken into consideration and hence only direct precipitation. Figure 3-9 illustrates the processes in this routine and the equations involved their in. The soil moisture accounting is based on a non-linear function that partitions the infiltration from rainfall and snowmelt (I) into recharge (R) to upper reservoir and change in soil moisture storage (ΔSM):

$$R = I\left(\frac{\mathrm{SM}}{\mathrm{FC}}\right)^{\beta},$$

where β is the 'non-linearity parameter' controlling the shape of the partitioning curve, SM is the actual soil moisture and FC is the field capacity or the maximum soil moisture holding capacity of the soil. If SM/FC exceeds LP, actual evapotranspiration (AET) is assumed equal to the potential (PET) otherwise the actual evapotranspiration decreases linearly with the decrease in soil moisture storage (i.e. AET/PET = SM/LP). The soil moisture accounting involves three free parameters FC, β and LP.

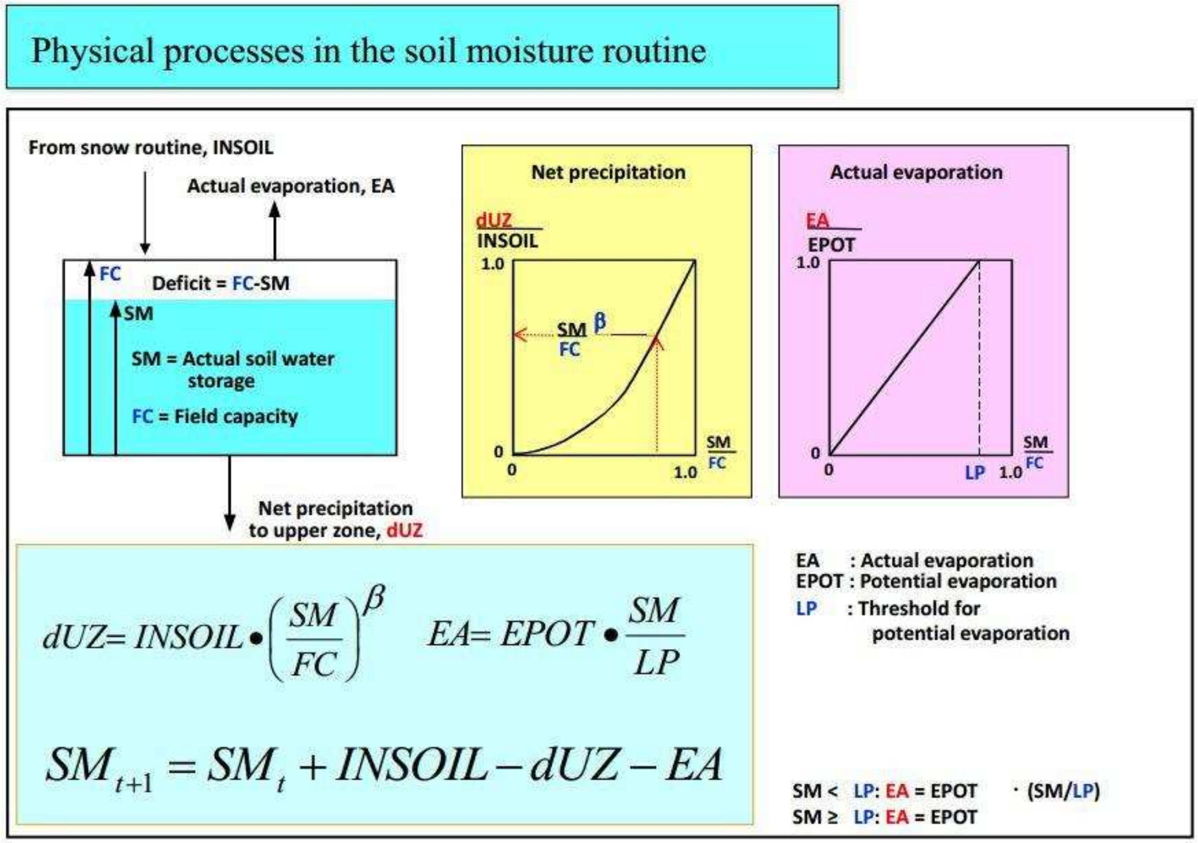

Figure 3-10: Soil Moisture Routine

3.6.7. Runoff response models

Based on the distributed version of the Swedish Meteorological and Hydrological Institute (SMHI)-HBV model (Bergström, 1976), the model contains two conceptual reservoirs. The upper reservoir contains two outlets while the lower reservoir has only one outlet. The response routine has five free parameters namely very quick and quick upper reservoir recession coefficients (respectively k_2 and k_1), slow base flow recession coefficient (k_0), percolation rate (*Perc*) and upper reservoir storage threshold (UZ_t). The runoff from the upper reservoir conceptually represents flow from overland and shallow depths while the runoff from lower zone represents a base flow from ground water:

$$Rf_l = Q_{UZ} + Q_{LZ} = \Big(max\big(0, k_2(UZ - UZ_t)\big) + \big(k_1\, min(UZ, UZ_t)\big)\Big) + k_0 LZ,$$

where the Rf_l is the total runoff from the land grid cells and the Q_{UZ} and Q_{LZ} respectively are outflows from the upper and lower zones in mm.

The routing between sub-basins can be described by the Muskingum method (Shaw, 1988). Each one of the sub-basins has individual response functions (SMHI). Schematic representation of runoff response routine shown on Figure 3-10.

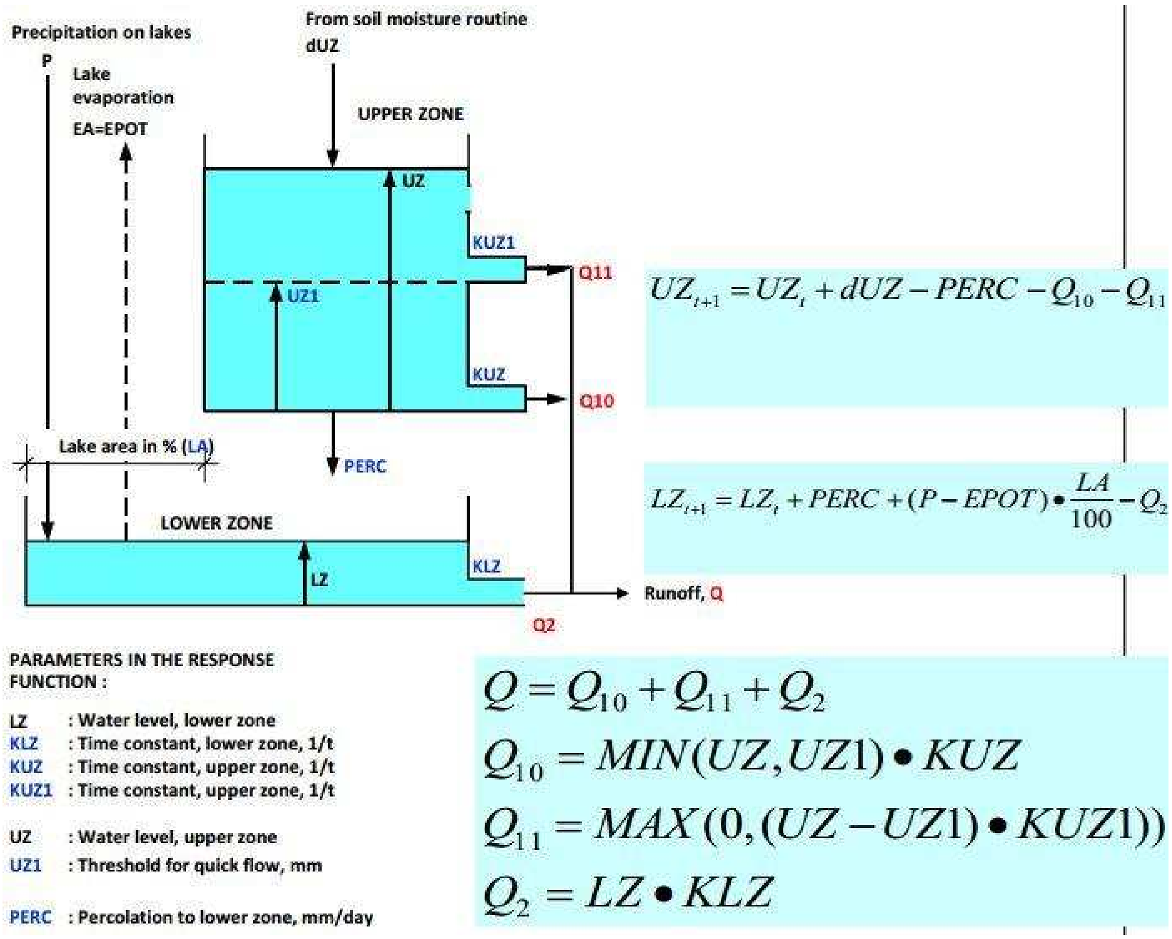

Figure 3-11: Runoff response for Upper and Lower tanks

3.6.8 Lakes in Enki Model

Consideration of the lakes in the ENKI structure is similar to the HBV setup with the precipitation un interrupted by the vegetation. In this study, since there is no data available for the lake bathymetry, the lake banks are considered as vertical and hence the storage is dependent of a constant surface area and the lake water levels. The actual evaporation form the lake was considered the same as the potential.

The water balance equation for simulation of the Lake storage volume is given as:

$SV_t = SV_{t-1} + RV_{lk,t} + RfV_{l,t} - EV_{lk,t} - OV_{lk,t},$

where SV denotes storage volume of the Lake in Million cubic meter (Mm3), RVlk is the volume of Lake areal rainfall (Mm3), RfVl is the runoff volume entering the Lake from land grids or rivers inflow to the Lake (Mm3) that is computed from the runoff response models (runoff from the land –which was an aggregated inflow from LVEMP, 2005), EVl is Lake evaporation volume (Mm3) computed from the PET (Preistley-Taylor equation) and OVl is the observed Lake outflow volume to the Nile River (Mm3). The observed Lake storage volume a day prior to the start of the simulation was used as an initial Lake storage volume. No calibration parameter in the water balance model to account for errors, for instance, as performed in Troin et al. (2010) was introduced.

3.7 Parameter Calibration and Validation

The calibration of the model was carried out in two ways. One was automatic and the other was manual calibrations in search of best fit. The Monte Carlo Markov Chain (MCMC) Random GLUE parameter auto calibration algorithm was used in this study. This is a global optimization method that is considered as an efficient optimization technique for calibrating watershed models. The Nash–Sutcliffe efficiency index (R^2) is used to assess the performance of a hydrologic model.

The validation of the model was aiming testing the models robustness and ability to describe the catchments hydrological response and further detect any biases in the calibrated parameters (Gupta et al. 2005). The calibrated values were used in comparison with the observed values. Further evaluation of the performance was done in terms of the accumulative difference, since the intention was to receive as much water as possible for the study.

$$NSE\ (R2) = 1 - \left(\frac{\sum\ (Qsim\ - \mathrm{Qobs})^2}{\sum\ \left(\mathrm{Qobs} - Qobs_{average}\right)^2} \right)$$

Where Qsim- Simulated runoff; Qobs, observed runoff or inflow.

The parameters in the model structure are classified into three cateogorie; namely the free, confined and the seni-confined parameters.

The confined are inherent catchment characteristics such as the catchment Area, Hypsographical distribution, Lake Area percentage and so on which are constants for a particular defined catchment. These parameters need are provided as input to the model.

Semi-Confined parameters are regional hydro-meteorological variables of the catchment under considerations. These include parameters such as the precipitation gradient (PGRAD), temperature gradient (TPGRAD and TCGRAD), Snow distribution parameters, Potential Evapotranspiration. These parameters are usually obtained from literature review of previous investigations within the catchment or may need to be obtained through field measurements.

Free parameters are those majorly used in the calibration process. They are proided as definitive inputs to the model but as well calibrated for the efficiency of the model. They include, Process Parameters and coefficients such as Field Capacity in the soil moisture routine, Degree-Day factor in the snow routine and the various coefficients within the Flow-Response routine belong to this category.

Hydrological model calibration is a trial and error procedure, where free parameters are chosen, model simulation performed and the computed and observed runoff compared. The most difficult part of the procedure is the evaluation of the difference between observed and simulated runoff, and to decide which parameters should be changed and for how much. To decide if another set of parameters really give better fit for the model, a method or criterion to determine the goodness of fit is also needed. Two main types of methods can be used: subjective and objective methods.
The subjective methods are usually based on study of plots of input data and observe and computed hydrographs. Flow duration curves and cumulative deviation curves may be used.

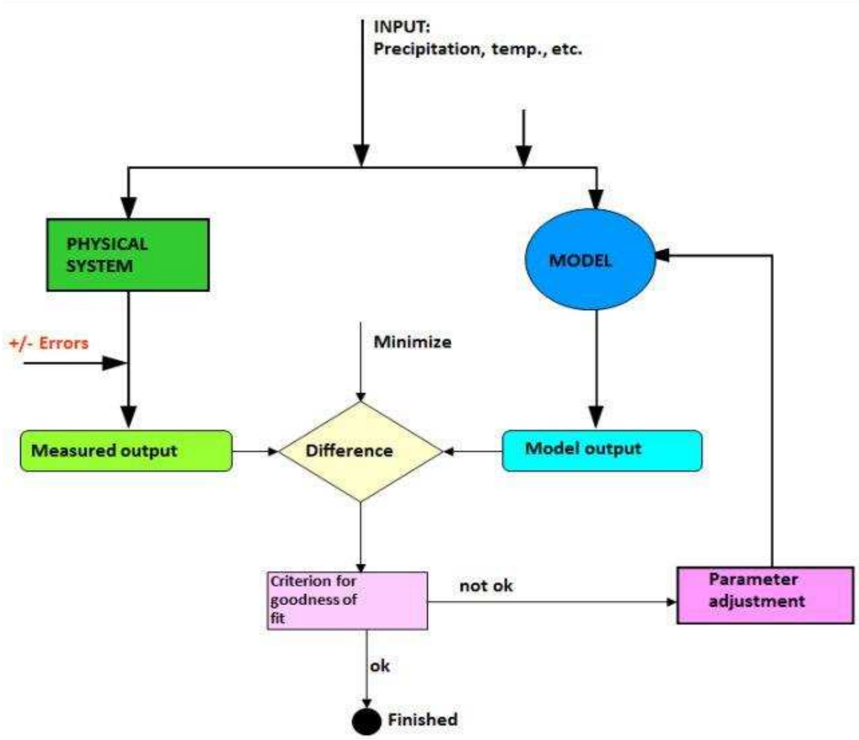

Figure 3-12: Automatic Calibration process

3.7 Climate Change Impact Studies

The term “Climate change” principally refers to any change in climate over time, whether due to natural causes or as a result of human activities (IPCC, 2001a). However, it is widely accepted that the term ‘climate change’ is equivalent to ‘global warming’. However, global warming is essentially a special type of climate change (Arnell, 1996).

Potential impacts of climate change on water resources are usually assessed by applying climate projections (temperature and precipitation) derived from global circulation models (GCM) using a hydrologic model. In this study, we investigate the impact of global climate change on the floods generated from the runoff of the Lake Victoria Basin in East African region. Climate change issues have been a concern for water planners throughout the world (Sene et al., 2001). Climate change causes changes in rainfall, runoff and evaporation, which in turn affect the water availability and variability worldwide.

Signs of the impacts of climate change observed around the world include the increase in surface temperature, sea-level rise, changes in precipitation and decreased in snow cover (IPCC, 2001). The chain effect of these impacts would likely bring in issues such as human health, shortage of water supply, biodiversity and ecosystem.

The stages for assessment cab be summarized as shown in the figure 3.13 below

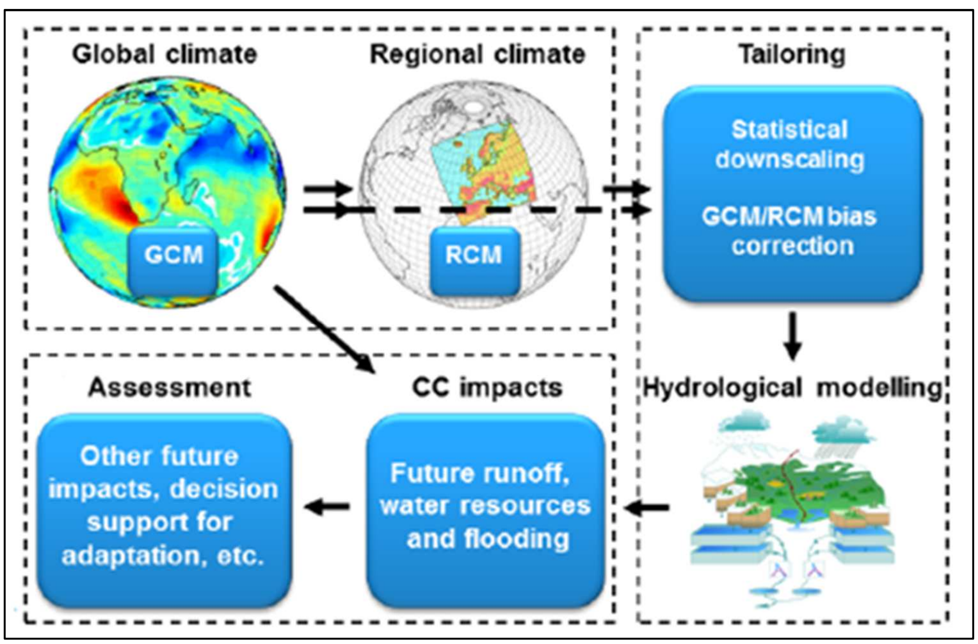

Figure 3-13: Climate change impact studies

Based on the above figure 3-13, the classification of the study stages are considered as two; namely Climate Modelling and Downscaling and Hydrological Modelling

In order to carry out a climate change impact assessment, simulations of the future hydrological scenarios using a hydrological model based on acquired climate data from the GCM and RCM models were downscaled. Downscaling is the derivation of local to regional-scale (10-100 kilometers) information from larger scale modeled or observed data. There are two main approaches: dynamical downscaling and statistical downscaling.

3.8 Climate Modelling and Downscaling

Climate data with a daily time series was used. This included the simulated historical and future climate data (precipitation and temperature). Two emission scenarios were used for the future simulations. These were the Representative Concentration Pathways (RCP), RCP45 and RCP 85 for the two Global Circulation Models (GCMs). The period of simulation for the future was 2041-2065 and 2073-2097(end of 21st century). Usually the period would be some how overlapping eg 2040-2070 and 2071-2100, but due to the relation of simulated GCM historical data with the observed data, the time periods were adjusted. The GCM simulated historical data had a period from 1976-2005 while the available observed data was from 1980-2010.

Global Circulation models (GCMs) are advanced numerical tools describing global climatic scenarios employing vast amount of real-time input data from dedicated satellites orbiting the globe. They also describe atmospheric, oceanic and biotic processes, interactions and feedbacks. ‘A GCM is composed of many grid cells that represent horizontal and vertical areas on the Earth’s surface. In each of the cells, GCMs compute the following: Water Vapor and cloud atmospheric interactions, direct and indirect effects of aerosols on radiation and precipitation, changes in snow cover and sea ice, the storage of heat and moisture, and large-scale transport of heat and water by the atmosphere and oceans.

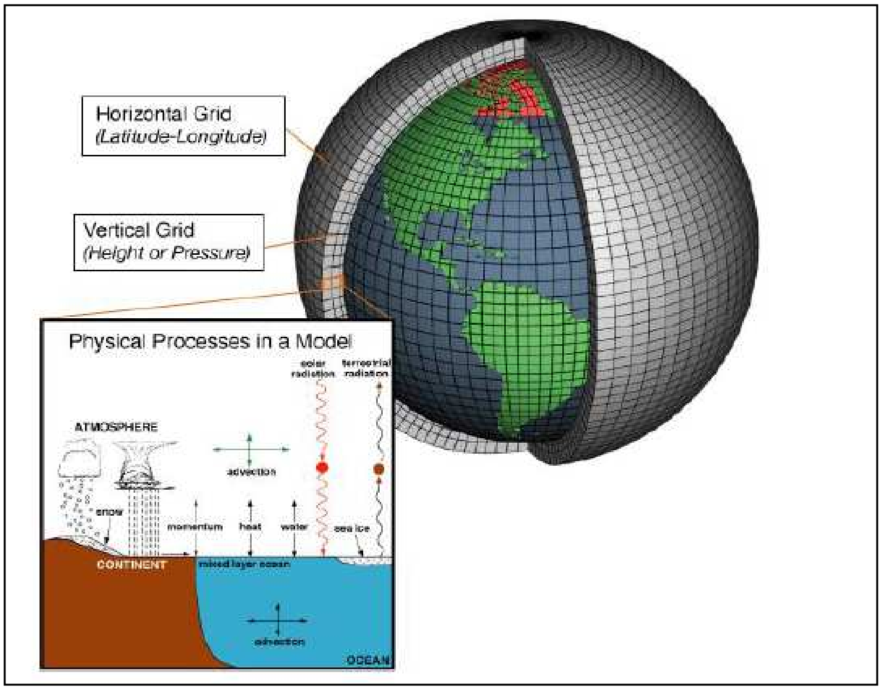

Figure 3-14: Conceptual Structure of GCM NOAA,2012)

One of the challenges of the GCM data is the spatial resolution. Most GCMs have the resolution the order of 100-500km due to the computations limitations. However the hydrological models are calibrated for catchments of quite small sizes. Downscaling is used to aid in modifying the accuracy of the climate data on a finer spatial esolution.

3.9 Climate Data and Downscaling Techniques

To derive fine-scale climate information, an assumption based on local climate is conditioned through the interactive climate states of large scale atmospheric features and the features. The principle of downscaling as illustrated by the figure below shows the downscaling process working principle. Dynamic Downscaling techniques attempt at obtaining climate data at sub-grid scales of the driving GCM models which can add accuracy to the climate data obtained by the GCM at a much finer resolution.

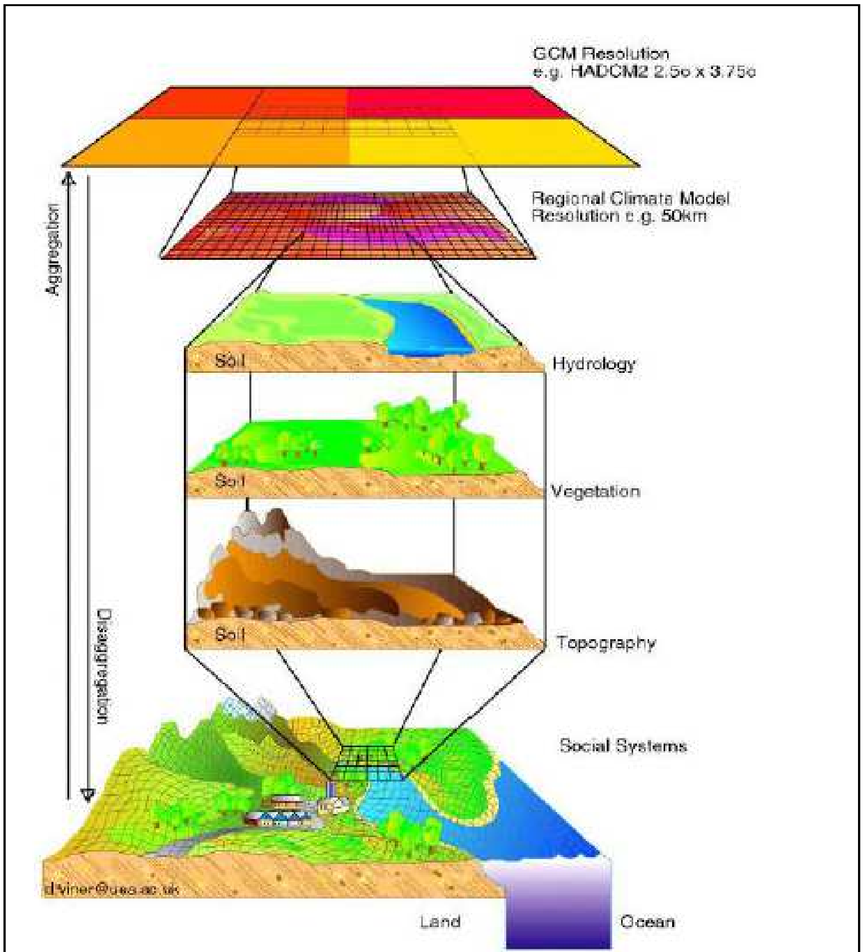

Figure 3-15: Spatial Downscaling concept (Viner, 2012)

Downscaling techniques are directed at obtaining better representation of the spatial and temporal aspects as the driving GCMs are usually designed to function at much coarser scales.

Dynamical downscaling deals with incorporation of a Regional climate model (RCM) on a sub grid level of the parent GCM. That is, RCMs can derive climate data to a finer resolution compared to the driving GCM. RCMs take the large scale atmospheric information supplied by the GCM output at the lateral boundaries and incorporate more complex topography, the land-sea contrast, surface heterogeneities, and detailed descriptions of physical processes in order to generate realistic climate information at a spatial resolution of approximately 20-50 kilometer Some of the RCMs developed by scientists are PRUDENCE (Europe), ENSEMBLES (Europe), CLARIS (South America), NARCCAP (North America), CORDEX (Africa) are some of the well-established RCMs.

Some of the prominent shortcomings of dynamical downscaling are:

1. Although RCMs can derive climate data to a finer resolution, they are still bound to inherit some systematic biases which needs further processing and corrections and also, the output quality of an RCM is directly linked to the output quality of the driving GCM.
2. Dynamical downscaling can be data intensive and demanding in terms of requirement of computational power.

Statistical downscaling aims at deriving an empirical relationship between the GCM output data with the observed climate data at the desired location/station. Hence, statistical downscaling can yield site specific datasets. This method is computationally much more efficient and less data intensive when compared to dynamical downscaling. This method also eliminates the need for a RCM which simplifies the entire process. However, this approach relies on the critical assumption that the relationship between present large-scale circulation and local climate remains valid under different forcing conditions of possible future climates, **(Zorita and Von Storch, 1999).**

The most important feature of statistical downscaling is that it is computationally convenient and is ideal for usage of institutions without access to sophisticated RCM capabilities. Statistical downscaling is broadly divided into three categories:

1. Linear Methods
2. Weather Classifications
3. Weather Generators

Linear methods are intended to arrive at linear relationships with the GCM output data and the observed climate data at the station which can be helpful in elimination of systematic biases. Weather classification deals with establishment of an atmospheric ‘State’ based on large scale weather patterns. The state predictions of GCMs are correlated with historical observed state to discern numerical relationships. Weather Generators are used to derive temporally finer resolution data (eg., Daily data from monthly series) from coarse GCM data employing statistical analysis.

Dynamical-Statistical downscaling is a hybrid approach incorporating the essence of both the dynamical and statistical downscaling methodologies. The GCM output data series is first processed to a spatially finer resolution employing a validated RCM. Further, the RCM output data is processed employing statistical tools to further eliminate systematic biases. This method is often known to give satisfactory results with reduced computational requirements.

Currently, there are no standardized international guidelines or national government specifications which provide researchers with assistance to choose the right models to obtain data sets and to choose ideal downscaling techniques.

3.10 Uncertainties Involved in Climate Modeling and Downscaling

There are four main sources of uncertainty in climate projection:

1. Difficulty in representing inter-annual and decadal variability in long-term projections
2. Uncertainty linked to imperfect model representation of climate processes
3. Uncertainty in future levels of anthropogenic emissions and natural forcings (eg., Volcanic eruptions)
4. Imperfect knowledge of current climate conditions that serve as a starting point for projections

Complex numerical models such as the Global Circulation models are inevitably based on some assumptions and simplifications at various stages of conceptualization and computation. These assumptions add inherent biases and uncertainties to the model output

One of the most important aspects of climate modeling which imparts uncertainty to model output is the representation of current and future state of carbon emissions on a global scale. Qualitative and Quantitative representation of current climatic conditions and prediction of possible future scenarios are highly dependent upon multitudes of socio-technical scenarios such as national economy, development of green technology and governing policies. Hence, it is always advised to consider multiple possible scenarios as this can give a sense of variability in model output which can greatly facilitate researchers and policy makers in the process of decision making. Almost all of the GCMs and RCMs are designed to foresee multiple emission scenarios and an ensemble analysis would be highly informative.

4 Data Acquisition and Control

4.1 Introduction

One of the challenging aspects in this study was retrieving data, especially observed data (meteorological and hydrological) since the catchment lies in five different countries. However, the data collected for the study was observed data, reanalysis data (from ERA-Interim) and the simulated historical and future GCM data. The data will be checked for quality and for further processes depending on the availability.

4.2 Data Acquisition

4.2.1 Observed Data

The sources of the observed data were from Uganda National Meteorological Authority, the Directorate of Water Resource Management-Uganda, the National Climate Data Centre (-https://www.ncdc.noaa.gov/) and Lake Victoria Environment Project. The data obtained from these sources included lake water levels, the outflows, inflows into the lake. Also included from the reanalysis data was the climate data. These were available in daily time series.
The observed (gauged) precipitation data on the land surface, available from 1970 to 2017 (not all stations had similar period observations) was retrieved from NCDC and had 13 gauged stations as indicated in the *figure 4-1 below*. However, most of the stations had data averaging to a period ending 1989 and three stations, Kasese, Tororo and Bujumbura out but close to the catchment. Further to this, three stations in the catchment (Eldoret, Kitale and Kigali) had data not exceeding a 50% availability. The stations in Uganda besides the NCDC data were supplemented with the information available from UNMA since the data was similar, hence missing gaps easily filled for these stations.

The information from other four stations in Tanzania and Burundi were available from the NCDC and was available upto 1989. The most of these stations had above 75% precipitation data and the gaps were filled by correlating with the neighboring stations.

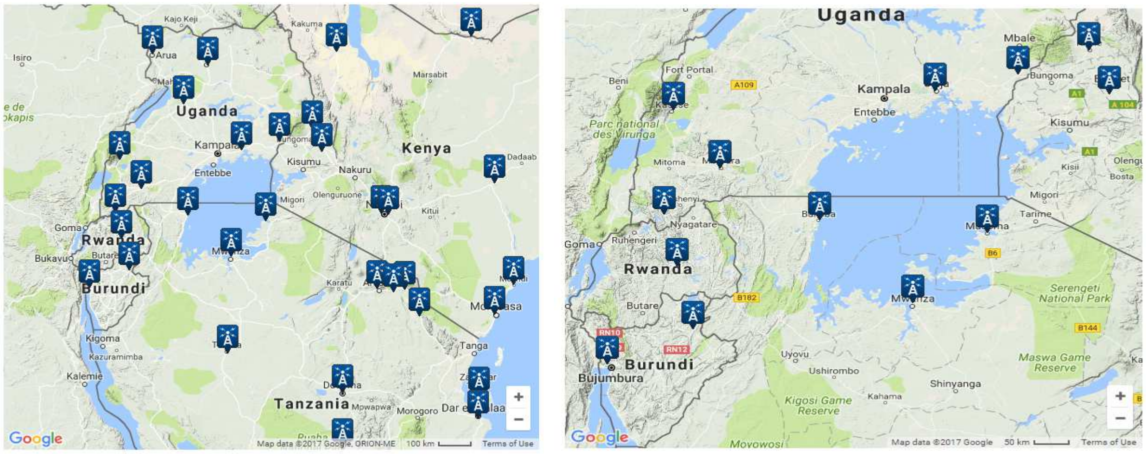

Figure 4-1: GHCN-D Precipitation stations in East Africa

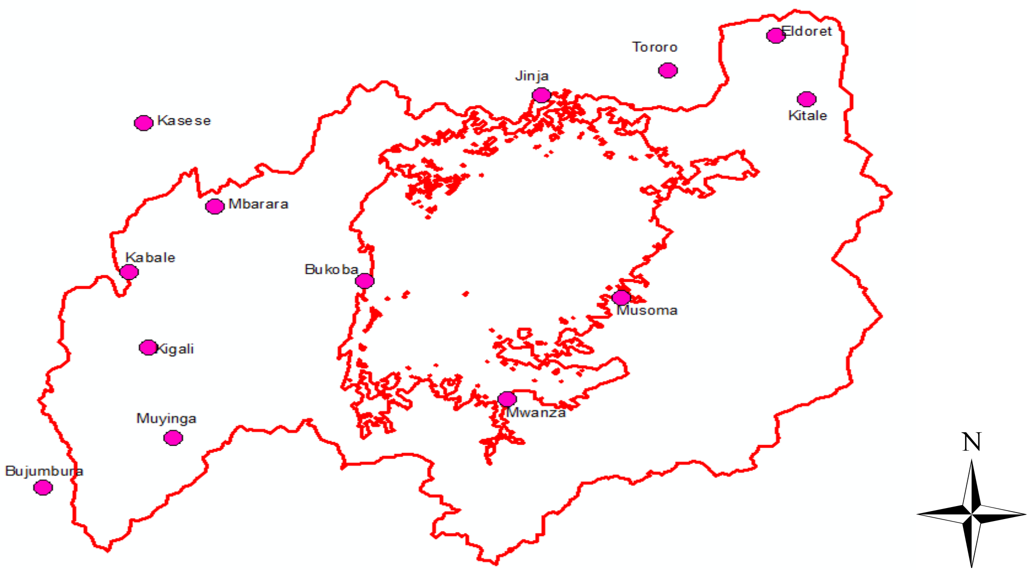

Figure 4-2: Precipitation stations in the LVB

The observed historical discharges from the lake outlet near Jinja and the water levels from Jinja and Entebbe stations were obtained from the DWRM-Entebbe, Uganda. Whereas these values (runoff and water levels) were available since 1900’s to 2017, in order to be consistent with other data series, the data for the period 1980-2010 was considered for further processing.

Due to the difficulties in obtaining the data attributed to the runoff from sub catchments from the basin, an aggregated land runoff series data from a study conducted by LVEMP, (LVEMP, 2005) was used as inflow series for this study. The data series was for a period 1950-2005, hence useful data taken was from 1980-2005.

4.2.2 Reanalysis Data

In many developing and arid regions of the world, the assessment and management of water resources is still a major challenge due to data scarcity [Buytaert et al 2012]. According to Gorgoglione et al, 2016, the difficulty in collecting data in semi-arid and other remote regions can be attributed to several reasons:

(i) lack of reliable equipment;

(ii) absence of good archiving system and software to store and process the data,

(iii) lack of funds to organize data collection campaigns.

Another challenge in these regions is that even when data is collected and archived, the effort and money required to access them can be quite substantial [Liu et al, 2008]. Hydrological models are designed to fill some of these gaps, and their application to enhance water resources management is widely acknowledged [Worqlul et al, 2014].

Rainfall is one of the most important inputs used to drive hydrological models; hence it is important to obtain rainfall data of sufficient temporal and spatial resolution. Nevertheless, due to the high spatiotemporal variability of rainfall, it can only be accurately captured by a dense network of rain gauge stations, which could be located outside the area of interest or even exhibit significant gaps in spatial coverage, especially in remote and ungauged areas.

Therefore, to try to solve this challenges, a multiyear global **gridded representation of weather** called **reanalysis** are available.

The reanalysis daily time series climate data, (temperature, precipitation, radiation, wind speed and relative humidity) corresponding to the observed hydrological data, was retrieved from the CORDEX -Africa region ERA Interim data base managed by the ECMWF and covered a period from 1980 -2010. The data was retrieved on a spatial resolution of 0.25^o x 0.25^o (equivalent to 50km x 50km) which could be managed by the hydrological model and within the time available for the study. In order to retrieve this dataset, a script from R-programming was used to convert files from ncdf to text files for further processing. This resolution generated 104 grids in the whole catchment including the area covered by the lake (land 79 and lake 25 grids).

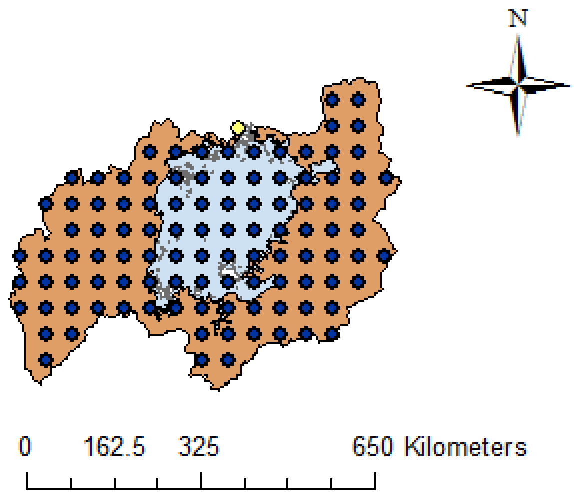

Figure 4-3: 50x50km Grid cells in the Lake Victoria Catchment

Developing Agency	ECMWF-ERAINT
Model Domain	AFR-44
Internal Initial model condition	r1i1p1

4.2.3 GCM Data

The Global Circulation Model data was required for the downscaling and projecting the future climate scenarios. The data included temperature and precipitation for both historical and future simulations. The historical and future simulated GCM data was used for the determination of the delta changes of the monthly precipitation and temperatures. The simulated GCM dataset for the future was used for simulation of the future inflows to the lake from the catchment based on two Greenhouse gas emission scenarios. The Period for the GCM simulated historical data was from 1980-2005 while for the future simulated was 2041-2097. The data from the GCM was obtained similar to the reanalysis with the same grids in the catchment.

Model Name	GFDL-ESM2M	HadGEM2-ES
Developing Agency	NOAA	MOHC
Model Domain	AFR-44	AFR-44
Greenhouse gas emission scenario	Rcp45 and 85-SMHI-RCA4	Rcp45 and 85-CLMcom-CCLM4
Internal Initial model condition	r1i1p1	r1i1p1

Table 4-1: Details of the GCM Models used

4.3 Data Quality Control

Bearing in mind that all hydrological models are simply calculators converting meteorological input into hydrological output, care has to be given to the quality of data used, hence one has to be sceptical to any data.

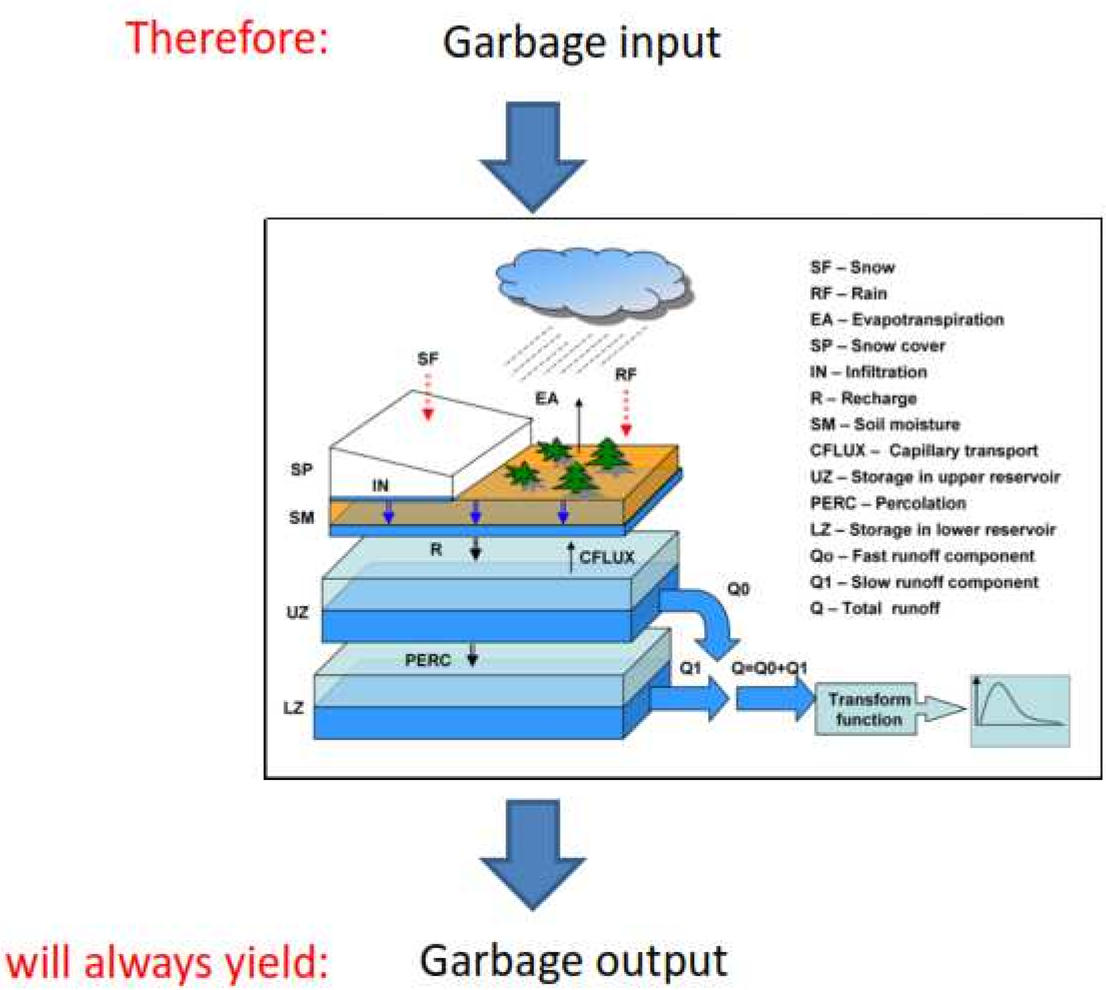

The reasons for the data quality control was to

- ✓ To minimise errors occurring by sound design and administration of the data collection system and processing line
- ✓ To detect and rectify error sources at sensor and in the processing line
- ✓ To detect and correct or reject erroneous data

The control system should be an integral part of the data collection and processing system, both technically and administratively. Data errors can be jumps, single errors, long term errors, variations.

The jumps and single errors types are easiest to detect, and should normally not pass the primary control. Trends are far more difficult to detect. Killingtveit and Sælthun, 1995, identified three stages in a quality control system; - a primary stage, run as the data is received – a secondary stage, run yearly, checking consistency – and a tertiary stage, checking homogeneity and trends

4.3.1 Observed Precipitation data

The GHCND/ground Stations				Elevation	Lat	Lon	X	Y
	Station	**Stn ID**	**Country**	masl	Deg	Deg	metres	metres
1	Jinja	GHCND:UG000063682	Uganda	1173	0.45	33.183	520362.73	49738.79
2	Kabale	GHCND:UG000063726	Uganda	1869	-1.25	29.983	164206.68	-138355.78
3	Kasese	GHCND:UG000063674	Uganda	961	0.183	30.1	177165.44	20253.11
4	Mbarara	GHCND:UG000063702	Uganda	1413	-0.617	30.65	238445.08	-68254.85
5	Tororo	GHCND:UG000063684	Uganda	1171	0.683	34.167	629857.75	75507.82
6	Eldoret	GHCND: KE00063686	Kenya	2115.6	0.404	35.239	749202.34	44688.49
7	Kitale	GHCND:KE000063661	Kenya	1875	1.016	35	722560.65	112367.54
8	Bukoba	GHCND:TZ000063729	Tanzania	1143	-1.333	31.817	368387.7	-147368.43
9	Musoma	GHCND:TZ000063733	Tanzania	1147	-1.5	33.8	588992.58	-165811.71
10	Mwanza	GHCND:TZ000063756	Tanzania	1140	-2.467	32.917	490772.68	-272679.6
11	Kigali	GHCND:UG000063682	Uganda	1481	-1.969	30.139	181696.16	-217907.75
12	Bujumbura	GHCND:BY000064390	Burundi	787	-3.317	29.317	90574.26	-367394.46
13	Muyinda	GHCND:BY000064397	Burundi	1755	-2.833	30.333	203482.66	-313475.46

Table 4-2: **Observed/GHCND Precipitation data stations**

Observed Precipitation from the catchment was obtained from the GHCN (Global Historical Climatology Network)-Daily, managed by NCDC. Table below shows the details of the land surface gauged stations which are sparsely distributed in the catchment. From the figure showing the sparse distribution of the land stations, the concentration of the stations with fair data was found to be to the western part as compared to the eastern part. Moreover, the eastern stations of Eldoret and Kitale did not have adequate data in the study period of 1980-1989 compared to other stations.

The accumulative plots for both the overall precipitation from all these stations and by individual stations, is further shown in the figures below

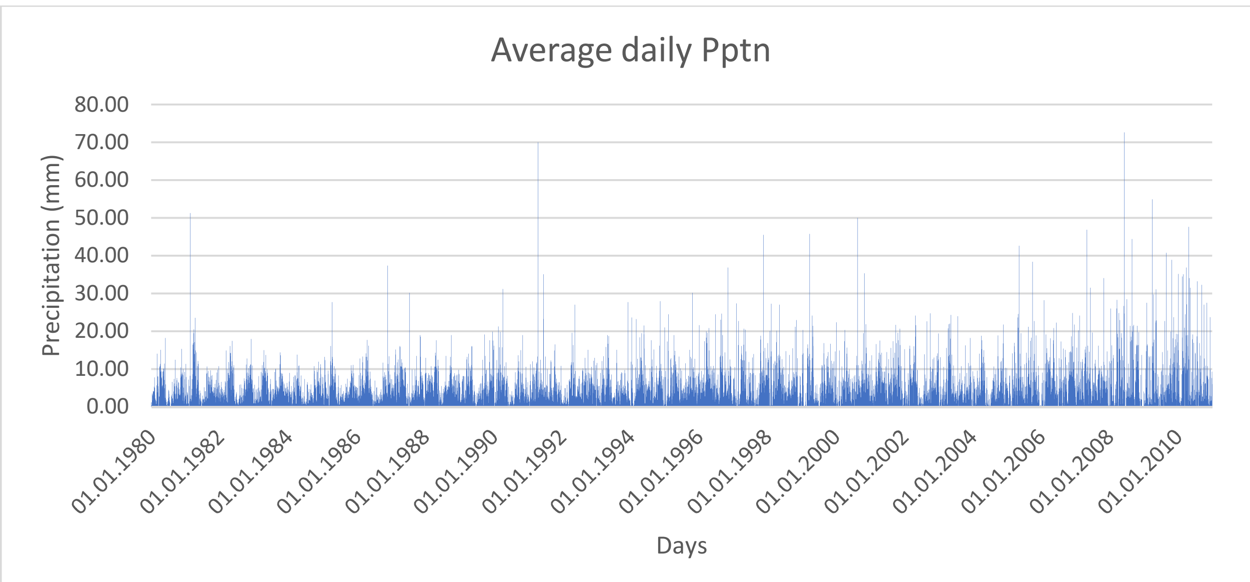

Figure 4-4: Observed average daily precipitation plot

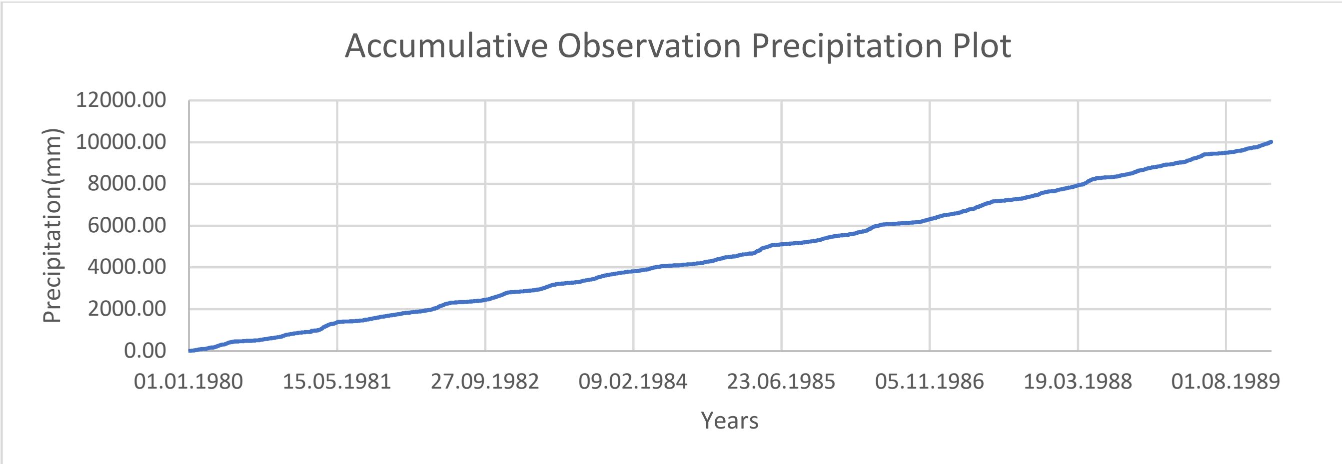

Figure 4-5: Accumulation plot for all stations in the catchment

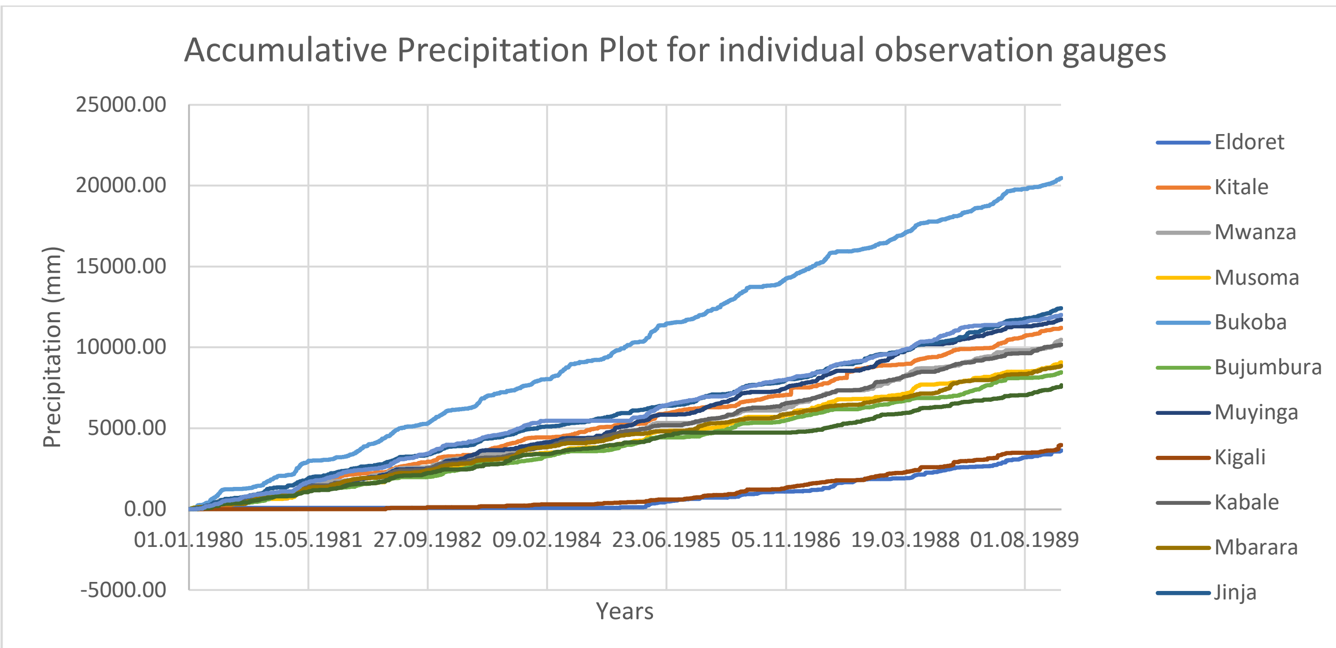

Figure 4-6: Accumulation precipitation plots for individual stations

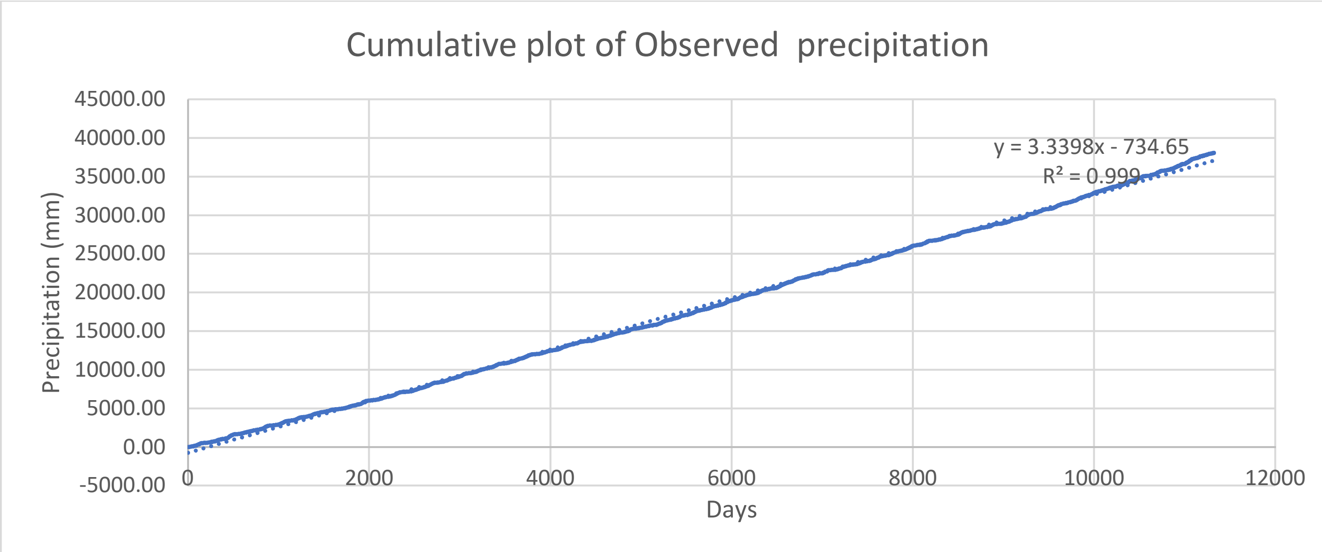

Figure 4-7: Cumulative plot after some of the gaps of fair stations were filled

From the graph above, Bukoba station shows the highest amount of precipitation by accumulation while the lowest are Kigali and Eldoret.

Comparing the two accumulation plots, it shows that the overall accumulation plot has low precipitation accumulation compared to the individual accumulation like Bukoba station. This is due to the effect caused by stations with lots of missing data dragging down the precipitation from others.

However, the model setup for ENKI enables interpolation for the missing data for stations without data. But this as well led to underestimation of the rain since the stations are sparsely distributed.

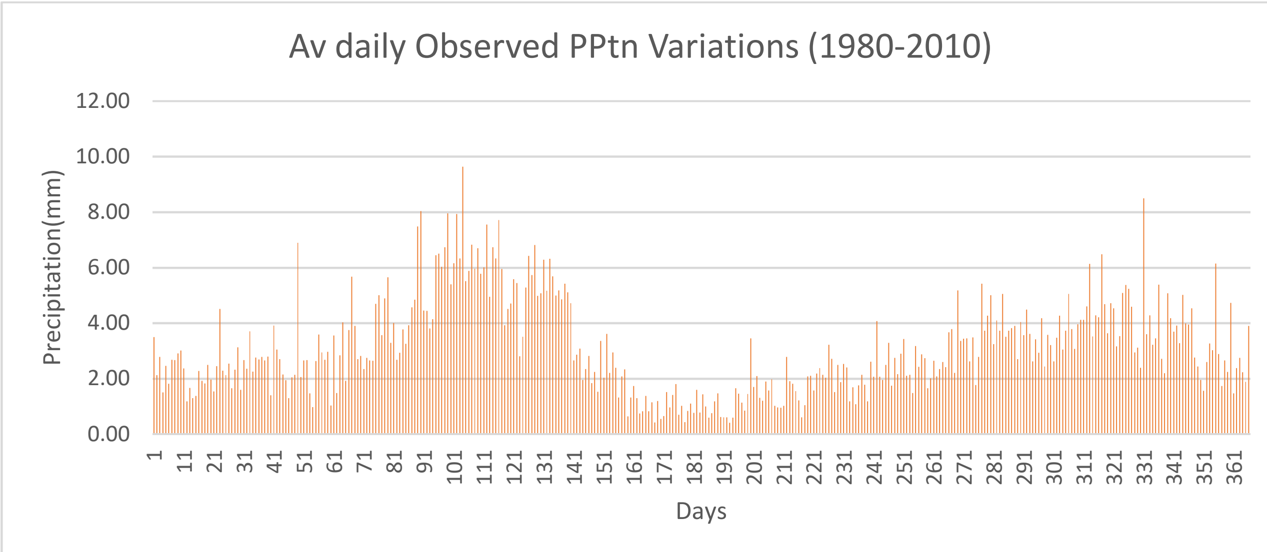

Figure 4-8: Average daily observed Precipitation

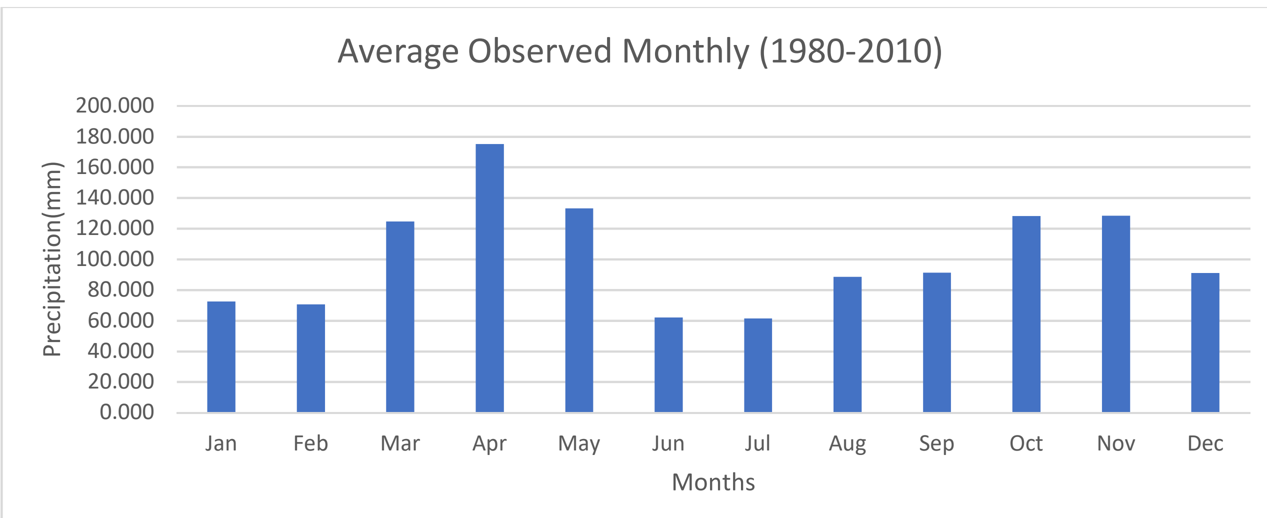

Figure 4-9: Mean monthly observed precipitation

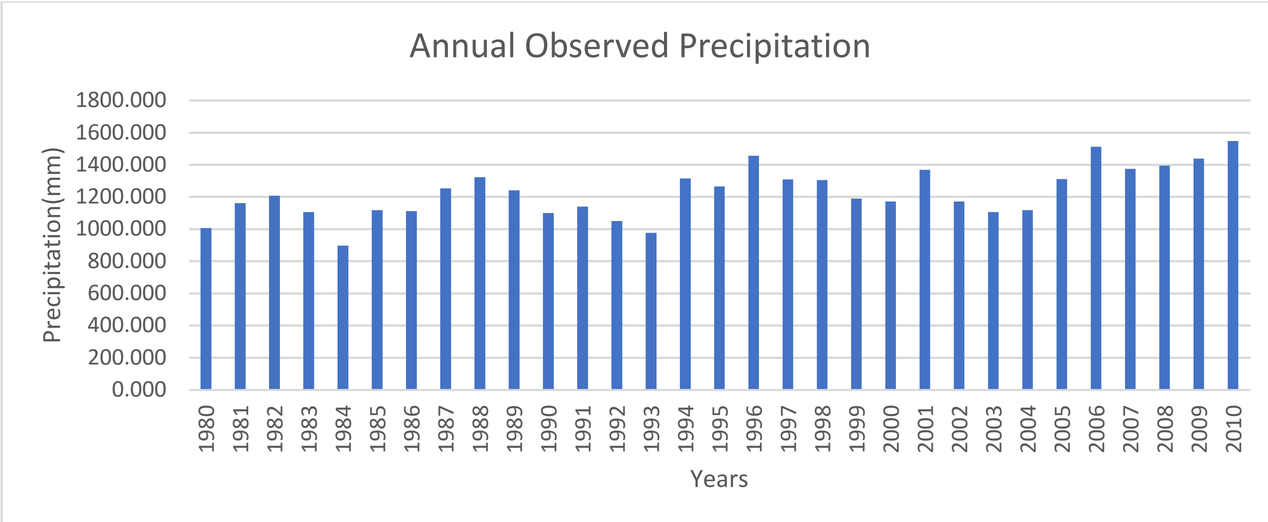

Figure 4-10: Mean annual precipitation for observed data

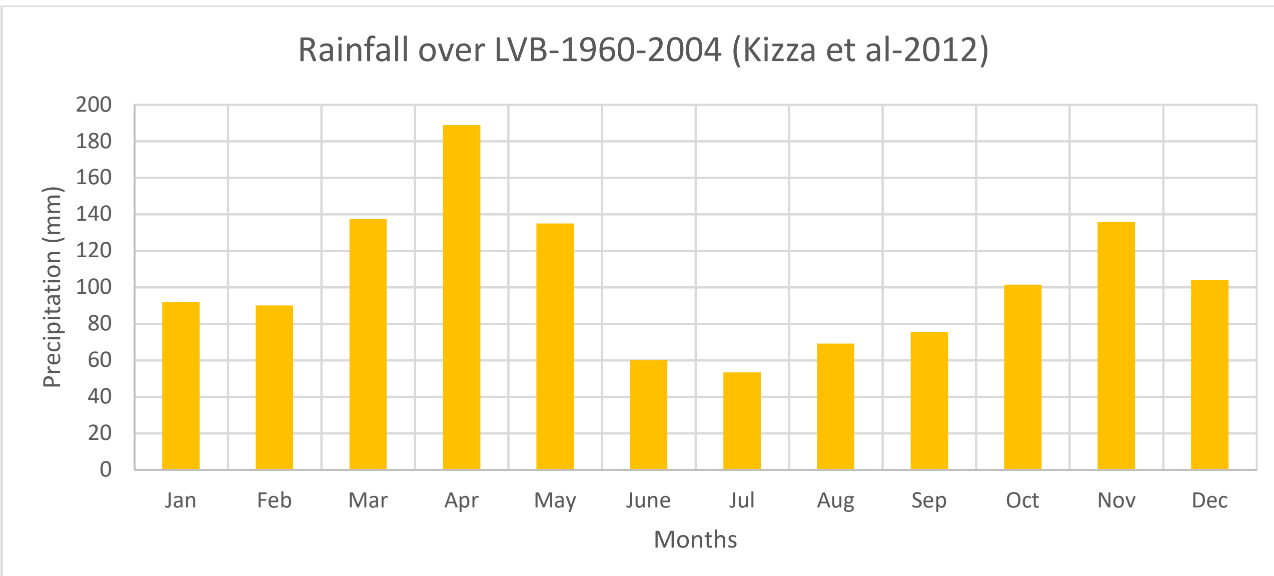

Figure 4-11: Monthly modeled precipitation year the catchment (Kizza et al., 2012)

From the observed precipitation variations, it was noted that;

- ✓ Higher precipitations occur in the months of March, April and May (MAM) and in October, November and December (OND) with the maximum monthly precipitation of about 175mm in the month of April. This is comparable with previous scholars whose maximum is 188mm occurring in the month of April.
- ✓ The lowest period of precipitation was noted in the months of June and July with lowest precipitation being 60mm which is comparable 55mm like previous study.

- ✓ Based on the annual precipitation, it was noted an average annual precipitation of 1227mm over the study period with the maximum being 1547mm for 1980-2010 period and 1322mm for the period 1980-1989. The overall lowest was 896mm recorded in 1984. Kizza et al., 2012 had an annual precipitation almost similar to the study observed precipitation.
- ✓ From the annual precipitation plot, it shows some kind of pattern of rainfall drops in every ten (10) ie 1984, 1993, 2003.
- ✓ In the period 1980 to 2010, a gradual average increase of about 35% can seen on the annul plot.

Previous studies on precipitation on Lake Victoria catchment.

In order to evaluate the observed data, it was prudent to compare the results obtained with the previous studies on the LVB.

The table below details the monthly estimated precipitation by Kizza et al, 2012 the different sub catchments on LVB

4.3.3 Precipitation from reanalysis data

The global gridded precipitation (reanalysis) data was prepared in two ways. Firstly, the data was considered the original retrieved format and in the second part, a ***linear bias correction*** to the data was made. Due to the fact that satellite and reanalysis data have biases and random errors which are caused by various factors such as sampling frequencies, non uniform field- of- view of the sensors, and uncertainties in the rainfall retrieval algorithms, many algorithms have been developed for bias correction (eg Yang et al. 1999; Li et al. 2010; Piani et al. 2010)

Original reanalysis precipitation (unbiased)

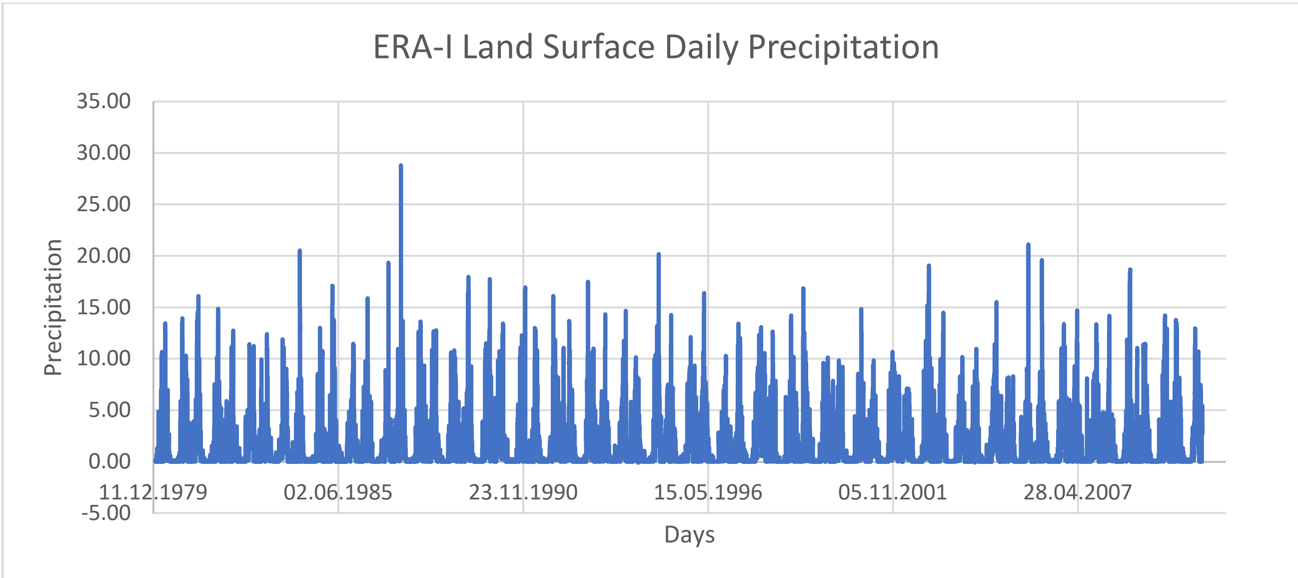

Figure 4-12: Av daily land precipitation for uncorrected ERAI

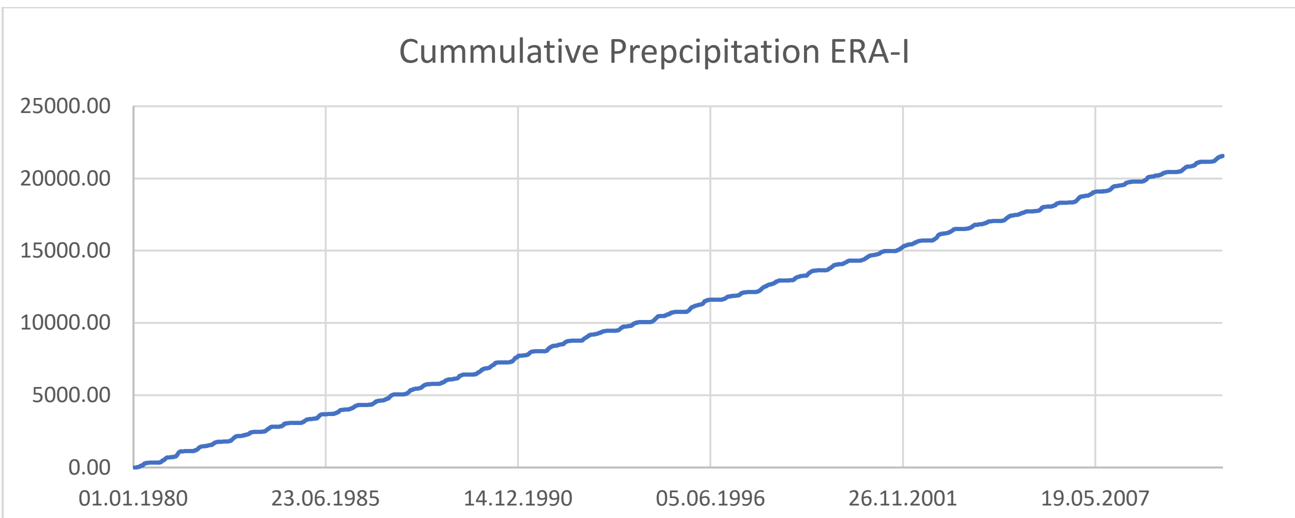

Figure 4-13: Cumulative plot for the uncorrected ERAI precipitation

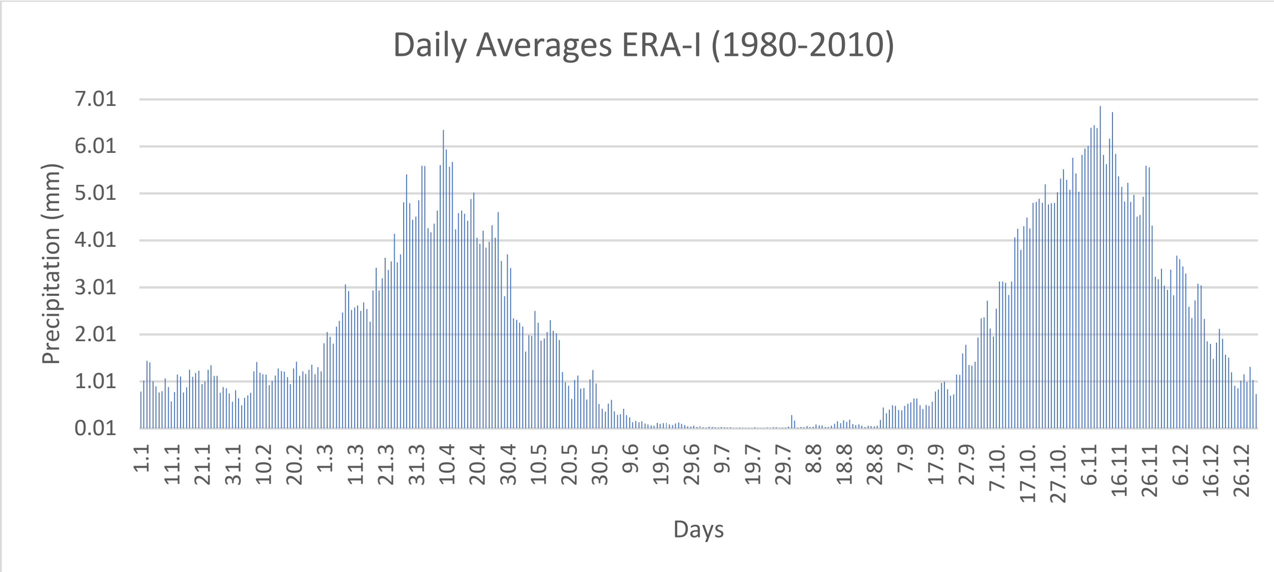

Figure 4-14: Average daily ERAI precipitation over the period 1980-2010

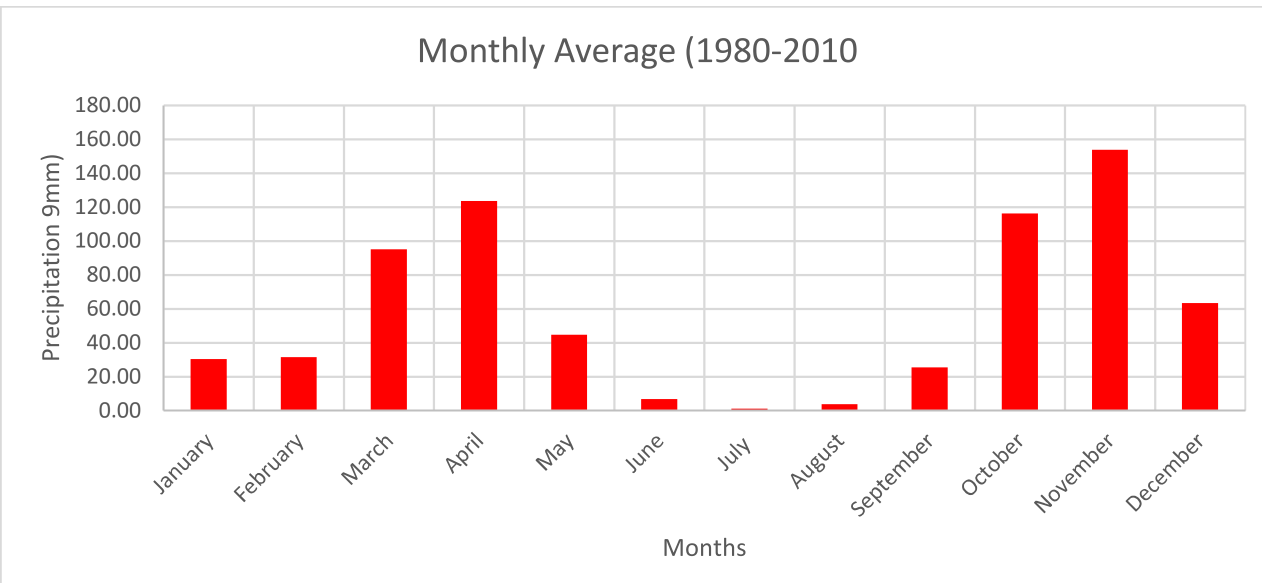

Figure 4-15: Mean Monthly ERAI precipitation

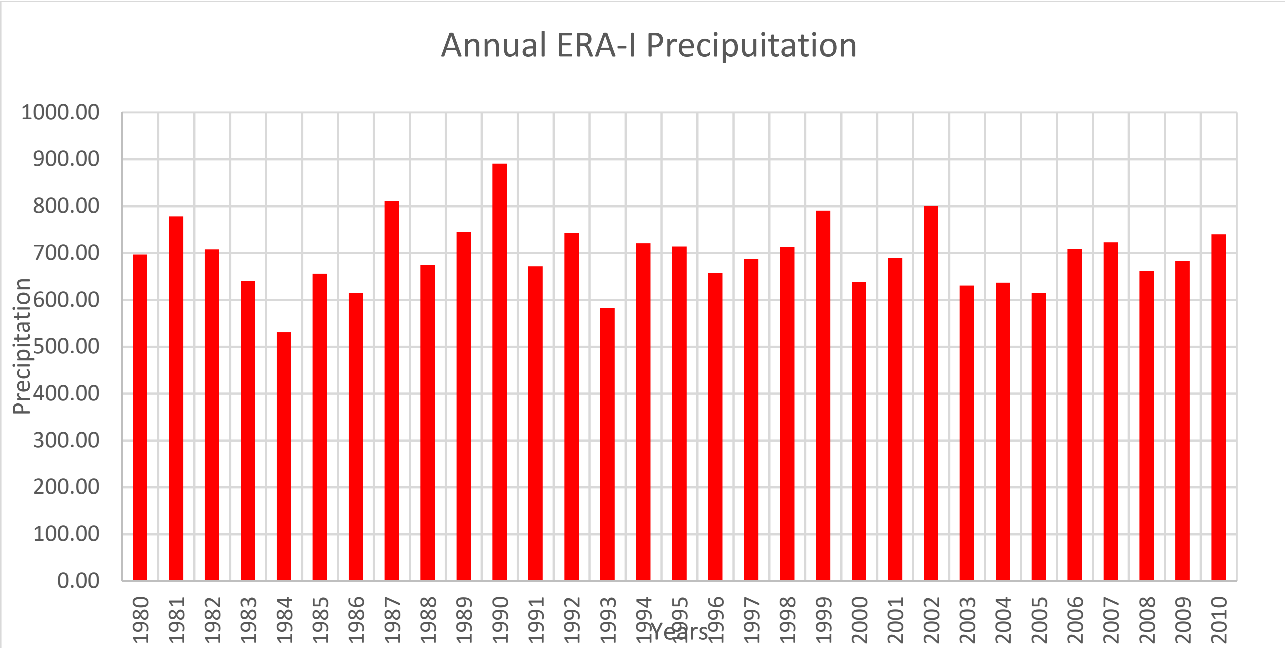

Figure 4-16: Mean annual ERAI precipitation

To note in the un-biased reanalysis data (land surface precipitation)

- ✓ The precipitation pattern is like the observed data with more precipitations in the months of MAM and OND and low in June and July.
- ✓ Worth to note in the pattern of precipitation is that, whereas in the observed data the precipitation is more in the April, in the reanalysis, the more rain is registered in November. This can be seen in the average daily and monthly precipitation plots.
- ✓ The maximum annual rainfall in the observed is 1547mm and average of 1227mm, the maximum and average for the reanalysis data was 890mm and 695mm respectively over the same period. This shows a deference of more than 40% underestimation (ie 657mm and 532mm respectively).
- ✓ The annual precipitation increased while approaching 2010 in the observed, whil in the reanalysis, it is almost uniform throughout the period much as the highest were recorded in 2010 for observed and in 1990 for the reanalysis.
- ✓ Similar to the observed annual precipitation, in every after 10 years, there is a lower drop in precipitation. However, it shows that over this period of study, the precipitation seems to be constant.

4.3.4 Biased reanalysis precipitation data

There are two methods of doing a bias correction. The linear (Teutschbien and Seibert, 2012) and Nonlinear (Leander and Buishand, 2007) correction methods. In this study, the linear approach was considered due to its simplicity and wide application. Daily precipitation P is transformed into P^* such that $P^* = aP$, using a scaling parameter, $a = \bar{O}/\check{Z}$, where $\bar{O}$ and $\check{Z}$ are monthly mean gauged and ERAI precipitation data. The monthly scaling factor was applied to each ungauged daily ERAI data of that month to generate the corrected daily time series.

The data used for correction of the reanalysis data was obtained from the Kizza et al.2012, estimation of areal precipitation on the Lake Victoria basin since the results were fairly comparable with the observation data obtained for this study.

Month	**mean obs ($\bar{O}$)**	**mean era ($\check{Z}$)**	**Correction (a)**
1	91.70	30.35	3.02
2	90.00	32.06	2.81
3	137.35	95.04	1.45
4	188.70	123.48	1.53
5	134.85	44.65	3.02
6	59.95	6.67	8.99
7	53.30	1.07	50.04
8	69.15	3.63	19.05
9	75.35	25.46	2.96
10	101.35	116.20	0.87
11	135.75	153.69	0.88
12	104.00	63.37	1.64
Sum	1241.45	695.66	96.26

Table 4-2: Factors for the Linear Correction of the ERAI rainfall

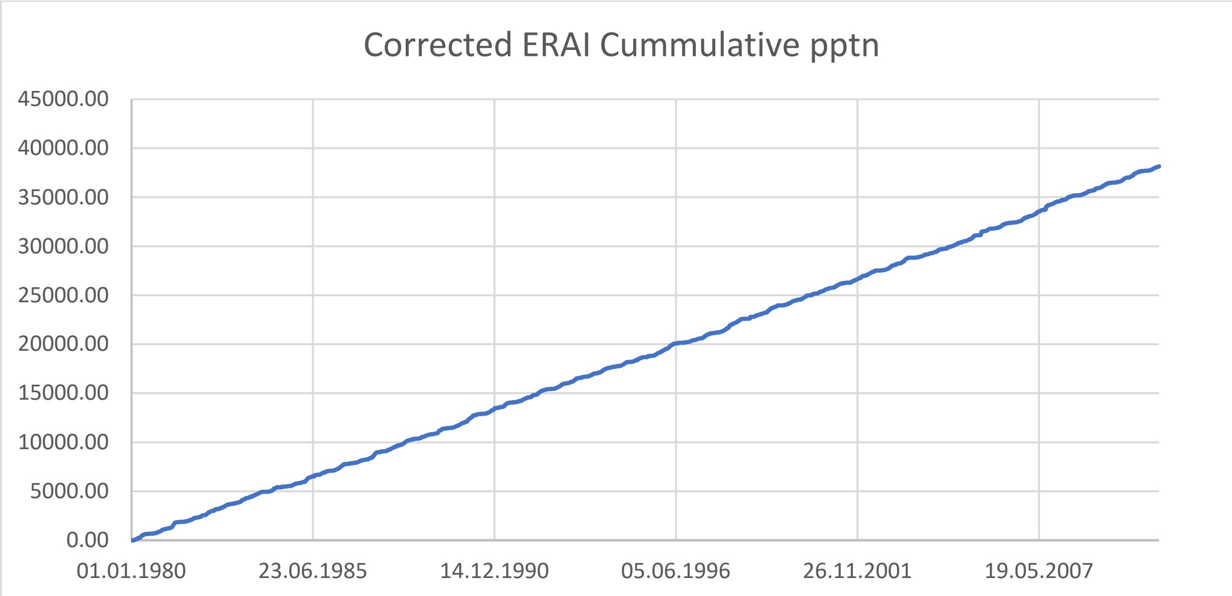

Figure 4-17: Cumulative precipitation is almost 39000mm as compared to the un corrected which is 21000mm (about 85% increase)

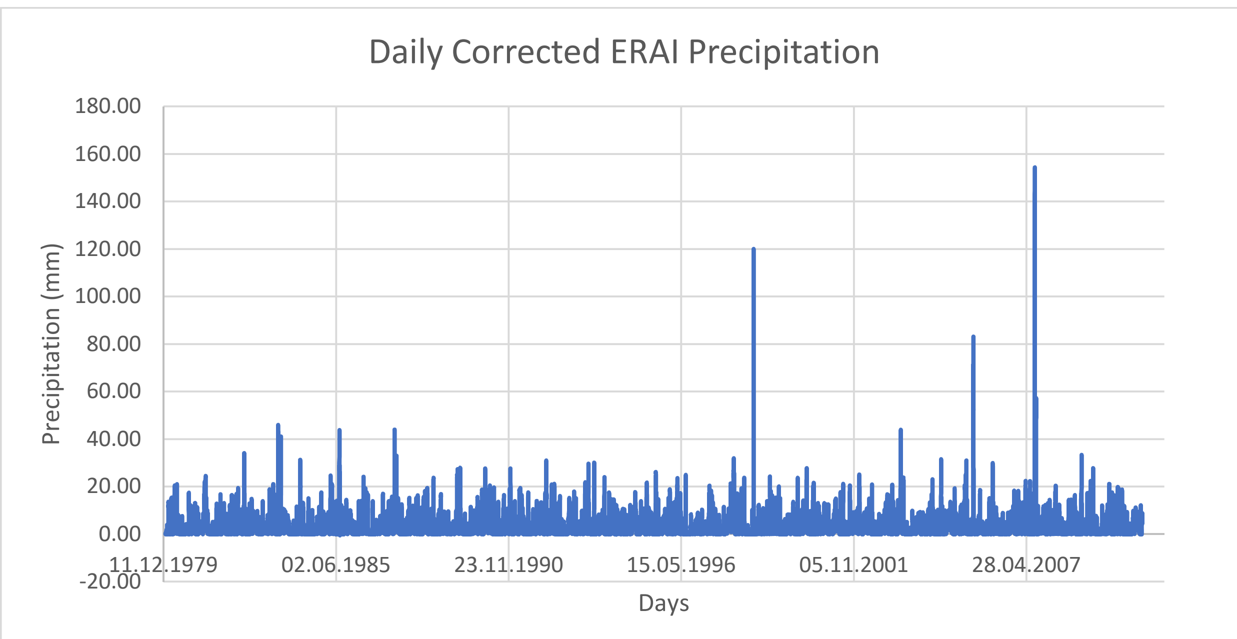

Figure 4-18: Daily Precipitation of the corrected ERAI

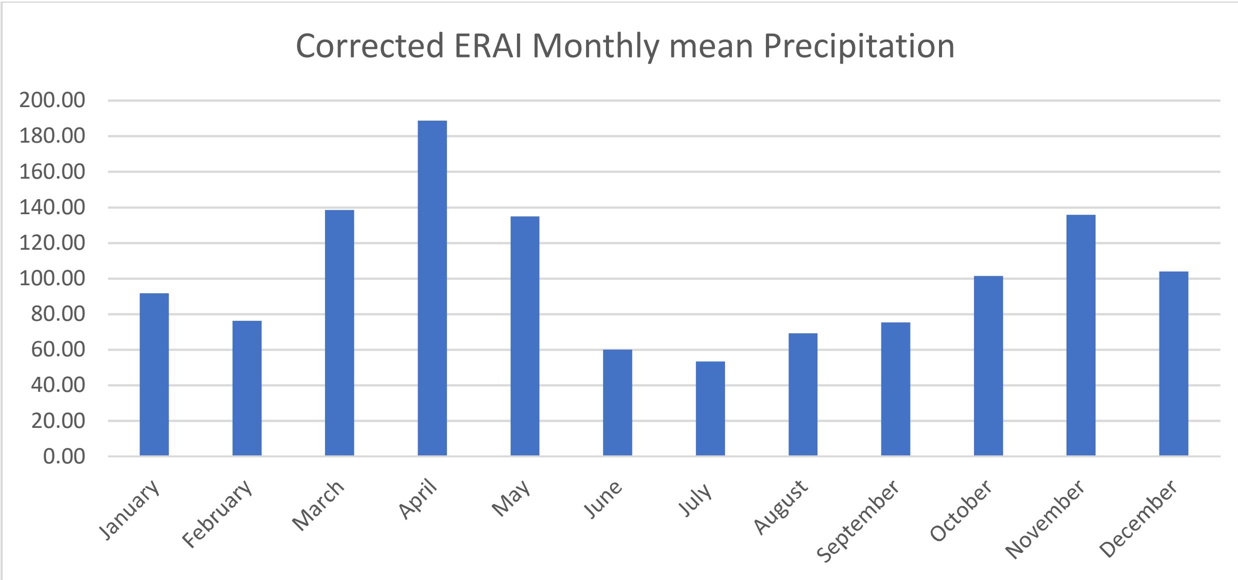

Figure 4-19: Monthly precipitation of the ERAI

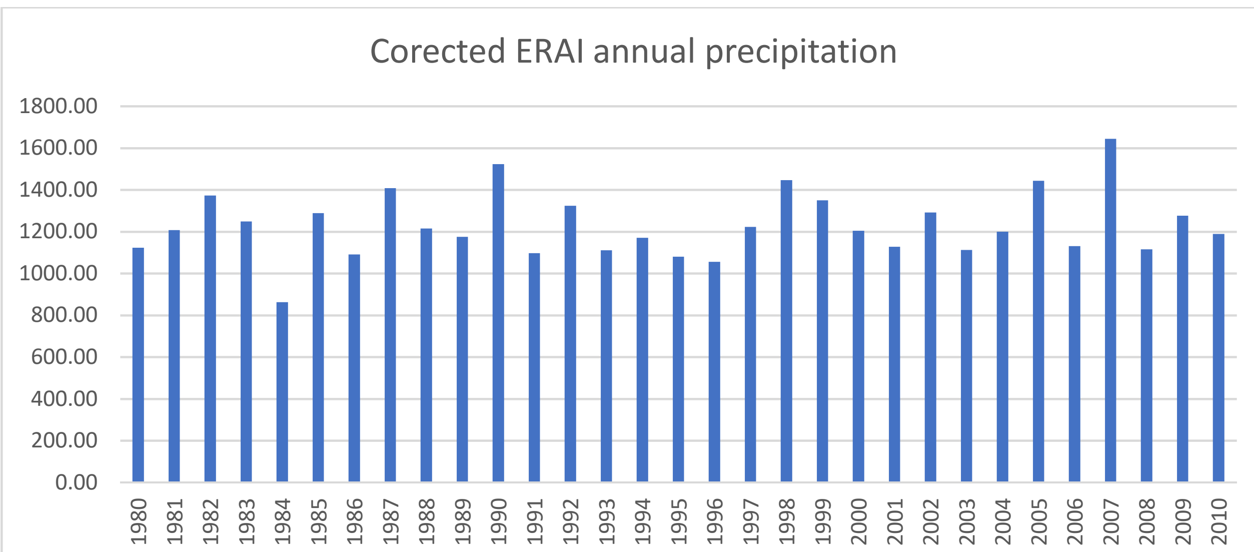

Figure 4-20: Mean annual corrected ERAI precipitation

After the linear bias correction, the average monthly and annual precipitations were 102mm and 1229mm an increase of approximately 76% and 38% respectively.

Comparison with previous studies

The table and the figure hereunder shows the comparisons of the land precipitation results from previous studies and the current.

Year	Land Precipitation comparison with various previous studies						
	ERAI -orig	ERAI crtd	Kizza, 2012	Yin, 2002	Tate, 2001	Mutenyo	GHCND
1981	777.69	1207.64	1150	1313.83	1403	1184	1161.45
1982	707.34	1372.93	1330	1440.18	1585	1387	1206.81
1983	640.29	1248.01	1140	1256.19	1359	1115	1105.31
1984	530.84	862.70	1040	1106.18	1363	1185	896.14
1985	655.69	1288.61	1200	1351.51	1541	1308	1116.37
1986	613.74	1090.66	1125	1321.95	1516	1280	1111.13
1987	810.68	1407.66	1140	1323.43	1497	1272	1252.59
1988	674.74	1214.28	1320	1500.04	1665	1375	1322.22
1989	744.88	1174.17	1245	1365.55	1570	1346	1241.12
1990	890.36	1523.34	1165	1359.64	1490	1269	1099.66
1991	671.52	1096.28	1200	1396.59	1585	1430	1140.11
1992	743.07	1322.71	1080	1159.39	1359	1193	1050.51
1993	582.33	1109.79	975	1128.35	1352	1174	975.42
1994	720.57	1170.43	1270	1401.76	1730	1400	1314.14
Max	**890.36**	**1523.34**	**1330.00**	**1500.04**	**1730.46**	**1430.00**	**1322.22**
Min	**530.84**	**862.70**	**975.00**	**1106.18**	**1351.59**	**1115.00**	**896.14**
Average	**697.41**	**1220.66**	**1170.00**	**1316.04**	**1500.95**	**1279.86**	**1142.36**

Table 4-3: Annual precipitation comparison with previous studies

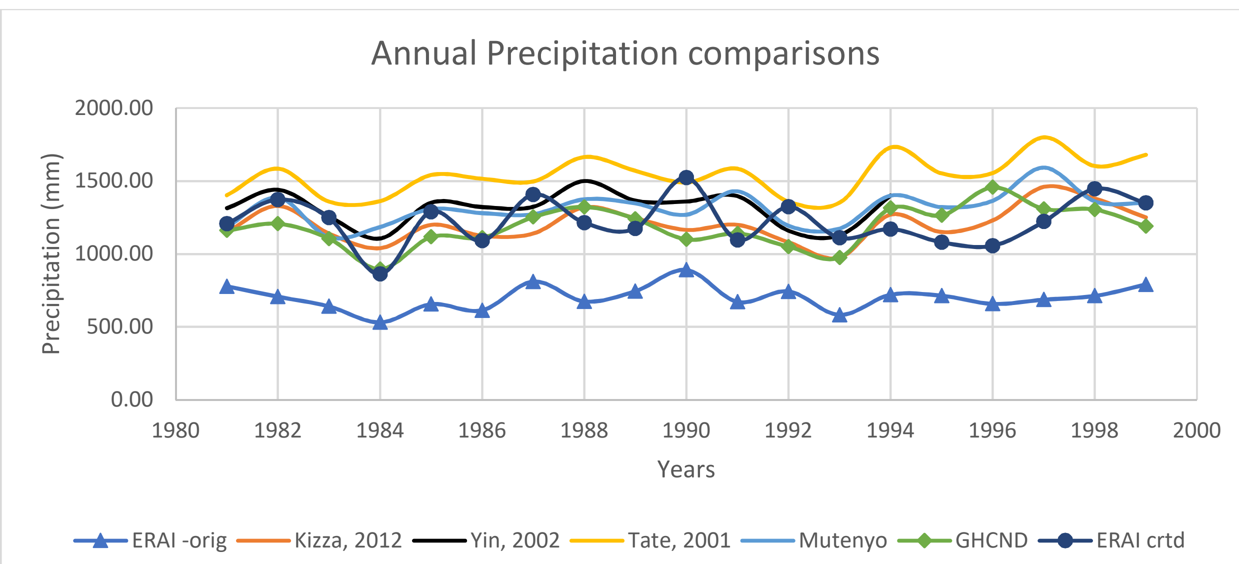

Figure 4-21: Comparative precipitation plot for current and previous studies

From the above table (table 4-3) of previous studies and its plot, it was worth noting that

- The original reanalysis data underestimated that precipitation by more than 60%. This relates with observations of the author. Zhu et al., 2014.
- After carryin out a bias linear correction of the precipitation, the pattern of the precipitation does not match others.

4.4 Temperature

The temperature data obtained from ERAI was used both in the reanalysis process and together with the observed precipitation further analysis. The temperature here considered is near surface temperature which is 2m above the ground of meteorological stations. Ta is conventionally observed at meteorological stations with high accuracy (Stisen et al. 2007). However, reanalysis Ta data is more accurate than the satellite data though it has high bias from complex topography and high local elevation (Zhao et al. 2008).

LVEMP, 2005 indicated that temperature reaches maximum in February, just before the March equinox (date when sun is overhead equator) and reaches its lowest records in July after the June equinox. Maximum temperature ranges from 28.6-28.7^{o} C while minimum temperature is from 14.7^{o} C in Tanzania 18.2^{o} C in Uganda. Although it is expected that the highest temperatures should occur after the March equinox when the sun is overhead the equator, the highest temperatures have been observed to occur before the March equinox. One possible explanation is that the dry North-east winds from the Ethiopian highlands exert their greatest influence towards the end of the dry season in February. This probably creates the highest temperatures that are manifested in the records.

The same can explain the low temperatures observed in July. This is when the sun is overhead the tropic of cancer and a predominance of maritime breeze is felt in the lake basin from the cool waters of Lake Victoria as well as monsoonal winds from the Indian Ocean. These observations are useful in understanding the limnology of Lake Victoria as well as the quantitative variations of hydraulic and limnological processes in the basin.

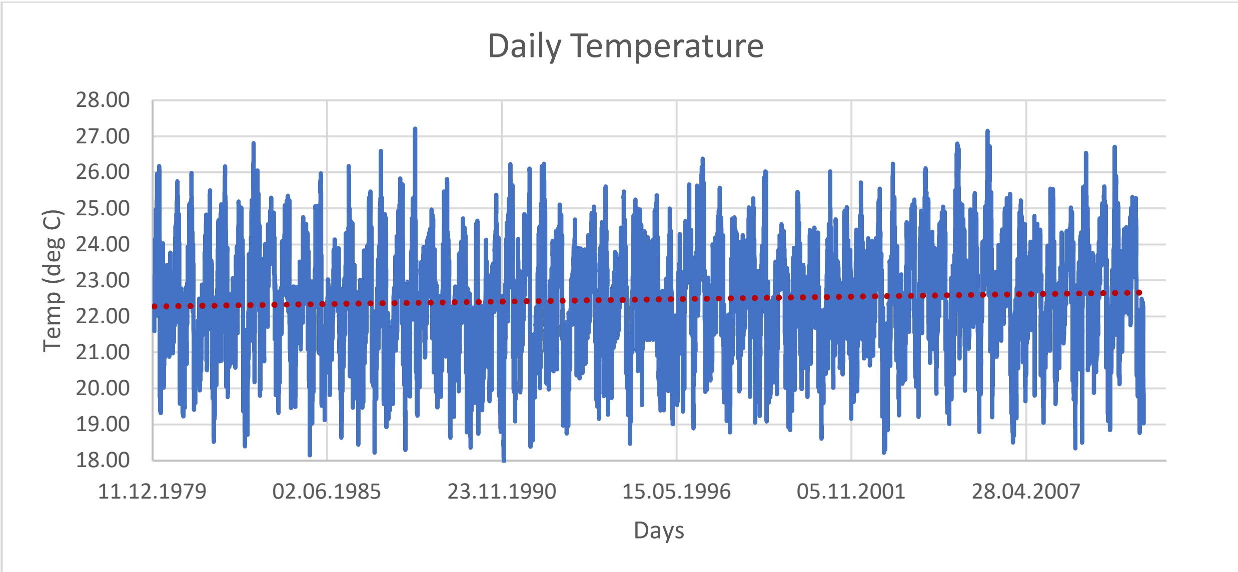

Figure 4-22: Daily temperature for land surface

From the daily temperature plot, it shows a slight gradual increase of about 0.5 deg C the temperature from 1980 to 2010.

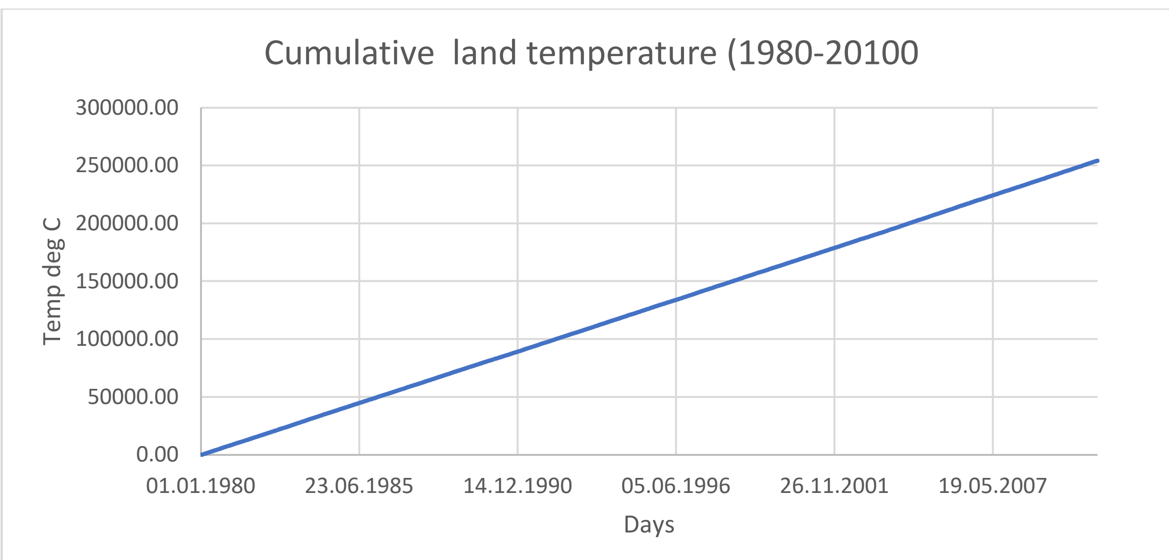

Figure 4-23: Cumulative land surface temperature

:

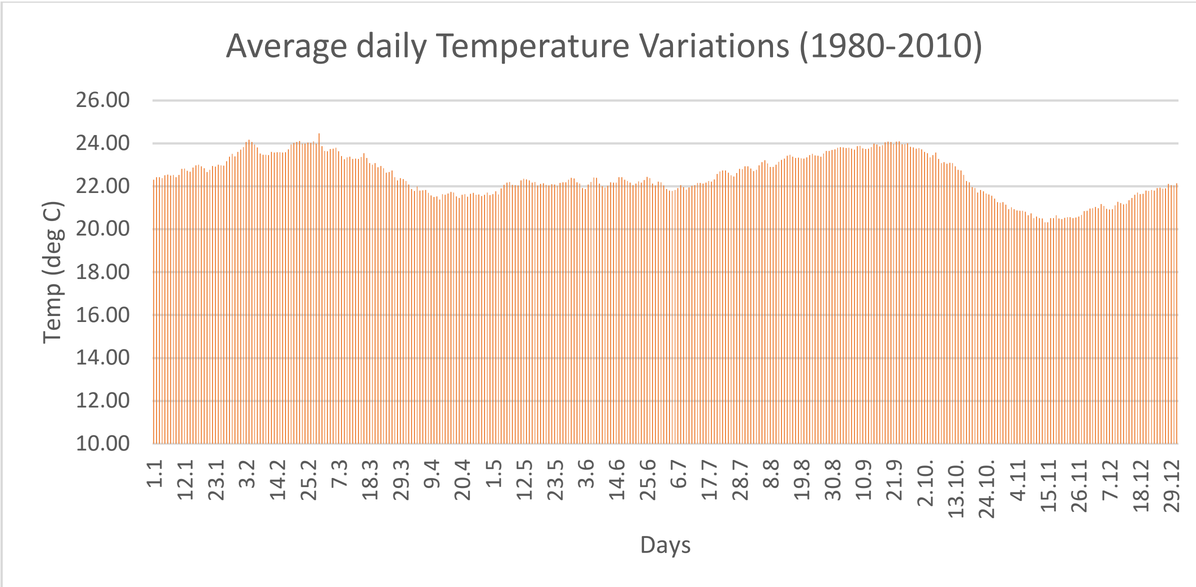

Figure 4-24: Average daily temperature variations

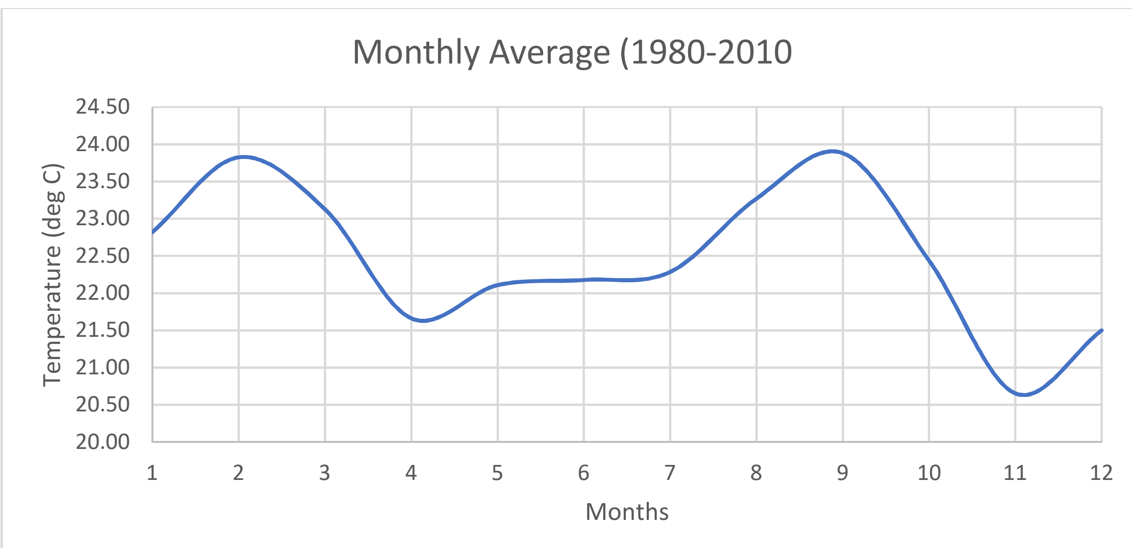

Figure 4-25: Average monthly temperature variations

Figure above shows the average daily and monthly temperature variations through the study period. It can be noted that around February and September, was when the temperature gets to the peak of about 24deg C. this is comparable with the results obtained in the LVEMP, 2005 study. The temperature also corresponds the precipitation pattern whereby it was high I February and September and low in the April and November, the months with higher rainfall.

4.5 Radiation data

Radiation is associated with the evaporation of the water from both the land and water surface. A net radiation was computed after retrieving the shortwave and longwave radiations. The Net radiation was computed as the sum of the Net shortwave radiation and Net Longwave radiation.

$R_{net} = SW + LW\ (Wm^{-2})$

The ranges of values of the radiation were between 120 Wm-2 to 160Wm-2 on a daily average. Higher radiation were experienced in the months of February and September and low in July and October.

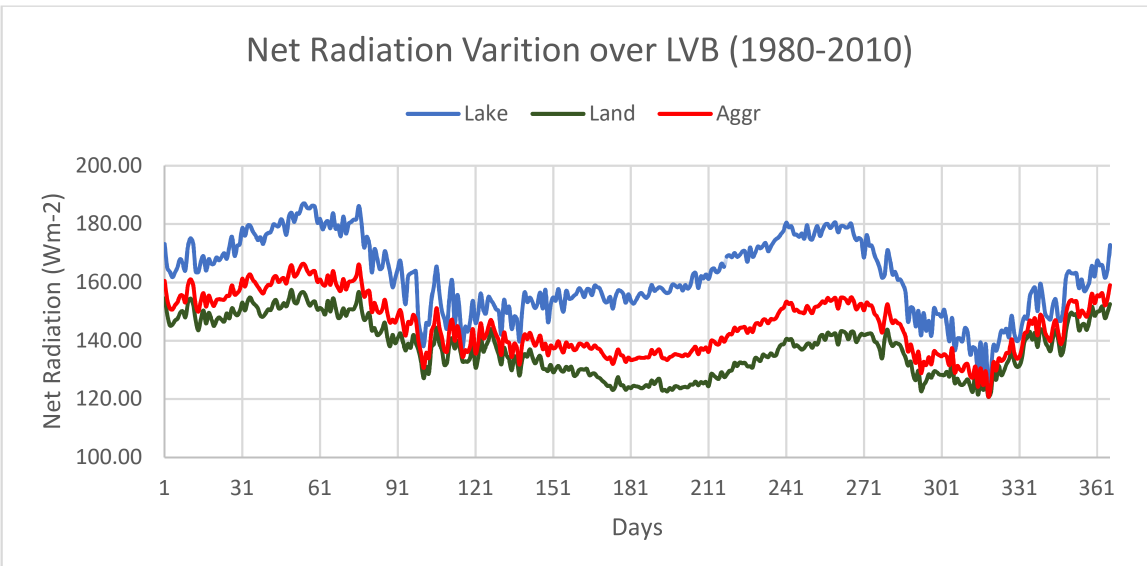

Figure 4-26: Average daily radiation variations

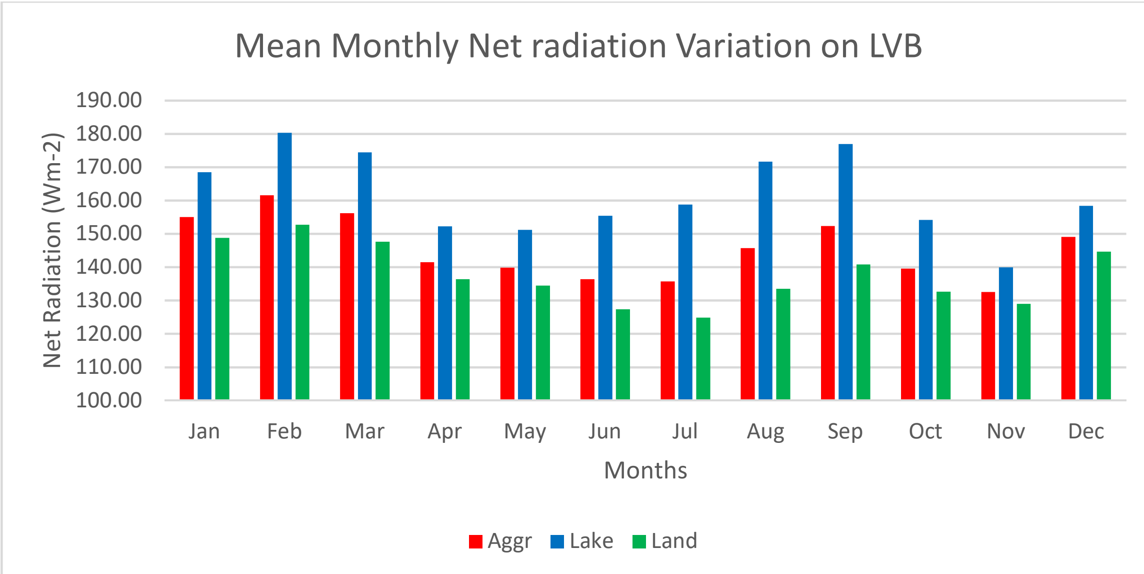

Figure 4-27: Mean monthly radiation variations

4.6 Wind speed data

Based on the plots, it showed that higher wind speeds are experienced in mid-year ie during the months of July and August. This is when there is quite low precipitation in the catchment,

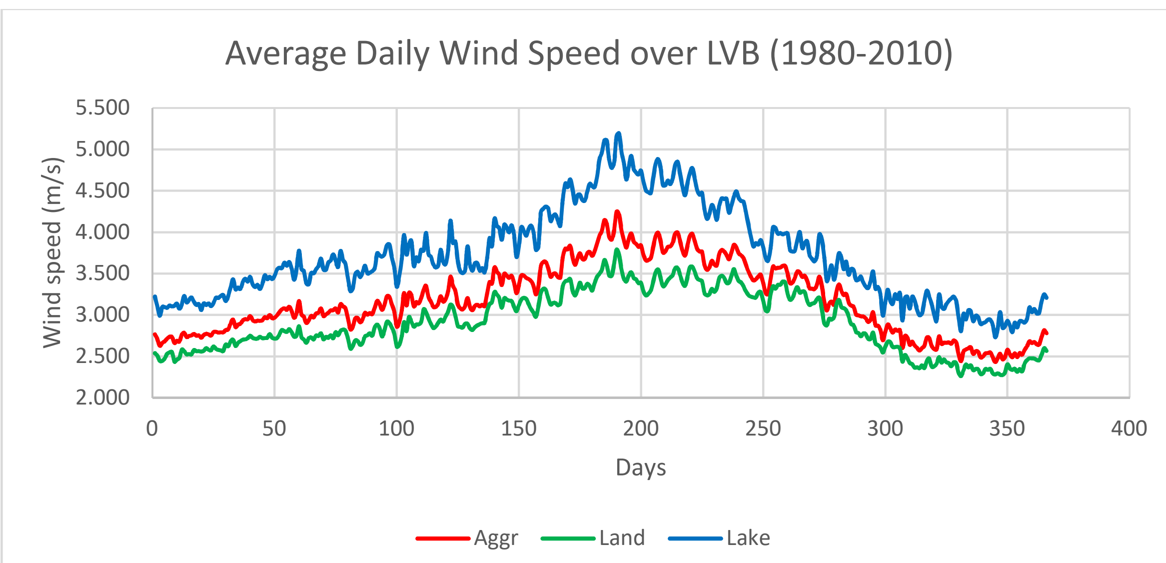

Figure 4-28: Average daily wind speed

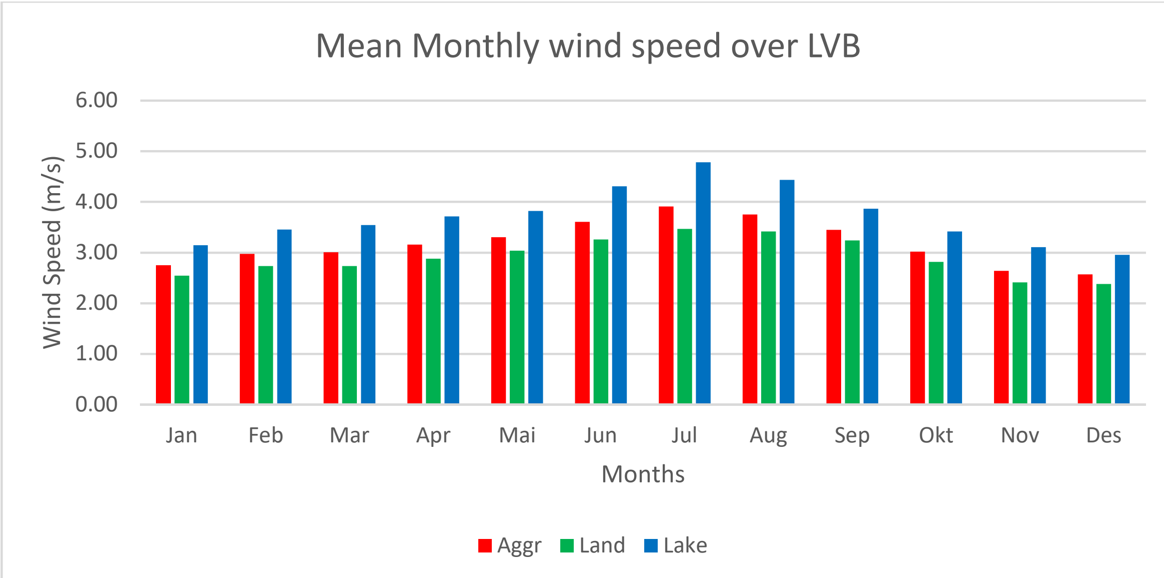

Figure 4-29: Average monthly wind speed

4.7 Relative Humidity

The relative humidity follwos the patten of the precipitation whereby it high in the ntjos of April and November.

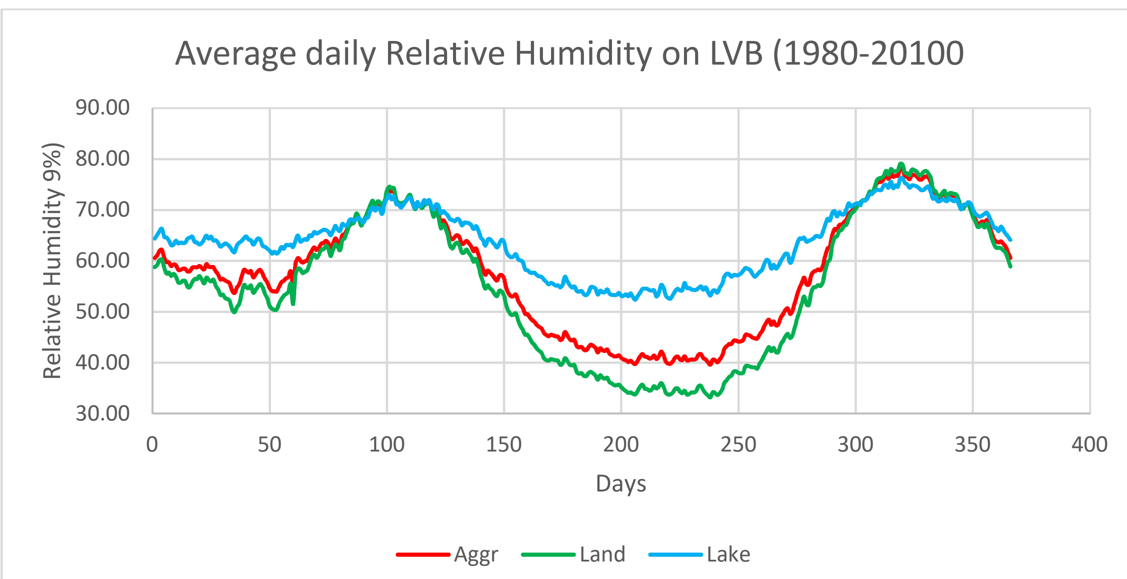

Figure 4-30: Daily Relative humidity variation

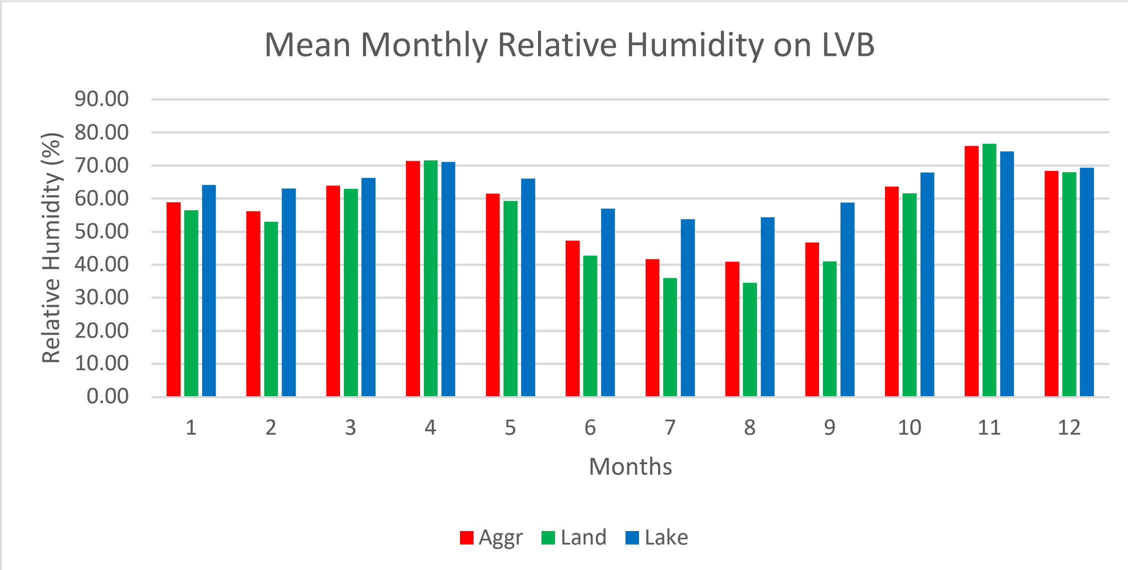

Figure 4-31: Mean monthly relative humidity variations

4.8 Hydrological Data

The major objective of this study was to investigate possible impacts of climate change on the natural hydrological regimes of Lake Victoria Basin and how they would impact the already built infrastructure at the exit of the Nile River. To achieve this objective, this involved the study of trends in the inflows from the sub catchments, the outflows from the lake and the water lake levels. Moreover, to further understand the afore mentioned changes, future climate scenarios were considered in order to investigate the future flood developments from the catchment.

The results from the future climate simulations will be used to compute the future flows generated from the catchment and thereafter determine the floods which will be compared with the previous design floods.

The analysis of the floods was done using the Gumbel EV 1 distribution method based on the peak stream flow data. Furthermore, the analysis were carried out based on the annual peak flows and seasonal flows of the year with high precipitation.

The table below (

Average annual tributary discharge into the lake for long term flow (Andjelic et al 1999)

Country	Basin	Discharge mm	Discharge m3/s
Kenya	Sio	5.5	12.0
	Nzoia	55.3	121.1
	Yala	18.0	39.5
	Nyando	8.7	18.9
	North Awach	1.8	3.9
	South Awach	2.8	6.2
	Sondu	20.3	44.3
	Gucha-Migori	27.8	60.9
	Sub total		
Tanzania	Mara	18.0	39.4
	Grumeti	5.5	12.1
	Mbalageti	2.1	4.5
	E. shore stream	8.9	19.5
	Simiyu	18.7	41.0
	Magogo moame	4.0	8.7
	Nyashishi	0.8	1.7
	Issanga	14.7	32.1
	S. Shore stream	12.3	26.9
	Bihamuro	8.5	18.7
	W.Shore stream	9.9	21.7
	Kagera	125.2	273.9
	Subtotal		
Uganda	Bukora	1.5	3.4
	Katonga	2.4	5.4
	N. Shore stream	0.7	1.6
	Sub total		
Average Inflow		373.4	817.3

Table 4-4: Summary of Discharges from tributaries of LVB

Figure 4-32: LVB and the major sub catchments

Figure 4-29

Annual Mean flows (cumecs) of the Major Rivers of the Lake Victoria basin and their Relative Ranking of Contribution to the total flow into the lake are shown in the table 4-4 above. Studies by LVEMP indicated that rainfall contributes more than 80% of the water inputs into Lake Victoria. The exact contribution is not known due to lack of adequate rainfall monitoring network in the lake. LVEMP also noted that Kagera River has the highest contribution of river flows into Lake Victoria with River Nzoia coming a far second with less than half the annual flow of the Kagera River.

Further literature from previous studies Kizza et al. 2008 on the temporal variability of rainfall in LVB concur with LVEMP.

In this study, the generation of the future trends of runoff from the aggregated flow into the lake was used to simulate the volumes of water into the lake and hence will be used to check with the existing design floods used for previous computations of the infrastructures in the river course. The reason for considering the inflow data from the LVEMP studies was due to the outflow being regulated since the construction of the Owen Falls Dam in 1954. By the end of 1998, another power plant (Kiira Power Station) was constructed in parallel with Owenfalls Dam. As a result, the excess water which used to spill over Owen Falls Dam was diverted to Kiira power dam with a canal

4.8.1 Inflow and Outflow data

Lake Victoria Environment Project carried out studies on the quality of Lake Victoria and hence incorporated the hydrological studies too from the basin. The project generated inflow data from the sub catchments of LVB from the period 1950-2004. Further to this, the original period which was considered during this study was from 1980-2010, with the model interpolating the remaining years to fill up from 2005-2010. However, in order to match the simulated historical GCM data, whose range ends in 2005, further analysis of the observation data was reduced to 1980-2005.

Comparative results from other previous studies on the inflows were also used to check the validity of the LVEMP data series, except that the previous studies were done on monthly resolution as compared to LVEMP's daily. LVEMP also filled the missing data, especially the out. Figure a shows the in and outflow data.

The daily outflow data was obtained from the Directorate of Water Development which was in a daily time series. The location of the gauging station is near Jinja Town and about 2.3km upstream of the Owen Falls Dam. The guage (considered as zero gauge) is in an altitude of **1122.90 masl** and with coordinates **(X=517803.53m, Y=46975.46m)**

However, some of the years had missing data but the gaps could be filled on monthly series since the Institute of Hydrology (IH-ODA, 1993) had similar monthly outflow data from 1970-1990. Figure b shows a comparative plot for monthly in and outflows from 1970-1990 from various compilations (DWD, IH and LVEMP)

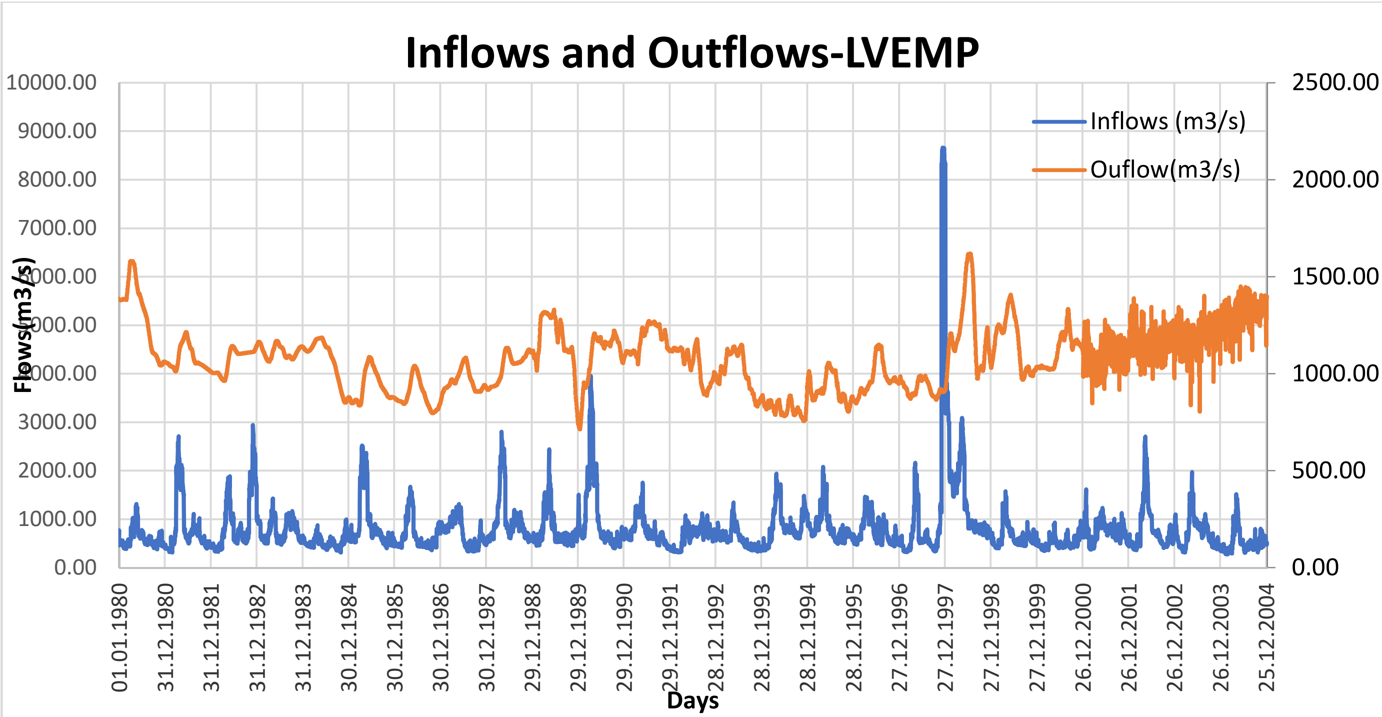

Figure 4-33: Inflows into and Outflows from Lake Victoria

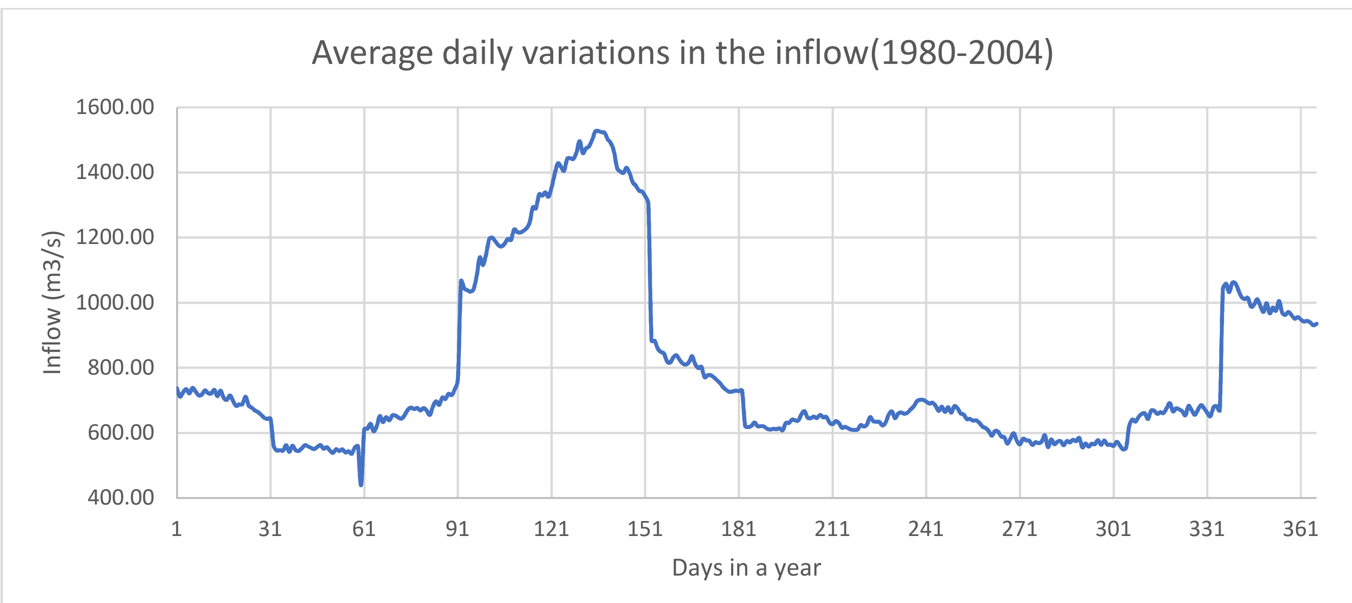

Figure 4-34: Daily variations of inflows for the LVB

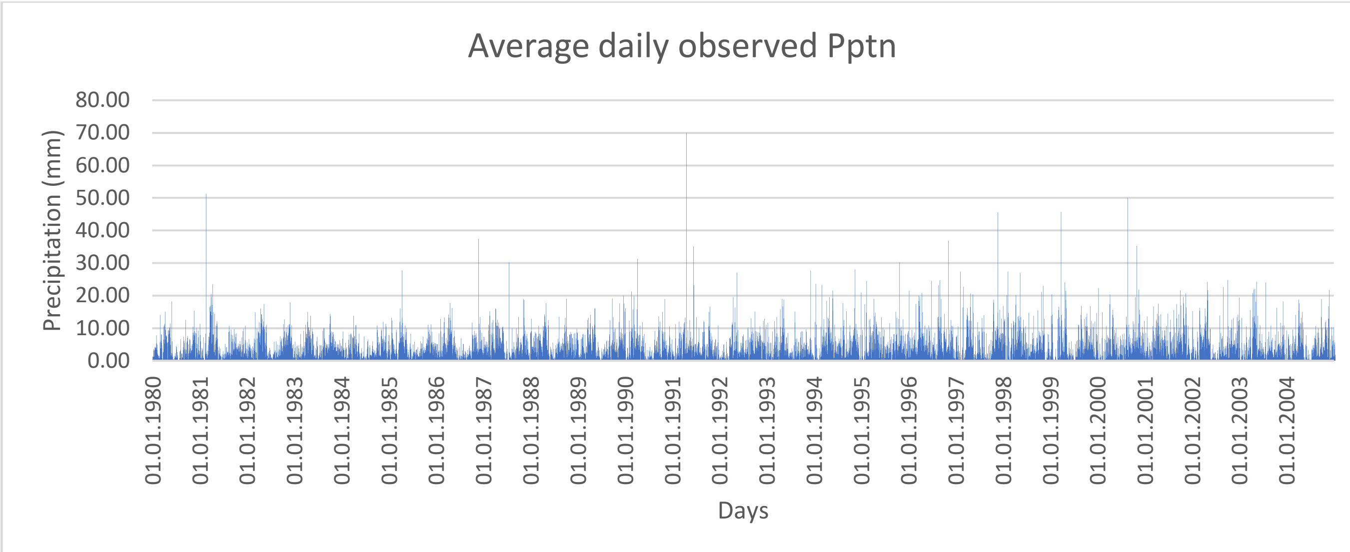

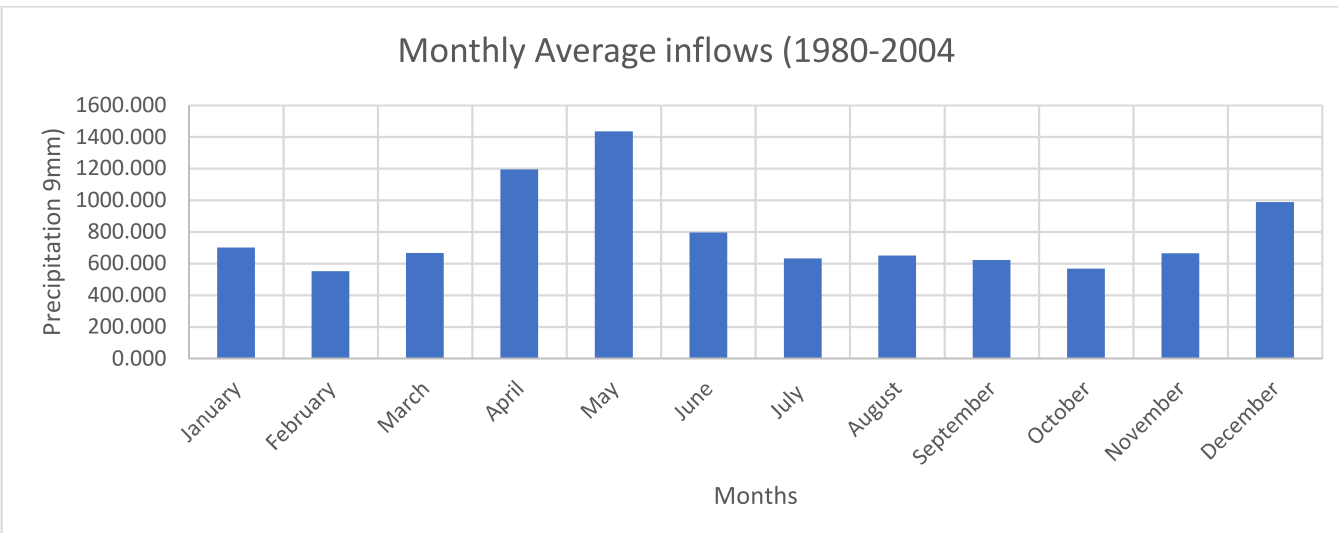

Figure 4-35: Mean monthly variations of inflows for the LVB

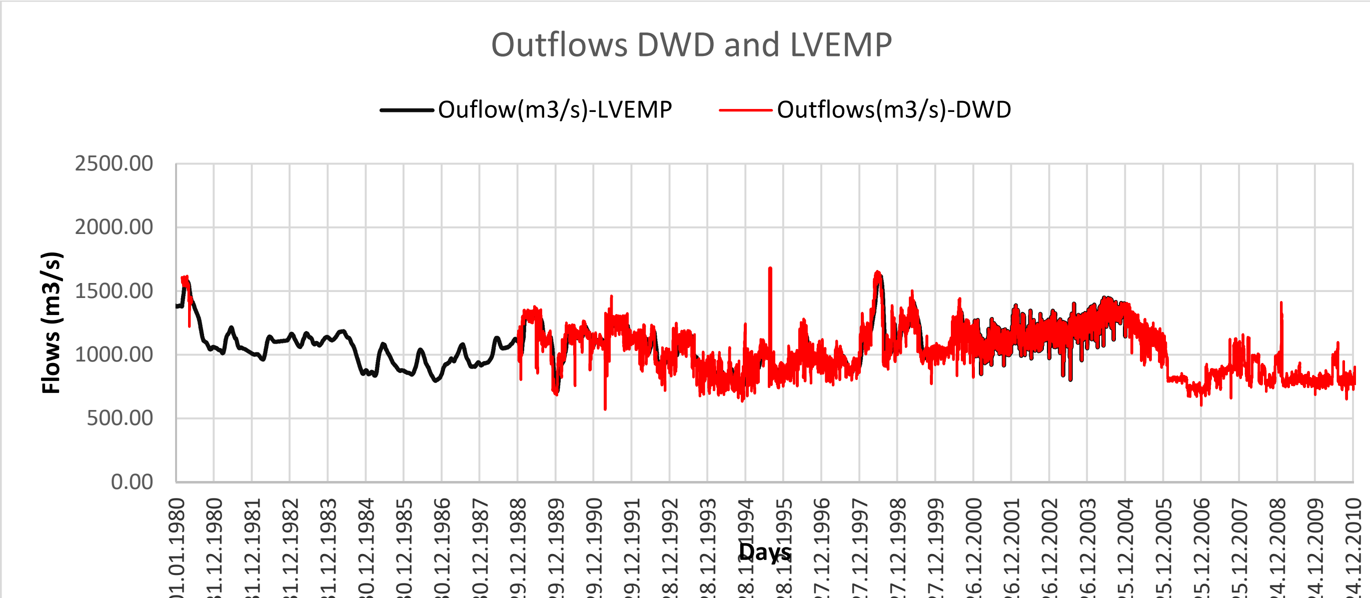

Figure 4-36: Comparative Outflow values between DWD and LVEMP

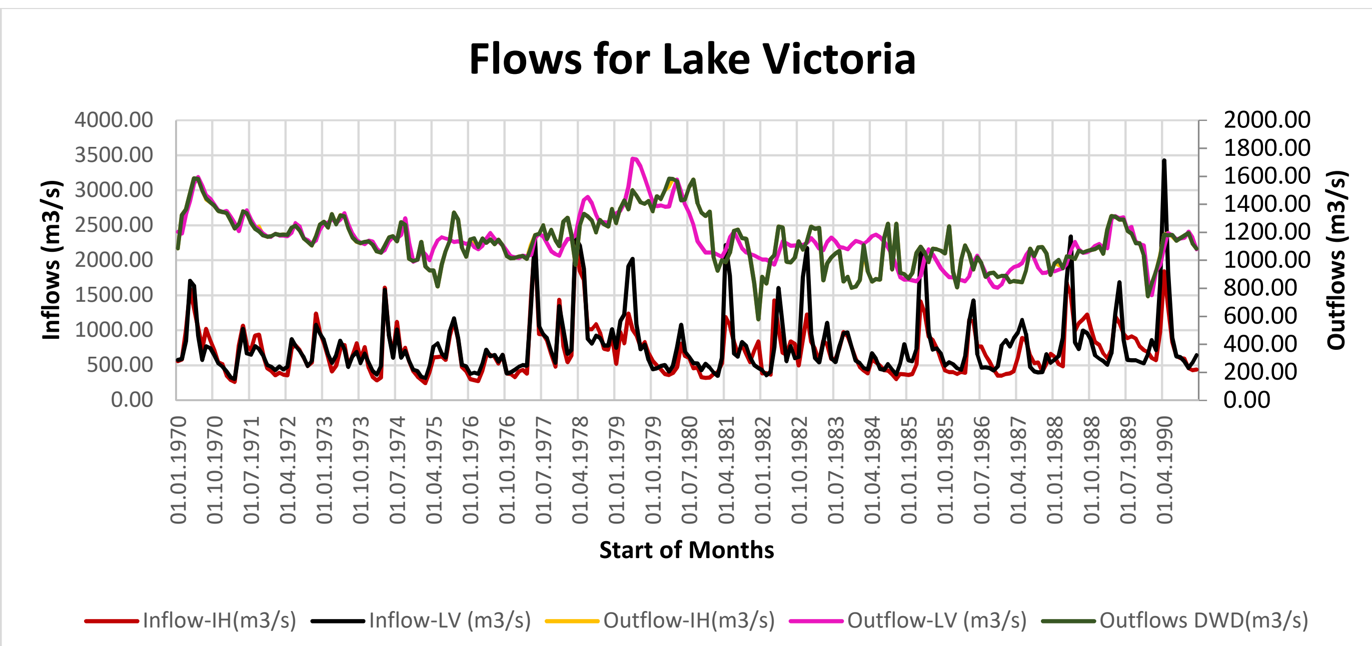

Figure 4-37: Comparative flow values on monthly means from IH, LVEMP and DWD sources

It can be noted from the inflow and outflow plots that

- There are inconsistencies in the outflow even when the inflows seem to increase. This could be due to the dampening effect of the lake.

- There is no direct comparable pattern between the daily precipitation and the inflows, however, there are similarities in the monthly patterns with the inflow responding to the precipitation increase in the months of May and December due to increased precipitation in the months of April and November.

- Based on inflow hydrograph, it shows that all the three sources of data came from the same source with slight discrepancies. However, the IH (Institute of Hydrology, UK) and LVEMP almost have the same inflow hydrographs, while for the outflows, IH and DWD have similar hydrographs with a slight difference from LVEMP.

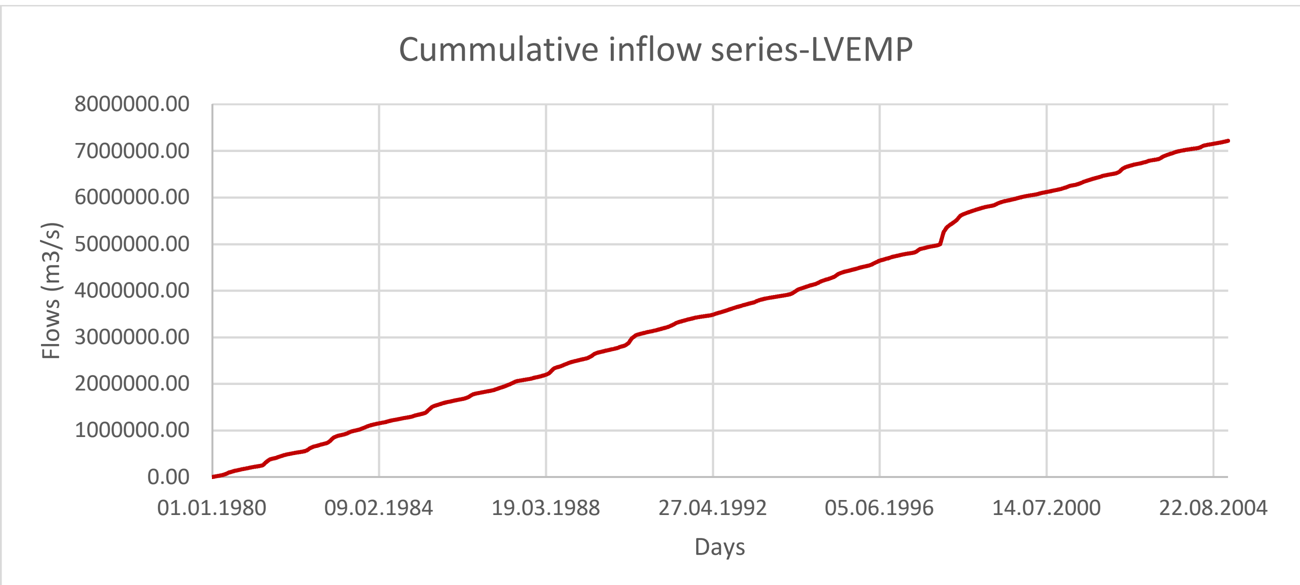

Figure:4-38: Plot of the cumulative inflow.

From the cumulative inflow plot, there is a sudden change of gradient in the year 1997, this corresponds to the daily inflow hydrograph shown in figure 4-30. Moreover, this sudden increase also triggers a sudden response to the outflow hydrograph. This could be as a result of an increased precipitation during that time. Is evident both in the ERAI mean annual precipitation hydrograph and also in the table of comparison of mean annual precipitations.

4.8.2 Lake Victoria Water Levels

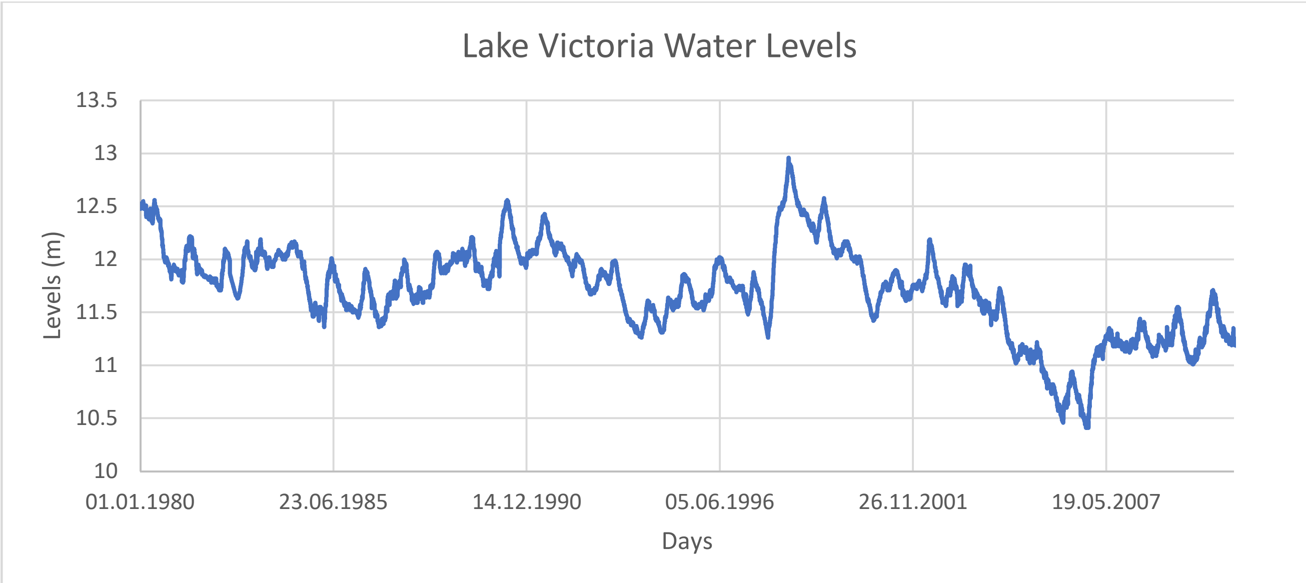

Figure 4-39: Lake water levels

Between 1980 and 2007, it shows that the lake levels have been falling. However, the plot also shows a sharp increase around 1997. This correlates with increased precipitation during that period and subsequent inflow into the lake. The cumulative plot for the lake levels shows good data.

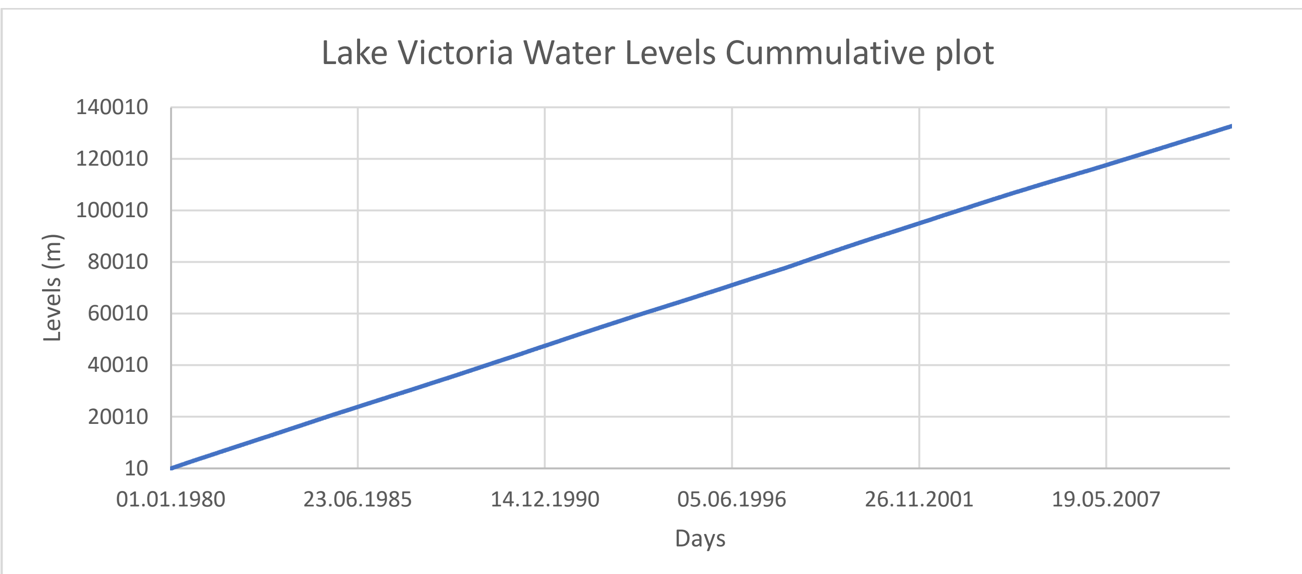

Figure 4-40: Lake Victoria water levels

4.9 Catchment Characteristics

Having obtained the climate and hydrological data for the catchment, the next step determines the characteristics. These characteristics are influential to the climate and the hydrology of the catchment. Some of these include the elevation distribution of the catchment, the lake percentage. These were retrieved using the ArcGIS application. The delineation of the watershed was done using ArcGIS 10.3. The watershed or catchment is the area upstream of the given outlet point, from which all the water drains to the lowest point (in this study the lowest point was at Elev 1122.9masl).

To delineate the LVB watershed, the DEM for Africa was used and it was obtained from free website (http://earthexplorer.usgs.gov/). A Digital Elevation Model (DEM) is a digital representation of a terrain's surface. It represents the bare ground surface without any objects like plants and buildings (http://www.wikipedia.org/). The DEM in this study was represented in raster map format with 1km x 1km resolution.

The LVB watershed, lying in five countries in East Africa, had its DEM clipped out African DEM and later using the discharge station near Jinja as the outlet from the lake, the LVB watershed was delineated by ArcGIS from the website (http://downloads.weidmann.ws/cshapes/Shapefiles. LVB is located in the UTM zone 36 from which the geographic coordinate system was projected for distance and or area measurements. Below is the flow chart for the water shed delineation.

The GIS data can be represented in vector and raster format. Vector data can be in the form of point, polylines or polygons. It stores the spatial data and attributes and topology information, as well as the catchment boundaries and river network.

Raster data is the representation of data in an array of points. The grid spacing determines the resolution of the raster. (Alfredsen, 2013)

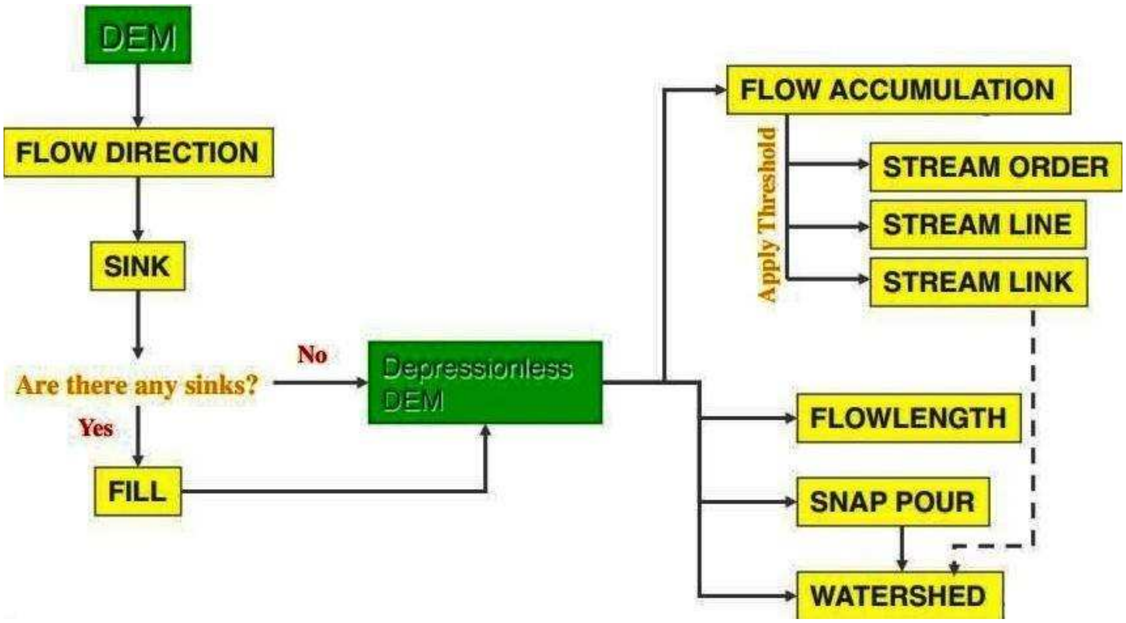

Figure 4-41: 1 Watershed delineation process

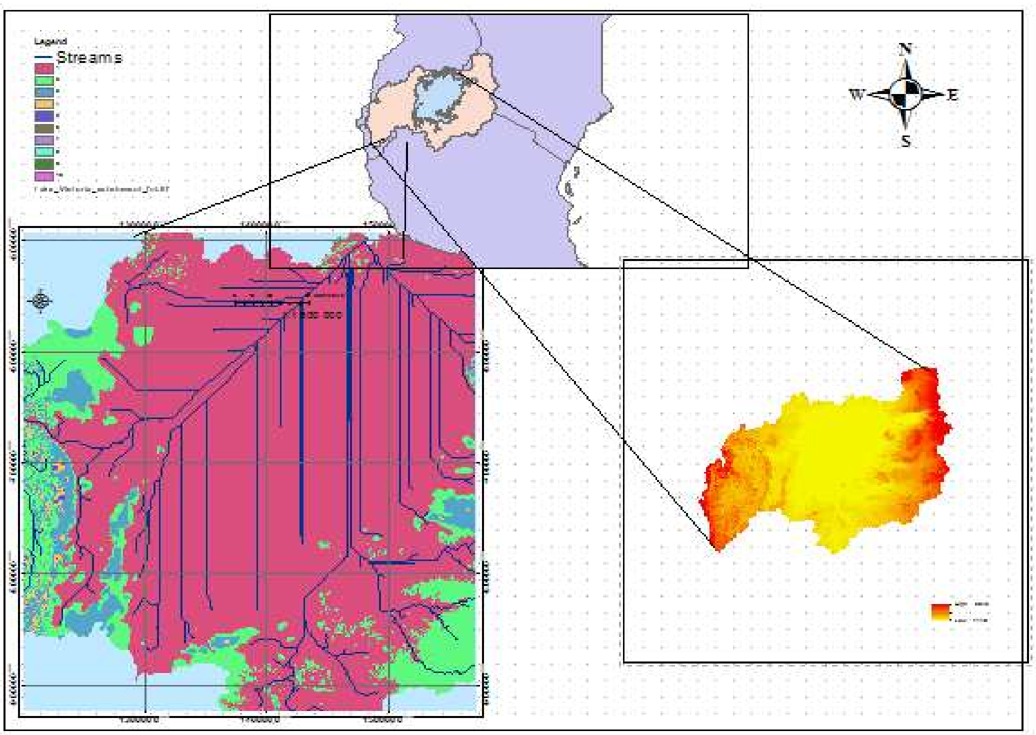

Figure 4-42: Catchment of Lake Victoria

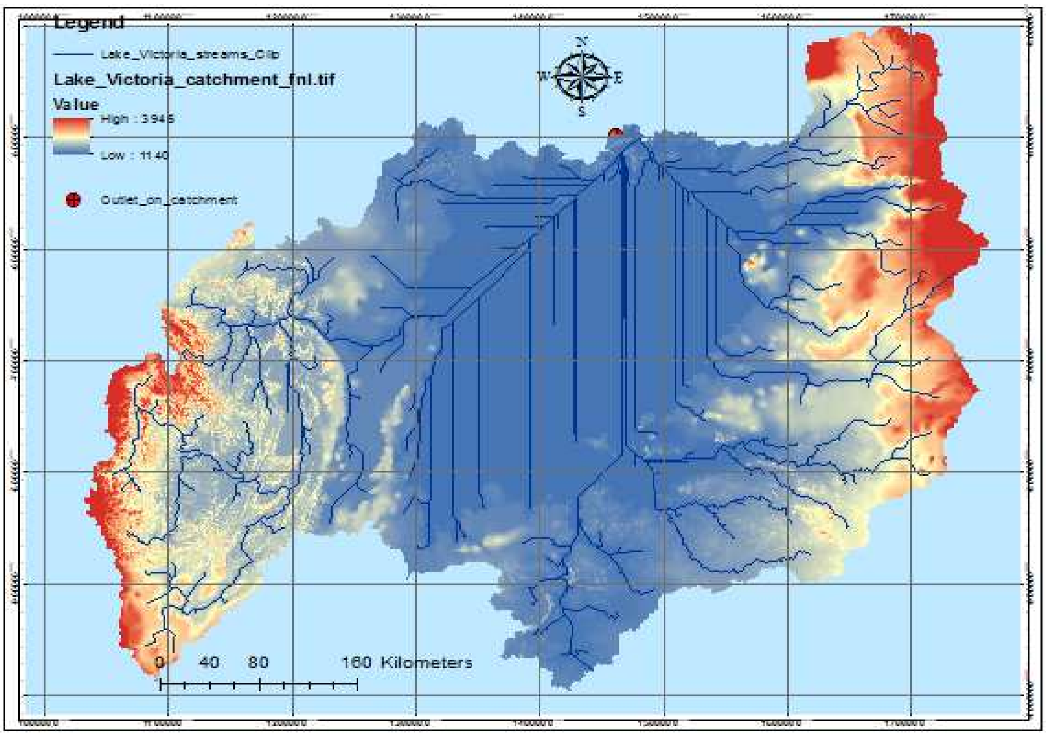

Figure 4-3: Digital Elevation Map for the LVB

Elevation Zones in the LVB

These are areas divided into 10 zones in order to derive the hypsographic curve. The hypsographic curve is a plot of the accumulated area percentage against the elevations. This curve is useful for the rainfall-runoff modelling.

MEAN Elev (masl)	% cumm area
1172	56.18
1442	80.87
1739	91.96
2035	97.03
2329	99.01
2608	99.77
2889	99.93
3200	99.97
3482	99.99

3787	100.00

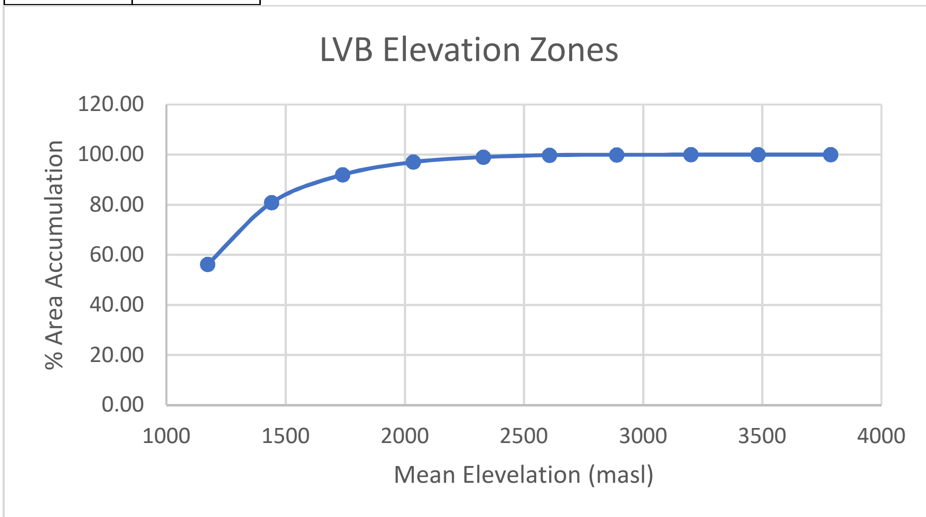

Figure 4-44: 2 Hypsographic curve for the LVB

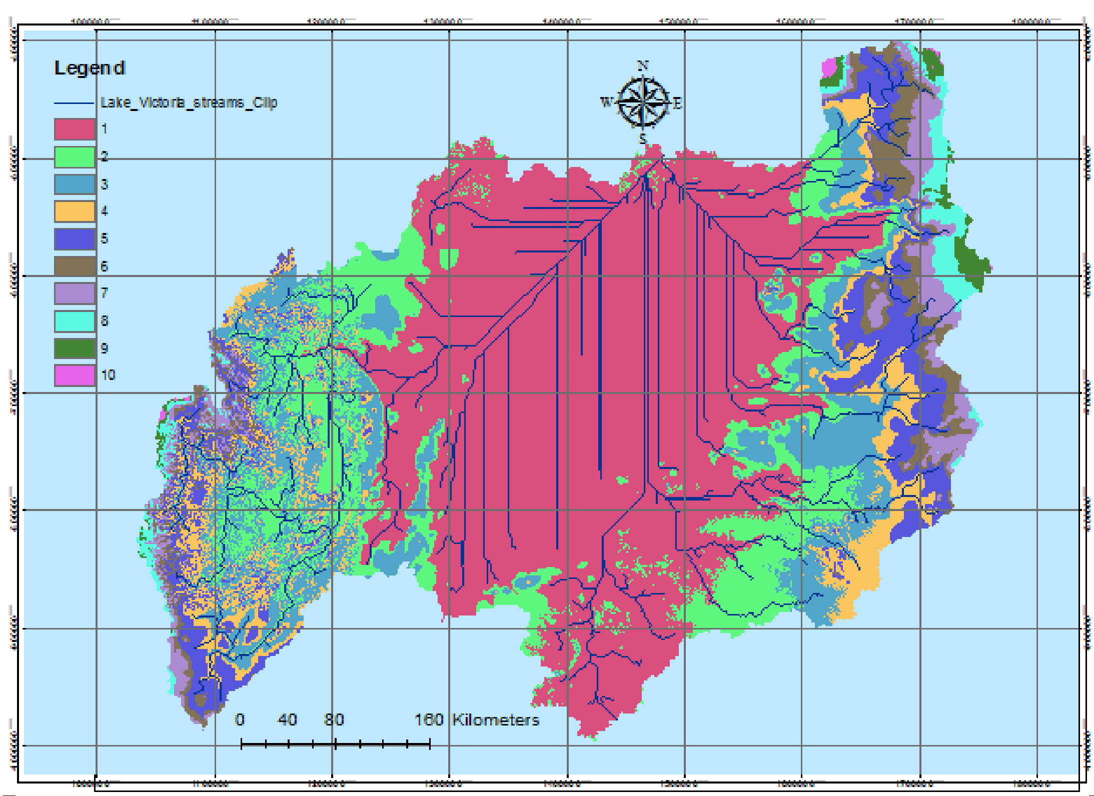

Figure 4-45: Elevation Zones for Lake Victoria Catchment

4.9.1 Data input for the Model-ENKI framework

For every hydrological model, care has to be taken on which type of dataset is required as its input and what the intended outcome will be. For this study, a distributed hydrological model was considered suitable. ENKI, a hydrological modelling framework and evaluation of distributed rainfall-runoff was for the simulation of temporal processes in spatial variables.

ENKI extracts information based on the land use maps and lake area. To enable ENKI read data from two forms, the DEM map was reclassified such that the land area was assigned 1 while the lake area assigned 0. Outside the project area, it is considered -9999. This reclassification also took into consideration the spatial distribution of the input data, especially the climate data, hence reclassification corresponded to the 50 x 50 km climate data grids.

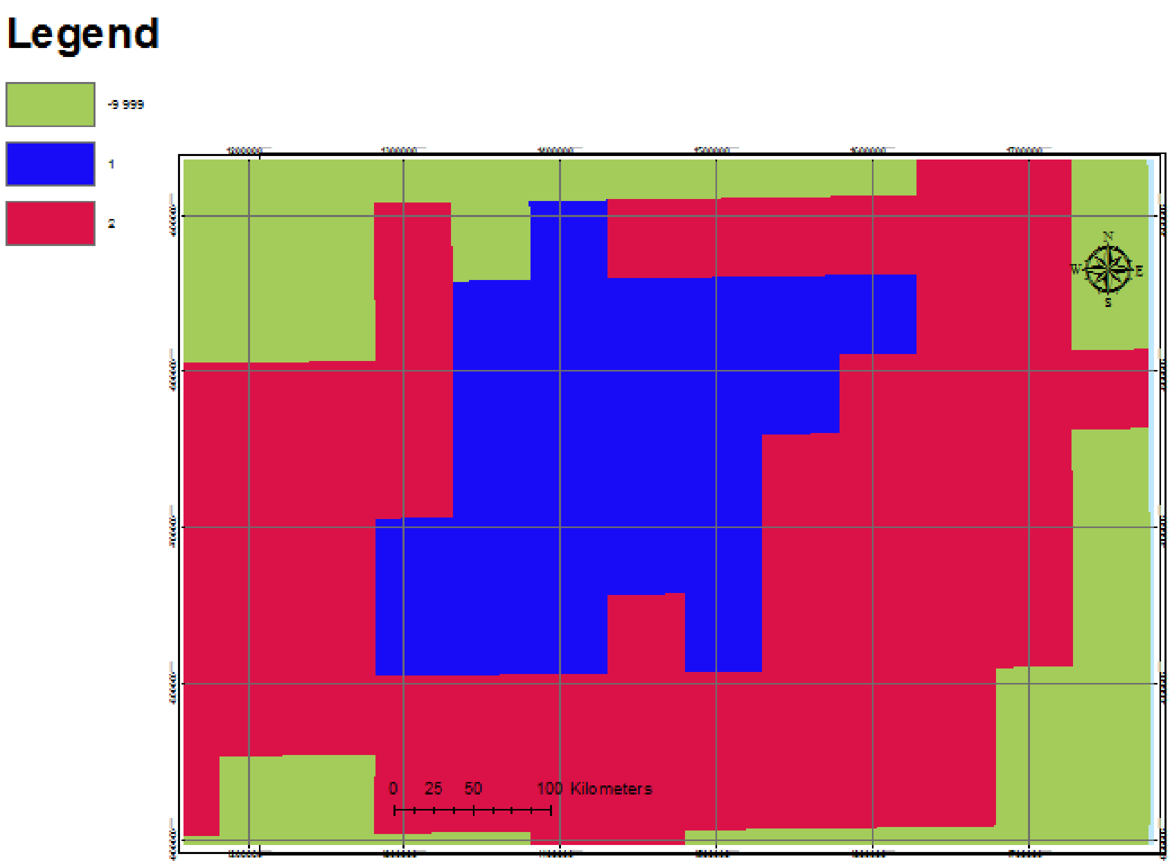

Figure 4-46: IDRISI map for the Catchment

For ENKI to interprete the data fed into the system, the GIS maps have to be converted to IDRISI. LSDTopoToolbox was used for the conversion of the DEM raster maps into the IDRISI (.rst) format. LSDTopo uses GDAL_translate as an interface for conversion.

For the climate and hydrological data, the data has to be converted to ASCII (.asc). This is a plain text format converted from the an excel file to text using the "Tab text delimited" For example see figure below;

A	B	C	D	E
Data Source	NCDC CDO/UNMA		ditto	ditto
STNR	GHCND:KEM00063686	GHCND:KE000063661	GHCND:TZ000063756	GHCND:TZ000063733
Name	Eldoret	Kitale	Mwanza	Musoma
Network	pstatscf	pstatscf	pstatscf	pstatscf
Point ID	1	2	3	4
Refsystem	utm-36n	utm-36n	utm-36n	utm-36n
xcoord	749202.34	722560.65	490772.68	588992.58
ycoord	44688.49	112367.54	-272679.60	-165811.71
HOH	2115.6	1875	1140	1147
Missing	-9999	-9999	-9999	-9999
01.01.1980	0.00	0.25	1.78	0.00
02.01.1980	-	0.00	0.00	0.00
03.01.1980	0.00	0.00	0.00	0.00

5.0 ENKI Model setup.

5.1 Calibration and Validation with Enki

Calibration by ENKI can be done in two ways; manual and automatic calibration. The Random Monte Carlo algorithm was used in this study due to its ability to perform computations by a probabilistic interpretation. This method is a robust optimization routine designed to find the global optimum also in highly irregular response surfaces. The routine may require thousands of model evaluations to converge, in particular if many parameters are optimized (SINTEF, 2003).

During the model setup, establishment of the parameter set was built based on the Tropical African climate and most of the parameters had references on lake Tana in Ethiopia. The main inputs to the model are climate data (temperature, rain, wind speed, relative humidity and net radiation) and the hydrological data (runoff, outflow and lake water levels).

In this study, the hydrological input used was the aggregated inflow from the sub-catchments into the lake as opposed to using the regulated outflow from the lake.

Calibrations were done based using two data types ie based on the reanalysis and the observed data sets. The Priestley Taylor method employed for estimation of the evaporation ***due to challenges in obtaining the detailed meteorological data like the wind speed and relative humidity for the catchment.***

The results from these calibrations and simulations were evaluated based on the model performance (NSE), the volume of water (Accumulative difference) and responses to the input parameters.

The period for the data sets that were entered into the models was from 01.01.1980-31.12.2010. During the calibration, the model considers the first year for calibration stabilization and hence termed as “warm up” period.

In computation of the water balance for the lake, it was assumed that the lake sides (banks) were vertical since there was no bathymetry data for determination of the Area-Volume curve for the lake.

5.2 Calibration using the Reanalysis data

Calibration of the reanalysis data was done based on two accounts. Firstly, with the precipitation not corrected and later with the corrected precipitation. Further, the period for calibration was chosen based on the fairness of the inflow data and this was from 1981-1989.

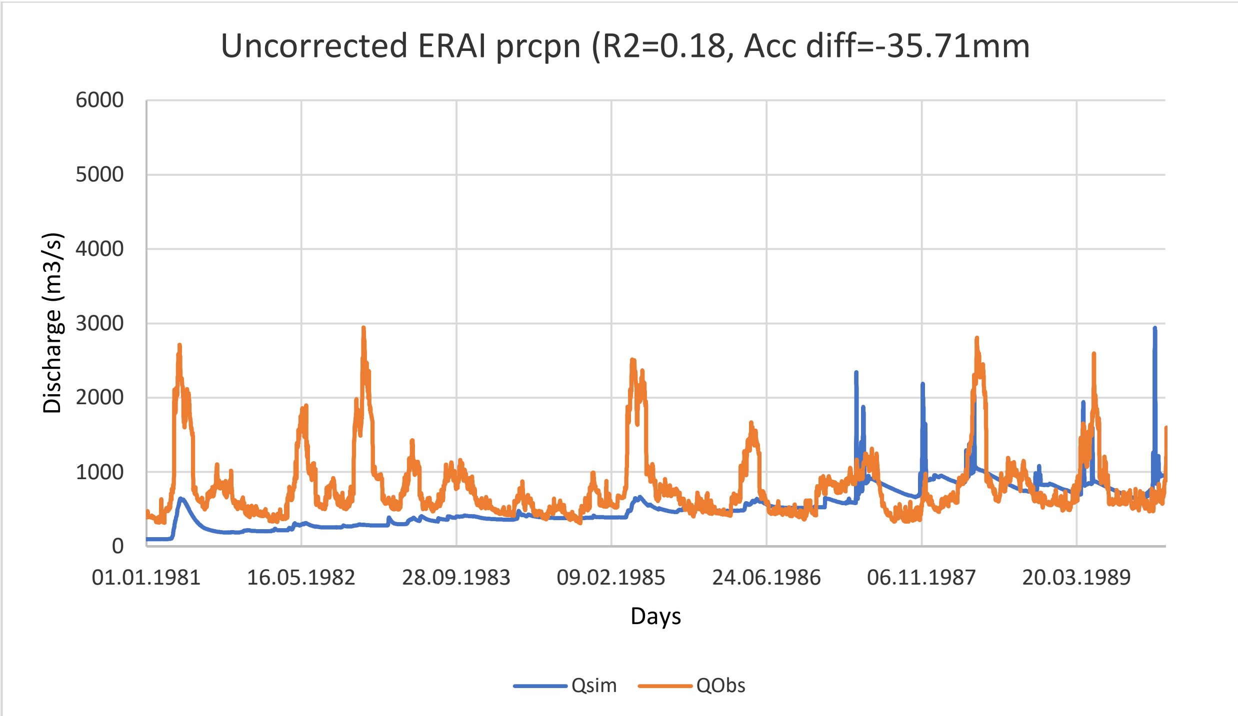

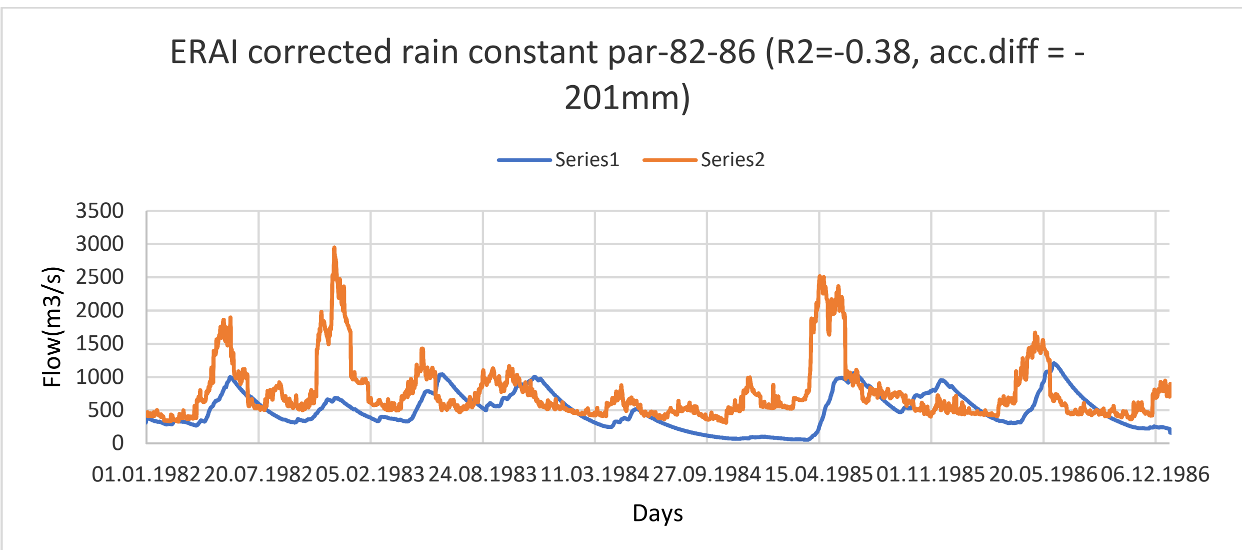

Figure 5-1: Calibration of Reanalysis data

5.3. Calibration using the GHCND/Observed data

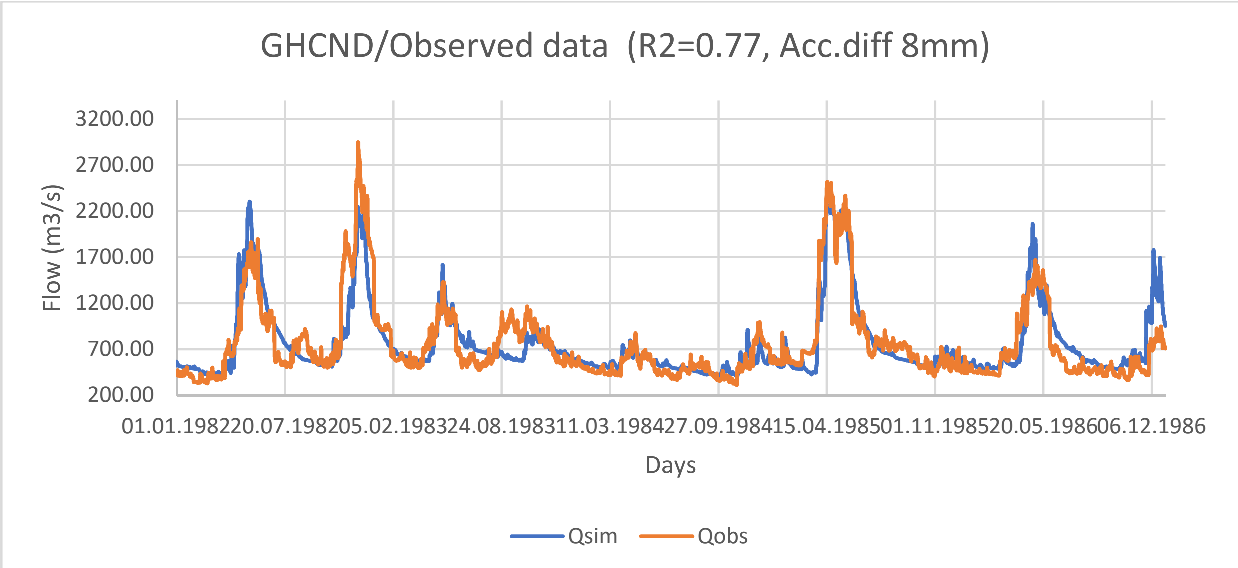

Figure 5-2: Calibration of the GHCND Data

The other possibility for the very low R2 could be as a result of the underestimation of the precipitation based on the reanalysis data. However, a correction to the precipitation was made to the data. Much as the precipitation values were improved, the calibration response was not good.

Calibration Results and analysis

1. **Calibration of the reanalysis data**

   a) **Not biased precipitation**

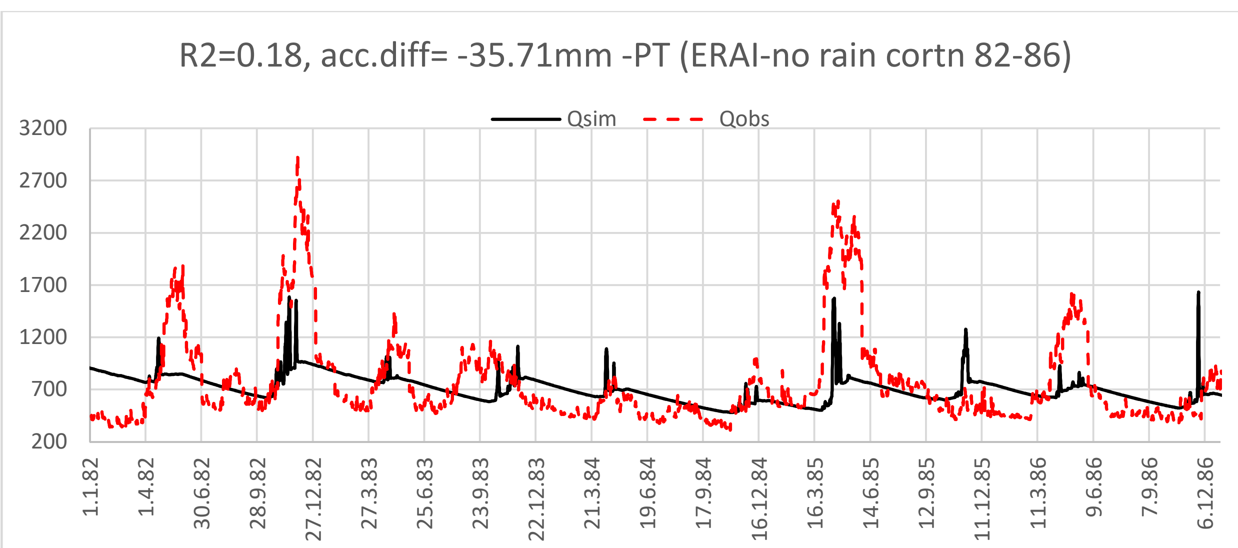

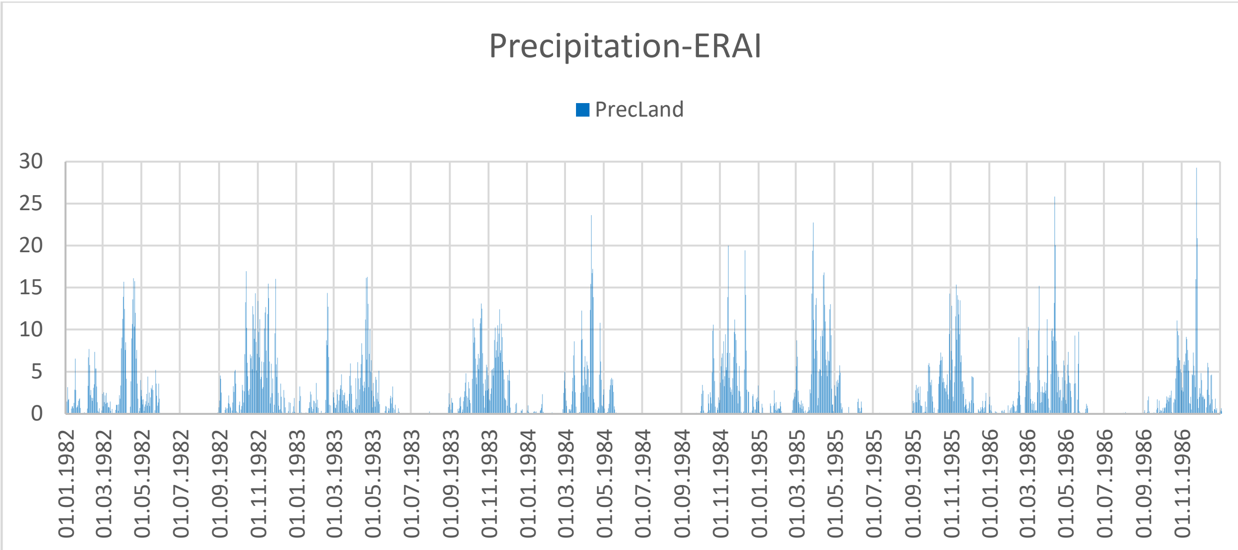

a) Biased Reanalysis precipitation calibration

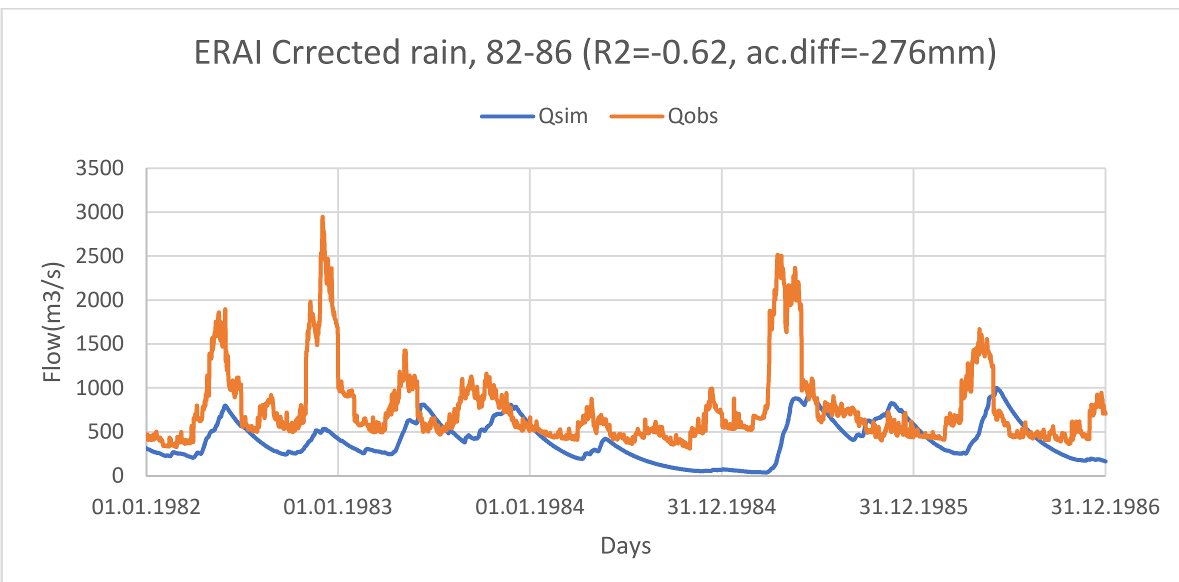

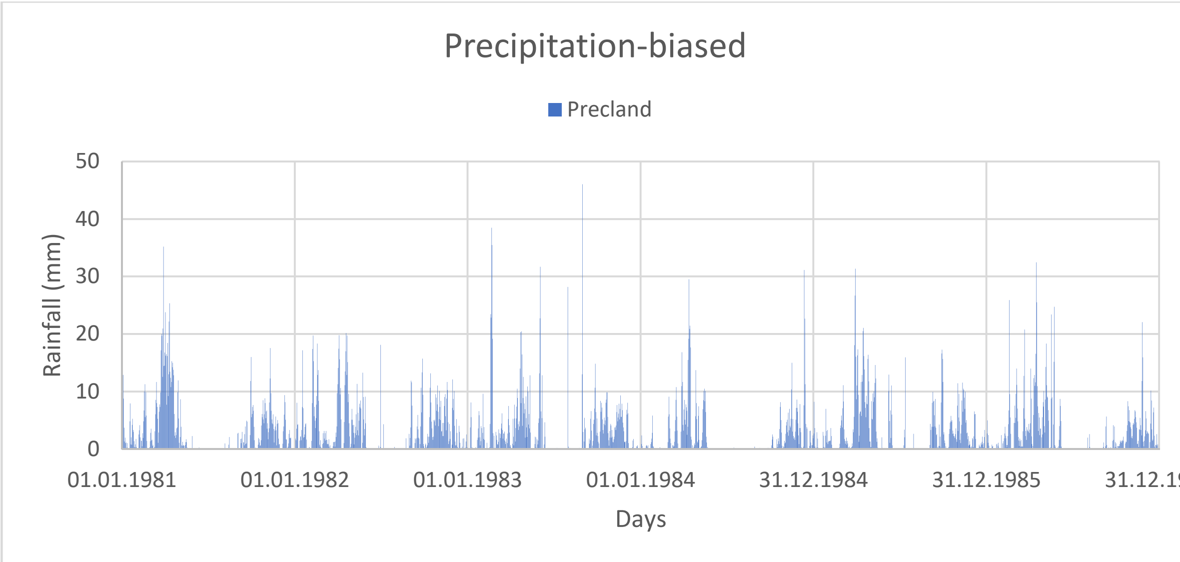

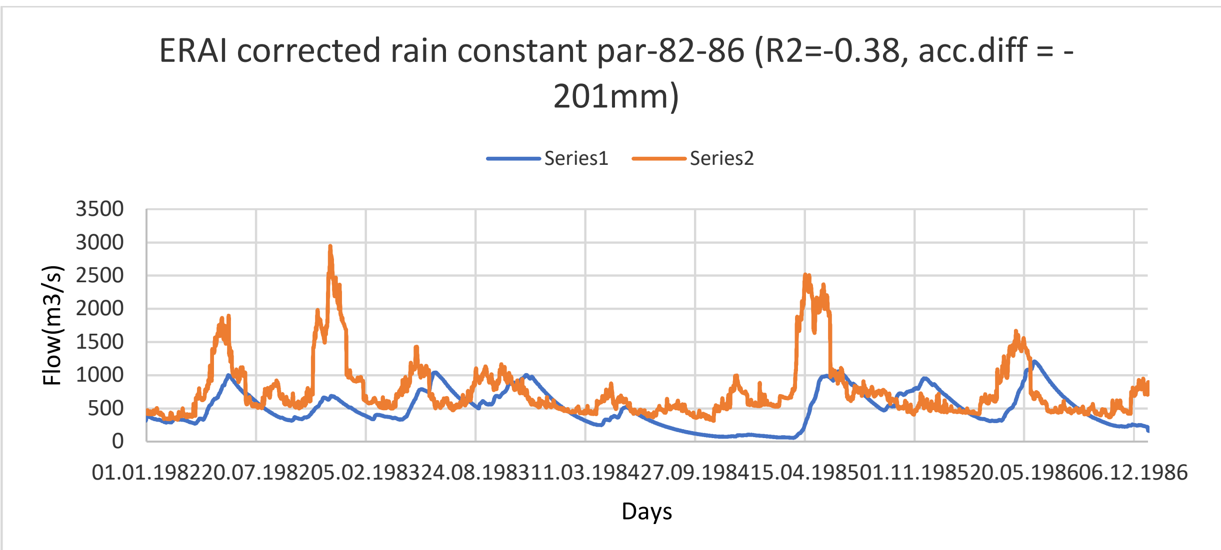

The figure above for calibration of the biased reanalysis data with some of the parameters made constant like the radiation correction, relative correction and wind correction. This was done to check how it would differ when the same parameters are not constant/uniform.

The result as seen has no much difference.

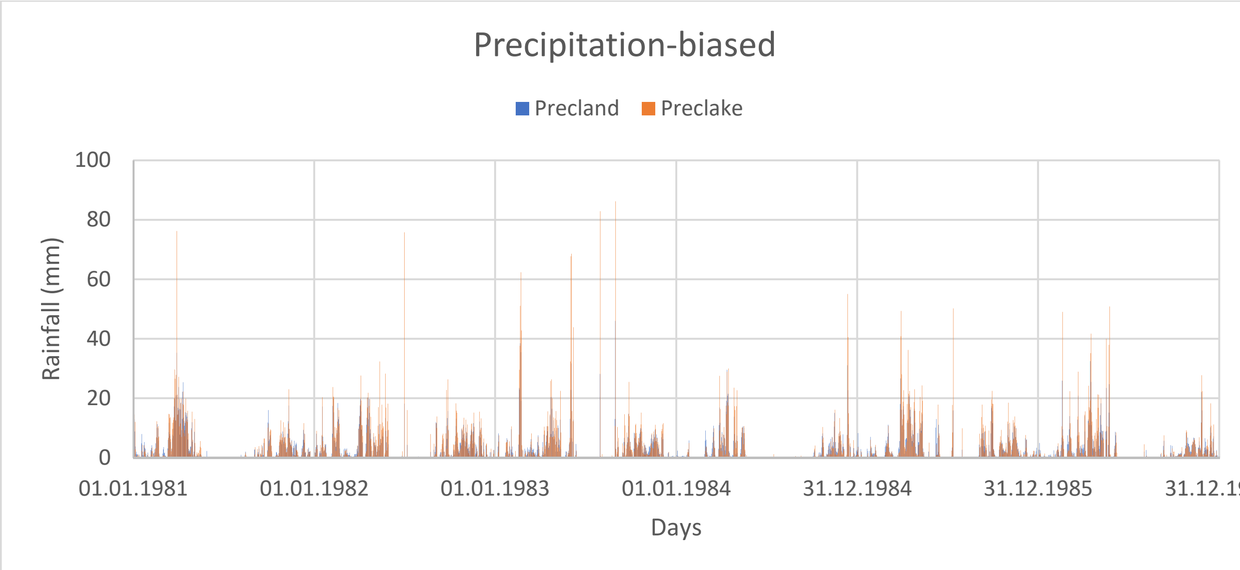
Precipitation-biased
Precland
Preclake
100
80
60
40
20
0
Rainfall (mm)
01.01.1981
01.01.1982
01.01.1983
01.01.1984
31.12.1984
31.12.1985
31.12.19
Days

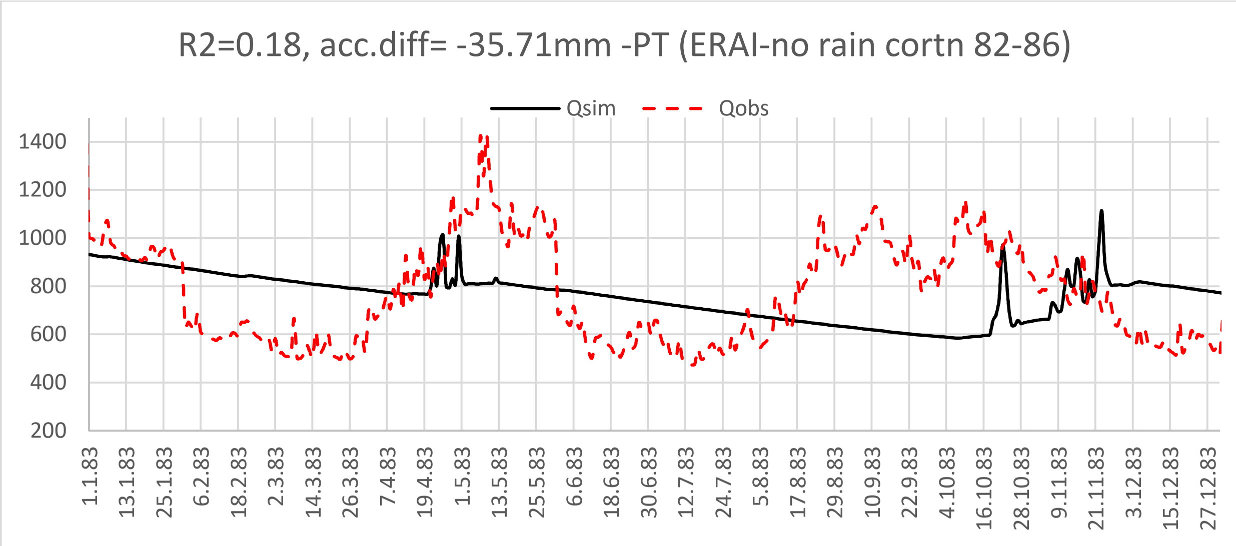
R2=0.18, acc.diff= -35.71mm -PT (ERAI-no rain cortn 82-86)
Qsim
Qobs
1400
1200
1000
800
600
400
200
1.1.83
13.1.83
25.1.83
6.2.83
18.2.83
2.3.83
14.3.83
26.3.83
7.4.83
19.4.83
1.5.83
13.5.83
25.5.83
6.6.83
18.6.83
30.6.83
12.7.83
24.7.83
5.8.83
17.8.83
29.8.83
10.9.83
22.9.83
4.10.83
16.10.83
28.10.83
9.11.83
21.11.83
3.12.83
15.12.83
27.12.83

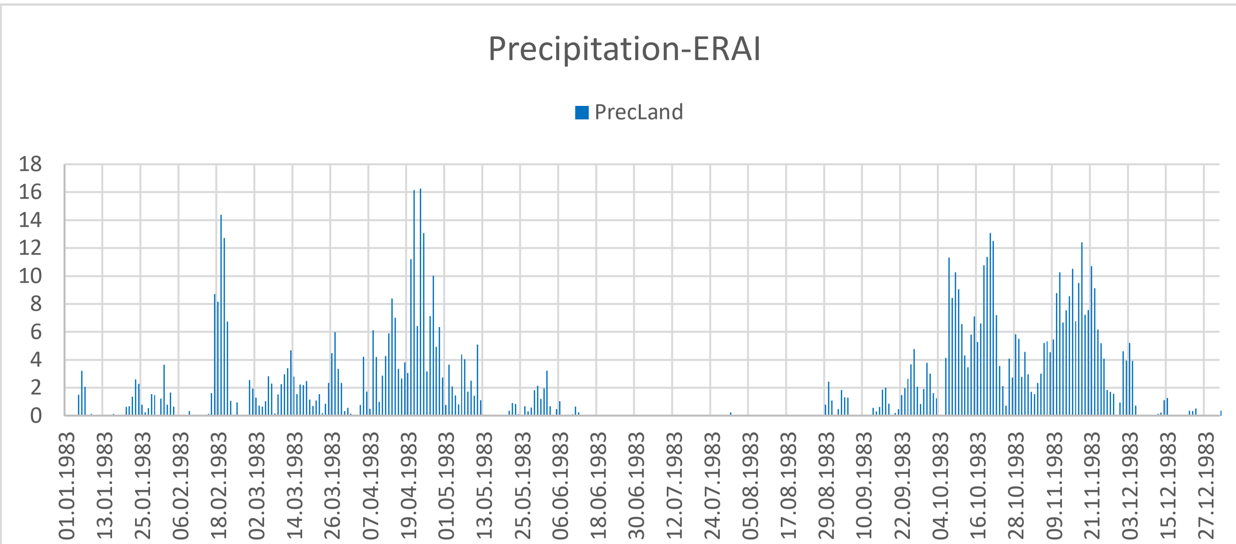
Precipitation-ERAI
PrecLand
18
16
14
12
10
8
6
4
2
0
01.01.1983
13.01.1983
25.01.1983
06.02.1983
18.02.1983
02.03.1983
14.03.1983
26.03.1983
07.04.1983
19.04.1983
01.05.1983
13.05.1983
25.05.1983
06.06.1983
18.06.1983
30.06.1983
12.07.1983
24.07.1983
05.08.1983
17.08.1983
29.08.1983
10.09.1983
22.09.1983
04.10.1983
16.10.1983
28.10.1983
09.11.1983
21.11.1983
03.12.1983
15.12.1983
27.12.1983

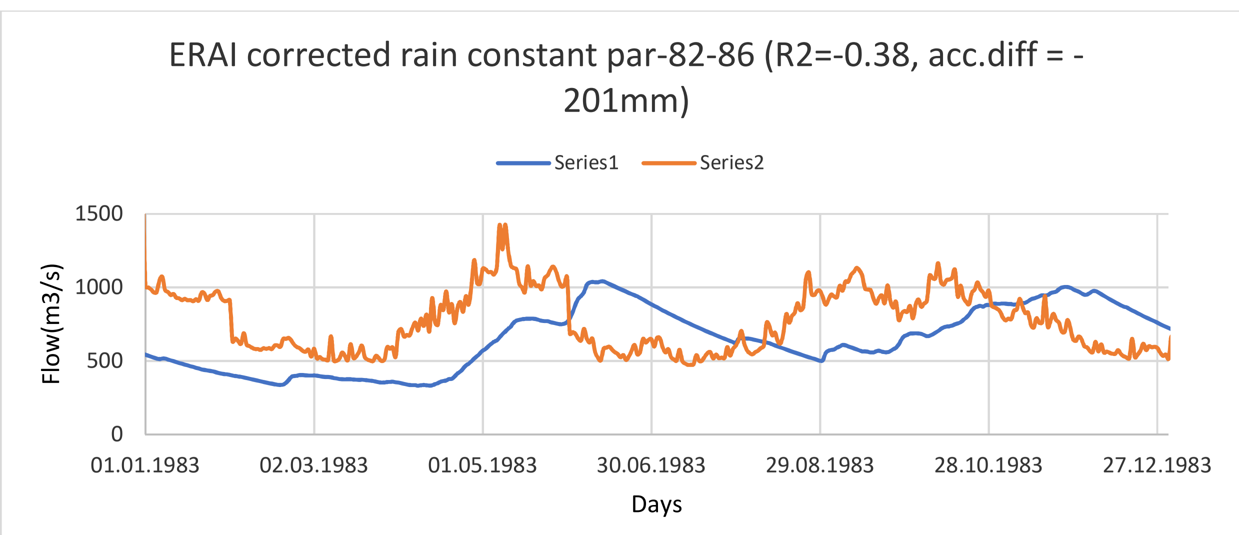
ERAI corrected rain constant par-82-86 (R2=-0.38, acc.diff = -201mm)
Series1
Series2
Flow(m3/s)
1500
1000
500
0
01.01.1983
02.03.1983
01.05.1983
30.06.1983
29.08.1983
28.10.1983
27.12.1983
Days

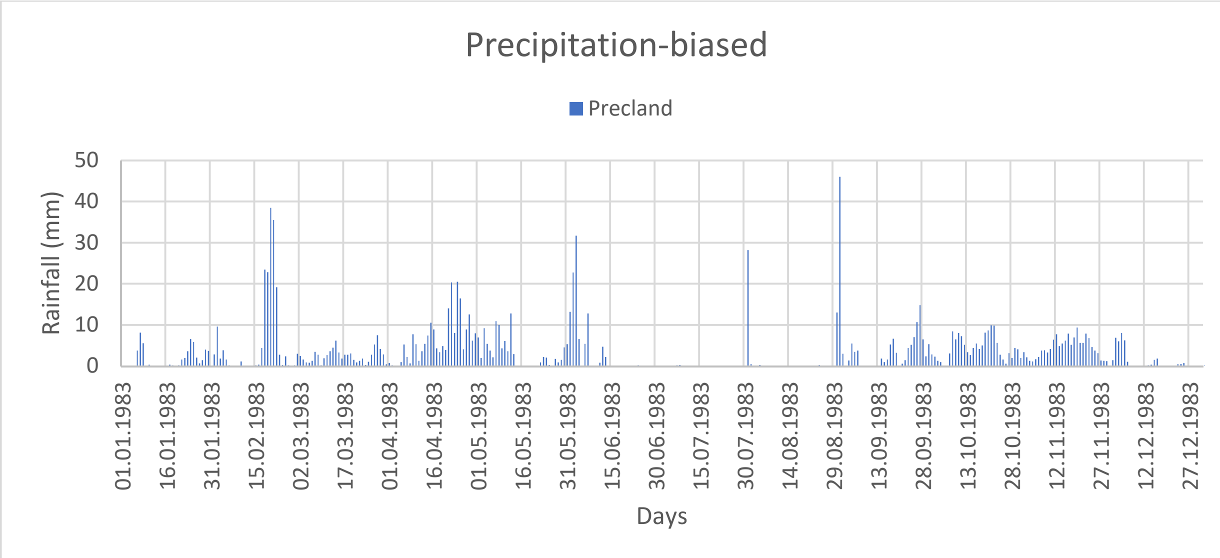

Explanation for the discrepancies in the hydrographs within the period of 1983 year.

- The precipitation pattern shows that there are two seasons in the year on both un-biased and biased simulations. These are between March and May and September and November. And due to low precipitations, it is quite difficult for the simulated flow to pick up the peak or even match the rhythm of the observed flow.
- For both situations, the simulated inflow tends to respond to the precipitation towards the end of the precipitation periods (end of May and November). This could be due to the expanse of the catchment whereby it takes time before the base flow is realized.
- From the parameter set table, it was noted that as the precipitation correction factor rcorr is high, the precipitation is low. Where as it suggests that about 13% of the rain into the catchment was lost by biasing *(table: calibration parameters for reanalysis data)*, it recorded higher precipitation compare to the u-biased with 8% increased precipitation.

2. **Calibration of the GHCND-observed data**

   a) **Automatic calibration**

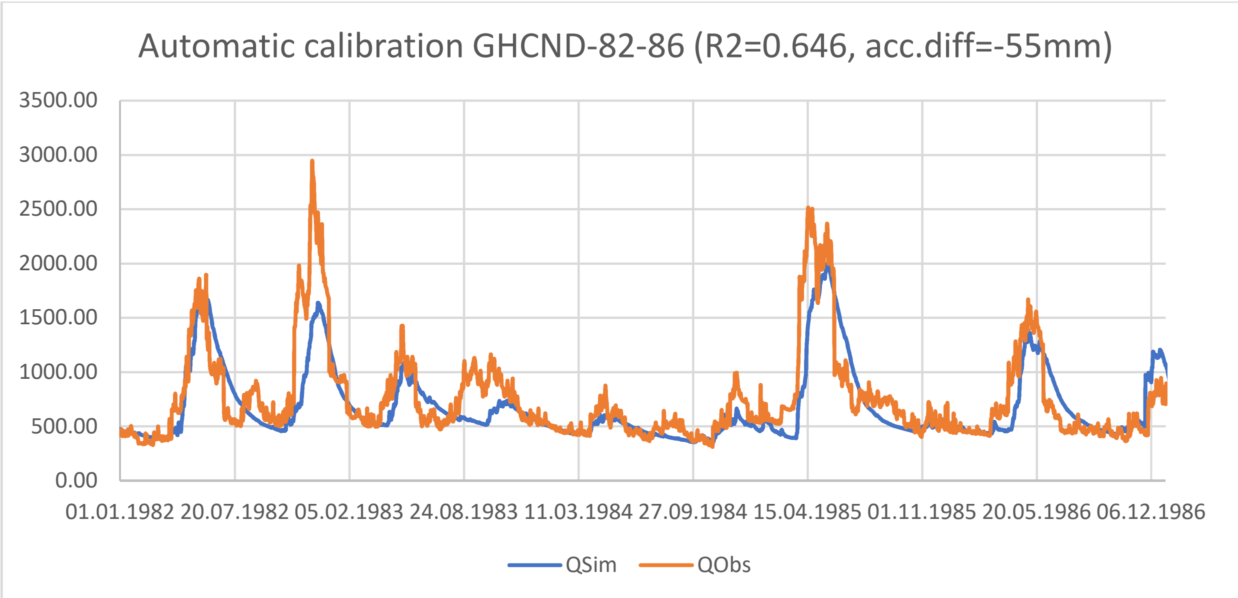

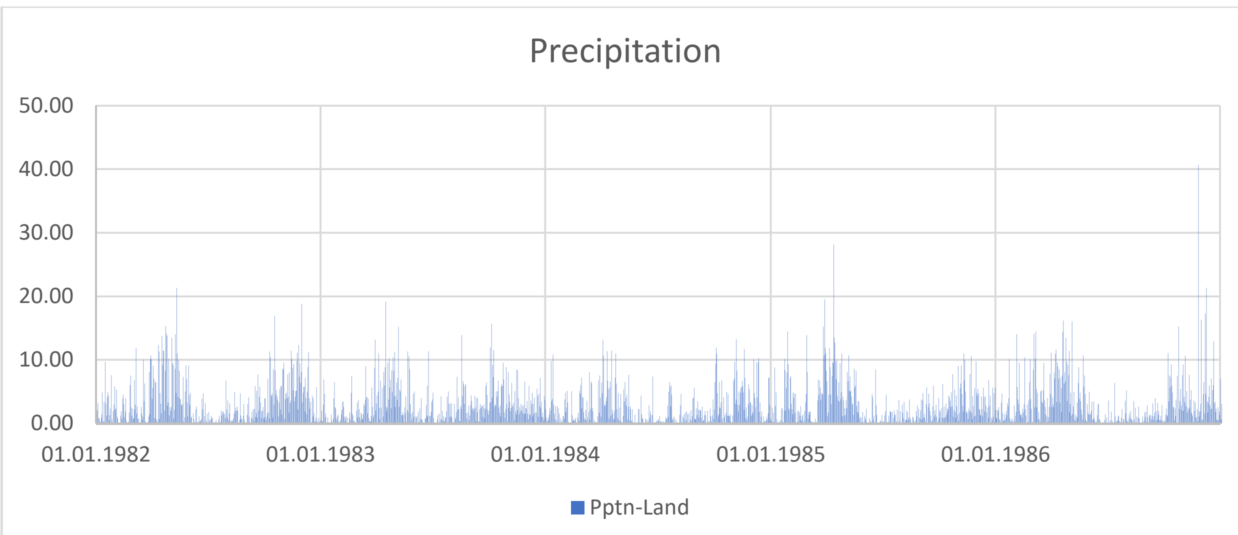

b) Manual calibration

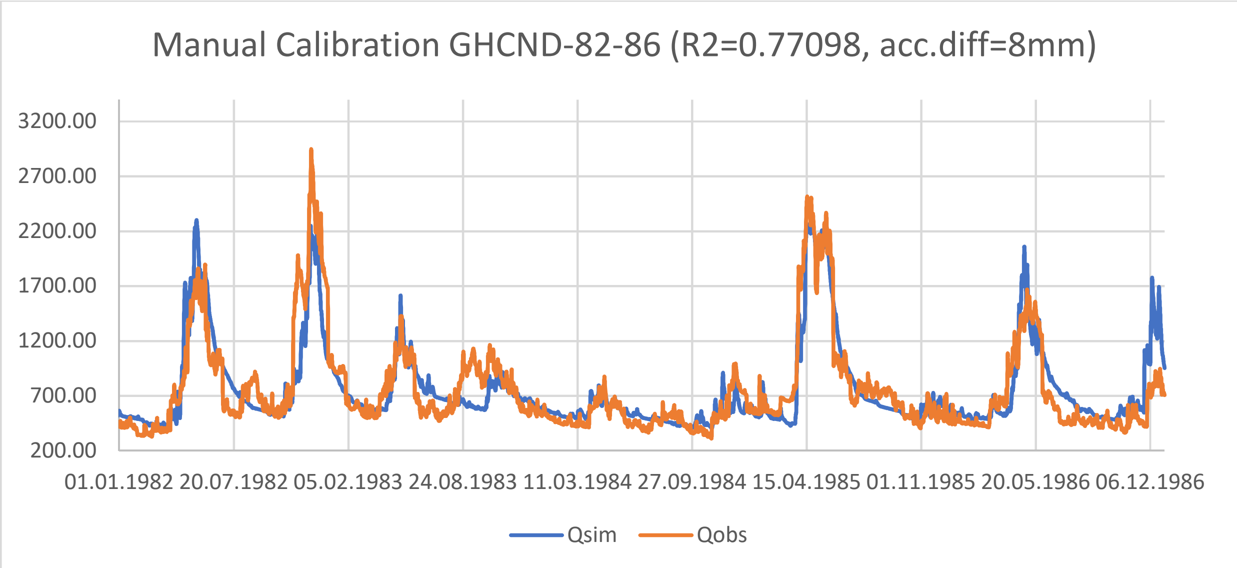
Manual Calibration GHCND-82-86 (R2=0.77098, acc.diff=8mm)
3200.00
2700.00
2200.00
1700.00
1200.00
700.00
200.00
01.01.1982 20.07.1982 05.02.1983 24.08.1983 11.03.1984 27.09.1984 15.04.1985 01.11.1985 20.05.1986 06.12.1986
Qsim
Qobs

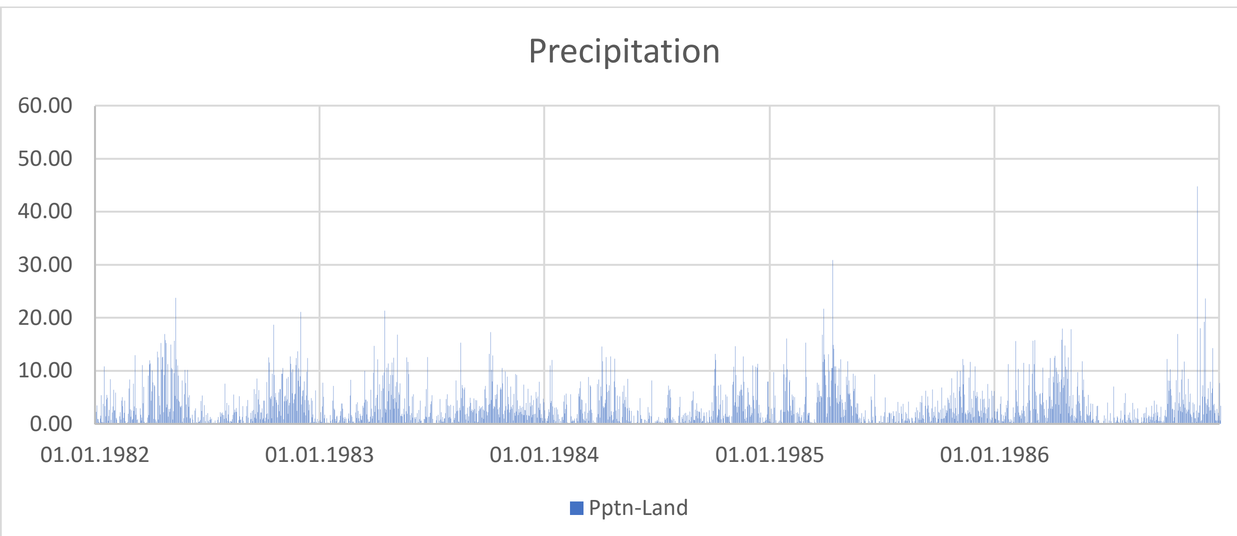
Precipitation
60.00
50.00
40.00
30.00
20.00
10.00
0.00
01.01.1982
01.01.1983
01.01.1984
01.01.1985
01.01.1986
Pptn-Land

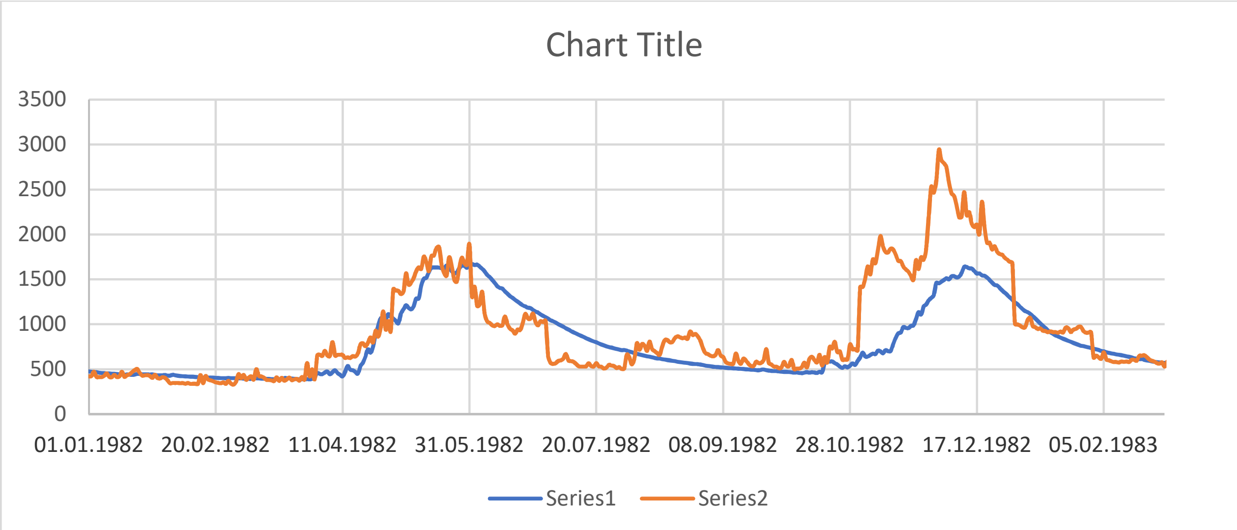
Chart Title
3500
3000
2500
2000
1500
1000
500
0
01.01.1982
20.02.1982
11.04.1982
31.05.1982
20.07.1982
08.09.1982
28.10.1982
17.12.1982
05.02.1983
Series1
Series2

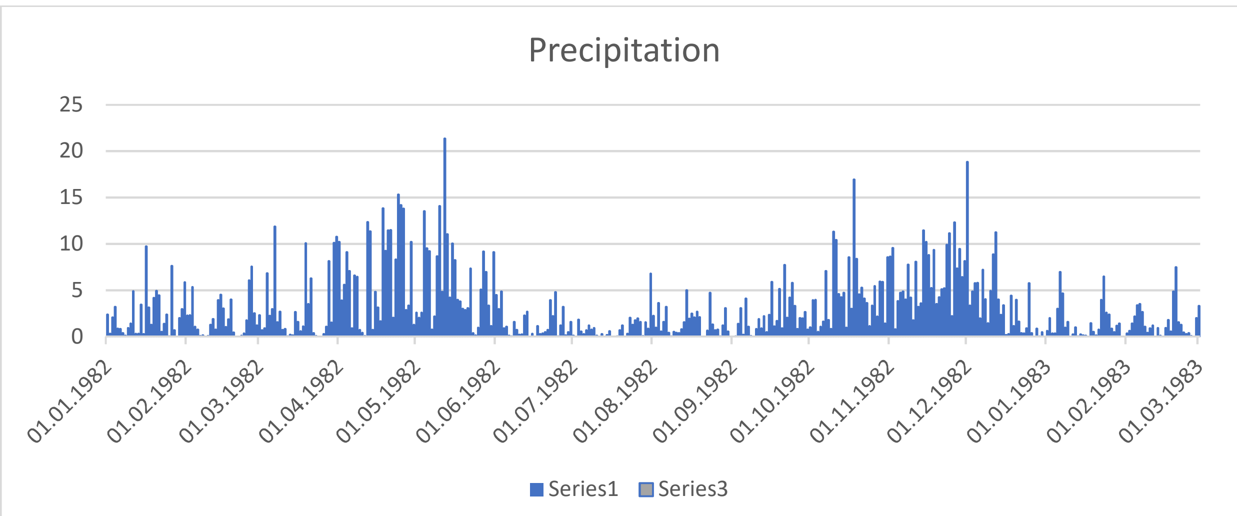
Precipitation
25
20
15
10
5
0
01.01.1982
01.02.1982
01.03.1982
01.04.1982
01.05.1982
01.06.1982
01.07.1982
01.08.1982
01.09.1982
01.10.1982
01.11.1982
01.12.1982
01.01.1983
01.02.1983
01.03.1983
Series1
Series3

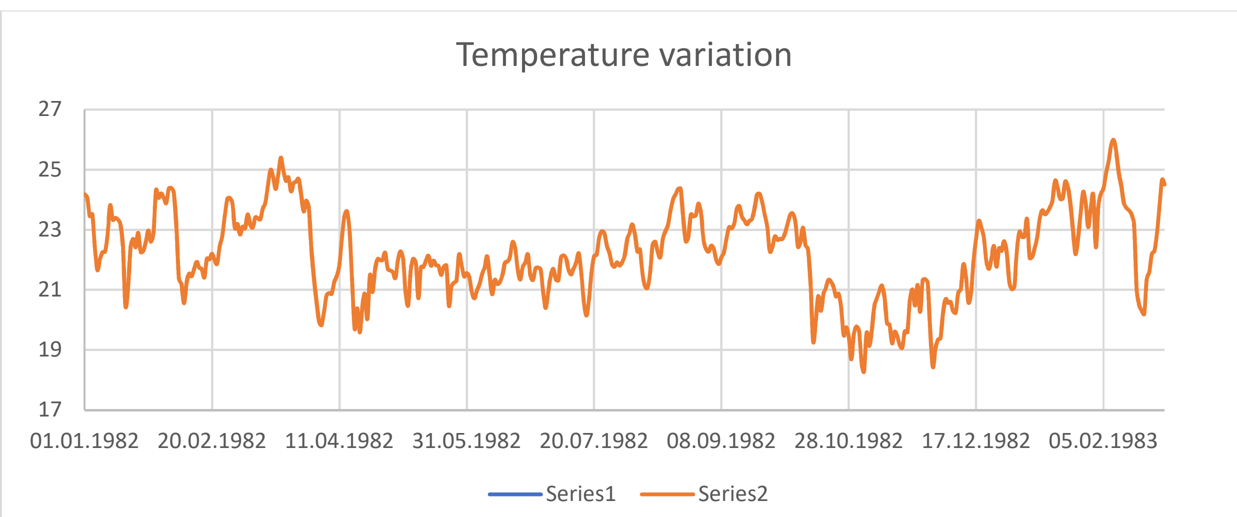
Temperature variation
27
25
23
21
19
17
01.01.1982
20.02.1982
11.04.1982
31.05.1982
20.07.1982
08.09.1982
28.10.1982
17.12.1982
05.02.1983
Series1
Series2

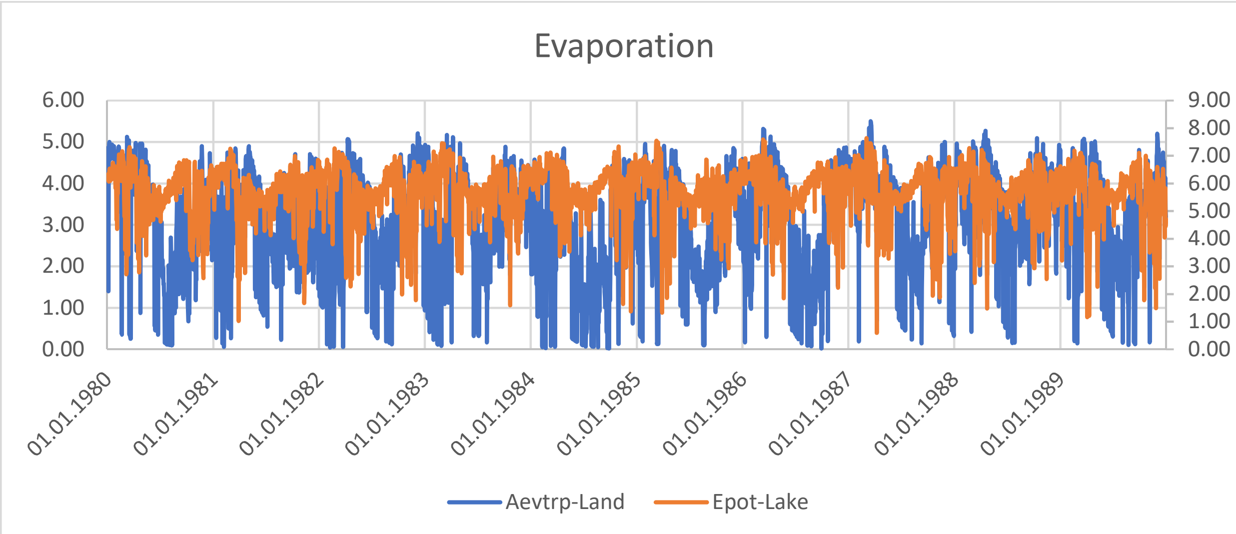

3. Discussions on discrepancies

a) Table of calibration parameters

Reanalysis Data	**Precipitation not biased**	**Biased Precipitation**
Calibration Period	1982-1986	1982-1986
Parameter:		
precgrad	4.68272	4.97615
raincorr	1.08486	0.867252
c1soil	-0.69468	0.823438
c2soil	1	1
alphaland	1.26	1.27589
alphalake	1.40765	1.40651
lakeZ	46.3094	46.3094
Kth	1	1.28134
soildepth	0.2	0.2
FC	392.032	563.128
LP	0.731721	0.972848
beta	1.433	4.47519
k2	0.426878	0.086219
k1	0.385633	0.031584

k0	0.002414	0.011795
perc	9.51719	9.09658
tresh	43.3206	0.751167
Tcorr	0.968192	1.11862
Windcorr	1.04033	1.1078
NRadcorr	0.819783	1.03471
RHcorr	0.919517	1.18039
PerfMeasure:		
Temporal R2	**0.18**	**-0.38**

Table 5-1: Reanalysis Calibration Parameters

Table of calibration parameters for Reanalysis data

Calib Period	**1981-88**	**1982-88**	**1982-86**	**1982-86**	**1982-86**	**1982-86**
Param Set	Auto Calib	Auto Calib	Auto Calib	Manual Cali	Manual Calib	Manual Calib
precgrad	3.958	2.21108	3.95843	4.850	4.58	4.58
raincorr	0.916	1.02928	0.918	0.924	1	1
c1soil	0.349	-0.348686	0.349284	0.754	-1.48	-1.48
c2soil	1.000	1	Uniform			
alphaland	1.204	1.20303	1.20427	1.206	1.21	1.21
alphalake	1.370	1.3376	1.36975		1.37	1.3697
lakeZ	46.309	46.3094		46.310		
Kth	0.973	0.602681	0.972621	1.086	0.6	0.62
soildepth	0.200	0.2	Uniform			
FC	299.538	430.261	299.538	299.540	455	455
LP	0.711	0.927676	0.71099	0.999	0.999	0.999
beta	1.176	1.23349	1.1762	1.150	1.22	1.22
k2	0.012	0.118524	0.01191	0.007	0.006	0.0006
k1	0.062	0.121044	0.062048	0.158	0.118	0.118
k0	0.002	0.005419	0.001975	0.002	0.004	0.004
perc	0.583	1.81014	0.58265	0.939	0.95	0.95
tresh	3.396	19.8659	3.39559	4.650	11.4	11.4
PerfMeasure:						

Temporal R2	**0.473**	**0.453814**	**0.646**	**0.770**	**0.758**	**0.7605**
Validation			**0.496**	**0.568**	**0.554**	**0.5681**
E/P (Lake)	1.79		1.59	1.85	1.70	
E/P(Land)	0.88		0.90	0.88	0.89	
Acc. Difference (mm)	-11.75	-74.46	-55.79	7.92	-5.31	

Table 5-3 : GHCND Calibration parameters

Paramater dataset for calibration of the model

b) Table of simulation results

	Land temp(°C)	Land pptn (mm)	Land actpot(mm mm)	runoff (mm)	Lake temp(°C)	Lakepptn(mm)	Epot (mm)	Av Qsim (m3/s)	Evp /Pptn	Epot/ lkpptn
GHCND Manual	22.75	3.06	2.70	0.33	23.40	3.10	5.73	762.86	0.88	1.85
GHCND auto	22.75	2.98	2.66	0.30	23.40	3.09	5.73	683.31	0.89	1.85
ERAI	22.03	2.09	1.81	0.31	22.66	2.13	4.78	708.38	0.87	2.24
ERAI-Biased	22.75	3.02	2.07	0.18	23.40	4.17	5.86	404.33	0.69	1.40

	R2	Acc.diff(mm)	RVE (%)	Av. Outflow ($Millm^3$)	Water balance
GHCND Manual	**0.77**	7.98	1.31	87.78	
GHCND auto	**0.65**	-55.79	-9.25	87.78	
ERAI	**0.18**	-35.71	-5.92	87.78	
ERAI-Biased	**-0.38**	-279.21	-46.30	87.78	

	Lake pptn(Milm^3)	Epotlake(Milm^3)	Inflow Qsim(Milm^3)	AvOutflow(Milm^3)	Water Balance(Milm^3)
GHCND Manual	211.09	389.72	65.91	87.78	-200.50
GHCND auto	210.33	389.72	59.04	87.78	-208.12
ERAI	144.93	324.88	61.20	87.78	-206.52
ERAI-Biased	283.68	398.32	34.93	87.78	-167.49

A water balance table

c) Testing the reanalysis data with the parameters from the manual calibration.

Having calibrated the reanalysis data both biased and un-biased, it was seen that the un biased gave a fair performance compared to the biased. However further calibration of the same did not yield fair results, hence adoption of the sparsely distributed ground based data.

It was later found it necessary to check the response of the reanalysis data to the parameters used in the ground based data by carrying out a simulation. The results from the simulation showed some amazing results on both cases as shown in the figures below

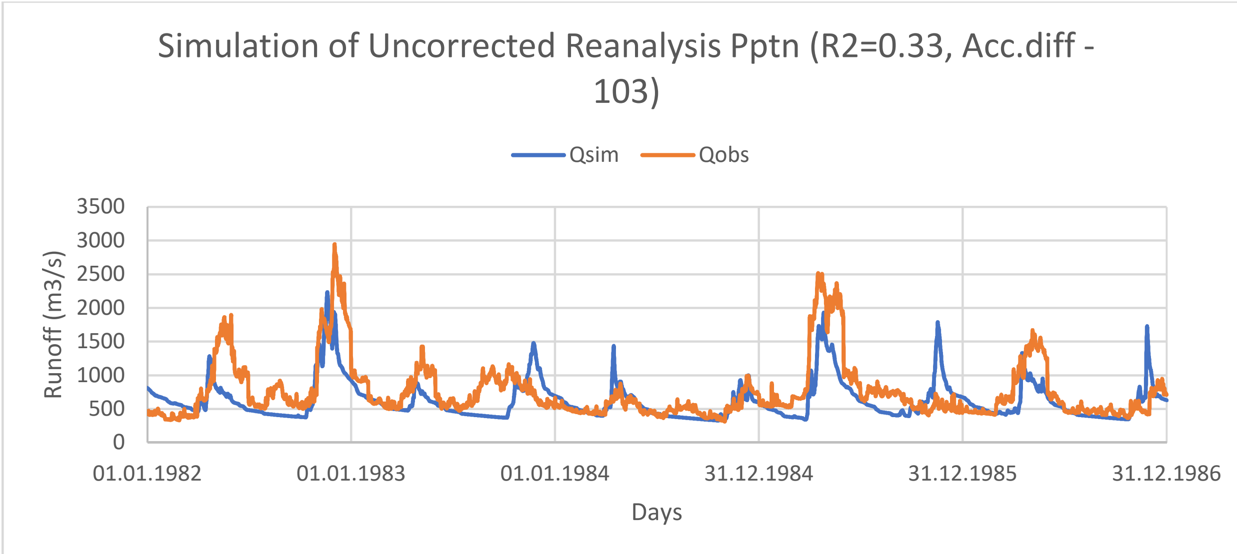
Simulation of Uncorrected Reanalysis Pptn (R2=0.33, Acc.diff -103)
Qsim
Qobs
Runoff (m3/s)
3500
3000
2500
2000
1500
1000
500
0
01.01.1982
01.01.1983
01.01.1984
31.12.1984
31.12.1985
31.12.1986
Days

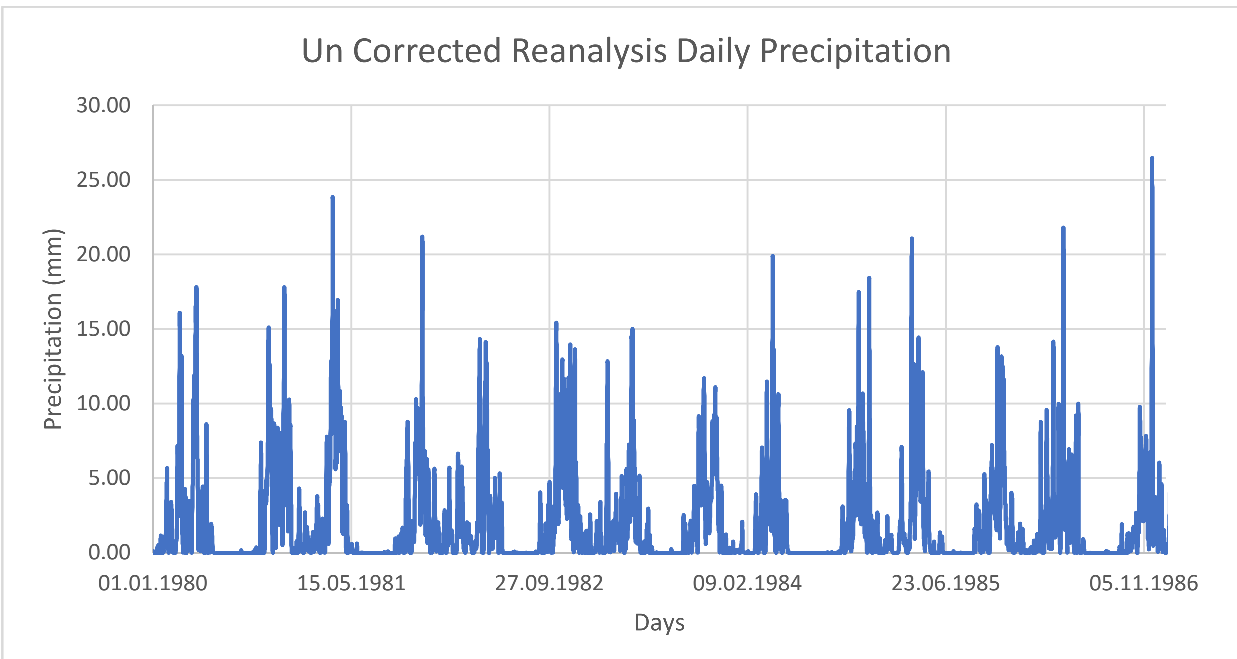
Un Corrected Reanalysis Daily Precipitation
Precipitation (mm)
30.00
25.00
20.00
15.00
10.00
5.00
0.00
01.01.1980
15.05.1981
27.09.1982
09.02.1984
23.06.1985
05.11.1986
Days

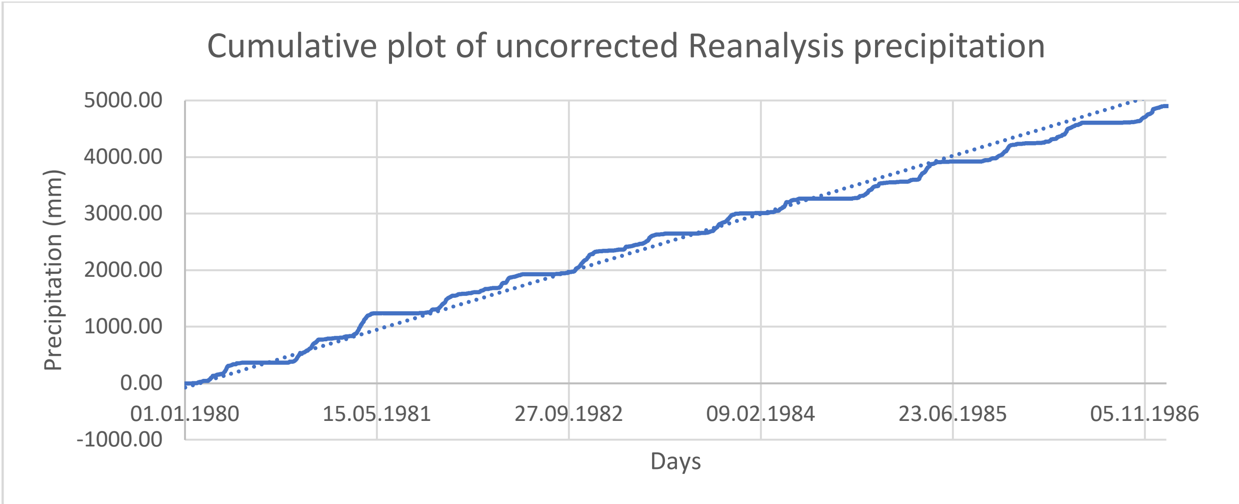
Cumulative plot of uncorrected Reanalysis precipitation
Precipitation (mm)
5000.00
4000.00
3000.00
2000.00
1000.00
0.00
-1000.00
01.01.1980
15.05.1981
27.09.1982
09.02.1984
23.06.1985
05.11.1986
Days

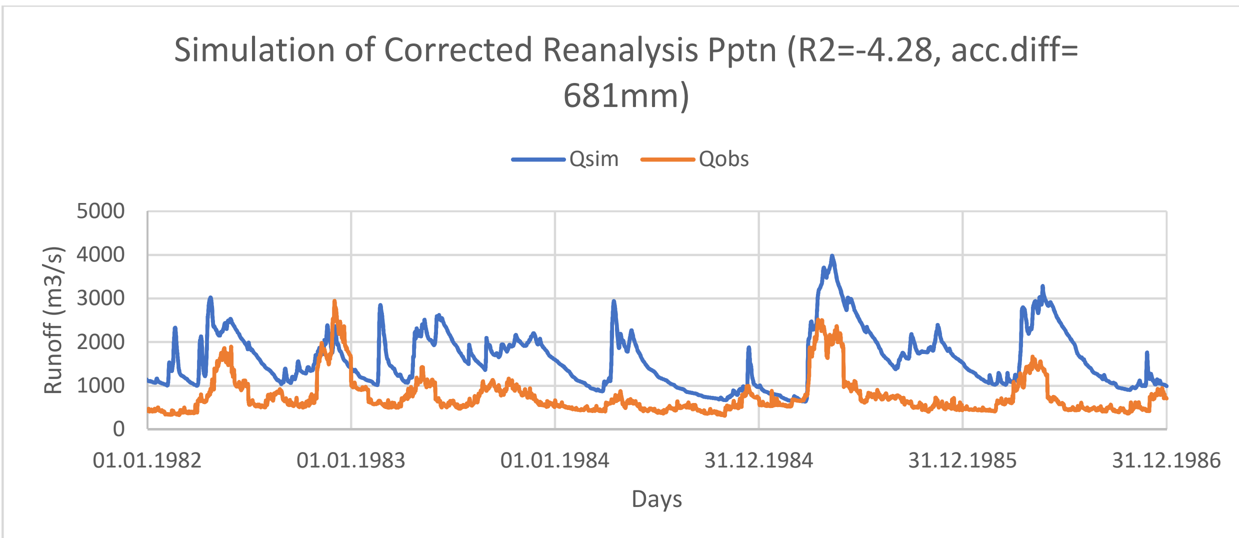
Simulation of Corrected Reanalysis Pptn (R2=-4.28, acc.diff= 681mm)
Qsim
Qobs
Runoff (m3/s)
5000
4000
3000
2000
1000
0
01.01.1982
01.01.1983
01.01.1984
31.12.1984
31.12.1985
31.12.1986
Days

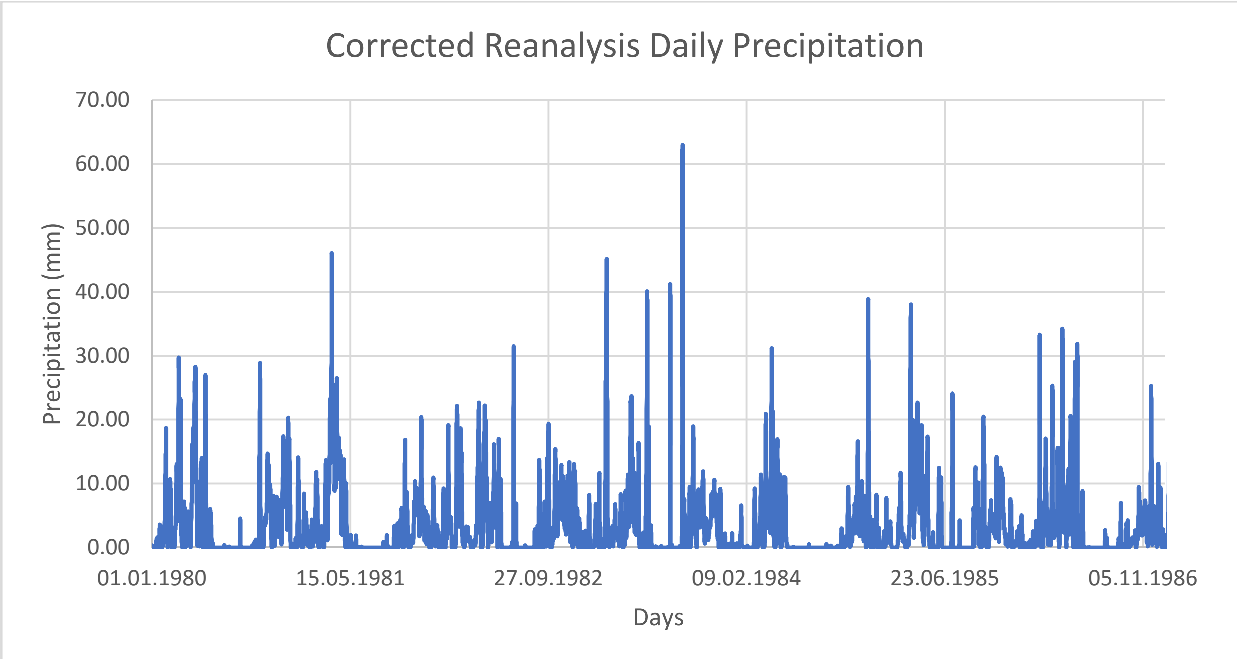

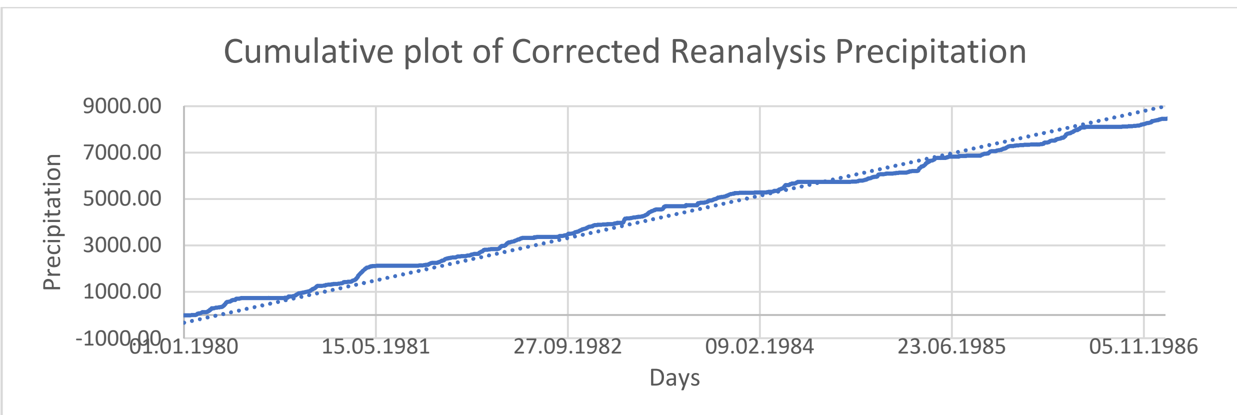

4. Conclusion on the simulations of the reanalysis data

- It was noted that the uncorrected data performance improved by more than 80% with the manual calibration parameters in terms of the R2 value ie from 0.18 to 0.33 and the accumulative difference also improved from -200mm to -103mm. This is attributed to the increase in the rainfall as seen in the simulated precipitation. Hence a prove that reanalysis underestimated the precipitation over the catchment.
- The corrected data too showed some improvement but instead showed that there was a lot of water added into the system. This is evident in the simulated hydrograph that has over shot the observed hydrograph. The accumulative difference is much greater than before the application of the manual calibrated parameters.

Discussion on the Reanalysis Calibration.

Two calibration approaches were adopted. One without bias in the rainfall and the other with rainfall bias. However, in both approaches, the corrections to the temperature, wind, radiation and relative humidity corrections were varying to be calibrate automatically. The reason for using satellite data is to aid in getting information in areas where their observation gauges are sparsely distributed or where adequate climate data cannot be achieved quite easily.

Similar to the observed GHCND data, the period of calibration was considered same ie 1982-1986 (five years) and validation for the remaining years. The study found that

- Whereas the precipitation by reanalysis data is underestimated compared to the observed data for same region, the un-biased precipitation data had fair performance in terms of the NSE, accumulative difference and RVE. Infact, judging by the accumulation difference and the RVE absolute figures, biased precipitation acc.diff and RVE percentages are about **8 times** more than the un biased.
- In the biased situation, the precipitation has improved a great extent, but the simulation indicates more inflow from the non-biased compared to the biased data. This could be attributed to the high simulated land temperature leading to a higher evaporation (in biased), hence low runoff from the biased precipitation data. Ratios of land evaporation to land precipitation is higher in un-biased than in biased (0.87 and 0.67 respectively).
- It could also be noted that there is a possibility of increased runoff from the un-biased calibration due to higher flow response parameters from the outlets of the upper tank (k2 and k1) compared to the those from the biased calibration.
- The Field capacity (FC), Treshold for minimum SM/FC (LP) and beta values for the un biased precipitation are lower than the biased. These are properties of the soil which are related to the flow of water.
- For the water balance, which is got from simulated inflow from land + lake precipitation – Epot- Outflow gives a low absolute value for the biased precipitation compared to the unbiased and even the GHCND simulations.

Discussion on the GHCND/ Observed data calibration

Explanations on the discrepancies between the observed and simulated inflow for the GHCND calibration for the period (01.01.1982-01.03.1983)

Possibilities

- The amount of precipitation over the period 01.01.1982-01.07.1982 was higher compared to the amount of precipitation over the period 01.07.1982 – 01.03.1983. This could possibly explain the discrepancies between the measured and simulated model runoff over the period. Hence, the under estimation of the flood peak could possibly be explained by the underrepresented precipitation data. Alternatively, the precipitation data quality is questionable. Furthermore, delineating discrepancies in temperature data was not easy as the correlation between the runoff and temperature is not well understood in the region.
- Further investigations were carried out to understand the discrepancies between the observed and simulated runoff by studying the calibrated parameter set within the ENKI model
- As could be inferred from the table of manual calibration parameters, the pcorr was set at 0.92 suggested that about 10% of the incoming precipitation was lost from the model. But simulations carried out by varying this parameter greatly reduces the model efficiency and hence this parameter was left unchanged.
- There are much similarities in the automatic and manual calibration of the model with exception of the simulated inflow which is about 70m3/s more than the manual simulation.
- Similar observations were made with respect to the flow response parameters k2, k1, and k0. For both calibrations, automatic and manual calibration, the k2<k1>ko, which could be difficult to explain in accordance with common hydrological practice. However, adjusting the values of these parameters manually greatly improved the performance of the model.
- Finally, iterations were carried out by varying the parameter precgrad from its initial value of 3.95, model performance was monitored with increase in precgrad and observation showed performance of the model from 0.65 to 0.77 when this parameter was increased from 3.95 to 4.85. Further increase in the parameter resulted in deterioration of model performance.
- Also noted was that during the validation of the model, it was seen to be stable even beyond the chosen period of investigation. The period chosen was between 1981-1989 (due to fair

quality of data in this period). Validation was first done for period of 1987-1989 and 1981. Further validation was done for the rest of the data period ie from 1989 to 2010 and the temporal performance value was NSE value 0.38.

- These investigations depict the complexity in understanding influence of the parameter sets on the model performance and this also points at the over parametersed nature of the ENKI model. Due to time restraints, the investigations were halted at this point in time and it is highly recommended further work be carried out to improve the model performance in the future studies.

Conclusion on the calibration of the model

- It was found that whereas reanalysis data shows an underestimation of precipitation, carrying out a bias correction did not improve the performance of the model. In fact, it showed less simulation compared to the un-biased precipitation.
- In both approaches, it shows that there are two seasons for precipitation over the catchment and these are March, April and May and in September, October and November. However, the responses to the by the inflow to the precipitation was fair for the ground based data compare to the reanalysis data. This was evident on the peaks and recessions of the inflow hydrographs of both datasets.
- Availability of the water in the basin may be highly impacted by the seasons.
- Based on the evolution of the model performance, it was found that the ground observations were giving better performance even with the sparse distribution over the catchment for which the reanalysis data would have corrected. The performance was based on the NSE value, the relative volume error (RVE) and the accumulative difference. Much of the water balance could not be ascertained since the lake storage was considered more or less like a cylinder rather than a cone. Therefore, future studies with the lake bathymetry are required.
- The model that was considered for further investigation was the manually calibrated model with R^2 value of 0.77. From the simulations, it recorded the mean values of the land air temperature.
- Further, it would be interesting to carry out the calibrations based on the individual sub catchments and a regional performance determined.

6 Climate Change Impacts Modelling on the Lake Victoria Basin

6.1 Introduction

It is envisaged in this chapter that at the at its end, the calibrated hydrological model (ENKI) will be used to simulate flows for the control periods and for computation of the design flood which will be used to evaluate, against data from the observed flow series, the design floods for the infrastructure on River Nile. To achieve the above objective, regional data from CORDEX Africa for two GCM models was downscaled. Bias corrections were performed and the evaluation of the historical RCM for driving the hydrological simulations in comparison with the historical data was done.

The climate data was taken from two models; MOHC (AFR-44_MOHC-HadGEM2-ES_rcp45_r1i1p1_SMHI-RCA4_v1_day_20960101-20991130) and NOAA (AFR-44_NOAA-GFDL-GFDL-ESM2M_rcp45_r1i1p1_SMHI-RCA4_v1_day_20960101-21001231. For each of the models, they had two emission scenarios used. Ie Rcp45 and Rcp85). The climate data used for the simulated GCM historical and future analysis was to have been 30 years but due to the comparative observation data used, the number of study years was reduced to 25years. The simulated GCM historical data downloaded for both GCMs was in the period of 1976-2005 and for simulated future GCM was from 2036 till 2099. The reason for 2099 as opposed to 2100 was due one of the model NOAA having the future simulated data ending in 2100 while MOHC ended in 2099.

In light of the above introduction to the data to be used for the study and that the observed data was available for the period from 1980-2010 (31years) and that calibration and validation was done for the period 1981-2010, it was prudent to consider similar periods for both the simulated historical and future investigations. Therefore, the simulated historical data was considered for the period 1981-2005 which corresponded to the observed data for same period hence 25years.

However, for the future simulated GCM datasets, the periods were divided into two century sections; the middle century (2041-2065) and the far century (2073-2097). Based on the previous gridded reanalysis data, the same grid of the future climate was used .

6.1 Regional Circulation Models - Selection and Downscaling

The control period used for this study was 1981-2005. Reliable predictions of information in the scales of 1000 x 1000km can be obtained from a Global Climate Model. However, Regional Climate Models (RCM) and Empirical Statistical Downscaling (ESD) techniques, applied over a limited area and driven by GCMs can provide information on much smaller scales. Since the impacts of climate change and adaptation strategies required to deal with them occur more on regional and national scales, it is important to use Regional climate downscaled data that provide much greater detail and more accurate representation of localised extreme events.

CORDEX, a regional downscaling experiment, is founded by the World Climate Research Programme. It was used to downscale the RCM data. An R programming language script was used for the conversions from the RCM data base to the text files from which analysis were done using the excel application.

6.2 Evaluation of the downscaled data

Hydrological modeling for climate-change impact assessment implies using meteorological variables simulated by global climate models (GCMs). Due to mismatching scales, coarse-resolution GCM output cannot be used directly for hydrological impact studies but rather needs to be downscaled to a finer resolution that can be run by simple models. (1) an analog method (AM), (2) a multi-objective fuzzy-rule-based classification (MOFRBC) and (3) the Statistical Downscaling Model (SDSM. The reason for the coarse nature of the GCM data is for ease in storing the data based on the available resources.

6.2.1 Delta Change Approach

Delta Change is mean monthly changes in precipitation and temperature between the historical and the future downscaled climate data. The changes in temperatures are considered in terms of the differences between the individual mean monthly values between the simulated historical and the future (categorized) values. While for the precipitation is taken as the ratios of the simulated future to the historical mean monthly values.

The extraction of the delta change factors for the two GCM models ie MOHC and NOAA were done as below explained.

- Firstly, having gridded the catchment in grids of 50x50km, since the model for the simulations is based on gridded data, the climate data for every grid point had to be extracted for both the simulated historical and the future GCM climate analysis using the R programming script. The total number of grid points for the catchment were 104. Figure below 6.1 shows location of all grid points and the observed gauges within the catchment.

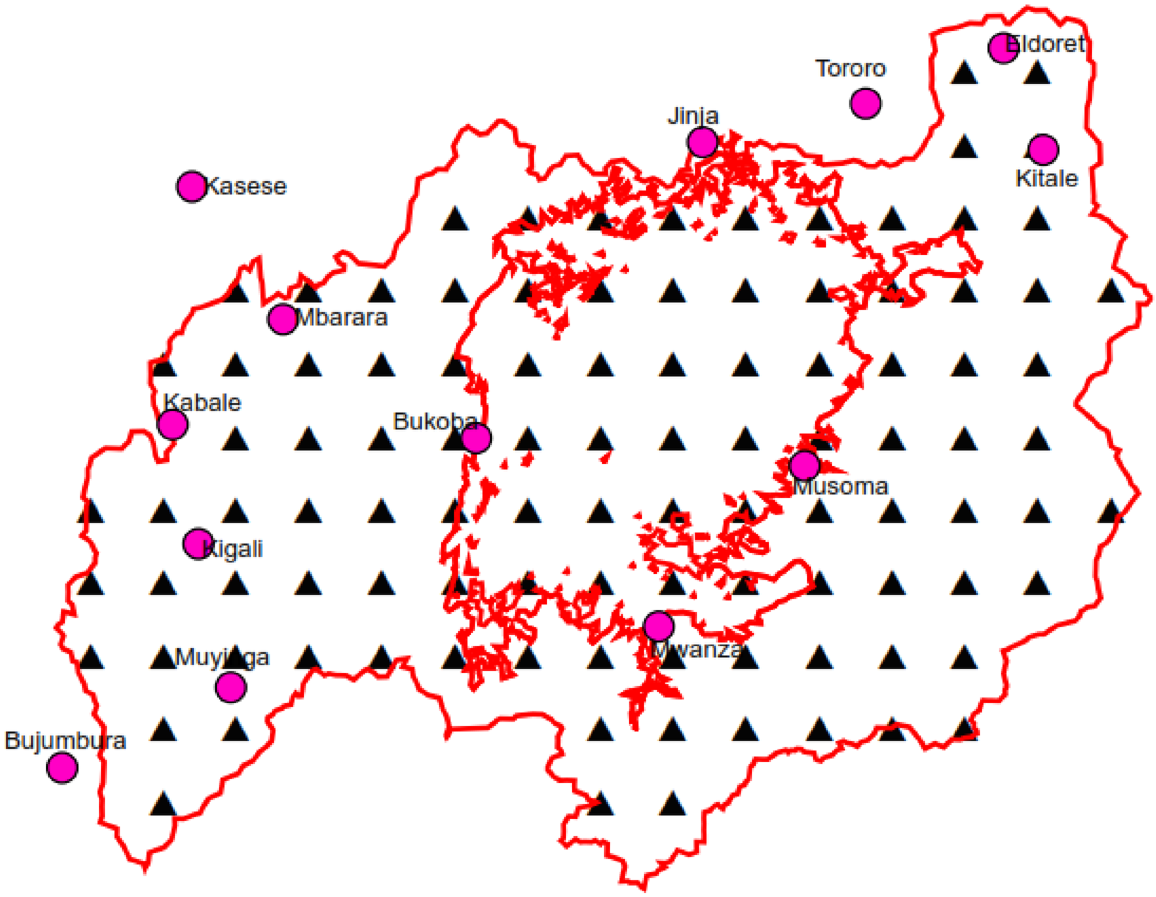

Figure 6-1: Gridded Catchment of LVB

Secondly the daily simulated GCM climate data, historical and future precipitation and temperature was then extracted for the catchment from the link https://esg-dn1.nsc.liu.se/projects/esgf-liu/ and prepared for analysis. At this stage, the simulated historical data was compared with the observed data to study their variability.

Figures below show the correlations between the observed data and the GCM simulated historical data for the two GCM models.

a) **Temperature – Observed and GCM simulated Historical data**

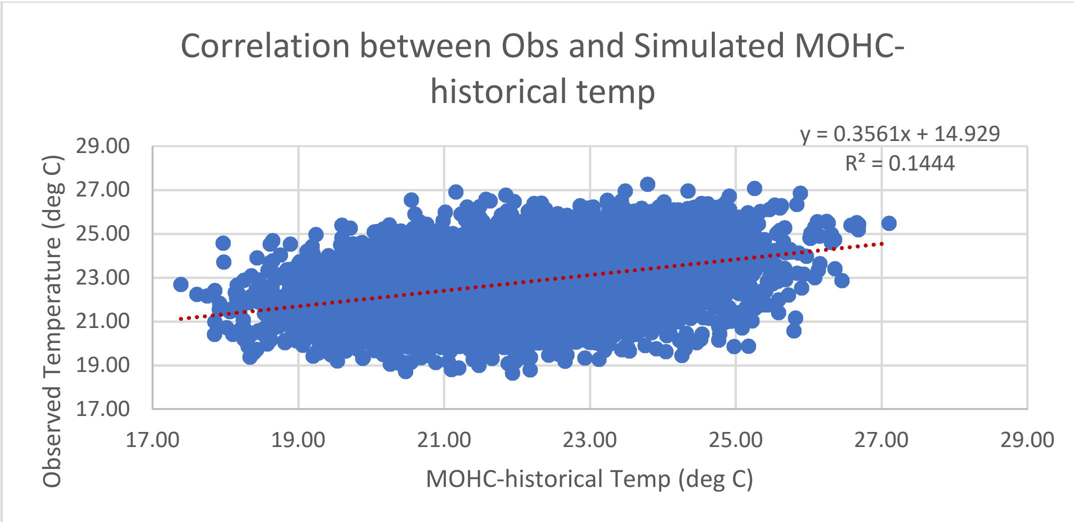

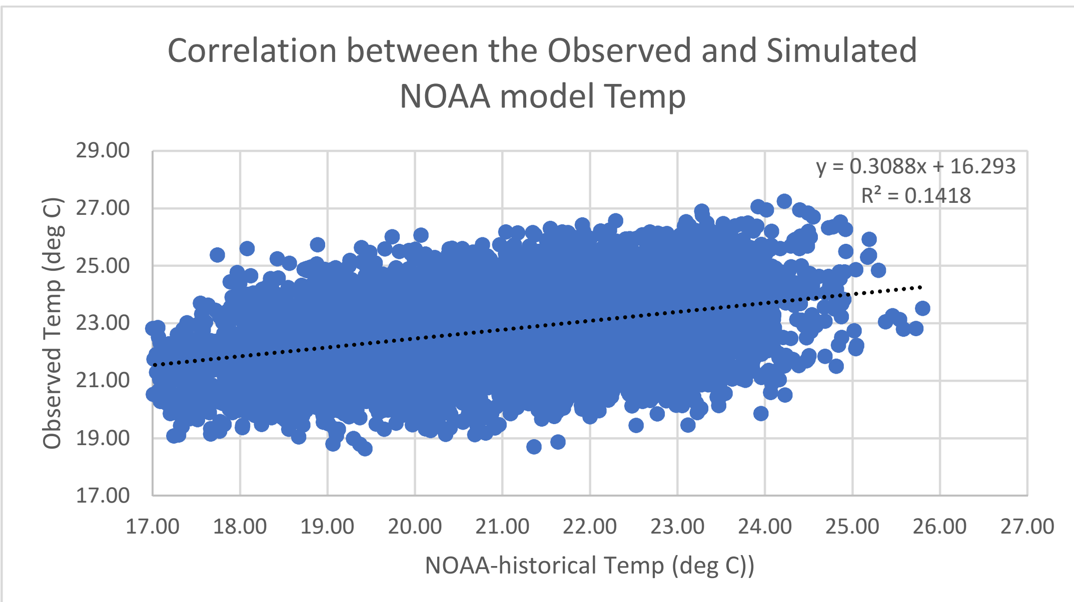

Figure 6-2: Correlations between Observed and GCM simulated historical temperature

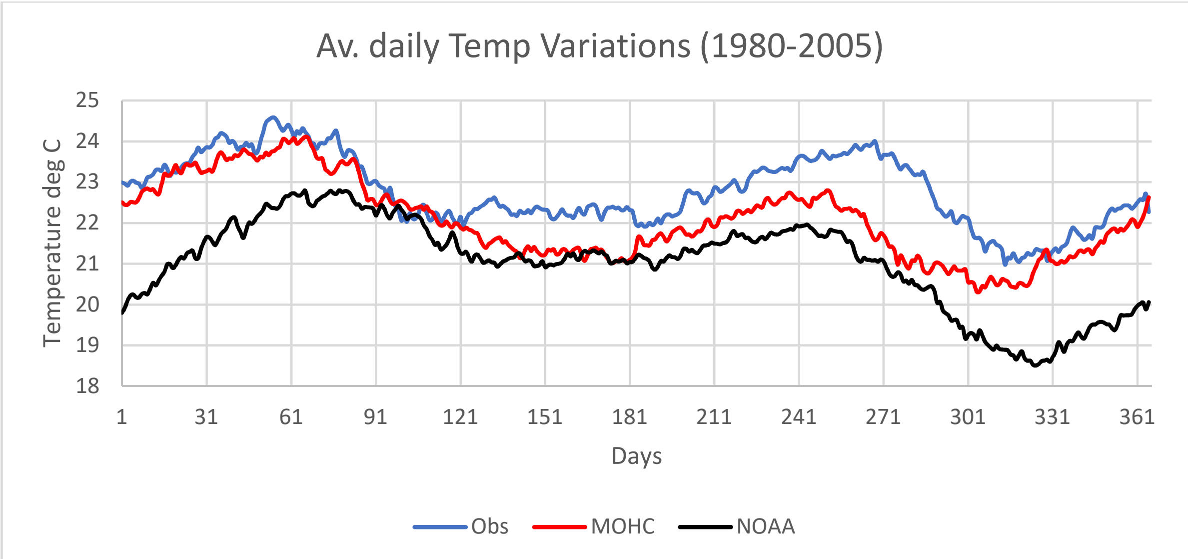

Figure 6-3: Average daily variability of Observed and GCM simulated historical climate (1981-2005)

	Observed	MOHC	NOAA
Maximum Temp (deg C)	24.58	24.11	22.80
Minimum Temp(deg C)	20.98	20.31	18.51

From the correlation figures, it shows that correlation between the GCM temperature data has a very low correlation with the observed temperature data. However, from the average daily temperatures annually for the study period, the pattern for the three observations is similar. The variations show that temperatures are higher in the month of February and October with the maximum recorded for each as 24.58° C, 24.11 ° C and 22.80 ° C for observed, MOHC and NOAA respectively. Whereas the lowest temperatures are 20.98 ° C, 20.31 ° C and 18.51 ° C respectively. All these show that there has been an increase in temperature on average of about 1.1 ° C overall.

b) Precipitation – Observed and simulated Historical GCM

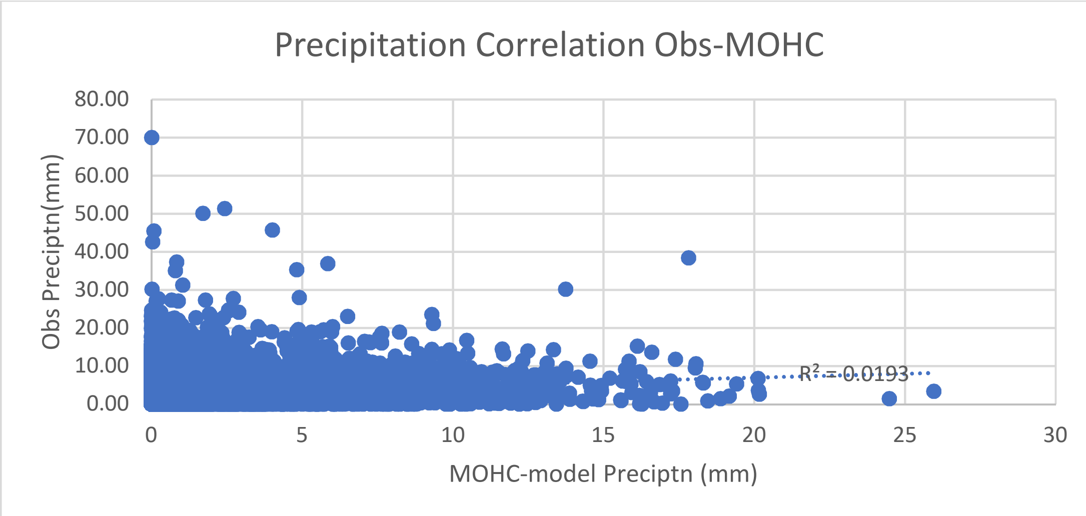

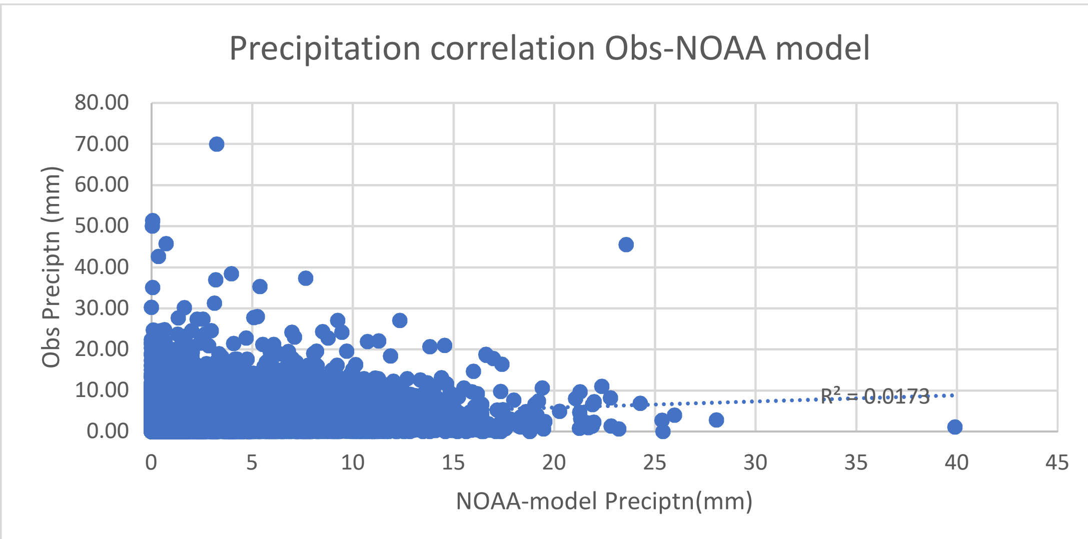

Figure 6-4: Precipitation correlation between the observed and the GCM simulated (1981-2005)

Model Name	Simulated Average number of rainy days (1980-2005)	Observed average number of rainy days (1980-2005)
NOAA	332	328
MOHC	299	328

Table 6-1: Comparative Rainy days

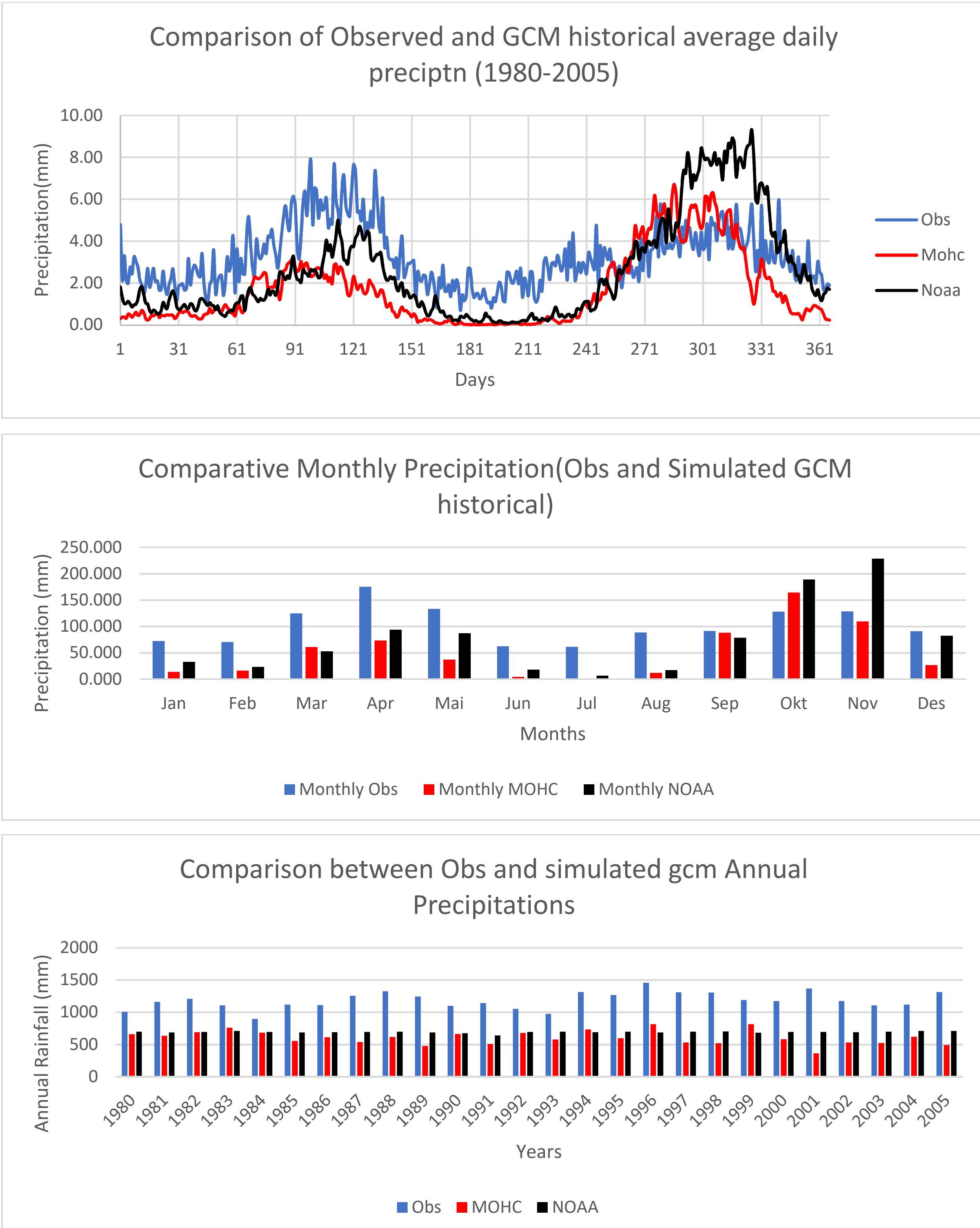

Figure 6-5: Comparative Av daily, Monthly and annually rain between Observed and GCM

i) A similar pattern between the average daily and monthly precipitation was recorded with increased precipitation in particular bands of months; March, April and May and September, October and November, with the low months of June and July.

ii) For the average, daily and monthly precipitation, highest precipitation was recorded in the month of April for the observed and October and November for MOHC and NOAA respectively.

iii) In the annual precipitations, both observed and MOHC recorded highest precipitation in 1996 (1457mm and 815mm respectively), while NOAA highest in 2004 (710mm). the lowest precipitation was seen in 1984, 896mm for observed, 2001, 361mm for MOHC and 1991, 637mm for NOAA.

iv) Looking at the temperature-precipitation patterns, they correspond in such a way that as the temperature increases, this creates more evaporation which results to more rain compared to the periods when the temperature is low.

v) Based on the comparison of the precipitations between the observed and the simulated historical values, the number of rainy days, it is evident on average that the observed precipitation is more than the simulated historical precipitation. In fact, more than 75% in the year showed higher precipitation for observed than for GCM historical model precipitations which only over shot the observed in the months of October and November. This therefore would not be used to drive the hydrological simulations and hence very little downscaling would have required for only these months.

As a result of the above evaluations of the GCM simulated historical data, which was compared with the observed data, and which showed that the historical precipitation could not drive the hydrological simulations, it was imperative that the next stage of analysis be studied. At this stage, delta changes for two emission scenarios were calculated for the two models with simulated future climate data. The delta changes were applied to the mean monthly data values of the historical and future.

The two emission scenarios considered were rcp45 and rcp85 for which both of the will be according to the to the periods of 2041-2065 and 2073-2097 respectively.

The historical monthly means for the two models were computed and plotted as shown below

Mean Monthly precipitation **1981-2005**			
Months	OBS	Simulated Historical GCM models	
		MOHC	NOAA
Jan	1.84	0.46	1.07
Feb	1.95	0.60	0.85
Mar	3.23	1.96	1.75
Apr	4.80	2.41	3.12
Mai	3.45	1.22	2.69
Jun	1.54	0.14	0.60
Jul	1.42	0.04	0.22
Aug	2.17	0.34	0.54
Sep	2.42	2.80	2.53
Okt	3.37	5.30	6.02
Nov	3.46	3.72	7.61
Des	2.32	0.86	2.69
Average	2.66	1.65	2.48

Table 6-2: Monthly Means of Observed and Simulated GCM-historical

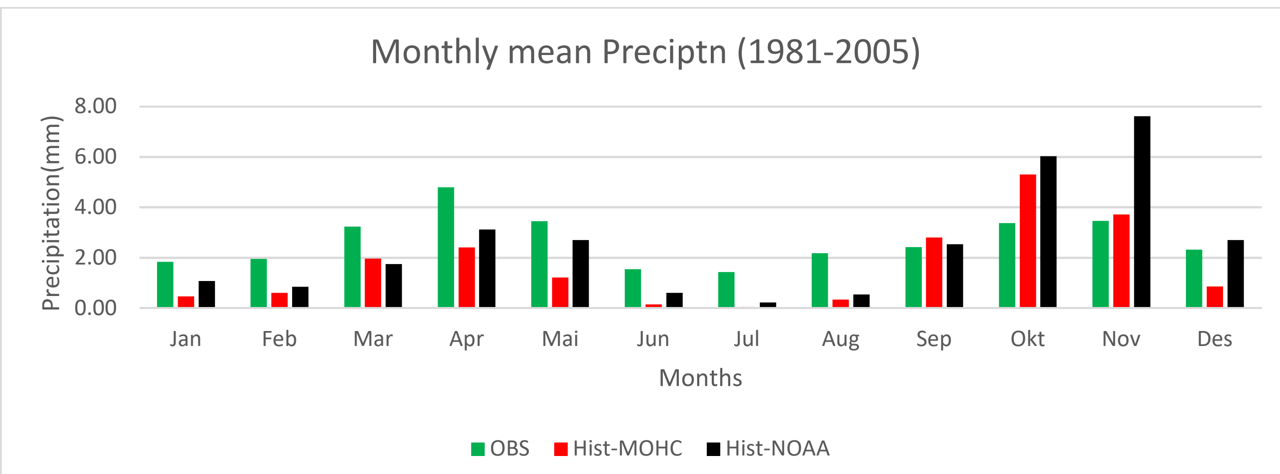

Figures6-6: Monthly mean plot for the observed and the simulated GCM historical rainfall

The plots in figures 6-7 (a and b) are the simulated future mean monthly temperature for the emission scenarios. In the subsequent discussions, the initials rcp45-M-MOHC or rcp45-F-MOHC the middle term **"-M-"or "-F-"** denotes midcentury and far century respectively.

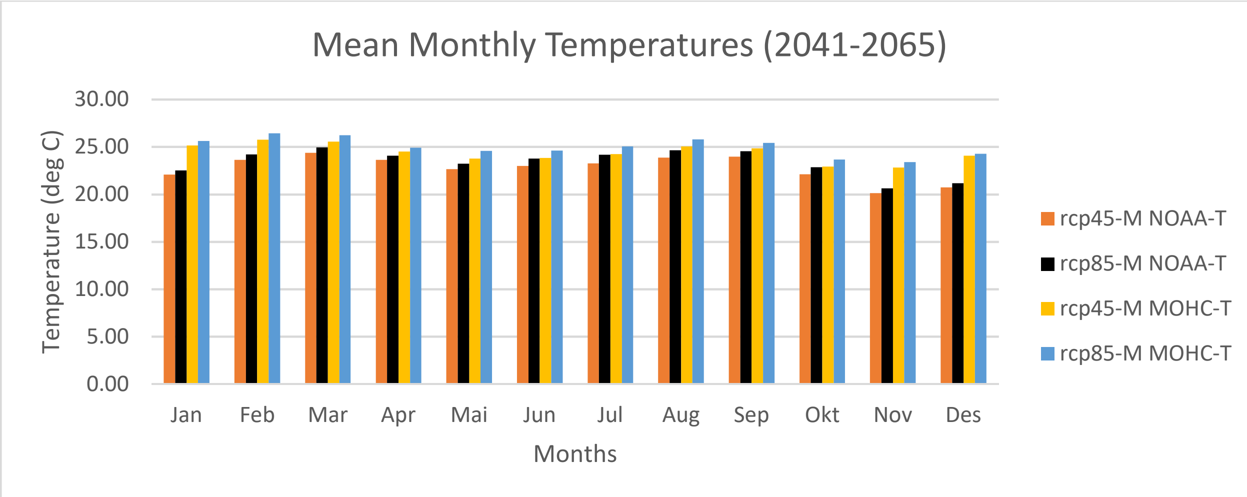

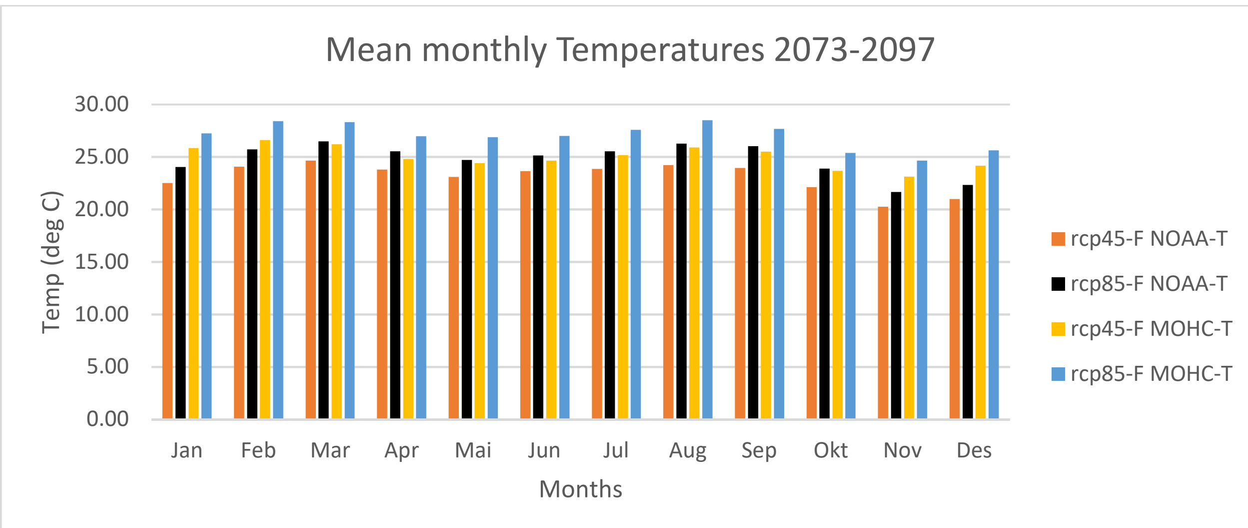

Figures 6-7(a and b): Mean Monthly Future Simulated GCM Temperatures

For the mean monthly GCM future temperature projections, it is seen for the mid-century that highest precipitation records are by scenarios Rcp85, model MOHC (26^{o}C in March) while the lowest is Rcp45, model NOAA (20^{o} C in November).

For the Far century, Rcp85, model MOHC (28^{o} C in March and August) and the lowest was Rcp45, model NOAA (20^{o}C in November).

Comparing this with the current observed of 24.5 deg highest and 19deg lowest, this shows an increase of about 1.5deg in the midcentury by MOHC and 4.5 deg by NOAA in the far century. The lowest temperatures were also noted to have increased by 1 deg in both models.

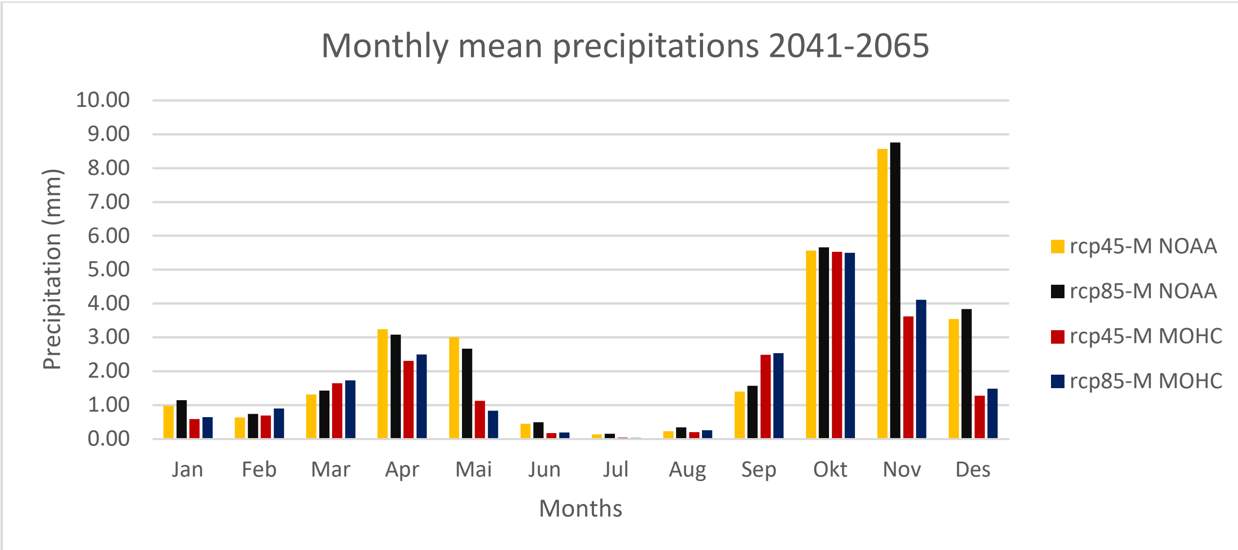

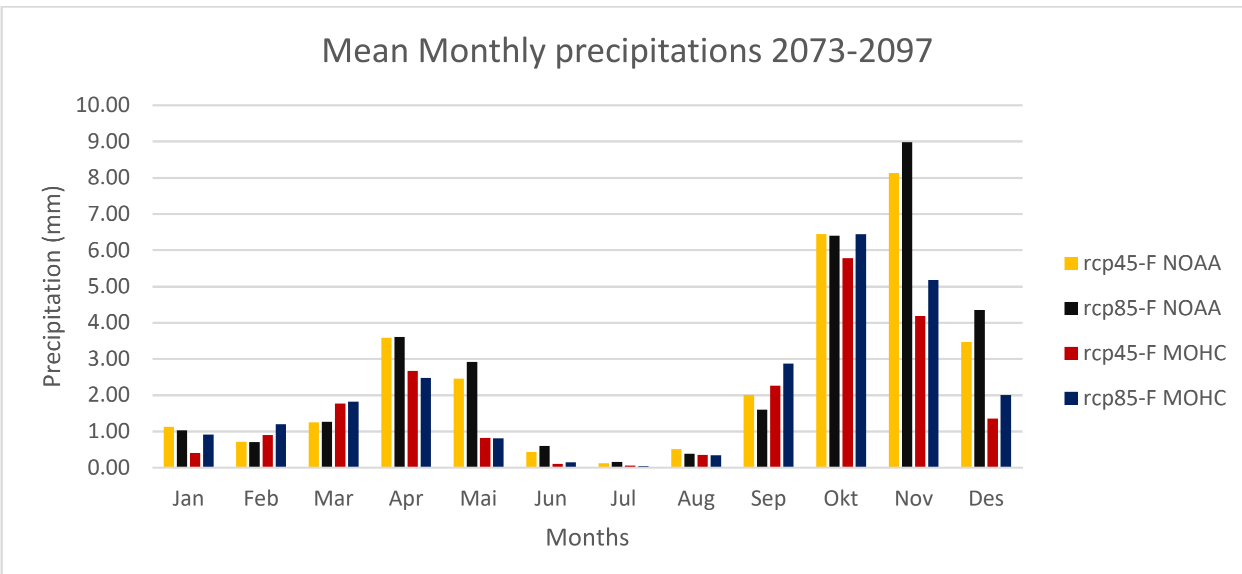

Figure 6-8 (a and b): Mean Monthly GCM future simulations

Figures 6-8 (a and b) represent the future simulated GCM precipitation and from them the following was deduced.

A similar pattern was registered in terms of the months with high precipitation like in the observed except there is a shift in increased amount of precipitation in October, November and December as opposed to the observed current that shows more rain in March, April and May.

Whereas for the temperature rcp85-MOHC indicates high temperature, for precipitation, rcp85-NOAA shows more rain.

6.2.2 Computation of the Delta Changes for Temperature and Precipitation

The delta changes for the temperature is the difference between the simulated future GCM and the simulated historical GCM models. The figures 6-9 and 6-10 shows the delta changes for mid and far centuries respectively for the two scenarios.

Delta Changes - Temperature

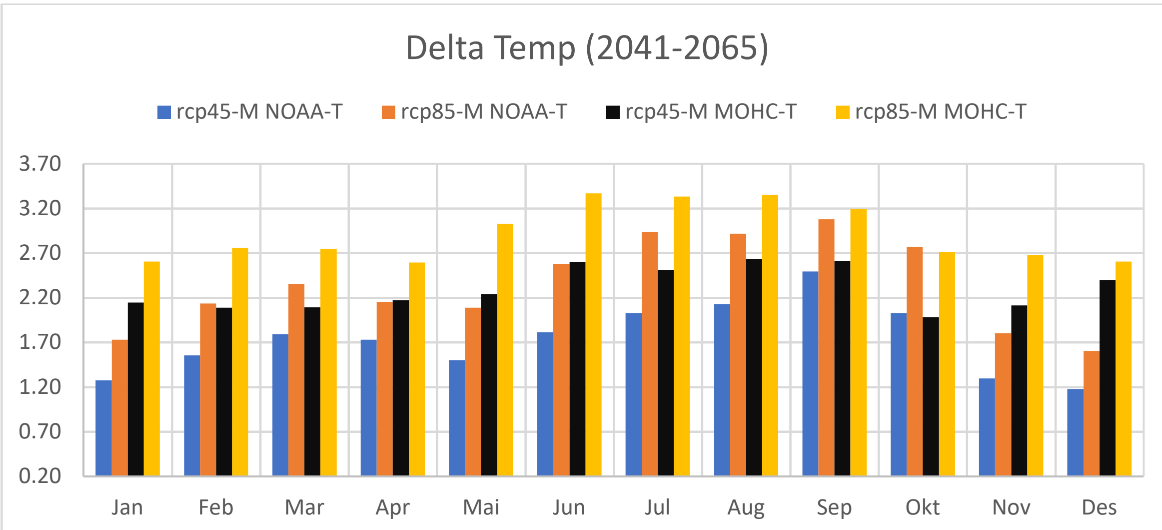

Figure 6-9: Temperature Delta Change-Mid Century

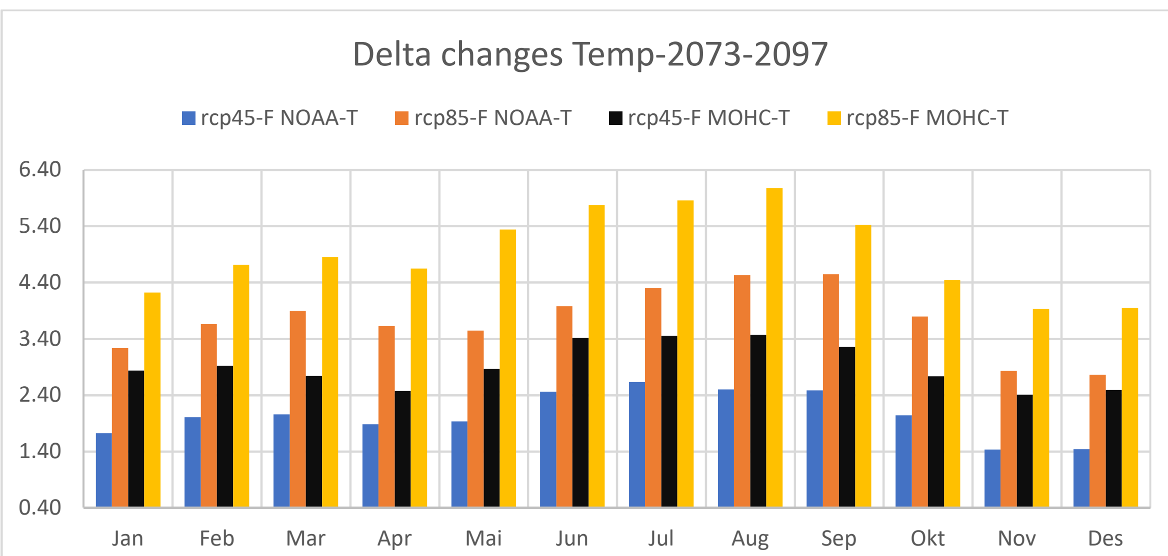

Figure 6-10: Temperature Delta Change - Far Century

	Delta Changes-Temp-MOHC				**Delta Changes-Temp- NOAA**			
	2041-2065		**2073-2097**		**2041-2065**		**2073-2097**	
	rcp45-M MOHC-T	rcp85-M MOHC-T	rcp45-F MOHC-T	rcp85-F MOHC-T	rcp45-M NOAA-T	rcp85-M NOAA-T	rcp45-F NOAA-T	rcp85-F NOAA-T
1	2.15	2.60	2.83	4.22	1.27	1.73	1.72	3.23
2	2.09	2.76	2.92	4.72	1.55	2.14	2.01	3.66
3	2.09	2.74	2.74	4.85	1.79	2.35	2.06	3.89
4	2.17	2.59	2.47	4.64	1.73	2.15	1.88	3.62
5	2.24	3.03	2.86	5.34	1.50	2.09	1.93	3.54
6	2.60	3.37	3.41	5.78	1.81	2.58	2.46	3.98
7	2.51	3.33	3.46	5.86	2.03	2.94	2.63	4.30
8	2.63	3.35	3.47	6.08	2.13	2.92	2.50	4.53
9	2.61	3.19	3.25	5.42	2.49	3.08	2.48	4.55
10	1.98	2.71	2.73	4.44	2.03	2.77	2.04	3.80
11	2.11	2.68	2.40	3.93	1.30	1.80	1.44	2.83
12	2.40	2.61	2.49	3.95	1.18	1.61	1.44	2.76

Table 6-3: Table showing the Delta Changes for different scenarios

From the table 6-3 above, the highest change expected in the temperature between the historical and future simulation would be by 6.08 deg and that is the month of August as expressed by the MOHC-rcp85 model in the far century (2073-2097). The lowest change is expected to be in December in the midcentury of 1.18 deg based on NOAA-rcp 45 (2041-2065).

The projected temperatures after the application of the delta change are shown in the figures…

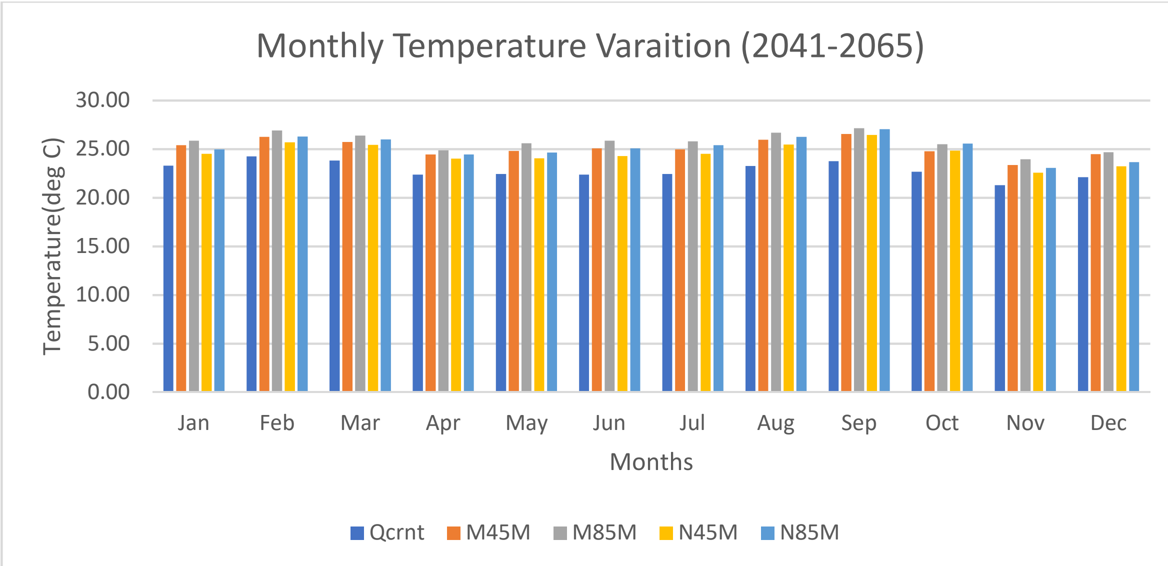
Monthly Temperature Varaition (2041-2065)
Temperature(deg C)
30.00
25.00
20.00
15.00
10.00
5.00
0.00
Jan
Feb
Mar
Apr
May
Jun
Jul
Aug
Sep
Oct
Nov
Dec
Months
Qcrnt
M45M
M85M
N45M
N85M

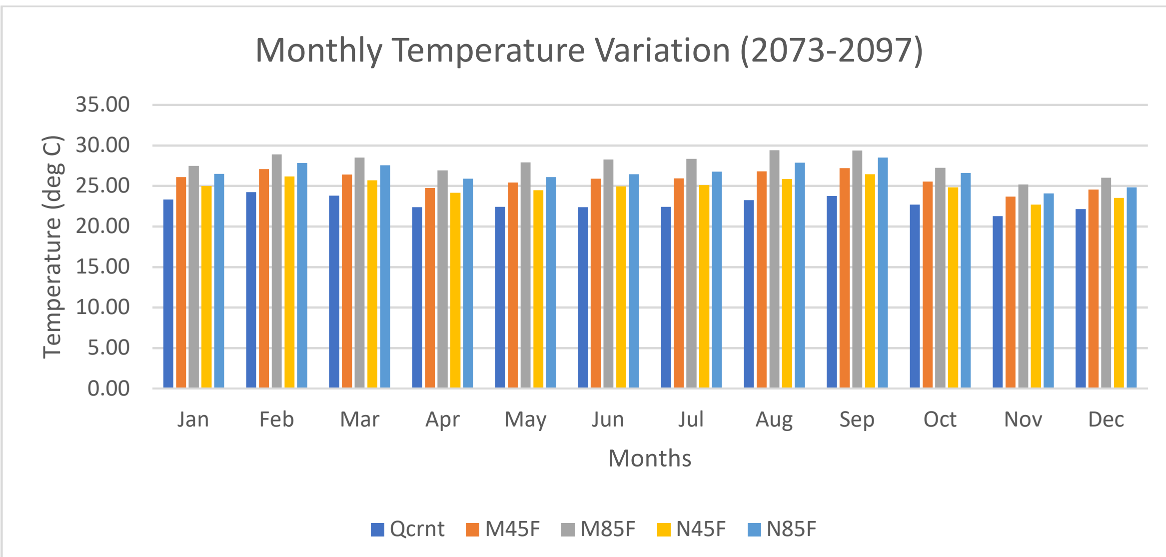
Monthly Temperature Variation (2073-2097)
Temperature (deg C)
35.00
30.00
25.00
20.00
15.00
10.00
5.00
0.00
Jan
Feb
Mar
Apr
May
Jun
Jul
Aug
Sep
Oct
Nov
Dec
Months
Qcrnt
M45F
M85F
N45F
N85F

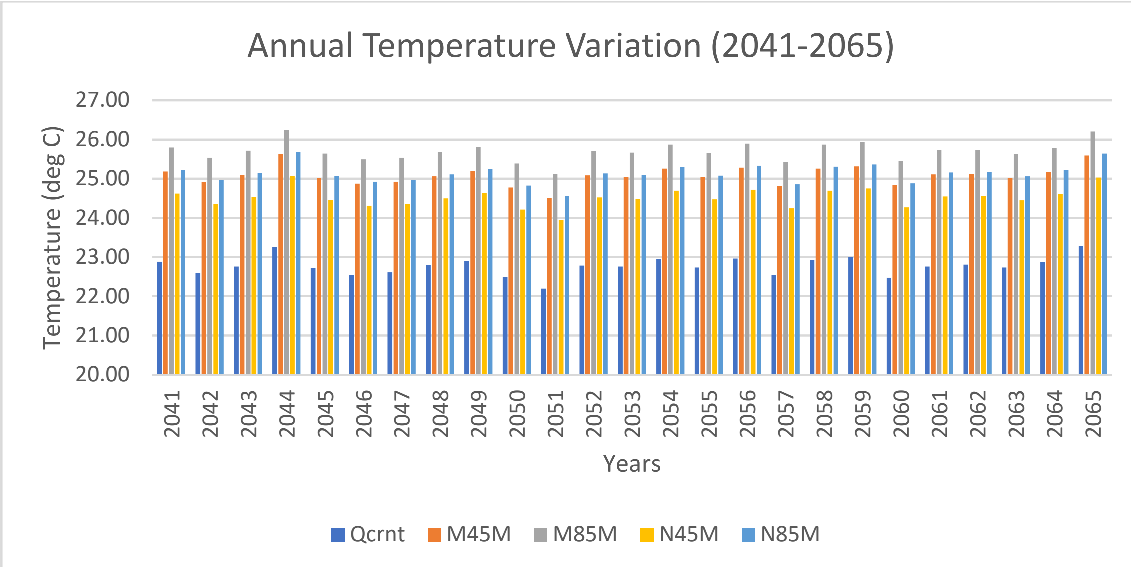

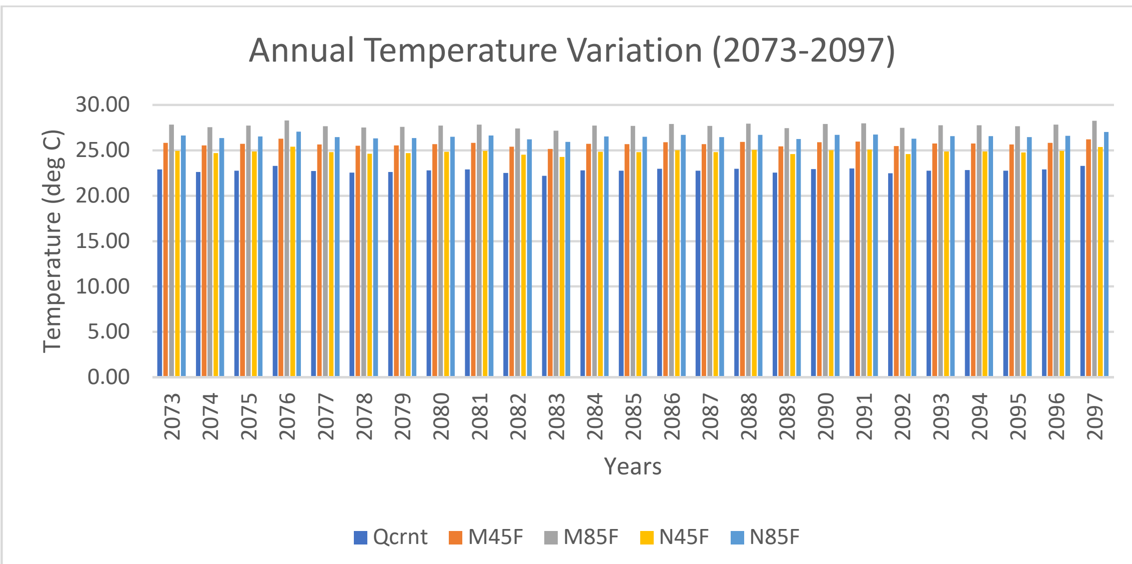

Precipitations Delta Changes

As earlier stated, this is the ratio of the future simulation to the historical simulation of the GCM models. They are taken as percentage increases or decreases of the result.

Figures 6-11 and 6-12 show the delta changes in the mid and far century respectively.

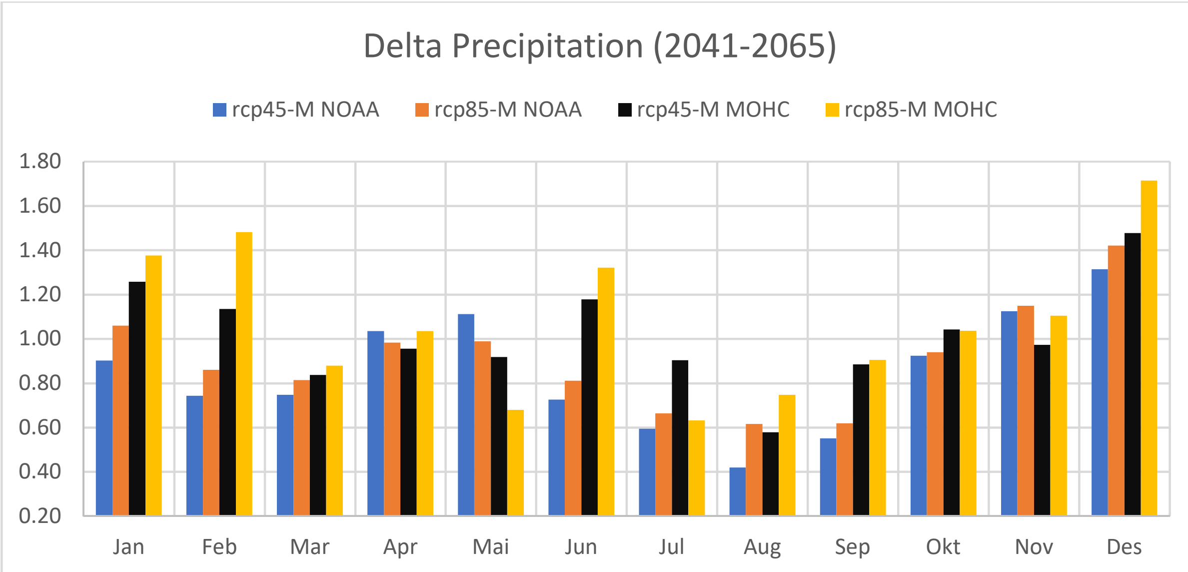

Figure 6-11: Delta Change in Precipitation (2041-2065)

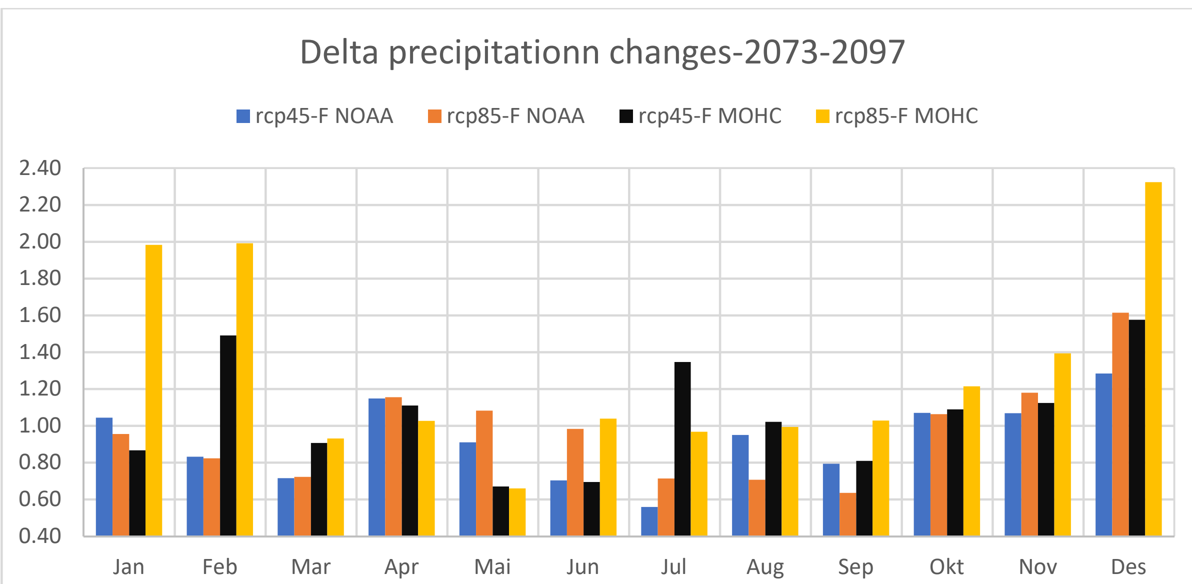

Figure 6-12 Delta Change-Precipitation (2073-2097)

	Delta Changes-Precipitation-NOAA				Delta Changes-Precipitation-MOHC			
	2041-2065		2073-2097		2041-2065		2073-2097	
Months	rcp45-M NOAA	rcp85-M NOAA	rcp45-F NOAA	rcp85-F NOAA	rcp45-M MOHC	rcp85-M MOHC	rcp45-F MOHC	rcp85-F MOHC
Jan	0.90	1.06	1.04	0.95	1.26	1.38	0.87	1.98
Feb	0.74	0.86	0.83	0.82	1.13	1.48	1.49	1.99
Mar	0.75	0.81	0.71	0.72	0.84	0.88	0.91	0.93
Apr	1.03	0.98	1.15	1.15	0.95	1.04	1.11	1.03
May	1.11	0.99	0.91	1.08	0.92	0.68	0.67	0.66
Jun	0.73	0.81	0.70	0.98	1.18	1.32	0.69	1.04
Jul	0.59	0.66	0.56	0.71	0.90	0.63	1.35	0.97
Aug	0.42	0.62	0.95	0.71	0.58	0.75	1.02	0.99
Sep	0.55	0.62	0.79	0.63	0.89	0.91	0.81	1.03
Oct	0.92	0.94	1.07	1.06	1.04	1.04	1.09	1.21
Nov	1.13	1.15	1.07	1.18	0.97	1.10	1.12	1.39
Dec	1.31	1.42	1.28	1.61	1.48	1.71	1.58	2.32

Table 6-4 Delta Changes- Precipitation

The precipitation delta changes shown in the table 6-4 above for the two GCM models has the following information to note,

The range of precipitation change is from the 55% (45% decrease) as the lowest and occurring in the month of September for rcp45-M-NOAA and the highest is 232% (132% increase) in the month of December, rcp85-F-MOHC. The similarities in the two emission scenarios show that rcp 85 for both MOHC and NOAA recorded the highest changes in the months of February and December in both far and midcentury. It will be of interest to understand the great 132% increase in the far future and as can be seen, there is a lot of precipitation anticipated in the December months compared to other months.

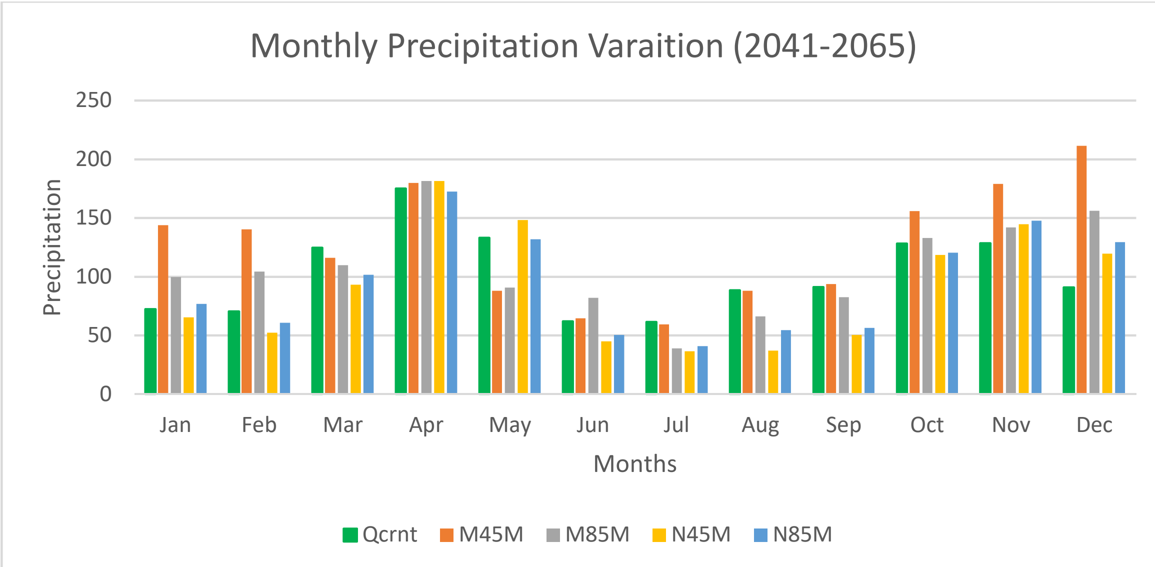

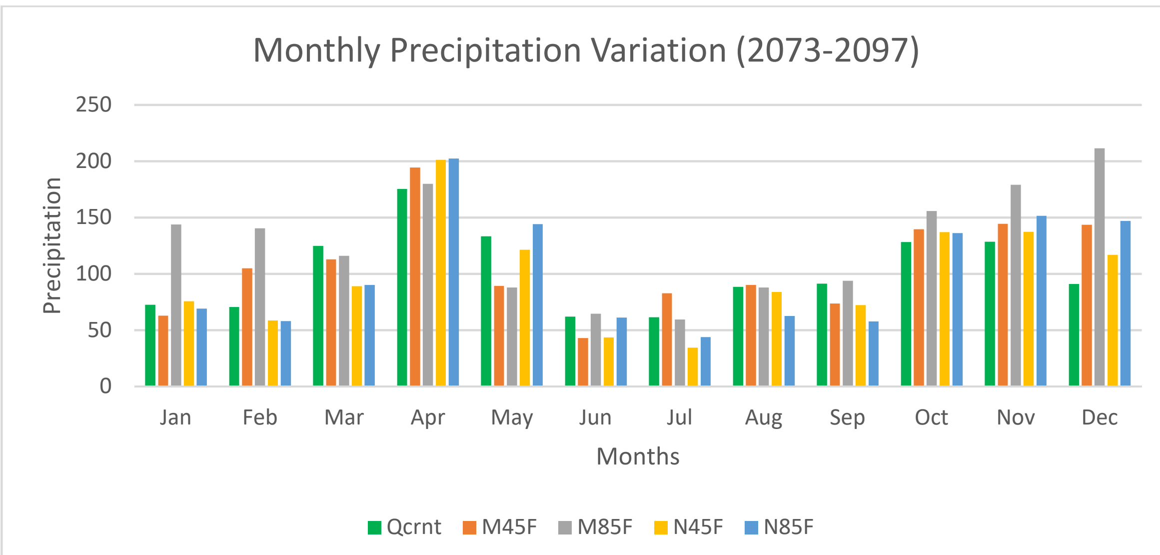

Figure Comparative Monthly precipitations

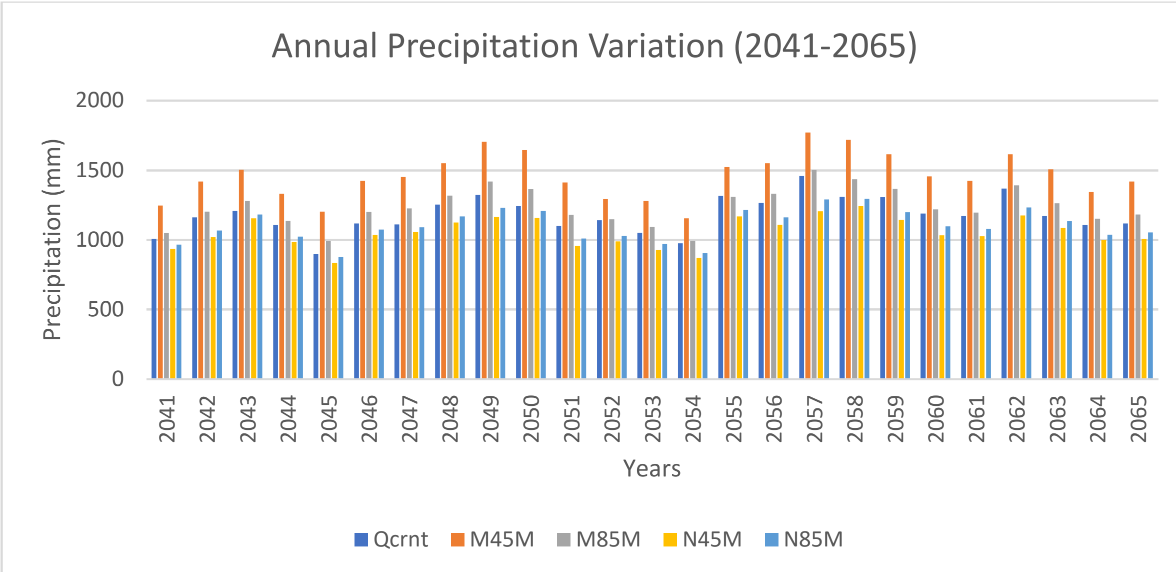

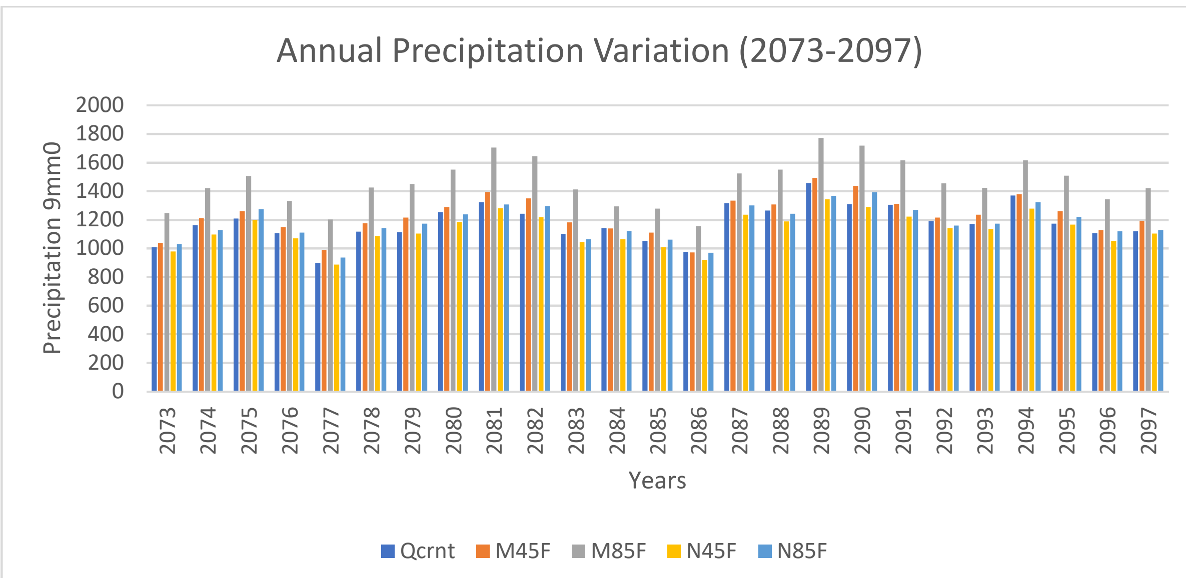

6.3 Simulation of the flows for the control periods

After the computation for of the delta changes, the next tasks was to generate the simulated flows using the ENKI model and based on the applied delta changes on the observed data in order to envisage floods caused as a result climate change.

First and foremost, it was found that there would be temperature increase in both scenarios to a highest of 6^{o} C by end of the far century while the lowest increase was by 1^{o} C. Further to this it was found that on average, there was a shift in the amount of precipitation from the current months of March, April and May to the months of October, November and December for the future projections, with December recording the higher increases compared to all other months.

After downscaling the future climate data and application of the delta changes, below is the plot of the monthly mean comparisons of the flows for the current and the future.

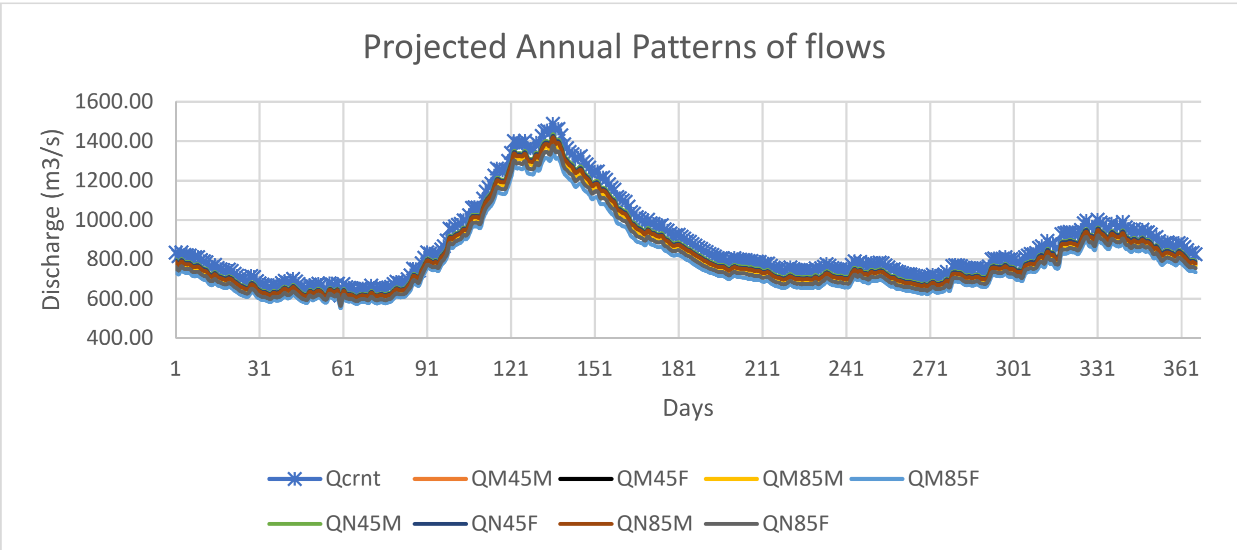

Figure 6-13: Comparison of the average daily flows

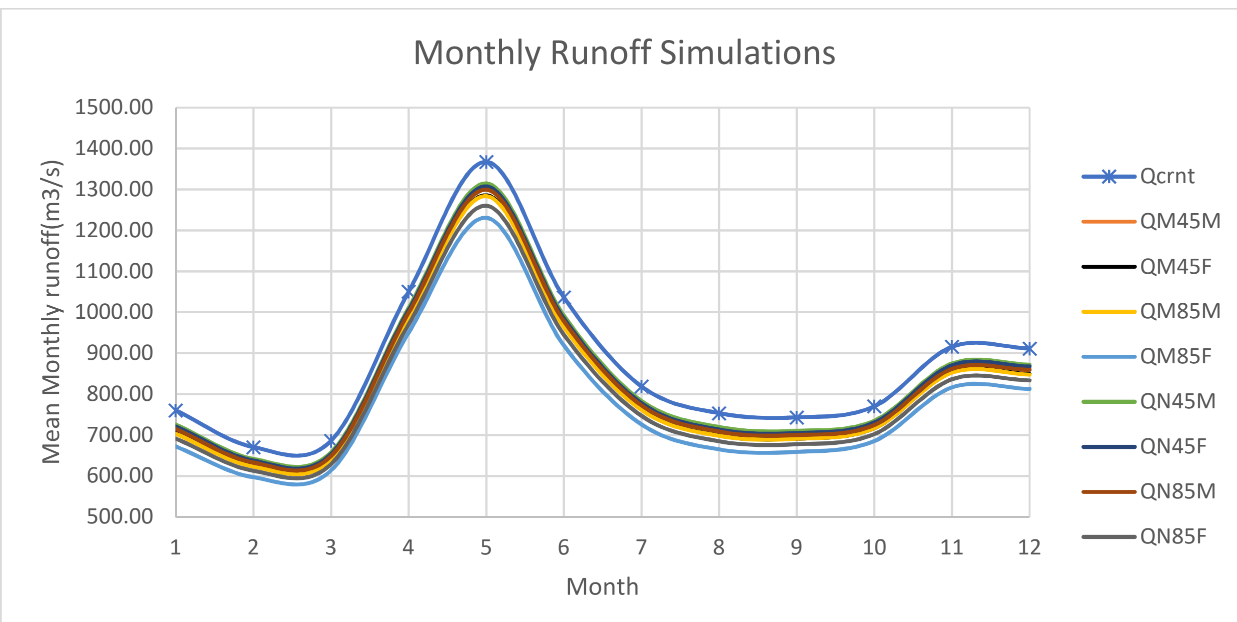

Figure 6-14: Comparison of observed with projected future runoffs

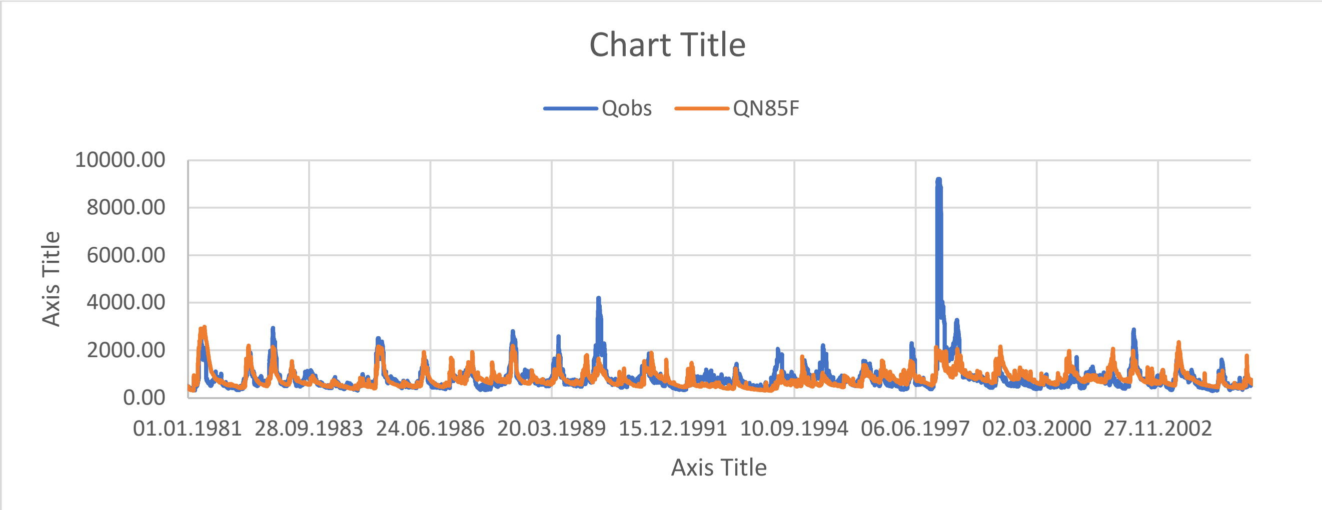

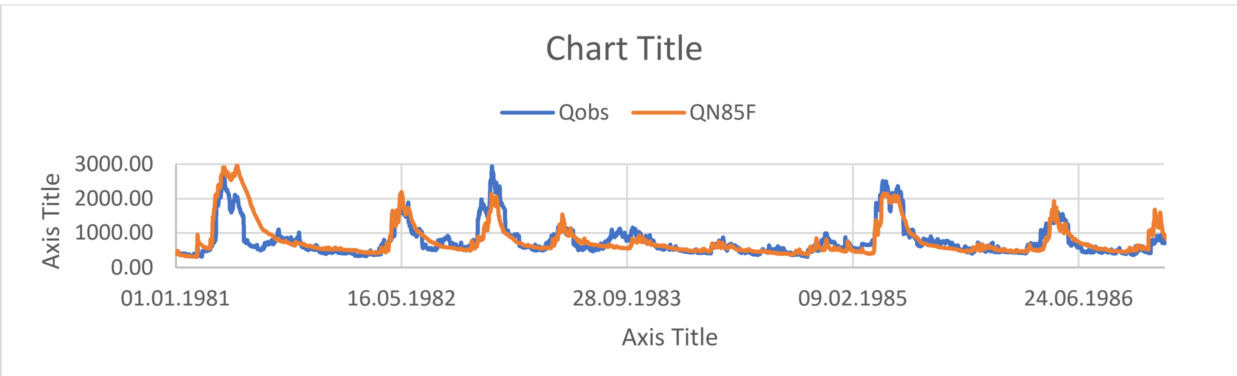

Comparisons of the simulated projected inflows with the observed show a very close match in terms of performance. With the exception of the years 1989 and 1997. In general, for all the simulations carried out, the temporal performance values of NSE (R^2) over the study period were in the ranges of 0.35-0.42. Hence this was considered for the flood frequency analysis.

6.4 Flood Frequency Analysis

Flood frequency analysis is the means by which flood discharge magnitude (Q) is related to the probability of its being equaled or exceeded in any year or to its frequency of recurrence or return period (T). The return period and recurrence interval (terms which are used interchangeably) are used to indicate the long-term average interval between floods of a given magnitude. The return period and exceedance probability are reciprocals.

Frequency analysis was applied to peak instantaneous discharges of the annual flows and the seasonal flows. The seasonal flows were based on the months with observed high flows.

The Gumbel distribution was applied for the flood frequency analysis because of the homogeneity of the peak flow data which are independent and lack long term trends, the inflows are not regulated hence not a lot of interference in the inflow by either diversions, or urbanization and the data of the flow is of long record (25 years) and of fair quality.

The equation for fitting the Gumbel distribution to observed series of flood flows at different return periods T is

$Q_T = Q_{av} + K\sigma$

where Q_T denotes the magnitude of the T-year flood event, K is the frequency factor, Q_{av} and σ are the mean and the standard deviation of the maximum instantaneous flows respectively.

The frequency factor K is expressed as

$K=-\sqrt{6}/\pi(\lambda-\ln(\ln(T-\ln(T-1)))$

where: π =3.14, λ is the Euler constant (=0.5772) and ln is the natural logarithm

The results of the analysis for the three different categories are show in the subsequent plots

a) Annual Maximum peaks

T	K	Qcrnt	QM45M	QM45F	QM85M	QM85F	QN45M	QN45F	QN85M	QN85F
5	0.72	2306	2228	2210	2208	2143	2247	2238	2227	2180
10	1.30	2560	2482	2464	2460	2392	2502	2493	2481	2431
20	1.87	2804	2726	2706	2703	2631	2747	2737	2725	2671
50	2.59	3119	3041	3020	3017	2940	3063	3053	3040	2983
100	3.14	3356	3277	3256	3252	3172	3301	3290	3277	3216
200	3.68	3591	3513	3490	3487	3403	3537	3526	3512	3449
500	4.39	3902	3824	3800	3796	3707	3849	3837	3823	3755
1000	4.93	4136	4058	4034	4030	3937	4085	4072	4057	3987

1000	6.7									
0	3	4916	4838	4810	4806	4701	4867	4853	4837	4757

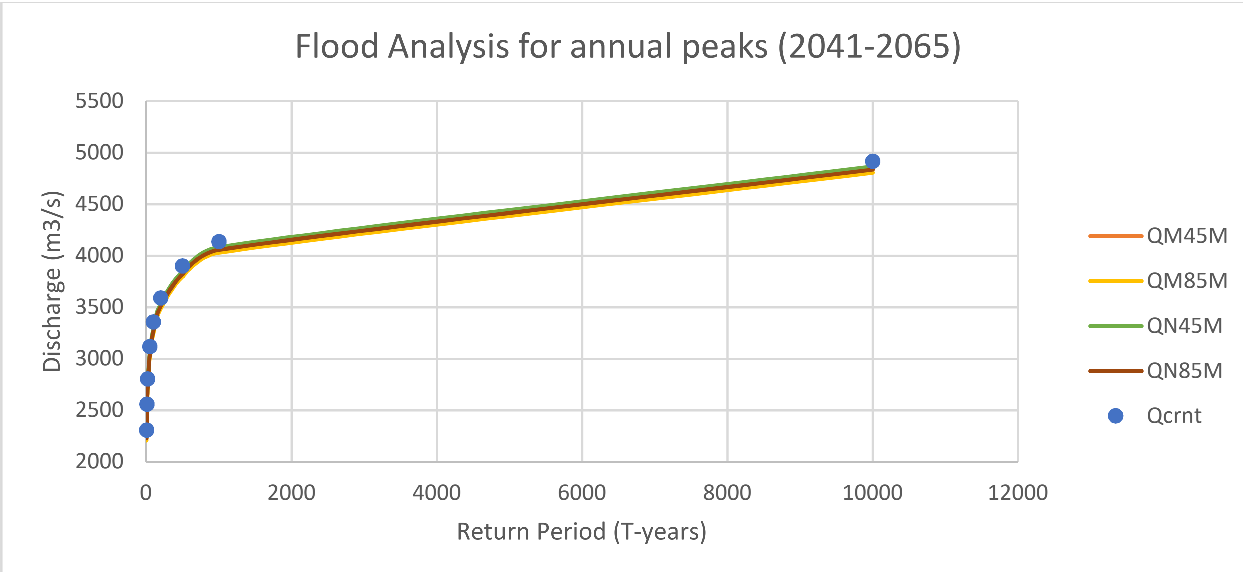

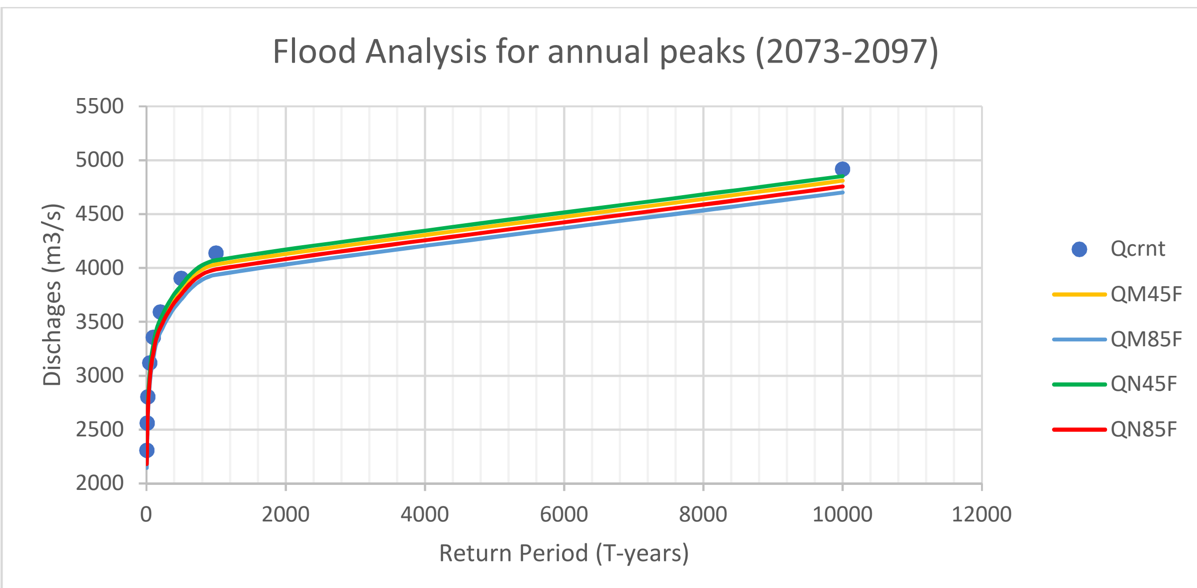

b) Season of March April and May (MAM) peaks

		Qcrn	QM45	QM45	QM85	QM85	QN45	QN45	QN85	QN85
T	K	t	M	F	M	F	M	F	M	F
	0.7									
5	2	2162	2084	2067	2065	2002	2101	2093	2083	2037
	1.3									
10	0	2467	2385	2368	2365	2299	2404	2395	2385	2335

20	1.87	2760	2674	2656	2653	2584	2694	2684	2674	2622
50	2.59	3138	3048	3029	3026	2952	3069	3059	3048	2992
100	3.14	3422	3329	3309	3306	3228	3351	3340	3328	3270
200	3.68	3705	3608	3587	3584	3503	3631	3620	3608	3547
500	4.39	4078	3977	3955	3952	3866	4001	3989	3976	3912
1000	4.93	4360	4255	4233	4229	4140	4280	4268	4255	4188
10000	6.73	5296	5180	5155	5151	5051	5208	5195	5180	5104

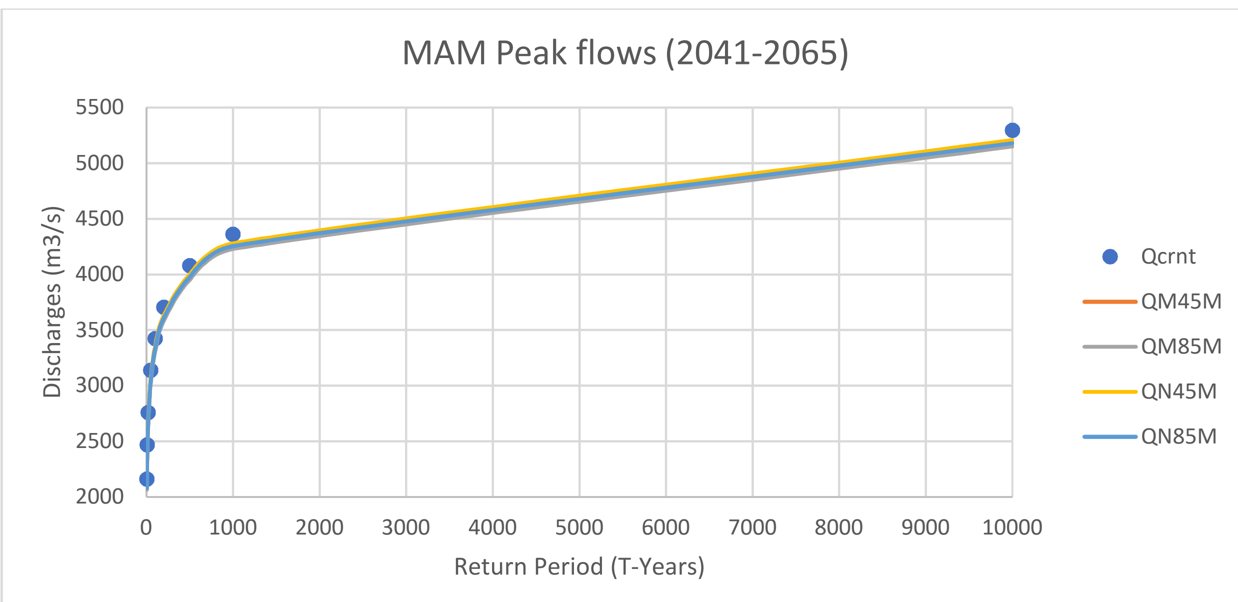

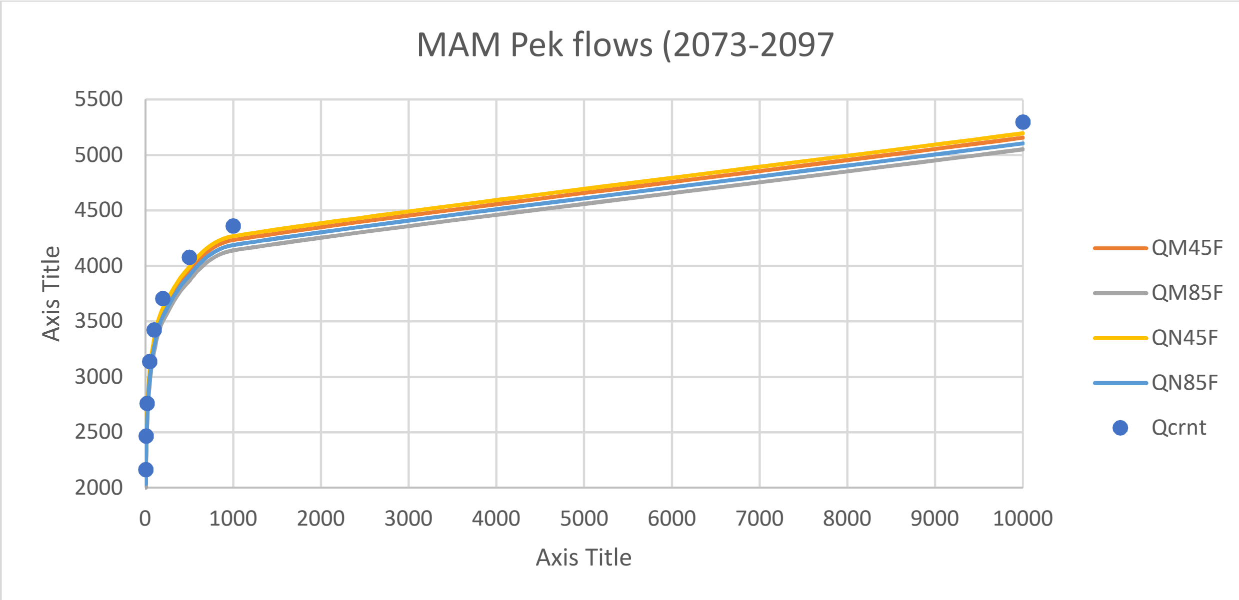

c) Season of October November and December (OND) peaks

T	K	Qcrnt	QM45M	QM45F	QM85M	QM85F	QN45M	QN45F	QN85M	QN85F
5	0.72	1814	1739	1722	1720	1669	1755	1749	1735	1698
10	1.30	2120	2036	2017	2015	1957	2053	2047	2032	1990
20	1.87	2413	2321	2300	2297	2233	2340	2334	2316	2271
50	2.59	2793	2690	2667	2663	2591	2711	2704	2684	2633
100	3.14	3078	2966	2941	2937	2860	2990	2982	2960	2905
200	3.68	3361	3242	3215	3209	3127	3267	3259	3235	3176
500	4.39	3735	3605	3576	3570	3479	3632	3624	3598	3533
1000	4.93	4018	3880	3848	3842	3746	3909	3900	3872	3803
10000	6.73	4957	4791	4754	4745	4631	4826	4816	4782	4700

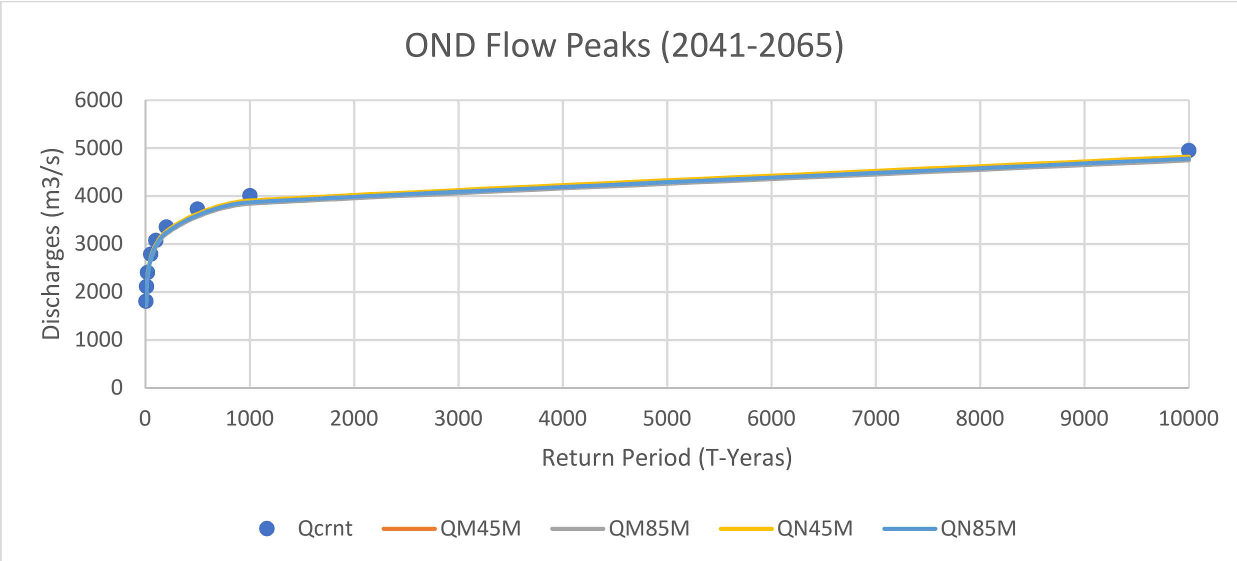

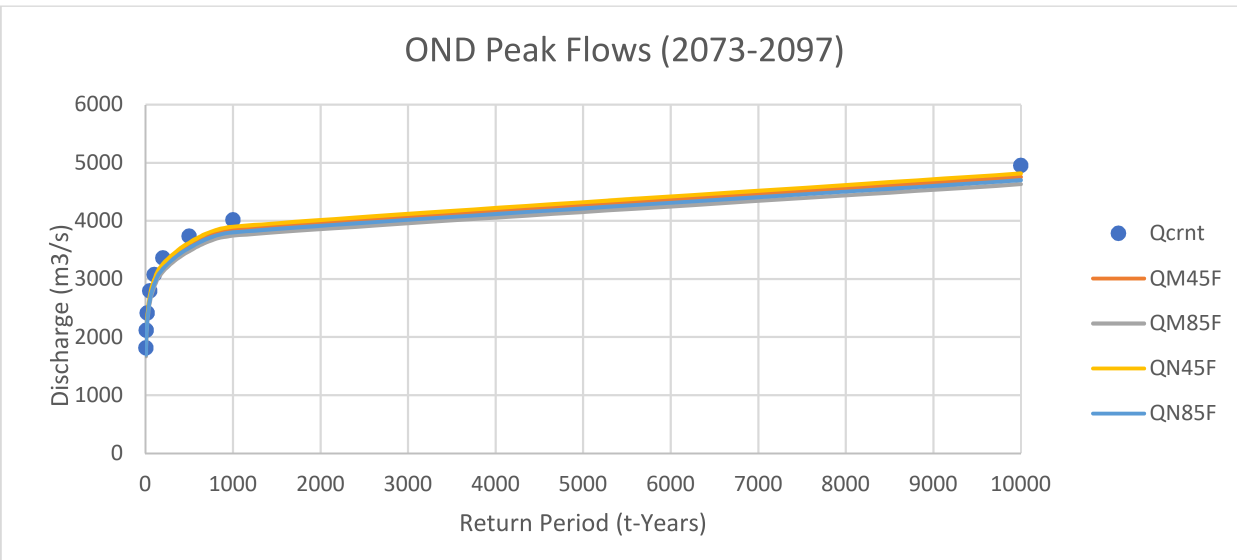

Analysis of the flood frequency results.

Based on the feasibility study report by Acres international May 1991 for the proposed extension to the Owen Falls Generating Station, below is the information.

- The maximum historic average inflow flood of 4000m3/s was recorded in the hydrologic years of 1961 to 1962 and this caused the rise of the water level by beyond 2.5m However the lake being low at that time due to the prolonged drought, it had no impact of the dam. At this period, 1964, the peak outflow was the highest recorded of 1700m3/s. Hence the spillway capacity was augmented by the turbine capacities.

A study was carried out which led to an increased capcity of the spillway by 2400m3/s from about 1900m3/s. This therefore improved the risk on a future overflooding and hence a design flood of 4500m3/s was adopted for a 1000-year return period.

- The analysis by Acres International are presented thus

Return Period (years	Maximum Spill(m3/s)	Maximum Lake level (m)
2	1743	1135.0
10	1860	1135.2
100	3515	1135.8
1000	4187	1136.0
10000	4782	1136.5

The indications from the climate change applications to the flows from the catchment show the following

- Generally, the trend of floods shows a decrease from the current state to the far century with high floods recorded in the season of MAM and the lowest in the season of OND.
- It was worth noting that the highest floods in the climate change period are predicted by the NOAA model in the mid-century
- In relation to the simulations of the inflows from catchment, the projected inflows don't exceed the observed series over the study period.
- The computed discharges from the flood analysis also show that the climate change will not lead to rise of the floods beyond the current state of inflows.
- From the GCM models, it is worth noting that the result from similar emission scenarios do not give a similar result, and therefore for a conclusive idea, there was a need to investigate the study based on more models.
- From the flood routing figure below, there are some discrepancies noted between the simulated outflow and the observed flow. This could be as a result of the regulation since the outflow from the lake is not free flowing.

6.5 Flood routing of the climate Scenarios.

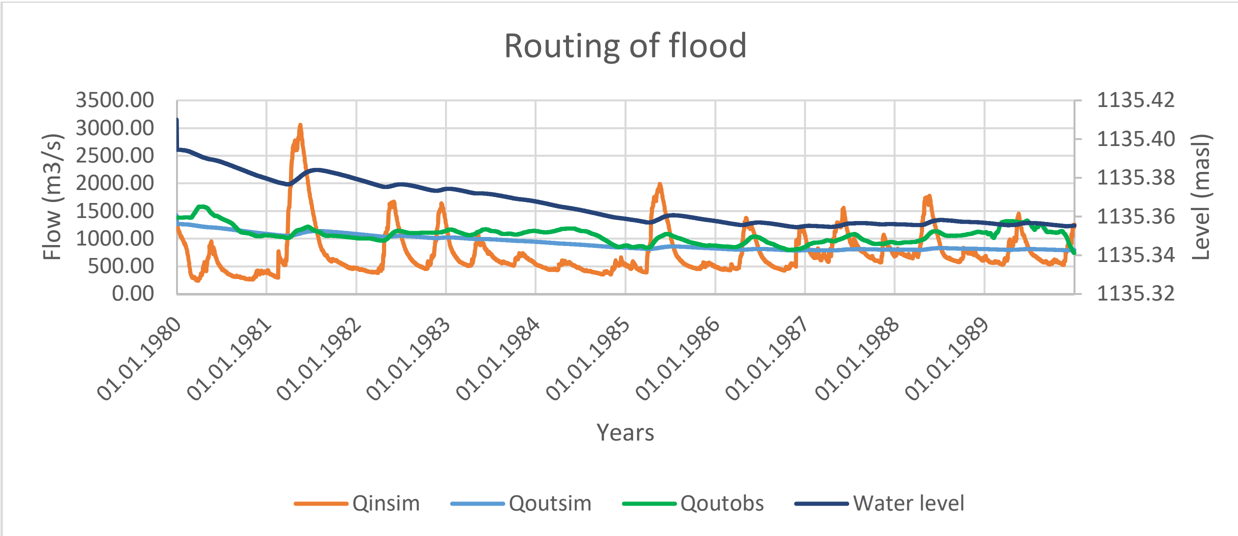
Routing of flood
Flow (m3/s)
Level (masl)
3500.00
3000.00
2500.00
2000.00
1500.00
1000.00
500.00
0.00
1135.42
1135.40
1135.38
1135.36
1135.34
1135.32
01.01.1980
01.01.1981
01.01.1982
01.01.1983
01.01.1984
01.01.1985
01.01.1986
01.01.1987
01.01.1988
01.01.1989
Years
Qinsim
Qoutsim
Qoutobs
Water level

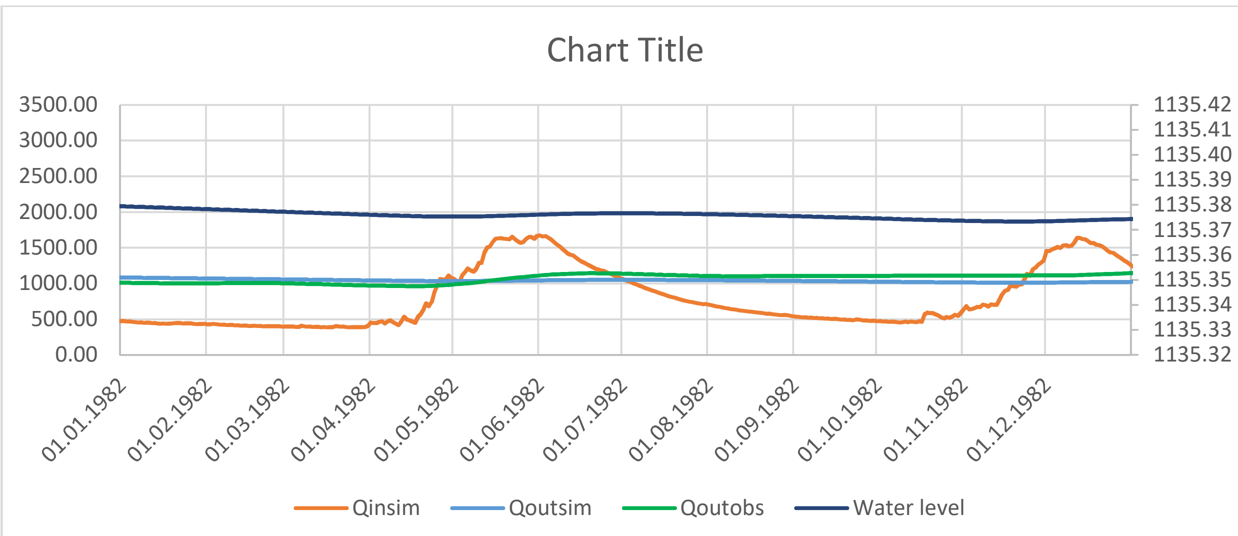
Chart Title
3500.00
3000.00
2500.00
2000.00
1500.00
1000.00
500.00
0.00
1135.42
1135.41
1135.40
1135.39
1135.38
1135.37
1135.36
1135.35
1135.34
1135.33
1135.32
01.01.1982
01.02.1982
01.03.1982
01.04.1982
01.05.1982
01.06.1982
01.07.1982
01.08.1982
01.09.1982
01.10.1982
01.11.1982
01.12.1982
Qinsim
Qoutsim
Qoutobs
Water level

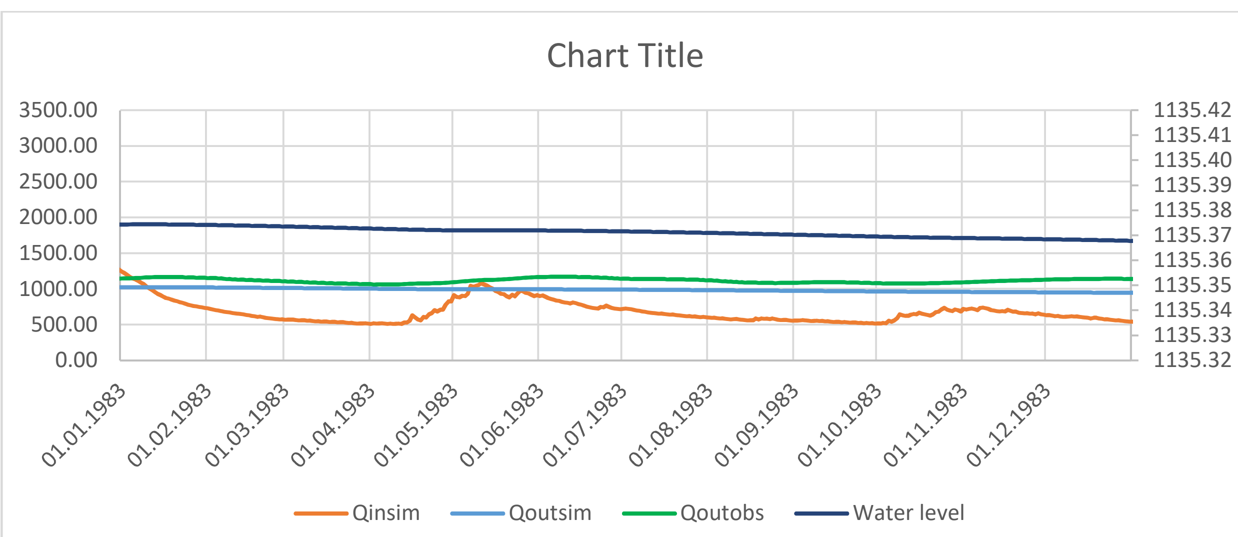
Chart Title
3500.00
3000.00
2500.00
2000.00
1500.00
1000.00
500.00
0.00
1135.42
1135.41
1135.40
1135.39
1135.38
1135.37
1135.36
1135.35
1135.34
1135.33
1135.32
01.01.1983
01.02.1983
01.03.1983
01.04.1983
01.05.1983
01.06.1983
01.07.1983
01.08.1983
01.09.1983
01.10.1983
01.11.1983
01.12.1983
Qinsim
Qoutsim
Qoutobs
Water level

The above figures show the simulated inflow after climate change application but with the observed water levels. It can be seen that the water levels have been dropping from 1980 till 1986. However, it can also be noted that as the QSim rises, there is a slight response by a rise by the water level.

But the simulated outflows have quite a lot of differences in response to the inflow, infact very little response. These could call for further investigations in the future studies.

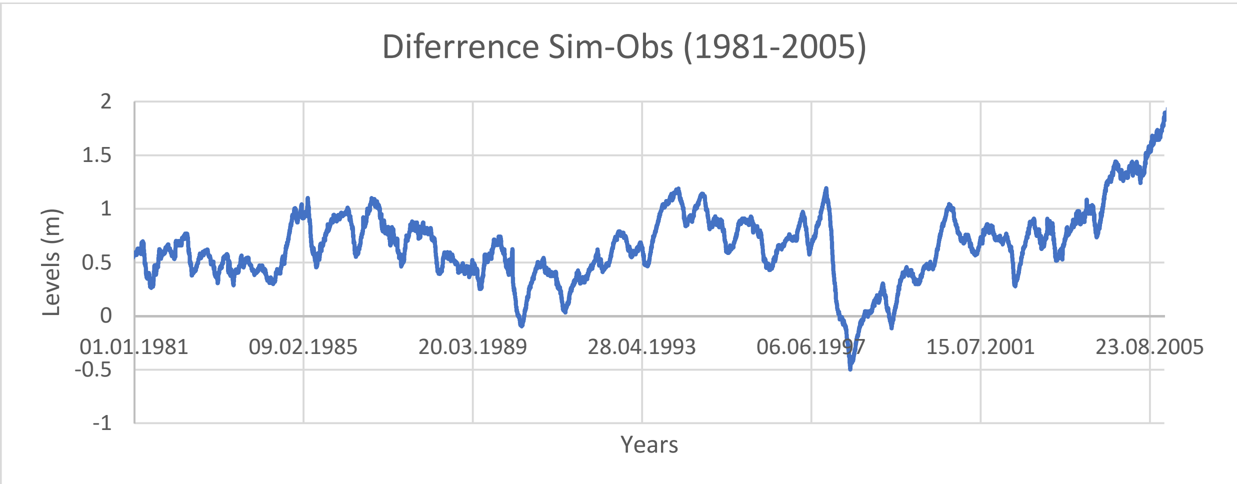

*1*Figure 6-: Difference in water levels between Simulated and Observed

Simulations of the future future outflows from the lake and the water levels are shown in the appendix A. In relation to the previous studies, it was assumed for this study the initial water level be at 1135.0m which is equivalent to maximum design water level. Below is the table showing the maximum and minimum flows and water levels after the inflows were routed through the lake.

Based on the DWD report for commissioning of the Bujagali dam, some 10km downstream of Owen Falls, "*the 100+ year average discharge from the lake is 870 cubic meters per second (m^3/s.) During the day, flows may vary between 400 m^3/s and 1300 m^3/s but rarely are the extremes reached and more typically the flows vary between 575 m^3/s m3/s to 1150 m^3/s m3/s.*" The quoted flows are supposed to be releases from the Owen falls based on the agreed curve. Therefore, the simulations not only justify the safety of the infrastructure downstream but also indicates that Owen falls dam, which ideally controls the flow downstream, can pass the generated flood. This can be attested by capacity of the spillways of both Nalubale and Kiira Power stations which have an overall release capacity of about 5240m^3/s from both their spillways and generating units.

Scenario	Inflows (m^3/s)		Outflows(m^3/s)		Water Levels (m)	
	Max	Min	Max	Min	Max	Min
	3119.37	32901	1157.29	720.00	1135.39	1135.35
2041-2065						
M45M	3041.95	311.58	1147.96	679.49	1135.38	1135.35
M85M	3022.61	307.36	1145.75	669.63	1135.38	1135.34
N45M	3059.41	315.67	1150.19	688.71	1135.39	1135.35
N85M	3041.66	311.44	1148.10	678.90	1135.38	1135.35
2073-2097						
M45F	3025.42	307.77	1145.90	670.53	1135.38	1135.34
M85F	2953.79	294.72	1138.46	639.88	1135.38	1135.34
N45F	3050.25	313.62	1149.04	684.07	1135.38	1135.35
N85F	2991.59	302.30	1142.52	657.23	1135.38	1135.34

Discussion of the Results

1. During the calibration of the model, it was noted that for the automatic calibrations, the flow response parameters k2>k1 while in the manual calibration, k2<k1. The explanation was not easily derived but this indicates that there was less of overflow from the land for the manual calibration.
2. After using the calibrated parameters from the ground based stations for the simulation of the reanalysis, it served as a confirmation that the reanalysis data underestimated the precipitation by more than 40%.
3. The reanalysis precipitation data correction needs to be studied further to ascertain why after the bias correction the performance was poor compared to the un-biased.
4. The study realizes that limitations in data can seriously constrain any efforts in regionalisation modelling. Collection of additional data in the Lake Victoria basin sub-basins would be very helpful as more advanced regionalization techniques can then be tested.

5. Whereas the climate change simulations indicate that the flood developments are lower than the current situation, there is a need for more study based on additional GCM models in order to get a fair accuracy of the result.
6. The temperature is expected to increase by 1.5deg C in the midcentury as indicated by MOHC and 4.5 deg C by NOAA in the far century. The lowest temperatures were also noted to have increased by 1 deg in both models.
7. From the routing results, and having fixed a starting point for the water levels, it was found that the water levels fluctuates between 0.3 and 0.4m above the chosen datum. The water released fluctuates within the range of $640m^3/s$ and $1150m^3/s$. this is within the release ranges of the current situation as documented by DWD.
8. The total annual precipitation is expected to increase by 3% and 6% for the period 2041-2065 and 2073-2097 scenarios respectively.
9. Uncertainties inherent in projections and additionally arising from applied downscaling are often not presented, quantified, nor discussed, leading the user to interpret the numerical results at face value.
10. Validation of downscaled results (on historical data) is often omitted; comparing downscaled results to high-resolution observed information would highlight systematic biases and the limitations of results
11. Information on downscaling and the limitations of the results are often not appropriately highlighted, leading the user to believe that the results are “true” and valid at the resolution presented. Extensive reading of technical documentation is often needed to uncover all the steps and assumptions that led to the final results.

Recommendations

To study future lake level changes, next to precipitation over the lake, also discharges of main inflowing rivers need to be studied. This requires future projections of precipitation and potential evapotranspiration over the Lake Victoria Basin river subcatchments, and impact modeling by means of catchment runoff models. A possible study could be GCM evaluations in precipitation simulation and analysis of future projections.

There should be increased frequency and consistency of relevant data collection in all the three countries.

There is need for the three countries to continue cooperating in updating the water budget for Lake Victoria.

Efforts should be made to determine the role played by groundwater in the water budget of Lake Victoria although work to date including isotopic analysis suggest the role of ground water is minimal in the budget.

Data collection equipment and instruments should be standardized so that uniform data can be collected and used.

Stations should be established in ungauged catchments so that actual data is used in the balance other than estimates.

Undertake intensive studies on the possibility of regulating the lake to optimize its multiple but potentially conflicting uses to achieve maximum and sustainable socio-economic benefits for the riparian states.

Having used the Delta change method for the climate change downscaling, which uses the monthly means, it would be interesting to find out what results are obtained from other methods of downscaling for a proper comparison. One of the approaches would be to use the Antinoise approach which could be tried out on a daily scale downscaling other than monthly.

References

Klemes, V. (1986) Operational testing of hydrological simulation models, Hydrological Sciences Journal 31 (1), pp. 13-24.

Priestley C. H. B., Taylor R. J. 1972 On the assessment of surface heat flux and evaporation using large-scale parameters. Mon. Weather Rev. **100**, 81–82. **CrossRefWeb of ScienceGoogle Scholar**

Vrugt, J. A., Ter Braak, C.J.F., 2011. DREAM(D): an adaptive Markov Chain Monte Carlo simulation algorithm to solve discrete, noncontinuous, and combinatorial posterior parameter estimation problems. *Hydrol. Earth Syst. Sci.* 15, 3701–3713.

Troin, M., Vallet-Coulomb, C., Sylvestre, F., Piovano, E., 2010. Hydrological modelling of a closed lake (Laguna Mar Chiquita, Argentina) in the context of 20th century climatic changes. Journal of Hydrology 393, 233–244.

Sene, K.J., Tate, E.L. and Farquharson, F.A.K. (2001) Sensitivity studies of the impacts of climate change on White Nile flows. Climatic Change. Vol. 50, pp. 177-208.

Buytaert, W.; Friesen, J.; Liebe, J.; Ludwig, R. Assessment and management of water resources in developing,semi-arid and arid regions. Water Resour. Manag. 2012, 26, 841–844. [CrossRef]

Gorgoglione, A.; Gioia, A.; Iacobellis, V.; Piccinni, A.F.; Ranieri, E. A rationale for pollutograph evaluation in ungauged areas, using daily rainfall patterns: Case studies of the Apulian region in Southern Italy. Appl. Environ. Soil Sci. 2016, 2016, 9327614. [CrossRef]

Liu, Y.; Gupta, H.; Springer, E.; Wagener, T. Linking science with environmental decision making: Experiences from an integrated modeling approach to supporting sustainable water resources management. Environ. Model. Softw. 2008, 23, 846–858. [CrossRef]

Worqlul, A.W.; Maathuis, B.; Adem, A.A.; Demissie, S.S.; Langan, S.; Steenhuis, T.S. Comparison of rainfall estimations by TRMM 3B42, MPEG and CFSR with ground-observed data for the Lake Tana basin in Ethiopia. Hydrol. Earth Syst. Sci. 2014, 18, 4871–4881. [CrossRef]

Kizza, M.; Westerberg, I.; Rodhe, A.; Ntale, H.K. Estimating areal rainfall over Lake Victoria and its basin using ground-based and satellite data. *J. Hydrol.* **2012**, *464–465*, 401–411.

Liu, T.; Willems, P.; Pan, X.L.; Bao, A.M.; Chen, X.; Veroustraete, F.; Dong, Q.H. Climate change impact on water resource extremes in a headwater region of the Tarim basin in China. *Hydrol. Earth Syst. Sci.* **2011**, *15*, 3511–3527.

Sutcliffe, J.; Parks, Y. *The Hydrology of the Nile*; International Association of Hydrological Sciences IAHS: Wallingford, UK, 1999; Volume 5.

Mutenyo, I.B. Impacts of Irrigation and Hydroelectric Power Developments on the Victoria Nile in Uganda School. Ph.D. Thesis, Cranfield University, Cranfield, UK, 2009; p. 258.

Kizza, M.; Rodhe, A.; Xu, C.-Y.; Ntale, H.K.; Halldin, S. Temporal rainfall variability in the lake Victoria Basin in East Africa during the twentieth century. *Theor. Appl. Climatol.* **2009**, *98*, 119–135.

Yin, X.; Nicholson, S.E. The water balance of Lake Victoria. *Hydrol. Sci. J.* **1998**, *43*, 789–811.

Tate, E.; Sutcliffe, J.; Conway, D.; Farquharson, F. Water balance of Lake Victoria: Update to 2000 and climate change modelling to 2100/Bilan hydrologique du Lake Victoria: Mise à jour jusqu'en 2000 et modélisation des impacts du changement climatique jusqu'en 2100. *Hydrol. Sci. J.* **2004**, *49*, doi:10.1623/hysj.49.4.563.54422.

Piper, B.S.; Plinston, D.T.; Sutcliffe, J.V. The water balance of Lake Victoria. *Hydrol. Sci. J.* **1986**, *31*, 25–37.

Kite, G.W. Analysis of Lake Victoria levels. *Hydrol. Sci. J.* **1982**, *27*, 99–110.

Anund Killingtveit, Nils Roar Saelthun **'Hydrology-Hydropower Development series #7**', 1995, Hydrological Models, Page 107, Section 6.5.2, Figure 6.7.

A Review of Downscaling Methods for Climate Change Projections', African and Latin American Resilience to Climate Change Project, September 2014, Page 2, Section 1.2, Paragraph-

APPENDIX C-Owen Falls Dam and Bujagali Dam Layout

APPENDIX C-Flood Routing

Simulated inflows from the different scenarios which are routed through the lake. An assumption of the lake level was taken as 1135.0m. from the routing equations, the storage level relation equation was found to be **s=7E+10H-8E+13**

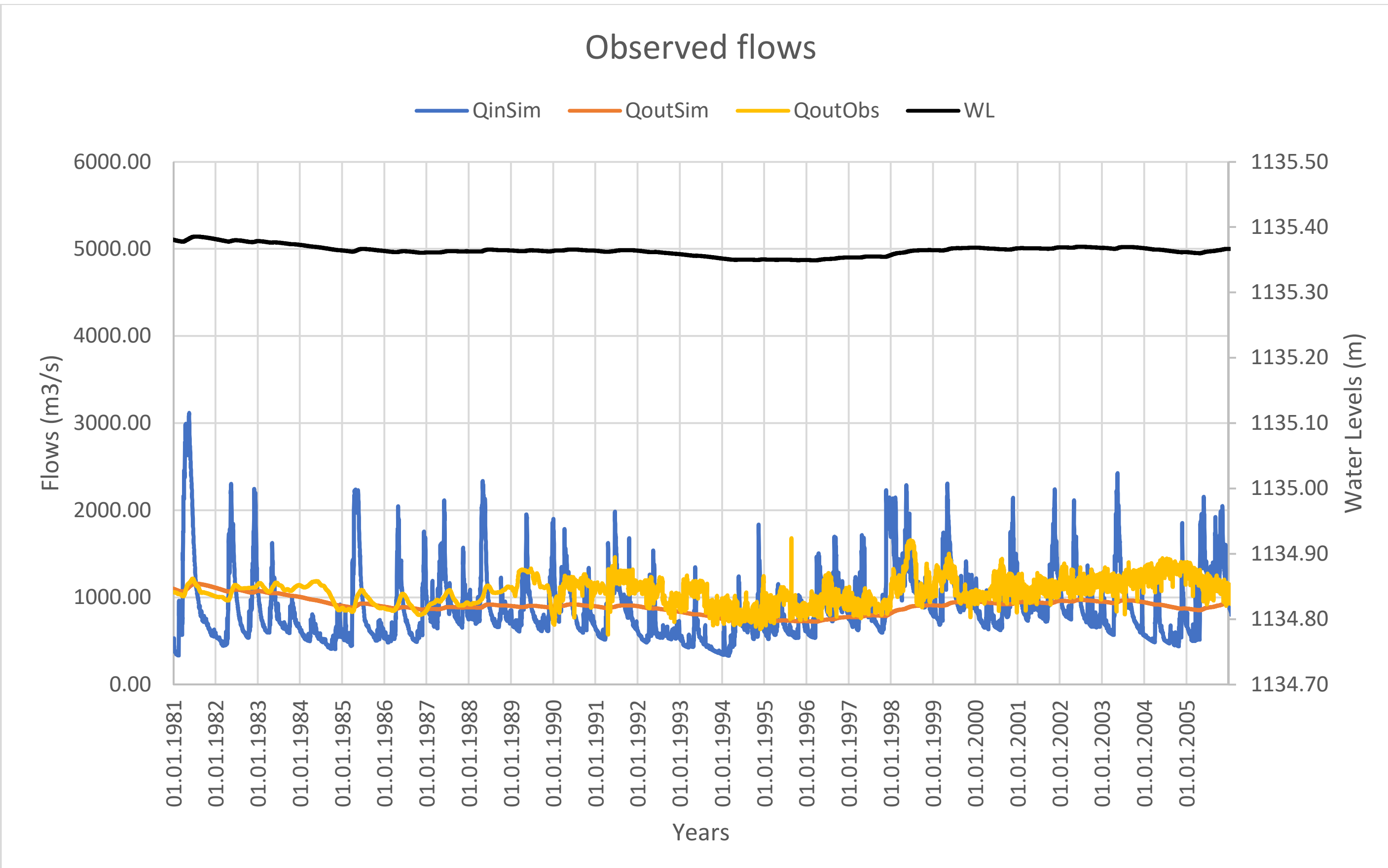

Mx Qin	MinQin	Mx Qo	MnQo	Mx Wl	MinWl
3119.37	329.01	1157.29	720.00	1135.39	1135.35

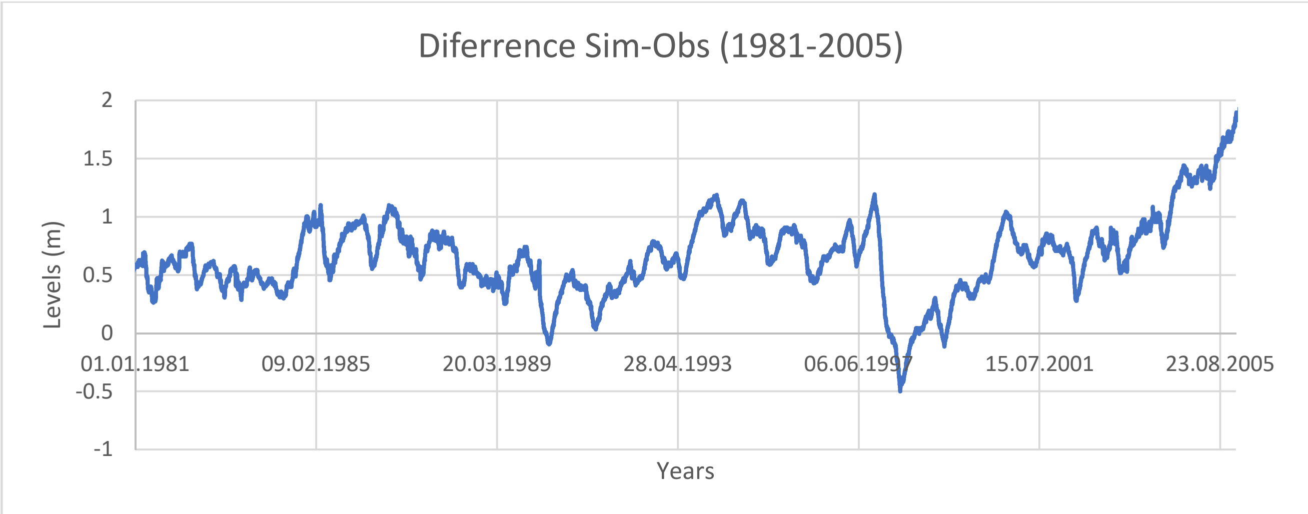

Routing floods 2041-2065

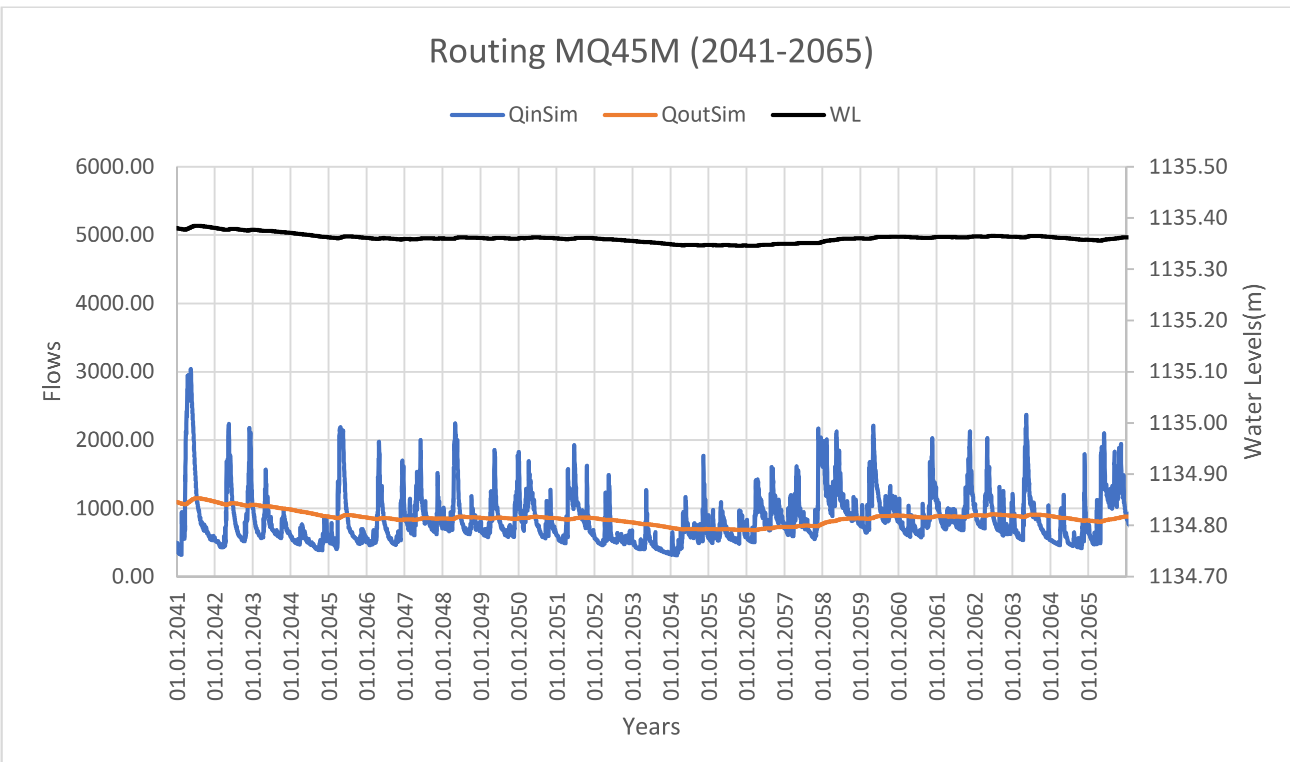

Mx Qin	MinQin	Mx Qo	MnQo	Mx Wl	MinWl
3041.95	311.58	1147.96	679.49	1135.38	1135.35

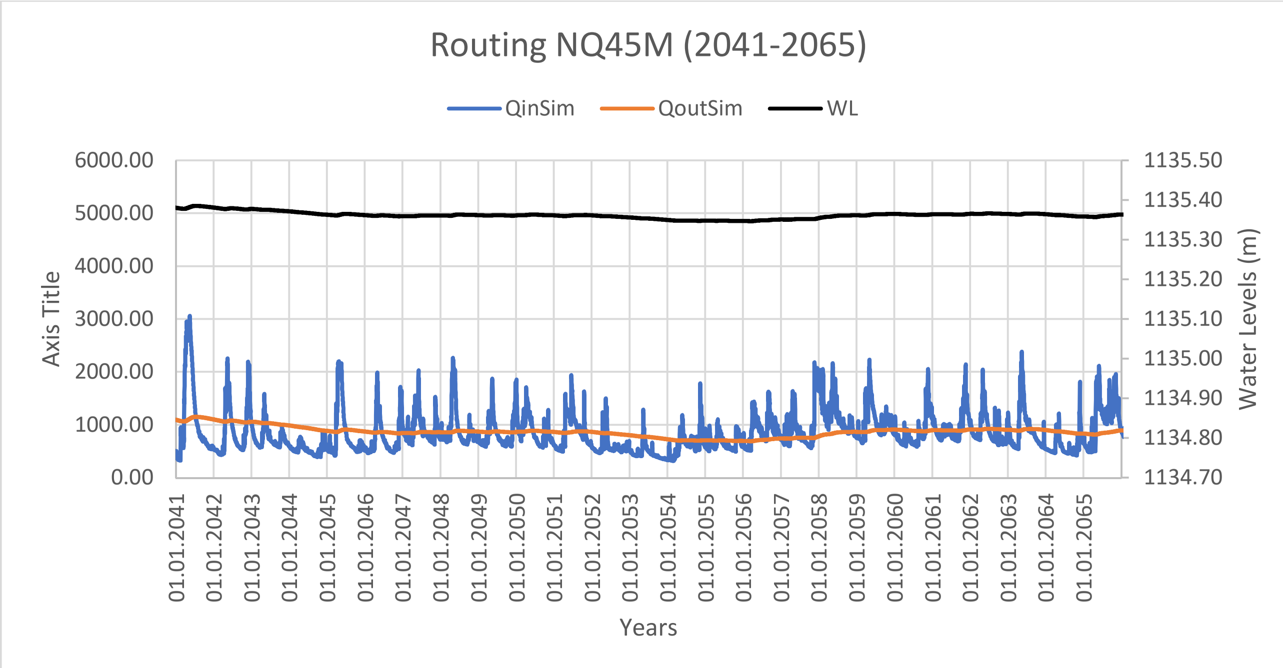

Mx Qin	MinQin	Mx Qo	MnQo	Mx Wl	MinWl
3059.41	315.67	1150.19	688.71	1135.39	1135.35

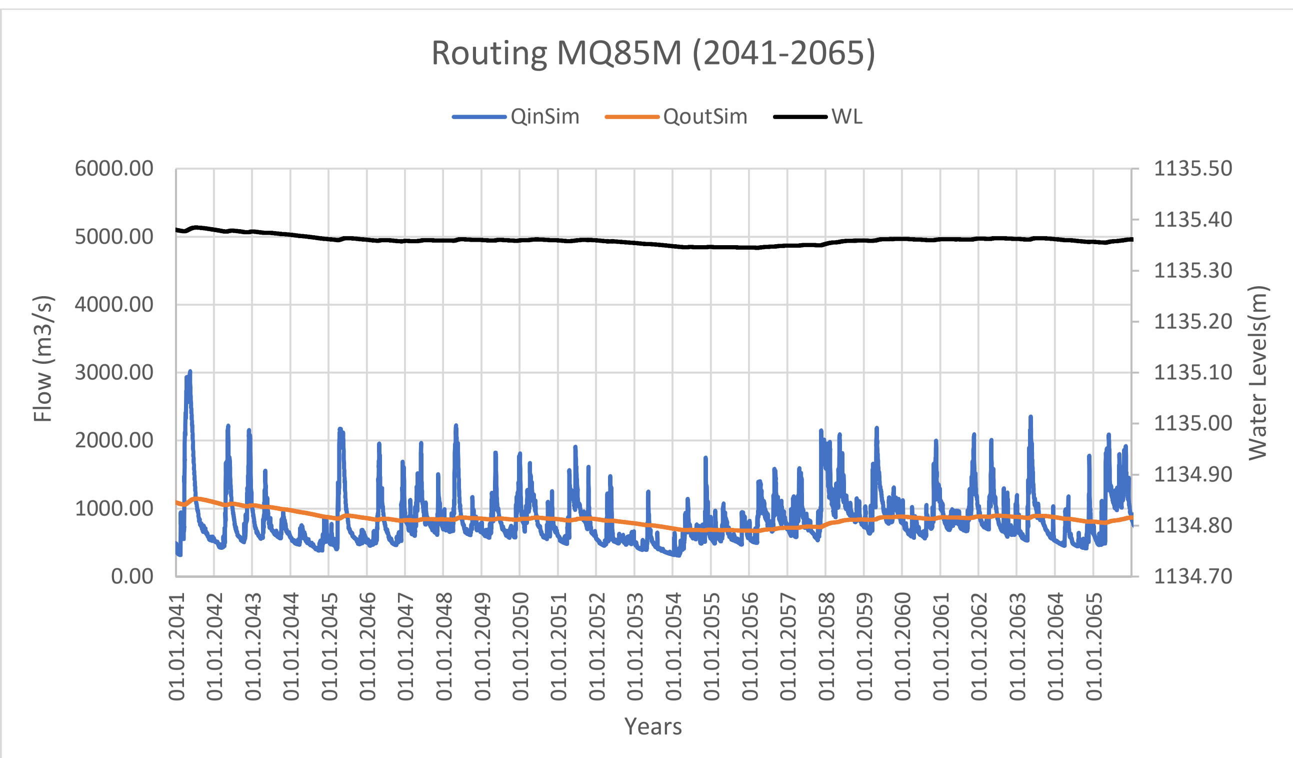

Mx Qin	MinQin	Mx Qo	MnQo	Mx Wl	MinWl
3022.61	307.36	1145.75	669.63	1135.38	1135.34

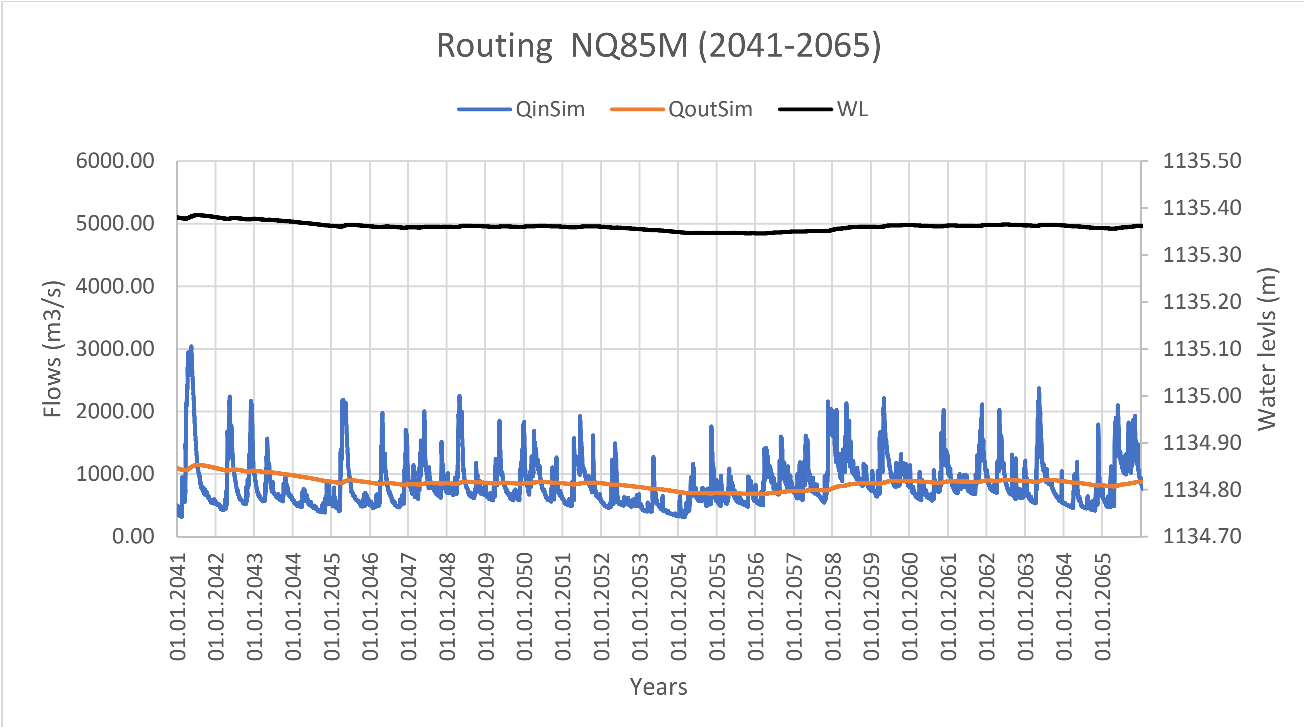

Mx Qin	MinQin	Mx Qo	MnQo	Mx Wl	MinWl
3041.66	311.44	1148.10	678.90	1135.38	1135.35

Period 2073-2097

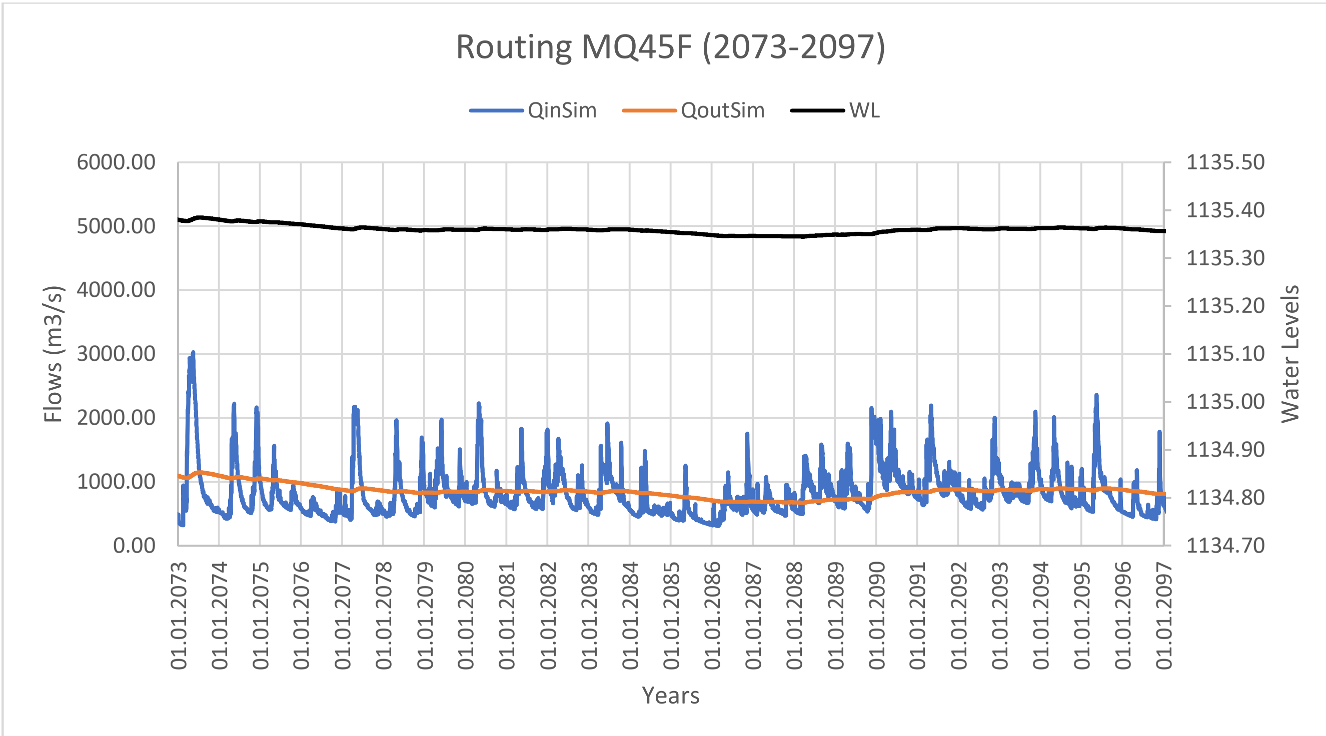

Mx Qin	MinQin	Mx Qo	MnQo	Mx Wl	MinWl
3025.42	307.77	1145.90	670.53	1135.38	1135.34

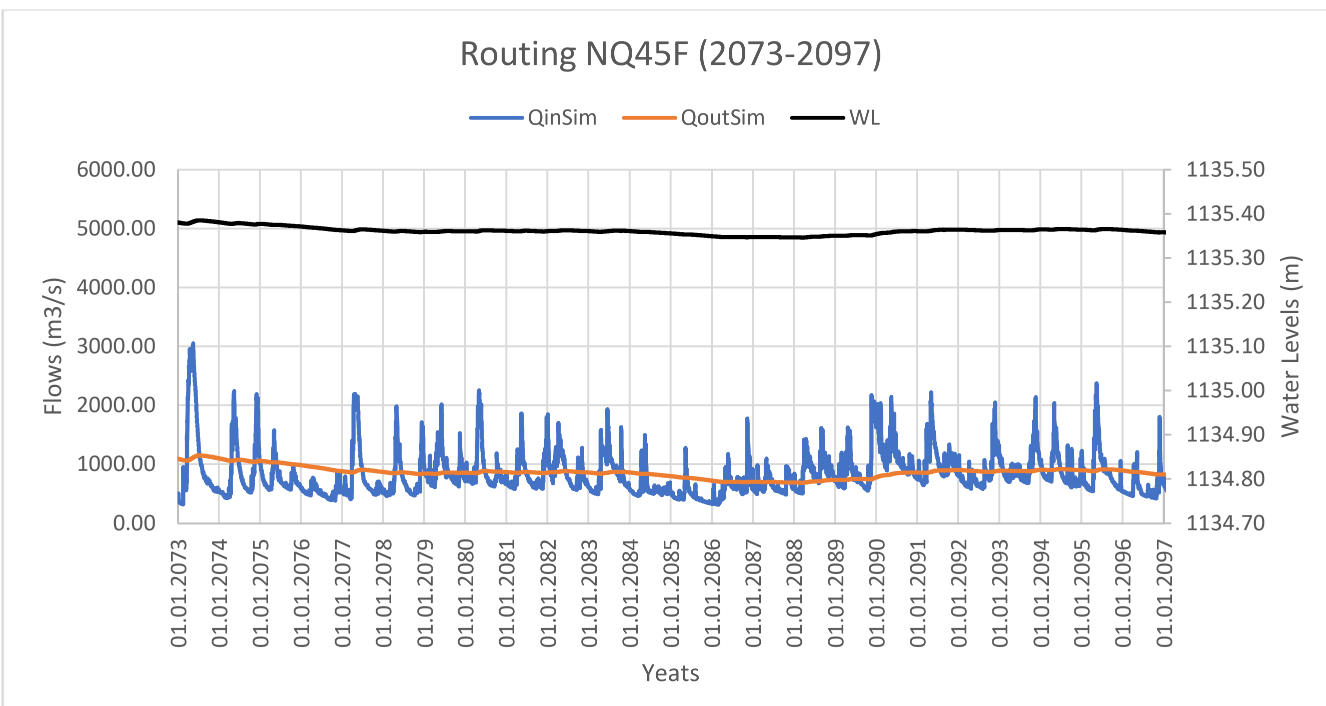

Mx Qin	MinQin	Mx Qo	MnQo	Mx Wl	MinWl

3050.25	313.62	1149.04	684.07	1135.38	1135.35

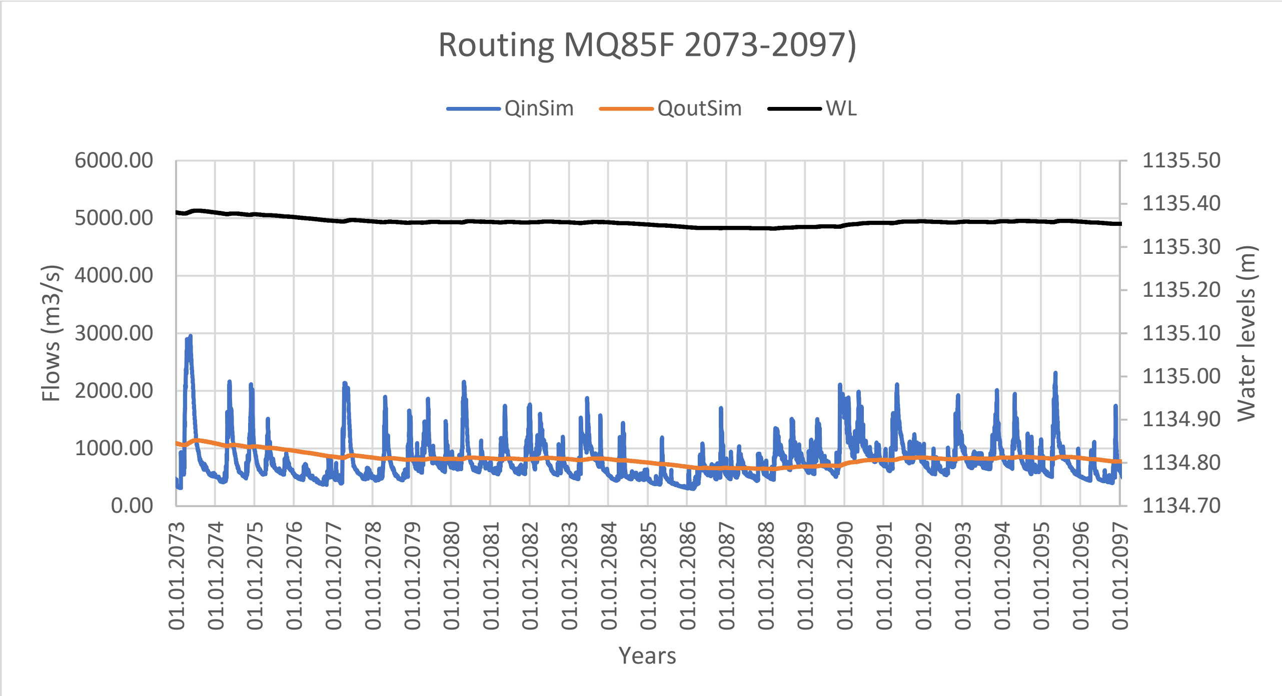

Mx Qin	MinQin	Mx Qo	MnQo	Mx Wl	MinWl
2953.79	294.72	1138.46	639.88	1135.38	1135.34

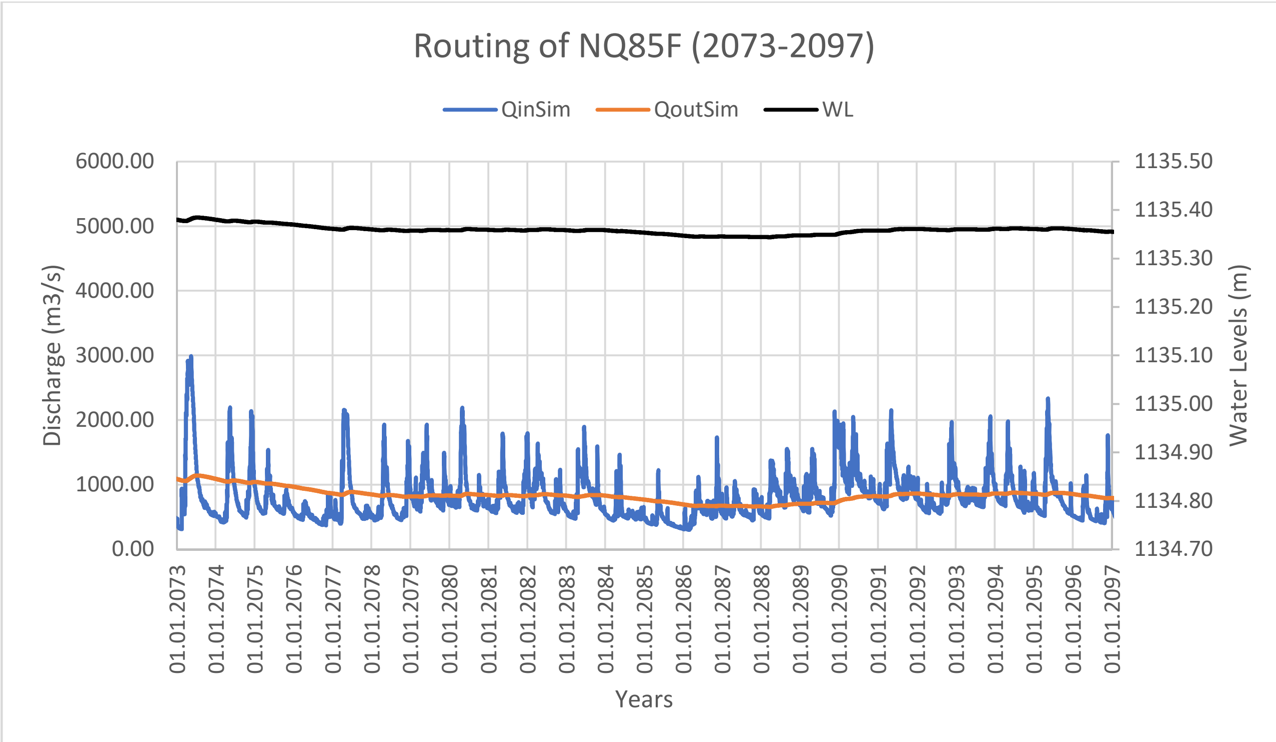

Mx Qin	MinQin	Mx Qo	MnQo	Mx Wl	MinWl
2991.59	302.30	1142.52	657.23	1135.38	1135.34

APPENDIX B- Simulated GCM inflows

2041-2065

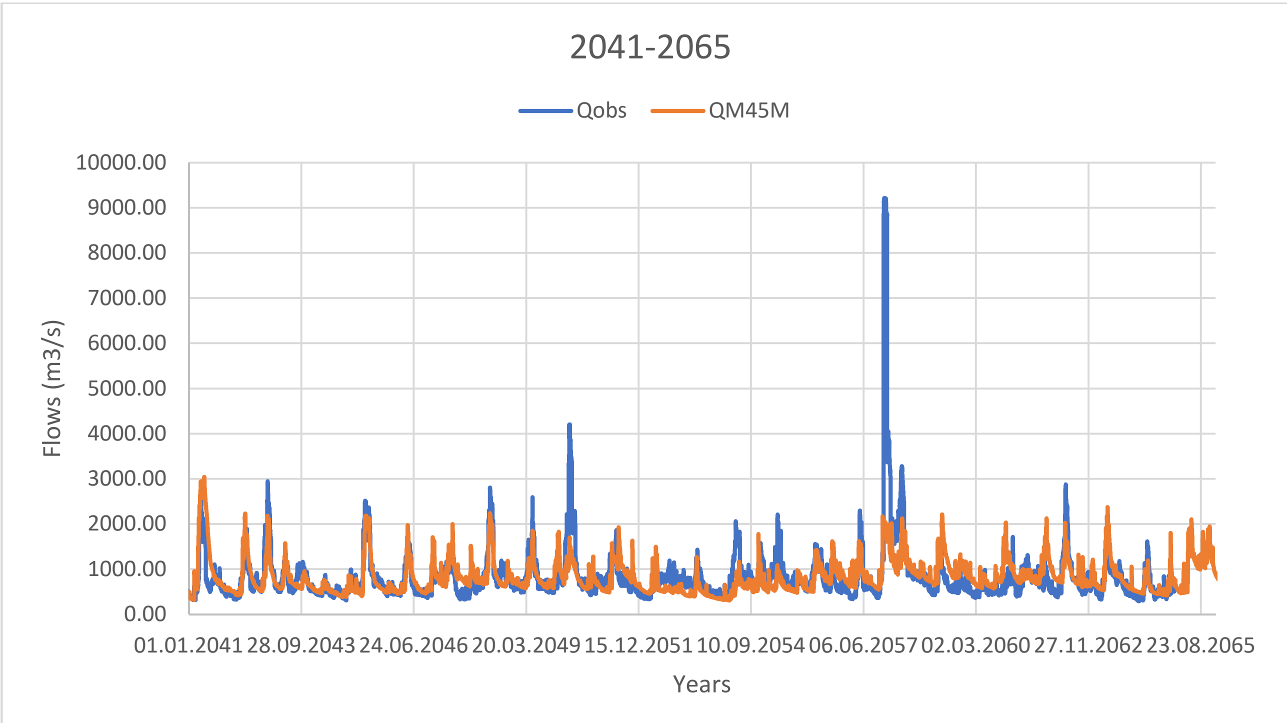

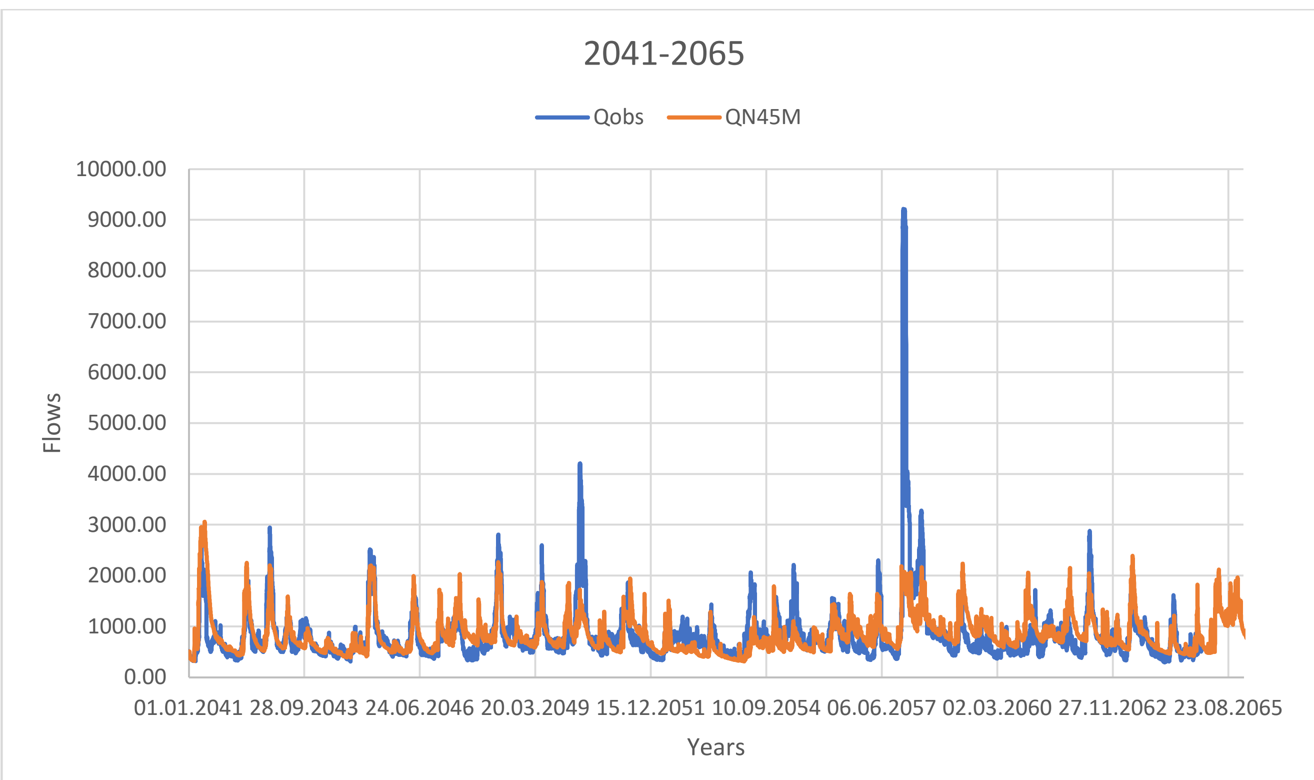

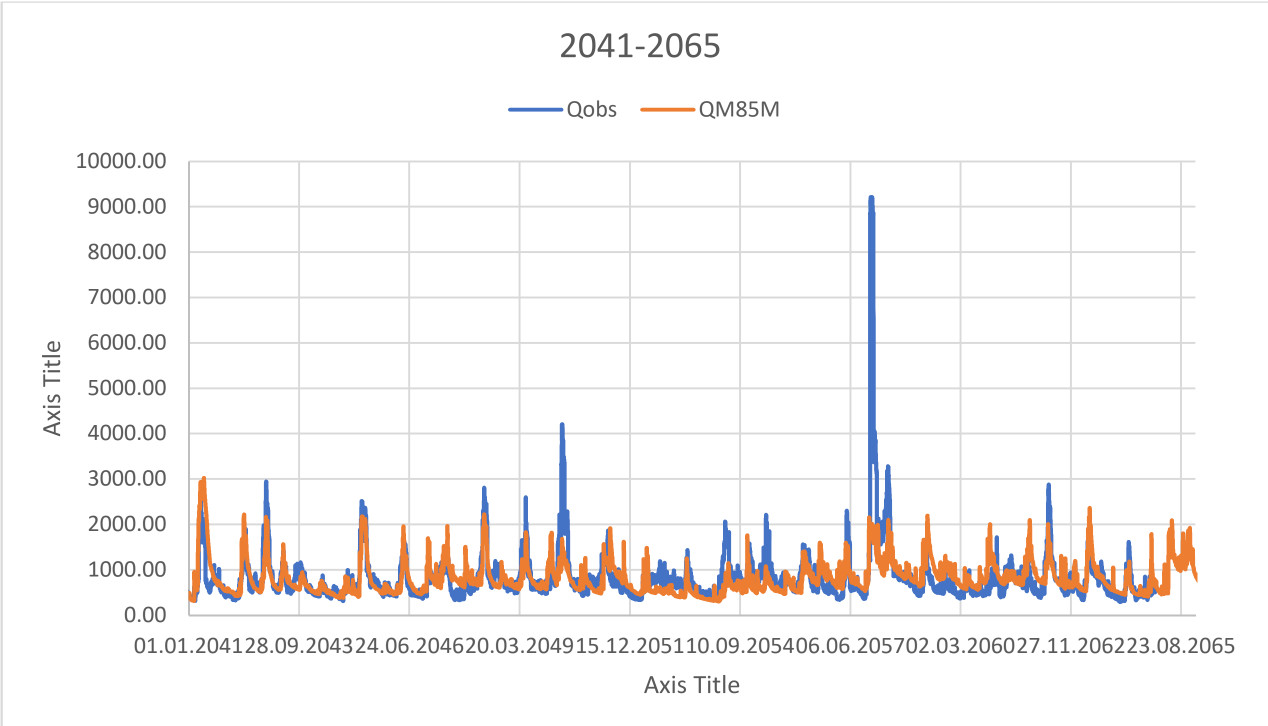
2041-2065
Qobs
QM85M
10000.00
9000.00
8000.00
7000.00
6000.00
5000.00
4000.00
3000.00
2000.00
1000.00
0.00
Axis Title
01.01.2041
28.09.2043
24.06.2046
20.03.2049
15.12.2051
10.09.2054
06.06.2057
02.03.2060
27.11.2062
23.08.2065
Axis Title

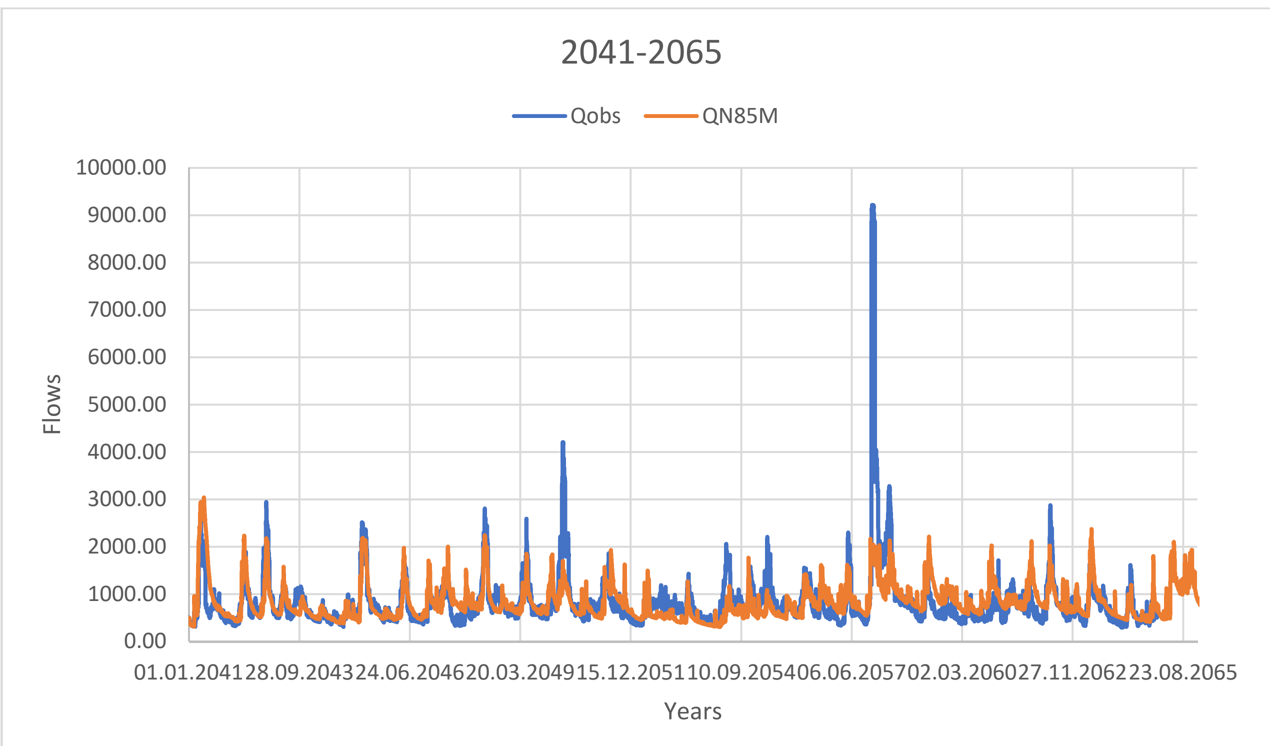
2041-2065
Qobs
QN85M
10000.00
9000.00
8000.00
7000.00
6000.00
5000.00
4000.00
3000.00
2000.00
1000.00
0.00
Flows
01.01.2041
28.09.2043
24.06.2046
20.03.2049
15.12.2051
10.09.2054
06.06.2057
02.03.2060
27.11.2062
23.08.2065
Years

2073-2097

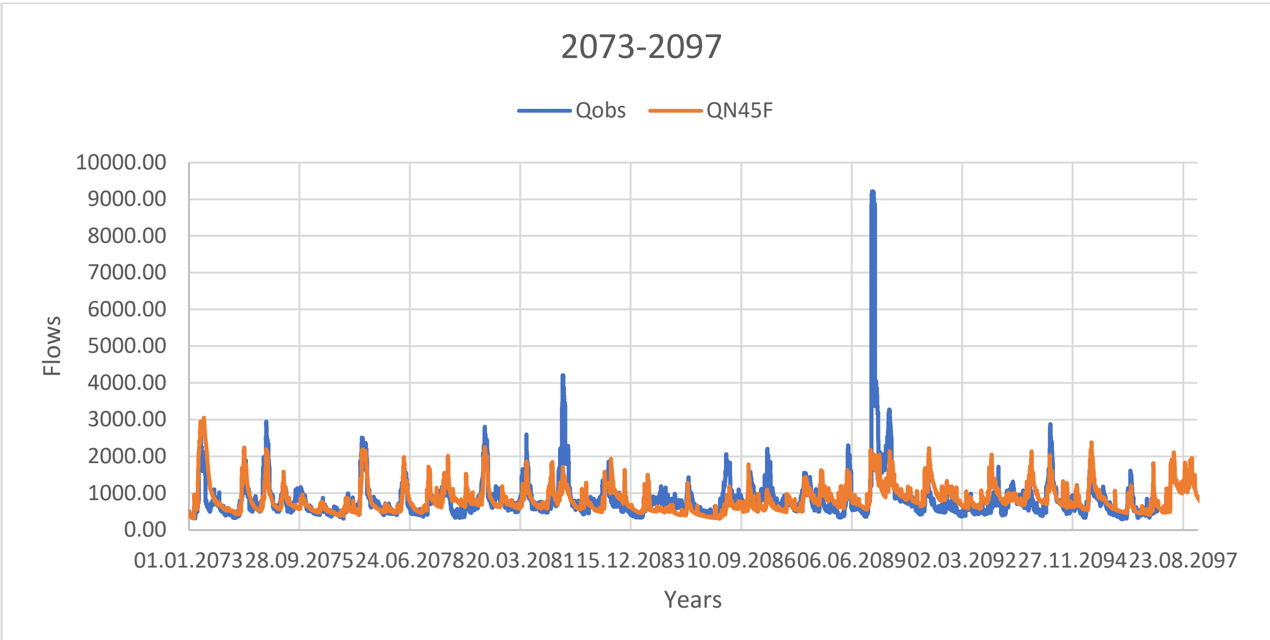
2073-2097
Qobs
QN45F
Flows
10000.00
9000.00
8000.00
7000.00
6000.00
5000.00
4000.00
3000.00
2000.00
1000.00
0.00
01.01.2073 28.09.2075 24.06.2078 20.03.2081 15.12.2083 10.09.2086 06.06.2089 02.03.2092 27.11.2094 23.08.2097
Years

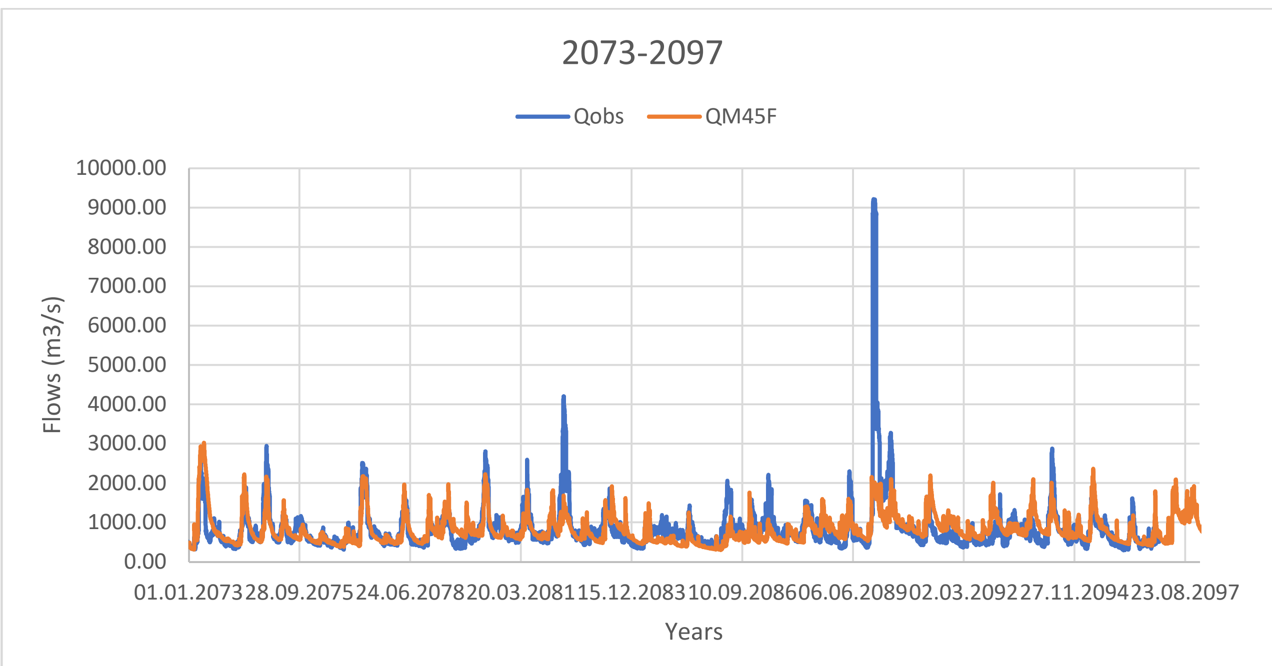
2073-2097
Qobs
QM45F
Flows (m3/s)
10000.00
9000.00
8000.00
7000.00
6000.00
5000.00
4000.00
3000.00
2000.00
1000.00
0.00
01.01.2073 28.09.2075 24.06.2078 20.03.2081 15.12.2083 10.09.2086 06.06.2089 02.03.2092 27.11.2094 23.08.2097
Years

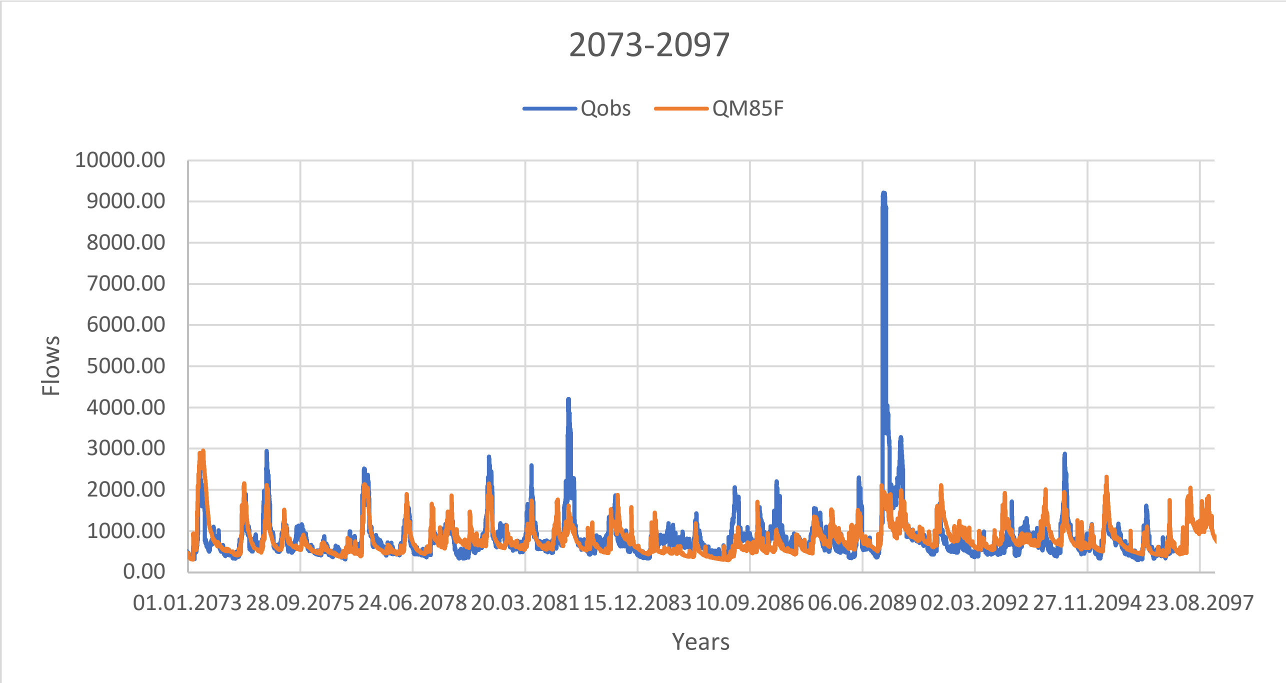
2073-2097
Qobs
QM85F
10000.00
9000.00
8000.00
7000.00
6000.00
5000.00
4000.00
3000.00
2000.00
1000.00
0.00
Flows
01.01.2073 28.09.2075 24.06.2078 20.03.2081 15.12.2083 10.09.2086 06.06.2089 02.03.2092 27.11.2094 23.08.2097
Years

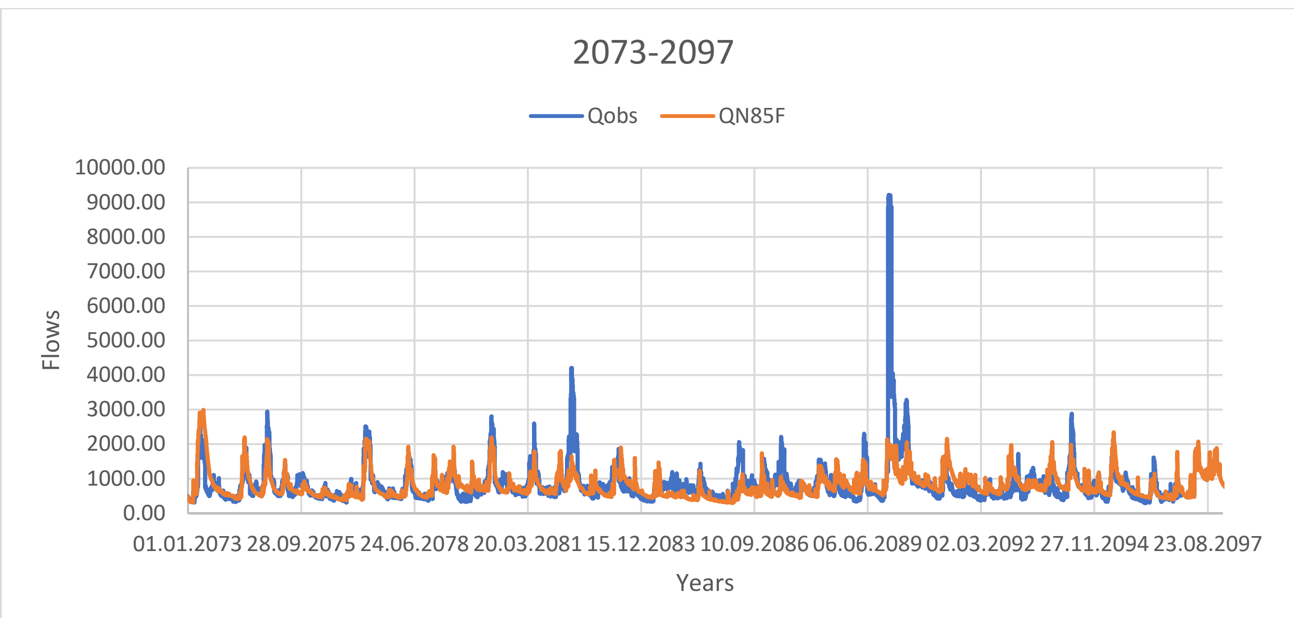
2073-2097
Qobs
QN85F
10000.00
9000.00
8000.00
7000.00
6000.00
5000.00
4000.00
3000.00
2000.00
1000.00
0.00
Flows
01.01.2073 28.09.2075 24.06.2078 20.03.2081 15.12.2083 10.09.2086 06.06.2089 02.03.2092 27.11.2094 23.08.2097
Years